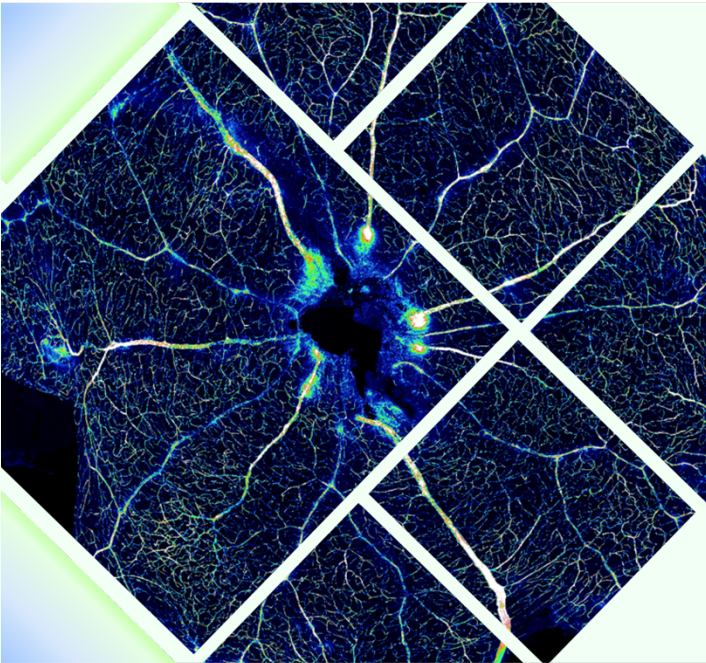


ADVERTIMENT. L'accés als continguts d'aquesta tesi doctoral i la seva utilització ha de respectar els drets de la persona autora. Pot ser utilitzada per a consulta o estudi personal, així com en activitats o materials d'investigació i docència en els termes establerts a l'art. 32 del Text Refós de la Llei de Propietat Intel·lectual (RDL 1/1996). Per altres utilitzacions es requereix l'autorització prèvia i expressa de la persona autora. En qualsevol cas, en la utilització dels seus continguts caldrà indicar de forma clara el nom i cognoms de la persona autora i el títol de la tesi doctoral. No s'autoritza la seva reproducció o altres formes d'explotació efectuades amb finalitats de lucre ni la seva comunicació pública des d'un lloc aliè al servei TDX. Tampoc s'autoritza la presentació del seu contingut en una finestra o marc aliè a TDX (framing). Aquesta reserva de drets afecta tant als continguts de la tesi com als seus resums i índexs.

ADVERTENCIA. El acceso a los contenidos de esta tesis doctoral y su utilización debe respetar los derechos de la persona autora. Puede ser utilizada para consulta o estudio personal, así como en actividades o materiales de investigación y docencia en los términos establecidos en el art. 32 del Texto Refundido de la Ley de Propiedad Intelectual (RDL 1/1996). Para otros usos se requiere la autorización previa y expresa de la persona autora. En cualquier caso, en la utilización de sus contenidos se deberá indicar de forma clara el nombre y apellidos de la persona autora y el título de la tesis doctoral. No se autoriza su reproducción u otras formas de explotación efectuadas con fines lucrativos ni su comunicación pública desde un sitio ajeno al servicio TDR. Tampoco se autoriza la presentación de su contenido en una ventana o marco ajeno a TDR (framing). Esta reserva de derechos afecta tanto al contenido de la tesis como a sus resúmenes e índices.

WARNING. The access to the contents of this doctoral thesis and its use must respect the rights of the author. It can be used for reference or private study, as well as research and learning activities or materials in the terms established by the 32nd article of the Spanish Consolidated Copyright Act (RDL 1/1996). Express and previous authorization of the author is required for any other uses. In any case, when using its content, full name of the author and title of the thesis must be clearly indicated. Reproduction or other forms of for profit use or public communication from outside TDX service is not allowed. Presentation of its content in a window or frame external to TDX (framing) is not authorized either. These rights affect both the content of the thesis and its abstracts and indexes.



Unravelling the underlying mechanisms involved in the beneficial effects of DPP-4 inhibitors in early stages of diabetic retinopathy

Hugo Ramos Abellán

Programa de doctorat en Bioquímica, Biologia Molecular i Biomedicina
Departament Bioquímica i Biologia Molecular

2023

Unravelling the underlying mechanisms involved in the beneficial effects of DPP-4 inhibitors in early stages of diabetic retinopathy

DOCTORAL THESIS
HUGO RAMOS ABELLÁN

Directors:

Dr. Rafael Simó Canonge

Dra. Cristina Hernández Pascual

Dra. Patricia Bogdanov Baruj

Tutor:

Dr. Miquel Vila Bover

Programa de doctorat en Bioquímica, Biologia Molecular i Biomedicina

Departament de Bioquímica i Biologia Molecular

Universitat Autònoma de Barcelona

2023

*Life is like a pencil, it will surely run out one day,
but what matters is the beautiful writing we can leave
with it before that happens*

Aknowledgments

Hace ya 5 años que abrí este capítulo de mi vida llamado doctorado y parece mentira lo rápido que ha pasado el tiempo y la cantidad de personas que se han cruzado en el camino, a veces incluso de la forma inesperada. Ahora, ya por fin a la puertas de cerrar esta etapa, es cuando vuelvo la vista atrás y veo que solo nunca lo habría conseguido. En primer lugar me gustaría agradecer a mis directores de tesis, el Dr. Rafael Simó, la Dra. Cristina Hernández y la Dra. Patricia Bogdanov, quienes desde un inicio apostaron por mí y me concedieron esta gran oportunidad profesional. También quiero daros las gracias por todas las enseñanzas, consejos y la confianza depositada durante todos estos años. Patri, darte la gracias también por el cariño diario que siempre me has mostrado y por estar dispuesta a ayudarme en todo momento, pese a que ello te implicase hacer horas extras. Al pensar en el día a día no puedo evitar acordarme de todas esas personas que han ido pasando por el laboratorio, ya haya sido coincidiendo todo este tiempo o de una forma más breve. Gracias Joel, rey de los Western Blots, por todas nuestras largas charlas en el estabulario y por enseñarme a ser un científico más crítico. Me alegra saber que las nuevas generaciones podrán disfrutar de un magnífico profesor. Gracias Angélica por tu alegría y por contagiarme siempre ese optimismo tan tuyo. Gracias a mi dúo dinámico Jordi y Anna, no sé qué hubiera hecho sin vosotros en mi día a día de los últimos 2 años. Gracias Jordi por tu humor y por ser el mejor cómplice a la hora de desquiciar a la buena gente del Collserola, con mención especial a Anna. Gracias Anna por siempre escucharme, aguantarme y ser la mejor compañera. También quería agradecerte el hacerme descubrir lo que es el miedo a no tener una poyata limpia e impoluta. Desearte lo mejor en tu recta final, sé que lo bordarás. Gracias David por tu amabilidad y paciencia durante tus clases magistrales en cultivos. No menos importantes, también están los integrantes del grupo del Dr. Josep Villena. Gracias Pep y Rosi por todas esas charlas durante las comidas, es fascinante el hecho de que uno nunca pueda intuir de qué forma intentaremos arreglar el mundo ese día. Gracias Marc i Maria por estar siempre ahí, sé que puedo contar con vosotros para cualquier cosa y sé que seguiremos viéndonos después de todo esto. Tengo a dos grandes personas a mi lado. Gracias Meri, Ingrid, Andrea, Aleix, Claudia y Laura por ayudar a hacer más ameno el día a día. Además quería agradecer a toda la gente de Mediterrània por su ayuda durante estos años. Gracias Lorena por tu infinita paciencia y empatía con todos mis problemas burocráticos, a los que siempre les ponías una solución acompañada con algún nuevo sticker para mi colección. Gracias Marta por

AKNOWLEDGMENTS

tu conocimiento de cultivos y por tu compañía durante los congresos del CIBER. Y aunque hayamos coincidido poco, gracias Maria por tus consejos para Belfast. En relación a Belfast, gracias a toda la buena gente del grupo del Dr. Tim Curtis (Tim, Peter, Tom, Evan, Adam, Sanaa, Niamh, y especialmente Burak y Josy) por acogirme tan bien y permitirme aprender y crecer en un ambiente laboral nuevo.

Otra piedra angular en todo este proceso, han sido todos los compañeros del Collserola. En primer lugar gracias a mis queridos vecinos kinasos, vuestro lab ha sido una segunda casa en el VHIR. Gracias a Sergio, Nora, Idoia, Maria, Anna, Clàudia y Gökhan por todos los buenos momentos y risas durante las comidas, no se qué hubiera hecho sin vosotros tampoco. Gracias a vosotros he descubierto que el origen del mundo está en Vitoria, que en Sevilla el límite de velocidad es distinto al resto de España y lo que es hacer magia con los pies dentro y fuera de un campo de fútbol. En cuanto a la ala este, gracias a la gente oftalmo, Anna, Helena, y Maddalen por vuestra ayuda y los buenos momentos entre laboratorios hermanos. Y gracias también a María por nuestras risas y por hacerme ser mejor persona. Y como no, a la dupla galáctica (Marta y Elena), a mi hermana Marina, Paula y Almudena, por animar siempre el edificio con vuestros eventos, incluso en los momentos más difíciles. Gracias también por hacerme ver que siempre podré vivir de TikTok en caso de que en esto de la ciencia no me vaya bien. Y no menos importantes, gracias al personal del Collserola (Andrés, Nieves, Rashira, Eulalia, y Rosa), a la gente del Biobanco, la UEB y la UAT (Maria, Pilar y Marta) por hacerlo todo siempre más fácil.

Gracias a los de toda la vida, Natalia, Riki y Ghis, simplemente por ser quiénes sois, no cambiéis nunca. Echo de menos nuestras largas conversaciones a las tantas de la madrugada. Gracias Mireia, las Martas, Adri, Laura, Miriam y Jordi por permitirme disfrutar de vosotros y por darme los mejores años de universidad que alguien pudiera desear.

Por último, me he reservado a los más importantes, a mi familia, especialmente a mis padres. Gracias papa y mama por estar siempre ahí con vuestro apoyo incondicional, por hacer que nunca me falte de nada, y sobre todo por haberme criado con unos buenos valores. Nunca podré agradecerlos lo suficiente. Gracias a los demás también, tía Guadalupe, tío Juan Manuel, Inma, “titos”, tía Mari, Montse, Carlos, yayos, etc., por contribuir a ser quien soy.

ABBREVIATIONS

Abbreviations

AbsLogFC: Absolute logarithmic fold change	Cat: Catalase (gene)
Actb: Actin beta (gene)	CAT: Catalase
AD: Alzheimer's disease	CCDC22: Coiled-coil domain-containing protein 22
ADA: American Diabetes Association	CCL5: Chemokine (C-C motif) ligand 5
Adj.P.Val: Adjusted p-value	cDNA: complementary DNA
AGEs: Advanced glycation end products	CNS: Central nervous system
AMPA: α -amino-3-hydroxy-5-methyl-4-isoxazolepropionic acid	CO₂: Carbon dioxide
Aβ1: amyloid beta precursor protein-binding family A member 1 (gene)	COL IV: Collagen IV
APBA1: Amyloid beta precursor protein-binding family A member 1	Commd8: Copper metabolism Murr1 domain-containing 8 (gene)
AR: Aldose reductase	COMMD8: Copper metabolism Murr1 domain-containing 8
ARE: Antioxidant response elements	COX: Cyclooxygenase
ARVO: Association for Research in Vision and Ophthalmology	Cplx1: Complexin 1 (gene)
ATP: Adenosine triphosphate	CTNF: Ciliary neurotrophic factor
B2m: Beta-2 microglobulin (gene)	CuZnSOD: Copper-zinc-superoxide dismutase
BB: Biobreeding	DAG: Diacylglycerol
BBB: Blood-brain barrier	db/+: BKS.Cg-Dock7 ^m + Lepr ^{db} /+
BCA: Bicinchonine acid assay	db/db: BKS.Cg-Dock7 ^m /+Lepr ^{db} J
BP: Biological process	DEGs: Differentially expressed genes
BDNF: Brain derived neurotrophic factor	DHE: Dihydroethidium (5-ethyl-5,6-dihydro-6-phenyl-3,8-diaminophenanthridine, hydroethidine)
BRB: Blood-retinal barrier	Dlg2: discs large MAGUK scaffold protein 2 (gene)
C1ql1: Complement C1q-like 1 (gene)	Dlg4: discs large MAGUK scaffold protein 4 (gene)
C1QL1: Complement C1q-like 1	DM: Diabetes mellitus
cAMP: Cyclic adenosine monophosphate	DME: Diabetic macular oedema
Cask: Calcium/calmodulin-dependent serine protein kinase (gene)	DNA: Deoxyribonucleic acid
CASK: Calcium/calmodulin-dependent serine protein kinase	

DPP-4: Dipeptidyl peptidase-4	<i>Grin2d</i>: Glutamate ionotropic receptor NMDA-type subunit 2D (gene)
DPP-4i: Dipeptidyl peptidase-4 inhibitors	<i>Gsr</i>: Glutathione reductase (gene)
DR: Diabetic retinopathy	GSEA: Gene Set Enrichment Analyses
EMA: European Medicines Agency	GSH: Glutathione
EPAC-1: Exchange factor directly activated by cAMP 1	h: Hour/s
EPO: Erythropoietin	H&E: Hematoxylin/eosin
ERG: Full-field electroretinogram	HRP: Horseradish peroxidase
ETC: Electron transport chain	iBRB: Inner blood-retinal barrier
EUROCONDOR: European Consortium for the Early Treatment of Diabetic	ICAM-1: Intercellular adhesion molecule-1
FDA: Food and Drug Administration	IF: Immunofluorescence assay
GADPH: glyceraldehyde-3-phosphate dehydrogenase	IkBa: Inhibitory protein nuclear factor of kappa light polypeptide gene enhancer in B-cells inhibitor alpha
GCL: Ganglion cell layer	IKK: IkB kinase
GDM: Gestational diabetes mellitus	<i>Il1b</i>: Interleukin-1 beta (gene)
GDNF: Glial cell line derived neurotrophic factor	IL-1β: Interleukin-1 beta
GFAP: Glial fibrillary acidic protein	IL-6: Interleukin-6
GIP: Gastric inhibitory polypeptide	INL: Inner nuclear layer
GLAST: Glutamate aspartate transporter 1	IPL: Inner plexiform layer
GLP-1: Glucagon-like peptide-1	IRBP: Interstitial retinol-binding protein
GLP-1R: Glucagon-like peptide-1 receptor	ISCEV: International Society for Clinical Electrophysiology of Vision
GK: Goto-Kakizaki	<i>Kif1b</i>: Kinesin family member 1B (gene)
GO: Gene Ontology	<i>Kif1bp</i>: Kinesin family member 1B binding protein (gene)
<i>Gpx1</i>: Glutathione peroxidase 1 (gene)	Lepr^{db}: Leptin receptor
GPX: Glutathione peroxidase	MCP-1: Monocyte chemoattractant protein-1
GR: Glutathione reductase	min: Minute/s
<i>Gria1</i>: Glutamate ionotropic receptor AMPA-type subunit 1 (gene)	MnSOD: Manganese superoxide dismutase
<i>Grin1</i>: Glutamate ionotropic receptor NMDA-type subunit 1 (gene)	mRNA: Messenger ribonucleic acid
<i>Grin2b</i>: Glutamate ionotropic receptor NMDA-type subunit 2B (gene)	Munc-13: Mammalian uncoordinated-13 protein
	Munc-18: Mammalian uncoordinated-18 protein

NAD⁺/NADH: Nicotinamide adenine dinucleotide

NADPH: Nicotinamide adenine dinucleotide phosphate

NaF: Sodium fluoride

Na₃VO₄: Sodium orthovanadate

NES: Normalized enrichment score

NF- κ B: Nuclear factor kappa-light-chain-enhancer of activated B cells

NGF: Nerve growth factor

NMDA: N-methyl-D-aspartate

NO: Nitric oxide

NOD: Non-Obese Diabetic mouse

NOS: Nitric oxide synthetase

NOX: Nicotinamide adenine dinucleotide oxidase

NPDR: Non-proliferative diabetic retinopathy

NPY: Neuropeptide Y

Nrf2: Nuclear factor (erythroid-derived 2)-like 2 (gene)

NRF2: Nuclear factor (erythroid-derived 2)-like 2

NSAIDs: Non-steroidal anti-inflammatory drugs

NVU: Neurovascular unit

O₂^{•-}: Superoxide anion

oBRB: Outer blood-retinal barrier

OCT: Optical coherence tomography

OLETF: Otsuka Long-Evans Tokushima fatty

ONL: Outer nuclear layer

OPL: Outer plexiform layer

PBS: Phosphate-buffered saline

PCA: Principal component analysis

PD: Parkinson's disease

PDR: Proliferative diabetic retinopathy

PEDF: Pigment epithelium-derived factor

PKC: Protein kinase C

PMSF: Phenylmethanesulfonylfluoride

PPY: Peptide YY

PRP: Pan-retinal photocoagulation

PSD: Postsynaptic density protein

PVCA: Principal variance component analysis

PVDF: Polyvinylidene difluoride

RAGE: Receptor for advanced glycation end products

RMA: Robust microchip average

RNA: Ribonucleic acid

ROS: Reactive oxygen species

RPD: Reactome Pathway Database

RPE: Retinal pigment epithelium

RT-qPCR: Quantitative reverse transcription polymerase chain reaction

SDF-1: Stromal cell-derived factor-1

SDH: Sorbitol dehydrogenase

SDS: Sodium dodecyl sulfate

SDS-PAGE: Sodium dodecyl sulfate polyacrylamide gel electrophoresis

SDT: Spontaneously diabetic Torii

SEM: Standard error of the mean

Slc17a7: Solute carrier family 17 member 7 (gene)

SNAP: N-ethylmaleimide-sensitive factor attachment protein

Snap25: Synaptosome-associated protein 25 (gene)

SNAP-25: Synaptosome-associated protein 25

SNAREs: N-ethylmaleimide-sensitive factor attachment protein receptors

SOD: Superoxide dismutase

Sod1: Copper-zinc-superoxide dismutase (gene)

Sod2: Manganese superoxide dismutase (gene)

SST: Somatostatin

Stx1a: Syntaxin-1A (gene)

Stxbp2: Syntaxin-binding protein 2 (gene)

Stxbp4: Syntaxin-binding protein 4 (gene)

Stxbp6: Syntaxin-binding protein 6 (gene)

STZ: Streptozotocin

Sv2b: Synaptic vesicle glycoprotein 2B (gene)

SV2B: Synaptic vesicle glycoprotein 2B

Syn1: Synapsin I (gene)

Syp: Synaptophysin (gene)

Syt: Synaptotagmin (gene)

T1DM: Type 1 diabetes

T2DM: Type 2 diabetes

Tnfa: Tumor necrosis factor alpha (gene)

TNF- α : Tumor necrosis factor alpha

TXNIP: Thioredoxin interacting protein

UAT: High Technology Unit

UEB: Statistics and Bioinformatics Unit

Unc13A: Unc-13 homolog A (gene)

Vamp2: Vesicle-associated membrane protein 2 (gene)

VAMP-2: Vesicle-associated membrane protein 2

Vcam1: Vascular cell adhesion protein-1 (gene)

VCAM-1: Vascular cell adhesion protein-1

VEGF: Vascular endothelial growth factor

VGLUT1: Vesicular glutamate transporter 1

VHIR: Vall d'Hebrón Research Institute

ZDF: Zucker diabetic fatty

INDEX

ABSTRACT.....	1
RESUMEN	3
RESUM	5
1. INTRODUCTION	7
1.1. DIABETIC RETINOPATHY.....	9
<i>1.1.1. Concept, epidemiology and risk factors.....</i>	<i>9</i>
<i>1.1.2. Pathophysiology of diabetic retinopathy: from the early impairment of the retinal neurovascular unit to the advanced stages of the disease</i>	<i>11</i>
1.1.2.1. The retina and the neurovascular unit in physiological conditions.....	11
1.1.2.2. Hyperglycemia: the underlying mechanism triggering early neurovascular unit impairment.....	14
1.1.2.2.1. Oxidative stress.....	16
1.1.2.3. The early neurovascular unit impairment	17
1.1.2.3.1. Glial activation and inflammation.....	18
1.1.2.3.2. Neurodegeneration	20
1.1.2.3.3. Early microvascular impairment	21
1.1.2.4. Advanced stages of the disease: diabetic macular oedema and proliferative diabetic retinopathy.....	23
<i>1.1.3. Treatment of early stages of DR: an unmet medical need</i>	<i>24</i>
1.1.3.1. Overview of current treatment of DR.....	24
1.1.3.2. Potential treatments for early stages of DR	27
1.2. GLP-1 AND DPP-4 INHIBITORS: A NOVEL THERAPEUTIC APPROACH FOR EARLY DIABETIC RETINOPATHY.....	29
<i>1.2.1. GLP-1 peptide: an incretin with neuroprotective effects in the central nervous system.....</i>	<i>29</i>
1.2.1.1. The beneficial effects of GLP-1 in the diabetic retina.....	30
<i>1.2.2. DPP-4 inhibitors: an alternative therapeutic approach based on GLP-1R activation</i>	<i>31</i>
1.2.2.1. The beneficial effects of DPP-4 inhibitors in the diabetic retina.....	32
1.3. ANIMAL MODELS FOR THE STUDY OF DIABETIC RETINOPATHY	34
<i>1.3.1. Inducible rodent models.....</i>	<i>35</i>

1.3.2. Genetic rodent models.....	37
1.3.2.1. The db/db mouse model.....	38
2. HYPOTHESIS AND OBJECTIVES.....	41
2.1. HYPOTHESIS	43
2.2. OBJECTIVES.....	43
3. MATERIALS AND METHODS	45
3.1. IN VIVO EXPERIMENTATION.....	47
3.1.1. Mice and housing conditions	47
3.1.2. Interventional studies: topical treatments.....	47
3.1.2.1. Transcriptomic study and evaluation of the potential beneficial properties of sitagliptin	47
3.1.2.2. Dose-effectiveness study with sitagliptin and saxagliptin	48
3.1.3. Full-field electroretinogram	49
3.1.4. Euthanasia and retinal tissue processing	51
3.2. NUCLEIC ACID ANALYSIS: GENOMIC APPROACHES.....	52
3.2.1. RNA extraction and quantification.....	52
3.2.2. Transcriptomic study: microarrays and gene set enrichment analysis.....	52
3.2.3. cDNA reverse transcription and quantitative reverse transcription polymerase chain reaction assay.....	53
3.3. ANALYSES OF PROTEIN LEVELS	56
3.3.1. Protein extraction and quantification	56
3.3.2. Western Blotting assay.....	56
3.3.2.1. Western Blot reproving: harsh stripping.....	57
3.4. HISTOCHEMICAL TECHNIQUES	58
3.4.1. Immunofluorescence staining	58
3.4.1.1. Measurements of glial activation	60
3.4.1.2. Evaluation of the nuclear translocation of NF- κ B.....	61
3.4.2. Hematoxylin-eosin staining.....	61
3.4.2.1. Cell counting of the ganglion cell layer and the inner nuclear layer	61
3.4.2.2. Analysis of retinal thickness	61
3.4.3. Evans Blue assay	62
3.5. STATISTICAL ANALYSIS	63

4. RESULTS.....	65
4.1. STUDY OF THE MECHANISMS UNDERLYING THE BENEFICIAL EFFECTS OF SITAGLIPTIN EYE DROPS DURING EARLY DIABETIC RETINOPATHY IN THE DB/DB MODEL	67
4.1.1. <i>Monitoring of body weight and systemic blood glucose levels.....</i>	67
4.1.2. <i>Transcriptomic study to identify the mechanisms mediating the protective effects of sitagliptin eye drops</i>	68
4.1.2.1. Multiple transcriptome comparison between all groups.....	68
4.1.2.2. Comparison of retinal expression patterns between diabetic animals treated with sitagliptin and vehicle	69
4.1.2.3. Assessment of the biological significance of the obtained results: gene set enrichment analysis	71
4.1.2.4. Evaluation of retinal gene expression of proteins related to synapse formation, maintenance and synaptic transmission	78
4.1.2.5. Examination of presynaptic protein content in the retina	81
4.1.3. <i>Study of the effect of sitagliptin eye drops on oxidative stress and inflammation</i>	84
4.1.3.1. Evaluation of antioxidant defenses	84
4.1.3.2. Assessment of superoxide anion levels and nitro-oxidative damage to biological macromolecules.....	88
4.1.3.3. Examination of the PKC content.....	89
4.1.3.4. Evaluation of the NF- κ B pathway and the pro-inflammatory cytokine production....	90
4.1.3.5. Analysis of the content of VCAM-1	93
4.1.4. <i>Study of neuronal proliferation.....</i>	95
4.1.5. <i>In vivo assessment of retinal functionality.....</i>	96
4.2. MINIMUM EFFECTIVE DOSE STUDY OF SITAGLIPTIN AND SAXAGLIPTIN FOR THE EARLY TREATMENT OF DIABETIC RETINOPATHY	97
4.2.1. <i>Dose-response effect on DPP-4 levels</i>	97
4.2.2. <i>Dose-response effect on glial activation.....</i>	99
4.2.3. <i>Dose-response effect on cell death and retinal thinning.....</i>	100
4.2.4. <i>Dose-response effect on vascular leakage</i>	105
5. DISCUSSION.....	107
5.1. PRESERVATION OF RETINAL NEUROTRANSMISSION: A PRIMARY MECHANISM OF NEUROPROTECTION OF SITAGLIPTIN IN EARLY STAGES OF DIABETIC RETINOPATHY	109
5.2. THE ANTIOXIDANT PROPERTIES OF SITAGLIPTIN	114

5.3. THE ANTI-INFLAMMATORY EFFECTS OF SITAGLIPTIN	116
5.4. THE RELEVANCE OF THE TOPICAL ADMINISTRATION	118
5.5. TRANSLATIONAL IMPLICATIONS: MINIMUM EFFECTIVE DOSE STUDY	119
5.6. LIMITATIONS OF THE STUDY	120
6. CONCLUSIONS	123
7. REFERENCES	127
8. ANNEXES	151
8.1. FUNDINGS	153
8.2. SUPPLEMENTARY DATA	153
8.3. LICENSES	160
8.4. SCIENTIFIC PUBLICATIONS	170

ABSTRACT

Abstract

Diabetic retinopathy (DR) is one of the most frequent complications of diabetes and it is considered the leading cause of blindness among the working age population in the most developed countries. Despite this, treatments are only available for the later stages of the disease when vision is already impaired. Moreover, current treatments are invasive, expensive and associated with undesirable side effects. Therefore treatment of DR and in particular in its early stages is considered an unmet medical need.

In the earliest stages of DR, before vision is impaired, there exist alterations in the retinal neurovascular unit (NVU), a functional coupling formed by neurons, glial cells and blood vessels, which modulates blood flow according to metabolic demands. Our research group found that glucagon-like peptide-1 (GLP-1) is locally synthesized by the retina and that a decreased production exist in diabetic patients. This is important because GLP-1 is a neuroprotective agent with vasculotropic actions. In this regard, we also found that topical administration of GLP-1 or GLP-1 receptor agonists were effective in the treatment of early stages of DR in experimental models. Another therapeutic approach related to GLP-1 receptor activation consists in administering topically inhibitors of the enzyme dipeptidyl peptidase-4 (DPP-4i), which degrades endogenous GLP-1. This enzyme degrades other substrates that have been linked to beneficial effects, which may be synergistic with the increase in GLP-1. For this reason, the greater stability and lower price, when compared to GLP-1 and GLP-1 receptor agonists, we hypothesized that topical administration of DPP-4i has great potential for treating early DR. First studies evidenced that these drugs can prevent the main pathophysiological processes of early DR (neuronal death, glial activation and vascular leakage), however more preclinical evidence is needed to reach clinical phases.

In the present thesis, and in order to shed light on the mechanisms of action behind these beneficial effects, a transcriptomic study was conducted between diabetic mice topically treated with vehicle or sitagliptin (a DPP-4i) and non-diabetic animals. The study revealed that the main mechanism of action of sitagliptin is neuromodulatory in nature, preserving key proteins in synaptic transmission at the pre- and postsynaptic level. These proteins are down-regulated in DR. Furthermore, sitagliptin also exhibits antioxidant and anti-inflammatory effects. Topical

ABSTRACT

administration of sitagliptin preserved the physiological balance between reactive oxygen species and antioxidant defenses, thus preventing oxidative damage to DNA and proteins. In addition, sitagliptin reduced the activation of inflammatory pathways in the retina and decreased the production of pro-inflammatory cytokines. These effects were accompanied by a functional improvement of the retina and a recovery of physiological neuronal proliferation rates. Furthermore, the minimum effective doses for sitagliptin and saxagliptin, another DPP-4i, were established. These findings could pave the way for clinical trials to test this new approach in the treatment of early stages of DR or even other retinal diseases.

Resumen

La retinopatía diabética (RD) es una de las complicaciones más frecuentes de la diabetes y es considerada la causa principal de ceguera entre la población laboralmente activa de los países más desarrollados. Pese a ello, los tratamientos disponibles están enfocados a los estadios más tardíos de la enfermedad, cuando la visión ya está afectada. Además, dichos tratamientos son invasivos, costosos y están asociados con graves efectos secundarios. Por lo tanto, el tratamiento de la RD y en particular sus etapas más tempranas está considerado como una necesidad médica no cubierta.

En las fases más tempranas de la RD, antes de que se dañe la visión, existen alteraciones en la unidad neurovascular de la retina (UNV), un acoplamiento funcional formado por neuronas, células gliales y vasos sanguíneos, que modula el flujo sanguíneo en función de las demandas metabólicas. Nuestro grupo de investigación descubrió que el péptido-1 similar al glucagón (GLP-1) es sintetizado localmente por la retina y que existe una menor producción en los pacientes diabéticos. Esto es importante porque el GLP-1 es un agente neuroprotector con acciones vasculotrópicas. En relación a este aspecto, también hemos observado que la administración tópica de GLP-1 o de agonistas del receptor de GLP-1 resulta eficaz en el tratamiento de las fases iniciales de la RD en modelos experimentales. Otro enfoque terapéutico relacionado con la activación del receptor de GLP-1 consiste en administrar por vía tópica inhibidores de la enzima dipeptidil peptidasa-4 (DPP-4i), encargada de degradar el GLP-1 endógeno. Esta enzima también degrada otros sustratos que han sido relacionados con efectos beneficiosos, los cuales pueden ser sinérgicos con el aumento de GLP-1. Por este motivo, la mayor estabilidad y el menor precio, en comparación con el GLP-1 y los agonistas del receptor del GLP-1, planteamos la hipótesis de que la administración tópica de DPP-4i podría tener un gran potencial para tratar la RD temprana. Los primeros estudios evidenciaron que estos fármacos pueden prevenir los principales procesos fisiopatológicos de la RD temprana (muerte neuronal, activación glial y fuga vascular), sin embargo son necesarias más evidencias preclínicas para llegar a fases clínicas.

En la presente tesis, y con el fin de arrojar luz sobre los mecanismos de acción que subyacen a estos efectos beneficiosos, se llevó a cabo un estudio transcriptómico entre ratones diabéticos

RESUMEN

tratados tópicamente con placebo o sitagliptina (un DPP-4i) y animales no diabéticos. El estudio reveló que el principal mecanismo de acción de la sitagliptina es de naturaleza neuromoduladora, preservando proteínas clave en la transmisión sináptica a nivel pre y postsináptico. Estas proteínas están reguladas a la baja en la RD. Además, la sitagliptina también presenta efectos antioxidantes y antiinflamatorios. La administración tópica de sitagliptina preservó el equilibrio fisiológico entre las especies reactivas del oxígeno y las defensas antioxidantes, previniendo así el daño oxidativo del ADN y las proteínas. Asimismo, la sitagliptina redujo la activación de vías inflamatorias en la retina y disminuyó la producción de citoquinas proinflamatorias. Todos estos efectos se acompañaron de una mejora funcional de la retina y una recuperación de las tasas fisiológicas de proliferación neuronal. Además, se establecieron las dosis mínimas eficaces de sitagliptina y saxagliptina, otro DPP-4i. Estos hallazgos podrían allanar el camino a ensayos clínicos para probar este nuevo enfoque en el tratamiento de las primeras fases de la RD o incluso de otras enfermedades de la retina.

Resum

La retinopatia diabètica (RD) és una dels complicacions més freqüents de la diabetis i és considerada la causa principal de ceguesa entre la població laboralment activa als països més desenvolupats. Malgrat això, els tractaments disponibles estan enfocats als estadis més tardans de la malaltia, quan la visió ja està afectada. A més, aquests tractaments són invasius, costosos i estan associats amb greus efectes secundaris. Per tant, el tractament de la RD en particular les seves etapes més primerenques és considerat com una necessitat mèdica no coberta.

En les fases més primerenques de la RD, abans que es danyi la visió, existeixen alteracions en la unitat neurovascular de la retina (UNV), un acoblament funcional format per neurones, cèl·lules glials i vasos sanguinis, que modula el flux sanguini en funció de les demandes metabòliques. El nostre grup de recerca va descobrir que el pèptid-1 similar al glucagó (GLP-1) és sintetitzat localment per la retina i que existeix una menor producció en els pacients diabètics. Això és important perquè el GLP-1 és un agent neuroprotector amb accions vasculotrópiques. En relació a aquest aspecte, també hem observat que l'administració tòpica de GLP-1 o d'agonistes del receptor del GLP-1 resulta eficaç en el tractament de les fases inicials de la RD en models experimentals. Un altre enfocament terapèutic relacionat amb l'activació del receptor de GLP-1 consisteix a administrar per via tòpica inhibidors de l'enzim dipeptidil peptidasa-4 (DPP-4i), el qual és l'encarregat de degradar el GLP-1 endogen. Aquest enzim també degrada altres substrats que han estat relacionats amb efectes beneficiosos, els quals poden fer sinergia amb l'augment de GLP-1. Per aquest motiu, la major estabilitat i el menor preu, en comparació amb el GLP-1 i els agonistes del receptor del GLP-1, plantegem la hipòtesi que l'administració tòpica de DPP-4i podria tenir un gran potencial per a tractar l'RD primerenca. Els primers estudis van evidenciar que aquests fàrmacs poden prevenir els principals processos fisiopatològics de la RD primerenca (mort neuronal, activació glial i fuita vascular), no obstant això són necessàries més evidències a nivell preclínic per a arribar a fases clíniques.

En la present tesi, i amb la finalitat d'esclarir els mecanismes d'acció que estan darrere d'aquests efectes beneficiosos, es va dur a terme un estudi transcriptòmic entre ratolins diabètics tractats tòpicament amb vehicle o sitagliptina (un DPP-4i) i animals no diabètics. L'estudi va revelar

que el principal mecanisme d'acció de la sitagliptina és de naturalesa neuromoduladora, preservant proteïnes clau en la transmissió sinàptica a nivell pre i postsinàptic. Aquestes proteïnes estan regulades a la baixa en la RD. A més, la sitagliptina també presenta efectes antioxidants i antiinflamatoris. L'administració tòpica de sitagliptina va preservar l'equilibri fisiològic entre les espècies reactives de l'oxigen i les defenses antioxidants, prevenint així el mal oxidatiu de l'ADN i les proteïnes. Així mateix, la sitagliptina va reduir l'activació de vies inflamatòries en la retina i va disminuir la producció de citocines proinflamatòries. Tots aquests efectes es van acompanyar d'una millora funcional de la retina i una recuperació de les taxes fisiològiques de proliferació neuronal. A més, es van establir les dosis mínimes eficaces de sitagliptina i saxagliptina, un altre DPP-4i. Aquestes troballes podrien aplanar el camí a assajos clínics per a provar aquest nou enfocament en el tractament de les primeres fases de la RD o fins i tot d'altres malalties de la retina.

INTRODUCTION

1.1. Diabetic retinopathy

1.1.1. Concept, epidemiology and risk factors

Diabetes mellitus (DM) is a group of chronic metabolic disorders characterized by abnormal and sustained high blood glucose levels caused by an absolute or relative insulin deficiency¹. DM is generally classified in three main categories, type 1 diabetes (T1DM), type 2 diabetes (T2DM) and gestational diabetes (GDM), being T2DM the predominant form (90-95%). T1DM results from autoimmune destruction of β -cells, typically leading to absolute insulin deficiency, whereas T2DM presents a progressive loss of insulin secretion, usually in the context of insulin resistance. GDM refers to the hyperglycemic state that appears during pregnancy in women without pre-existing diabetes. There exist also other forms of DM such as monogenic diabetes syndromes, chemical-induced diabetes or those derived from pancreatic diseases². In 2021, 536.6 million people worldwide aged between 20-79 years old suffered from one of these forms of the disease and its disabling complications, which are responsible for most of the societal and economic burden associated with DM. The prevalence of DM is expected to increase to 783.2 million by 2045 with the consequent high healthcare expenditures that DM and its complications entail³.

Diabetic retinopathy (DR) is one of the most common and feared complications of diabetes and the leading cause of preventable blindness among the working-age population in high-income countries^{4,5}. DR was classically defined as a microvascular disease, however the latest findings confirming the strong neurodegenerative component of this disease led the American Diabetes Association (ADA) to redefine it as a highly tissue-specific neurovascular complication, in which the interdependence between the multiple cell types of the retina is progressively compromised^{6,7}.

According to the severity and type of retinal lesions, we can classify the disease into four different stages. The first of these is mild non-proliferative DR (NPDR), which in the absence of treatment progresses to moderate and severe NPDR before the onset of advanced stages of DR which comprise proliferative DR (PDR) and diabetic macular oedema (DME). PDR is characterized by abnormal formation of new blood vessels⁶. In parallel and at any stage of the disease, the retinal vasculature gradually becomes hyperpermeable and the intraretinal fluid accumulates giving rise to the appearance of exudates and oedemas. The process in which the accumulation occurs in the macula, the central focal point of the retina, is known as DME and

INTRODUCTION

is currently the most common cause of vision loss among diabetic patients⁸. An schematic overview of the different stages of DR and the key players in the development of DME and PDR is displayed in **Figure 1**.

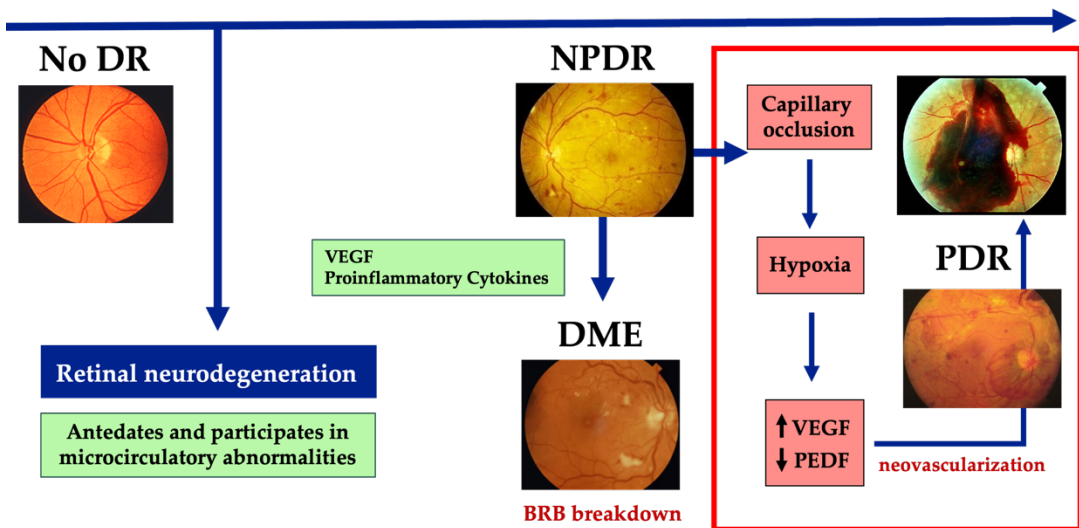


Figure 1. Schematic summary of the different stages of DR and the main players in DME and PDR development. Adapted from Simó & Hernández⁹. BRB (Blood-retinal barrier). VEGF (Vascular endothelial growth factor); PEDF (Pigment epithelium-derived factor).

DR affects approximately one-third of diabetic patients, of whom one-tenth will develop moderate or severe states of vision loss (PDR and/or severe DME)¹⁰. The probability of suffering any type of DR and PDR is significantly higher in type 1 diabetic patients when compared to type 2 (77.3 vs. 25.2 % for any DR, 32.4 vs. 3.0 % for PDR)^{11,12}.

The principal risk factors of DR are the duration of diabetes, hypertension and poor glycemic control^{7,13}. Nevertheless, the appearance of DR cannot only be associated to hypertension and hyperglycemia, since some studies have demonstrated that a significant proportion of diabetic patients with poor glycemic control and/or blood pressure control do not present DR¹⁴. In addition, and in contrast to them, other subjects with adequate monitoring and management of those parameters not only develop DR, but even progress to severe stages¹⁵. Therefore, other risk factors may play a relevant role. Low physical activity, caloric food intakes, obesity, vitamin D deficiency, puberty, pregnancy, dyslipidemia, diabetic nephropathy, endothelial dysfunction, cataract surgery, excessive sunlight exposure and genetic factors have been strongly associated to the onset of DR and its progression^{13,16–23}.

1.1.2. Pathophysiology of diabetic retinopathy: from the early impairment of the retinal neurovascular unit to the advanced stages of the disease

1.1.2.1. The retina and the neurovascular unit in physiological conditions

The concept of "neurovascular unit" (NVU) was first introduced to define the interdependent functional coupling that neurons, glial cells and the highly specialized vasculature of the central nervous system (CNS) form. The NVU regulates hyperemia in the brain, a homeostatic mechanism that regulates microvascular blood flow through vasodilatory or vasoconstrictive responses, which adapt to the neuronal demand for oxygen and nutrients based on metabolic activity²⁴. The retina is the innermost layer of the eye and is considered a full-fledged extension of the CNS due its embryological origin (it is formed from the diencephalon). For this reason, share similar properties with the brain and the spinal cord in terms of anatomy, functionality, immunology and response to stressful stimuli. In addition, multiple major neurodegenerative disorders present concomitant manifestations in the retina²⁵. Because of all these similarities, the NVU concept can be equally applied to the retina.

The retinal NVU is composed by neurons (photoreceptors, bipolar cells, horizontal cells, amacrine cells and ganglion cells), glial cells (Müller cells and astrocytes), professional immune cells (microglia and perivascular macrophages) and vascular cells (pericytes and endothelial cells)^{26,27} (**Figure 2**).

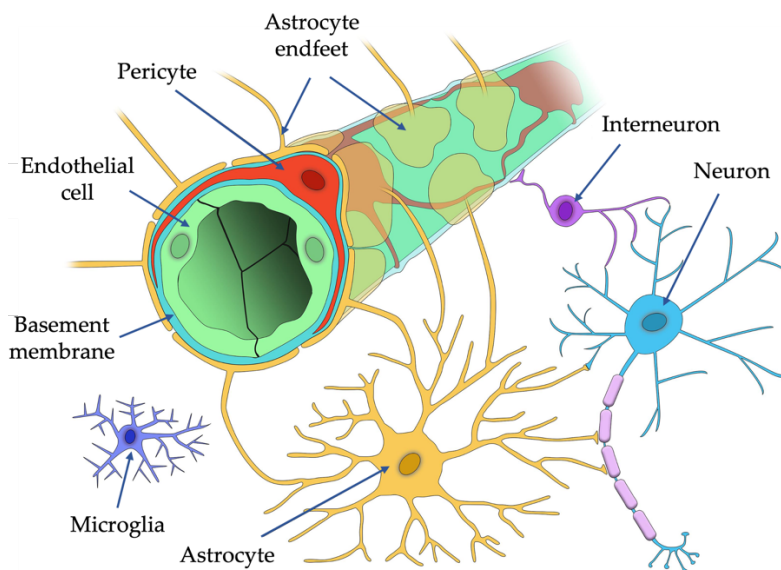


Figure 2. The cellular components of the retinal NVU. Adapted from Brown *et al*²⁸.

INTRODUCTION

The retinal neurons form a complex circuitry that allows the conversion of light energy from photons to three-dimensional images (phototransduction). Briefly, the outer segment of photoreceptors (cones and rods), which are a specialized group of neuroepithelial cells, capture light and convert into electrical signals that will reach the brain through the optic nerve, which is composed of retinal ganglion cell axons²⁹. Bipolar cells are responsible for transmitting information from photoreceptors to ganglion cells, either directly or indirectly through lateral interactions with amacrine and/or horizontal cells. Horizontal cells modulate the information flow from photoreceptors to bipolar cells while amacrine cells regulate the synapses between bipolar cells and ganglions cells^{30,31}. The cell bodies and processes of these neurons are stratified in five alternating layers that conform the neural retina. Photoreceptor somas conform the outer nuclear layer (ONL), cell bodies of bipolar cells are located in the inner nuclear layer (INL) and ganglion cell somas are situated in the ganglion cell layer (GCL). Synaptic contacts occur in the outer plexiform layer (OPL) and inner plexiform layer (IPL), where horizontal and amacrine cells operate respectively³⁰ (**Figure 3**).

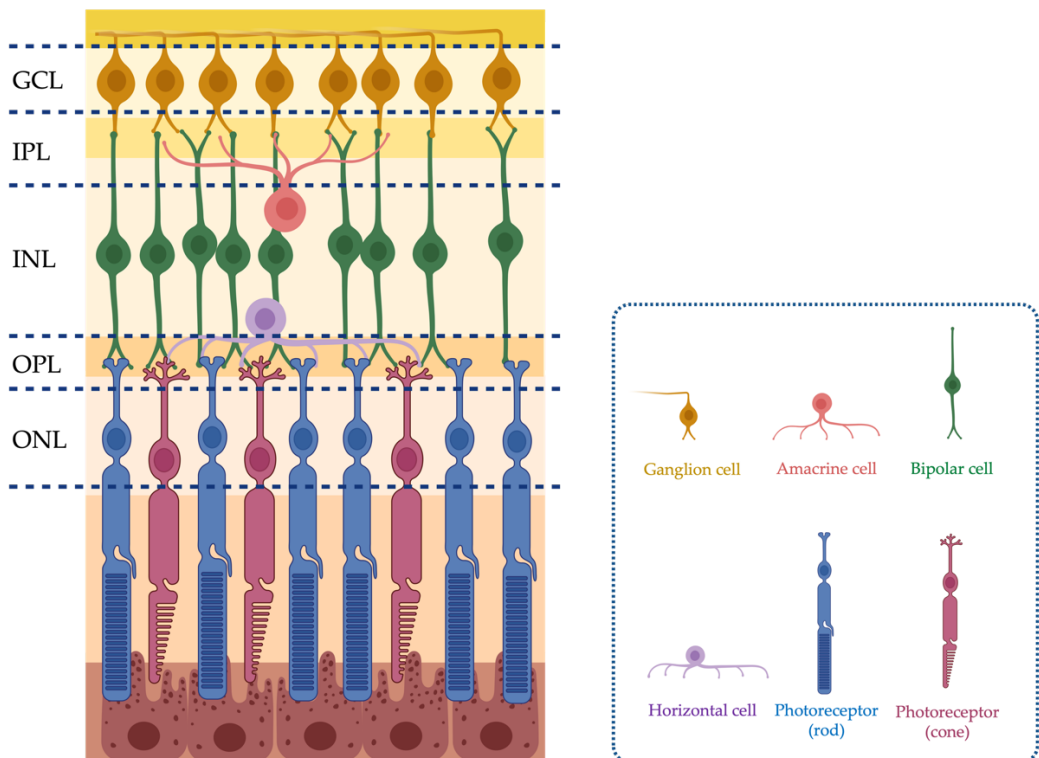


Figure 3. The structure of the retina and its main neuronal cell types. GCL (ganglion cell layer), IPL (inner plexiform layer), INL (inner nuclear layer), OPL (outer plexiform layer), ONL (outer nuclear layer).

As a result of phototransduction, the retina is one of the most metabolically active tissues in the body, with high oxygen consumption. The proper functioning of the retinal microvasculature, composed by endothelial cells and pericytes, is crucial to control retinal blood flow³². These two cell types are present in the retina in a ratio 1:1 and interact through gap-junctions, tight junctions, adhesion plaques, peg-and-socket connections and paracrine factors, such as secreted cytokines, growth factors or extracellular exosomes^{32,33}. These interactions are necessary not only to regulate blood flow but also are critical for the constitution of the inner blood-retinal barrier (iBRB). The iBRB and the outer blood-retinal barrier (oBRB) conform the blood retinal barrier (BRB), a highly-selective barrier that regulates the passage of ions, water, solutes and cells into and out the retina. The oBRB is formed by the retinal pigment epithelium (RPE) and controls the transport between the capillary lamina of choroid and the retina, while iBRB regulates transport across the retinal vascular bed to the delicate neural tissue³⁴.

Glial cells have been postulated to be the intermediaries between neurons and blood vessels in the control of the NVU, due to their capacity to release vasoactive factors in response to neuronal metabolic activity^{35,36}. Glial cells are able to sense synaptic activity through their P2Y purinergic receptors, which are stimulated through the neuronal release of adenosine triphosphate (ATP) in response to light stimuli³⁷. The intracellular concentration of ion Ca^{2+} in glial cells is consequently increased, influencing nitric oxide (NO) production since nitric oxide synthase (NOS) is sensitive to this ion. NO concentration acts as a modulator of the vasoconstrictive and vasodilatory responses through regulating the release of vasoactive factors and their downstream activities³⁵. In the retina, the main glial cell type are Müller cells, whose soma is located in the INL and which exhibit at least five apico-basal domains that extend from the apical stem around the photoreceptors to the basal end at the inner limiting membrane (the structural boundary between the vitreous and the retina). However, they are not only highly organized apico-basally, but also laterally to interact with almost all the retinal cells³⁸. Müller cells surround blood vessels and contact neurons, with their main functions being the regulation of retinal hyperemia, maintenance of extracellular pH, neurotransmitter recycling, metabolite transport and stabilization of tight junctions. Therefore, they can be considered a crucial structural and metabolic support for neurons and blood vessels. On the other hand, astrocytes encircle neuronal axons and major blood vessels to form an irregular network that supports the integrity of the iBRB³⁹. They play a major role in the proper development and functioning of the vascular system in the retina. Both Müller cells and astrocytes promote neuronal survival by providing neurotrophic factors, antioxidant support, clearing neurotransmitters and regulating synapse formation and removal⁴⁰.

Microglial cells, as highly specialized phagocytic cells, monitor constantly the local synaptic activity and contribute to the clearance of dying cells and metabolic debris. Under physiological conditions and during acute inflammation, microglia produce neurotrophic factors and anti-inflammatory cytokines that are necessary for retinal health³⁹.

In conclusion, retinal homeostasis requires the correct functioning of all retinal cell types, which act as an interdependent unit that modulates local blood flow to satisfy neuronal metabolic demands. Due to this interdependency, any minor alteration in one of the elements will, in the short or long term, cause damage to the rest of the components of the NVU, which can seriously compromise vision. A clear example of this is DR, where the diabetic milieu lead to early impairment of the NVU, even before any microvascular retinal lesions can be clinically apparent⁴¹.

1.1.2.2. Hyperglycemia: the underlying mechanism triggering early neurovascular unit impairment

DR pathogenesis is regulated by multiple factors and integrates several signaling pathways and cellular processes. Nevertheless, disrupted glucose homeostasis, which is essential for retinal cells, plays one of the most critical roles in the initial development of DR. This dysregulation occurs in many retinal cell types and it has been related to both neural and microvascular components of the disease. Glucose homeostasis is finely modulated by the coordinated interaction between glycolysis, Krebs cycle and oxidative phosphorylation, where glycolysis is the most accessible source ATP because it does not require neither oxygen nor compartmentalization by internal membranes⁴². Diabetic condition leads to an abnormal increase in glycolytic flux producing large amounts of intermediate metabolites that can trigger different damaging pathways in the retina, including hexosamine pathway, polyol pathway, diacylglycerol-dependent activation of the protein kinase C (PKC) pathway and advanced glycation end products (AGEs) pathway⁴³.

- **PKC pathway**: the high intracellular glucose concentration leads to the accumulation of on upper glycolytic intermediate named glyceraldehyde 3-phosphate, which further enhances the synthesis of diacylglycerol (DAG). DAG activates multiple isoforms of PKC in the interior of the cell. The activation of PKC- α , - β , - δ , and - ϵ isoforms has been associated to the pathogenesis of DR at different levels⁴⁴. They contribute to initial imbalance between the pro-oxidant and antioxidant species of different retinal cell types, inflammation, pericyte loss and vascular dysfunction^{42,44}.

- Hexosamine pathway: The increased glycolytic influx causes the accumulation of fructose-6-phosphate, another intermediate of glycolysis. Under euglycemic conditions, only a small fraction of fructose-6-phosphate is metabolized through the hexosamine pathway, whereas hyperglycemia impedes its full drainage by glycolysis and leads to an excessive stimulation of this pathway. In the hexosamine pathway, fructose-6-phosphate is metabolized to uridine-5-diphosphate-N-acetylglucosamine⁴⁵. This metabolite is a precursor for all other amino sugars necessary for the biosynthesis of glycoproteins, glycolipids, proteoglycans, and glycosaminoglycans. The overstimulation of hexosamine pathway results in excess of protein glycosylation, which alters normal gene expression and functioning of the retina, especially in neurovascular cells⁴². In the context of DR, high glucosamine levels have been related to the overproduction of reactive oxygen species (ROS), mitochondrial dysfunction, inflammation and vascular dysfunction⁴².

- Polyol pathway: Under high glucose concentrations, the enzyme aldose reductase (AR) oxidizes the nicotinamide adenine dinucleotide (NAD⁺/NADH) phosphate (NADPH) to NADP⁺ and reduces glucose to sorbitol, which is then metabolized by sorbitol dehydrogenase (SDH) to fructose, using NAD⁺ as cofactor. AR has a lower affinity for glucose compared to hexokinase, an enzyme that allows cells to obtain energy from glucose. Therefore, sorbitol levels under euglycemic conditions are minimal. Nevertheless, hyperglycemia saturates hexokinase and the excess of glucose enters in the polyol pathway increasing sorbitol levels and reducing NADPH availability⁴⁶. On one hand, sorbitol is a hydrophilic alcohol that does not diffuses properly across cell membranes and accumulates intracellularly causing osmotic stress⁴⁷. On the other hand, as NADPH is necessary for the reduction of the antioxidant glutathione (GSH), its decrease exacerbates oxidative stress. In addition, excessive oxidation of sorbitol by SDH promotes a higher NADH/NAD⁺ ratio that inhibits glyceraldehyde-3-phosphate dehydrogenase (GADPH) activity and increases triose phosphate concentration. High levels of triose phosphate could generate DAG (PKC activator) and methylglyoxal, which is precursor of AGEs formation⁴⁸. Excess of NADH can also be used by NADH oxidase, an enzyme that contributes to intracellular ROS generation⁴³. The fructose resulting from the polyol pathway also contributes to AGEs formation due it can be phosphorylated to fructose-3-phosphate and consequently broken down to 3-deoxyglucosone, two powerful glycosylating agents. In humans, retinal ganglion cells, Müller cells, endothelial cells and pericytes are provided with AR, making them the most exposed cells to polyol pathway during DR⁴⁷.

- AGEs pathway: Chronic hyperglycemia triggers a non-enzymatic reaction between carbonyl groups of reducing sugars, such as glucose, fructose or galactose, and free amino groups of

amino acids, proteins and peptides. During this reaction, known as Maillard reaction, Schiff bases are generated after reducing sugars react with the amino group of biological amines. Schiff bases are unstable and are converted into relatively more stable molecules, the Amadori products (ketoamines). Schiff bases are also especially prone to be oxidized and to generate ROS. From this moment on, reactions become not reversible⁴⁹. During the intermediate stage, Amadori products are metabolized to different reactive dicarbonyl compounds such as methylglyoxal, glyoxal or deoxyglucosone. Finally, these products, after complex chemical rearrangements, such as oxidations or dehydrations, and cross-linkings with macromolecules, become irreversible and stable AGEs^{43,50}. The best-characterized AGEs receptor is RAGE (receptor for AGEs), through which these compounds exert their detrimental effects. RAGE is expressed in almost all retinal cell types, especially in Müller cells. In the diabetic retina, the AGEs-RAGE axis predominantly affects to Müller cells, microglia, endothelial cells, pericytes and RPE. Apart from their capacity of generating ROS during its production, AGEs damage Müller cells through RAGE, which is overexpressed in this cell type during DR. The AGEs-RAGE axis activates the production of vascular endothelial growth factor (VEGF), promotes inflammation and it has been associated with the formation of glial fibrillary acidic protein (GFAP)⁵¹.

1.1.2.2.1. Oxidative stress

Oxidative stress reflects an imbalance between ROS production and the antioxidant defense mechanisms of a biological system⁵². This imbalance is very detrimental to the retina, an organ particularly sensitive to oxidative conditions due to the high presence of fatty acids in the photoreceptors⁵³. High-metabolic rate, high-oxygen consumption and exposure to light also contribute to the increased susceptibility of the retina to ROS⁵⁴.

In DR, hyperglycemia not only alters the balance of pro-oxidant agents through the activation of abnormal pathways associated with glutamate metabolism, but it also has a direct effect on it. Elevated glucose levels disrupt the electron flow of the electron transport chain (ETC) leading to higher electron leak, higher production of superoxide anion ($O_2^{\bullet-}$) and mutations in the mitochondrial deoxyribonucleic acid (DNA) resulting in impaired ETC complexes that further increase ROS generation, even if glucose levels are restored (epigenetic modifications)⁵⁵. It has also been reported that high glucose levels increase the activity of several enzymes linked to physiological ROS production in the diabetic retina, such as NADPH oxidase (NOX) family, cyclooxygenases (COX), lipoxygenases and xanthine oxidase^{56–59}. Furthermore, although the retinal NVU possesses robust antioxidant mechanisms, chronic hyperglycemia diminishes

their effectiveness and activity, exacerbating the oxidative imbalance. These antioxidant mechanisms include both non-enzymatic and enzymatic antioxidants that counteract ROS, as well as various repair systems that address oxidized molecules⁴³. Low levels and impaired activities of crucial antioxidant enzymes such as superoxide dismutase copper-zinc superoxide dismutase (CuZnSOD), manganese superoxide dismutase (MnSOD), catalase (CAT), glutathione peroxidase (GPX) or glutathione reductase (GR) have been associated with DR^{43,60}. This anomaly can be explained in part by the disruption of the signaling pathway of the nuclear factor- erythroid 2-related factor 2 (NRF2), which is a redox sensitive transcription factor that promotes the expression of genes that encode antioxidant enzymes through its binding to the antioxidant response elements (ARE)⁶¹. It has been reported that elevated glucose concentrations have the potential to induce oxidative stress by inhibiting the expression of the NRF2 gene, particularly in Müller retinal cells⁶².

Finally, the accumulation of these harmful species enables their interaction with macromolecules [ribonucleic acid (RNA)/DNA, proteins and lipids] leading to oxidative damage and disrupting cellular homeostasis of the different components of the retinal NVU.

1.1.2.3. The early neurovascular unit impairment

All the molecular alterations above mentioned ultimately affect the balance and functioning of the four major cell populations of the retinal NVU, namely neurons, vascular cells, glial cells and immune cells, leading to processes of neurodegeneration, early vascular damage, glial activation and inflammation respectively (**Figure 4**).

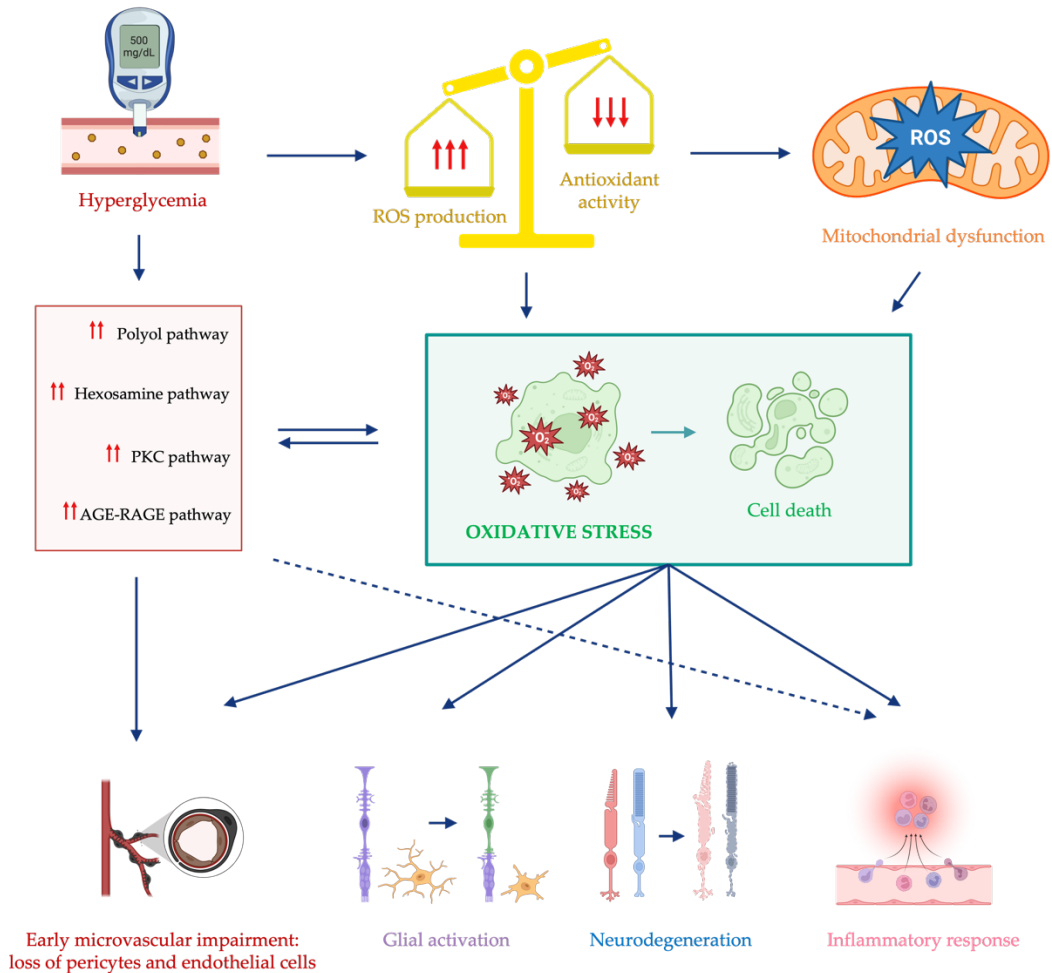


Figure 4. Schematic summary of the main mechanisms underlying the neurovascular impairment that occurs during early DR.

The complex interactions between the different cell types results in an interconnectedness impairment between all these processes, which lead to detrimental consequences. In the context of DR, the exact sequence of these events remains uncertain, and it seems that individual variability plays a significant role in determining the order of occurrence⁶³. Nevertheless, further research is needed to fully understand this circuitry and to precise the chronological order of these pathogenic events during early NVU impairment.

1.1.2.3.1. Glial activation and inflammation

Damage to Müller cells plays a pivotal role among early retinal cellular alterations. These cells, which constitute 90% of retinal glia and are distributed throughout the retina, serve

as crucial regulators of both normal and pathological interactions between neurons and vascular cells⁶⁴. Furthermore, Müller cells provide essential nutritional support to the retina due to their higher rate of glycolysis⁶⁵. Under conditions of chronic hyperglycemia, Müller cells undergo reactive gliosis at an early stage, which can be identified by the abnormal expression of GFAP. Gliosis involves biochemical, physiological, and morphological changes that lead to the upregulation of VEGF and activation of innate immune pathways, resulting in increased production of proinflammatory cytokines. These changes contribute to the disruption of the BRB, as Müller cell-derived VEGF induces the loss of tight junction proteins (occludin and zonula occludens-1) in endothelial cells, compromising the integrity of the BRB^{66,67}. Additionally, VEGF activates nuclear factor kappa-light-chain-enhancer of activated B cells (NF- κ B) and promotes a new excessive release of multiple pro-inflammatory cytokines, including intercellular adhesion molecule-1 (ICAM-1) and tumor necrosis factor- α (TNF- α)^{64,68}. Elevated levels of glucose also disrupt the homeostasis of retinal astrocytes, which regulate ion homeostasis, neuronal signaling and the proper functionality of endothelial cells to preserve in the iBRB⁶⁵. This alteration leads to an increased production of ROS and inflammatory cytokines, primarily TNF- α and interleukin-1 beta (IL-1 β). As a result, the proliferative, migratory, and adhesive abilities of astrocytes are impaired⁶⁹. The overall consequence is the exacerbation of a neuroinflammatory environment by macroglia, which contributes to neurodegeneration and abnormalities in microvasculature.

Apart from macroglia, the microglia is also activated in the diabetic retina during early stages of DR. Microglial cells serve as the primary resident sentinel immune cells located within the inner regions of the retina. Microglial cells have the capability to migrate to the subretinal space and release cytokines, thus helping to bring about neuronal cell death⁷⁰. Its activation has been postulated as an early event that could be triggered by the AGEs pathway and that can be detected even before the activation of macroglial cells^{70,71}. Microglial activation involves a phenotype change from a ramified structure to an amoeboid shape, giving rise to two opposing roles depending on the polarization of the resident retinal immune cells triggering pro-inflammatory (M1) or anti-inflammatory (M2) actions^{66,68,70}. In the pro-inflammatory M1 state, activated microglia release pro-inflammatory cytokines, chemokines and ROS, thus promoting inflammation and contributing to tissue damage. By contrast, in the anti-inflammatory M2 state, activated microglia release anti-inflammatory cytokines and growth factors, participating in tissue repair, promoting neuroprotection and suppressing the inflammatory response⁷⁰. In early stages of DR, the M2 response occurs concurrently with the M1 response ameliorating inflammation and delaying the progression of the disease. However, as DR progresses, the M1 response is sustained while the M2 response diminishes. This leads to chronic activation of

classical pro-inflammatory signaling pathways. Notably, the activation of these pathways, such as NF- κ B and extracellular signal-regulated kinase, triggers the release of various pro-inflammatory cytokines [particularly TNF- α , IL-1 β , and interleukin-6 (IL-6)], chemokines, caspases, and glutamate⁷². These molecular mediators contribute to the activation of macroglial cells, BRB breakdown, NVU impairment, and ultimately neuronal cell death^{73,74}.

Therefore, DR is considered a chronic low-grade inflammatory condition in which a multitude of inflammatory mediators and adhesion molecules are implicated⁷⁵. This condition is closely intertwined with all the characteristic features of DR by playing a crucial role in the progression of neurodegeneration and the development of vascular abnormalities in the diabetic retina.

1.1.2.3.2. Neurodegeneration

Retinal neurodegeneration is primarily characterized by neural apoptosis and glial activation. The first neuronal cells in the retina in which apoptotic processes can be detected are ganglion cells and amacrine cells³⁶. However, photoreceptors also present high apoptotic rates⁷⁶. Cell death mediated by apoptosis reduces the thickness of inner retinal layers and the nerve fiber layer, a morphological change that can be detected through optical coherence tomography (OCT). Neuronal death also causes functional impairment in the processing of visual stimuli, which can be detected by full-field electroretinogram (ERG)⁷⁷. The main mechanisms behind the early neurodegenerative process of the retina are oxidative stress, neuroinflammation (both detailed previously), glutamate-mediated excitotoxicity, downregulation of neuroprotective factors production, and disruptions in axonal transport and neurotransmission processes^{78–80}.

Glutamate is the predominant neurotransmitter in the retinal visual pathway playing a major role in signaling transmission. Once released from the presynaptic neuron, glutamate reaches the postsynaptic neurons where, through activation of its receptors, it enables membrane depolarization. However, abnormally high levels cause excitotoxicity and cell death mediated by overstimulation of the receptors. Hence, efficient removal of glutamate from the extracellular space is critical for maintenance of retinal function. Glutamate is metabolized in the retina by Müller cells uptake, primarily through the major glutamate transporter GLAST (glutamate aspartate transporter 1), and subsequent conversion to glutamine by glutamine synthetase. Effective coordination between glutamate uptake and degradation is crucial for a functional glutamate-glutamine cycle⁷⁸. In experimental DR, decreases in the transcript levels of genes related to glutamate neurotransmission and transport have been reported, including

the gene encoding GLAST protein in Müller cells^{81,82}. Retinal ganglion cells are particularly susceptible to glutamate excitotoxicity⁸³.

In retinal synaptic transmission, not only the metabolism of the main neurotransmitter is altered, but also the machinery necessary for its release and processing at the pre- and post-synaptic level.

In this regard, there is evidence that diabetes reduces the retinal content of several presynaptic proteins such as synaptophysin, synapsin I or syntaxin 1A, which are critical to the exocytosis of neurotransmitters and synaptic maintenance in murine models^{79,84}. Studies on postmortem human retinas have shown that the protein content of presynaptic components is reduced in individuals with diabetes compared to non-diabetic donors⁸⁵. These changes in synaptic protein content could be attributed to alterations in the retrograde axonal transport, whose impairment has been reported in retinal ganglion cells from diabetic rat⁸⁰.

The retina of diabetic patients also presents an imbalance in the production of neuroprotective factors. Factors such as pigment epithelium-derived factor (PEDF), somatostatin (SST), interstitial retinol-binding protein (IRBP) and glucagon-like peptide-1 (GLP-1) are produced at lower levels, compromising their protective effects against neurodegeneration^{27,36,86,87}. PEDF, synthesized by the RPE, plays a crucial role in retinal homeostasis by preventing oxidative stress and glutamate excitotoxicity⁸⁸. SST, also mainly produced by the RPE, has antiangiogenic and neuroprotective properties⁸⁹. IRBP, synthesized by photoreceptors, is essential for their survival and maintenance^{90,91}. Additionally, neurotrophic factors like VEGF and erythropoietin (EPO) are overexpressed in the diabetic retina, potentially counteracting the reduction of neuroprotective factors. Other factors such as insulin, brain-derived neurotrophic factor (BDNF), glial cell line derived neurotrophic factor (GDNF), ciliary neurotrophic factor (CNTF), nerve growth factor (NGF)³⁶. The role of GLP-1 will be specifically commented in section 1.2. of this thesis. This is because its significant relevance to the topic addressed in this thesis. Understanding these imbalances could lead to the development of targeted therapeutic interventions.

1.1.2.3.3. Early microvascular impairment

Early DR involves different microvascular abnormalities: thickening of the capillary basement membrane, pericyte and endothelial cell death, vasoregression, BRB breakdown and

INTRODUCTION

blood flow disruption. These changes contribute to the pathology of the disease and can lead to vascular leakage and impaired retinal function⁷.

Vascular basement-membrane is a critical component of the retinal NVU and plays a crucial role in maintaining structural integrity and facilitating cell-matrix interactions⁹². During early stages DR, there exist an imbalance in the ratio of synthesis and degradation of its components (i.e. collagen IV and laminin), which impairs cell-cell communications and physiological selectivity properties of the membrane. These changes ultimately lead to the thickening of the basement membrane and vascular leakage⁹³.

The early pathological mechanisms triggered by hyperglycemia (AGEs, polyol, hexosamine, and PKC pathways) along with oxidative stress and inflammation, play a role in pericyte and endothelial cell death. In addition, pericytes, which are responsible for regulating vascular tone and perfusion pressure, exhibit dropout before endothelial cell loss⁹⁴. The death of pericytes compromises capillary integrity, weakening the iBRB and promoting vascular leakage. On the other hand, endothelial cell loss leads to vasoregression or vasodegeneration, characterized by the conversion of retinal capillaries into acellular capillaries, resulting in ischemia. Additionally, capillaries from diabetic retina present impaired autoregulation of blood flow, which contributes to vasoregression^{95,96}.

The disruption of the BRB, particularly the iBRB, plays a critical role in the development of DR. Other key factors contributing to BRB breakdown include VEGF, proinflammatory cytokines such as IL-1 β , TNF- α , IL-6, and monocyte chemoattractant protein-1 (MCP-1), and components of the complement system^{74,97}. These factors are released by various cells, including RPE, glia, and immune cells^{74,97}.

Furthermore, blood circulating leukocytes engage with adhesion molecules such as ICAM-1, vascular cell adhesion protein-1 (VCAM-1) and selectins on the surface of the endothelial wall (leukostasis) causing capillary occlusion and blood flow disruption. Additionally, leukocytes release cytokines and generate O₂^{*}, contributing to microvascular damage and NVU impairment in the retina^{74,97}.

Figure 5 illustrates the impaired interconnection among glial activation, inflammation, neurodegeneration and early microvascular impairment.

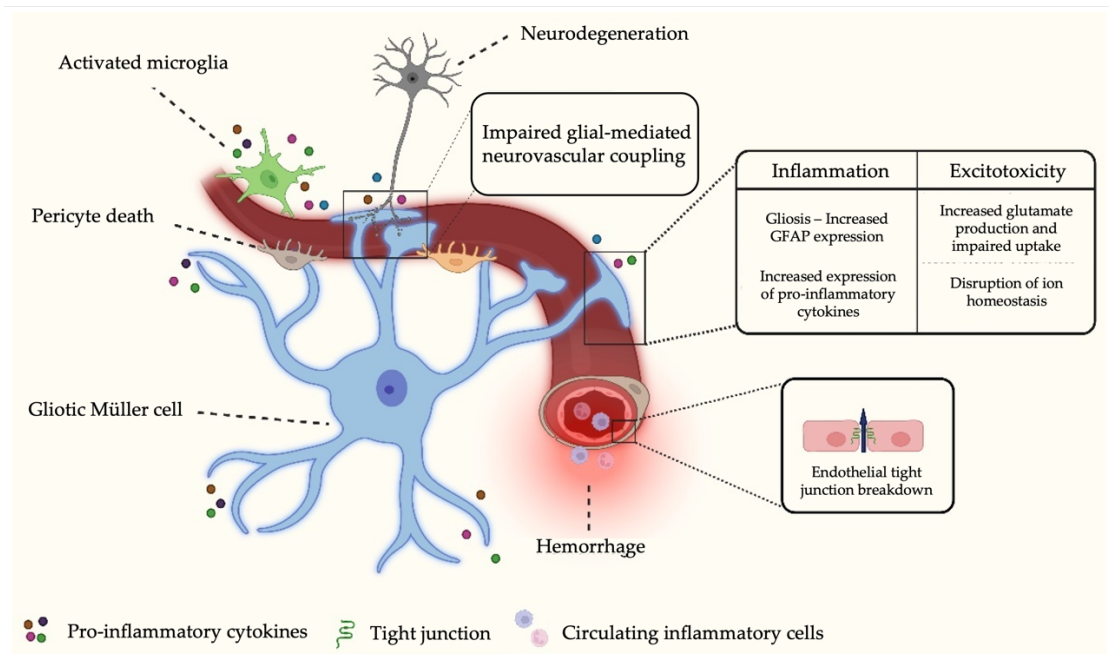


Figure 5. Illustration of the main processes underlying glial activation, inflammation, neurodegeneration and early microvascular impairment, and how they are interconnected. Adapted from Karan & Little *et al*⁹⁸.

1.1.2.4. Advanced stages of the disease: diabetic macular oedema and proliferative diabetic retinopathy

PDR represents an advanced stage of the disease characterized by hypoxia-induced pathological neovascularization at the vitreoretinal interface. This condition is frequently accompanied by vitreous hemorrhages, tractional retinal detachment, and DME. The progression of PDR involves a complex interplay of biochemical, immunological, and inflammatory factors, although the precise underlying mechanisms have yet to be fully understood.

In the vitreous fluid from patients with PDR have been detected elevated levels of various proangiogenic factors, including VEGFA, angiopoietin-2, platelet-derived growth factor, basic fibroblast growth factor, osteopontin, EPO and stromal cell-derived factor-1 (SDF1)⁹⁹. Conversely, the levels of anti-angiogenic factors such as PEDF are reduced in PDR¹⁰⁰. Among these factors, VEGFA has been extensively studied and is a key player in the pathogenesis of PDR, promoting vascular leakage and neovascularization. VEGFA interacts with its primary receptor, VEGF receptor-2, which is expressed on endothelial cells¹⁰¹. This interaction leads to the disruption of tight junctions between endothelial cells, triggering processes such as cell

proliferation and the sprouting of new blood vessels through angiogenesis¹⁰². However, it is noteworthy that not all PDR patients exhibit detectable or high intravitreal levels of VEGFA. This suggests the involvement of VEGFA-independent pathways in the development of PDR¹⁰³. New insights in mass spectrometry-based characterization of the vitreous proteome have shed light on additional processes contributing to PDR pathogenesis. These include inflammation, coagulation, complement activation, and other underlying mechanisms that extend beyond the realm of pathological angiogenesis¹⁰⁴.

DME is a common cause of vision impairment in diabetic individuals worldwide. It is characterized by the accumulation of fluid in the macula, leading to retinal thickening near the fovea. This fluid build-up results in increased central retinal or macular thickness, causing DME and affecting visual function¹⁰⁵. DME occurs as a result of an imbalance between fluid entry, fluid exit, and retinal hydraulic conductivity, leading to the accumulation of intraretinal fluid (extracellular spaces of INL, OPL and ONL,) or subretinal fluid. In normal conditions, the influx and efflux of fluid in the retina are balanced by the integrity of the BRB and the active drainage function of Müller glia and RPE. Müller glia remove fluid from the retinal interstitial tissue, while RPE transports subretinal fluid to the choroid. However, in DME, the breakdown of the BRB and reduced drainage functions by Müller glia and RPE contribute to increased fluid influx and decreased fluid efflux, leading to the development of DME^{106,107}. The pathogenesis of DME is complex and not yet fully understood, involving multiple intricate mechanisms⁸.

1.1.3. Treatment of early stages of DR: an unmet medical need

1.1.3.1. Overview of current treatment of DR

Despite improvements in terms of diagnosis, monitoring and treatment in the most recent years, DR stills representing a dramatic socio-economic cost for healthcare systems. This is because the continuous increase in the number of patients living with DM and, consequently, suffering DR. In addition, the limited knowledge concerning the onset of the pathology and the consequent lack of effective therapeutic approaches targeting the earliest stages of the disease is also an important reason to explain the huge economic burden associated with DR¹⁰⁸.

When referring to current treatments, it is important to mention that DR is often classified into two main stages, an early stage (mild and moderate NPDR) with mild retinal lesions and where visual acuity is generally preserved, and an advanced-stage (severe NPDR, PDR and severe DME) where retinal lesions become more significant and visual acuity is compromised⁵.

Current therapeutic approaches are indicated for the advanced-stage of the disease and are associated with severe adverse effects. These treatments include the following approaches:

- Laser photocoagulation: For many years, the gold standard treatment against PDR has been pan-retinal photocoagulation (PRP), which consists in the thermal destruction of the ischemic retina (Figure 6)¹⁰⁹. This intervention has demonstrated to be effective in reducing the rate of vision loss <50%, decreasing angiogenesis signaling, promoting regression of neovascularization and reducing the risk of developing hemorrhage or tractional membranes. Nevertheless, PRP has multiple limitations and side effects, such as loss of peripheral vision, reduction in night vision, transient decline in visual acuity, diminishment of color vision, reduction in contrast sensitivity, worsening or development of DME, choroidal neovascularization, damage to ciliary nerves, angle closure glaucoma or retinal detachment¹⁰⁹⁻¹¹¹.

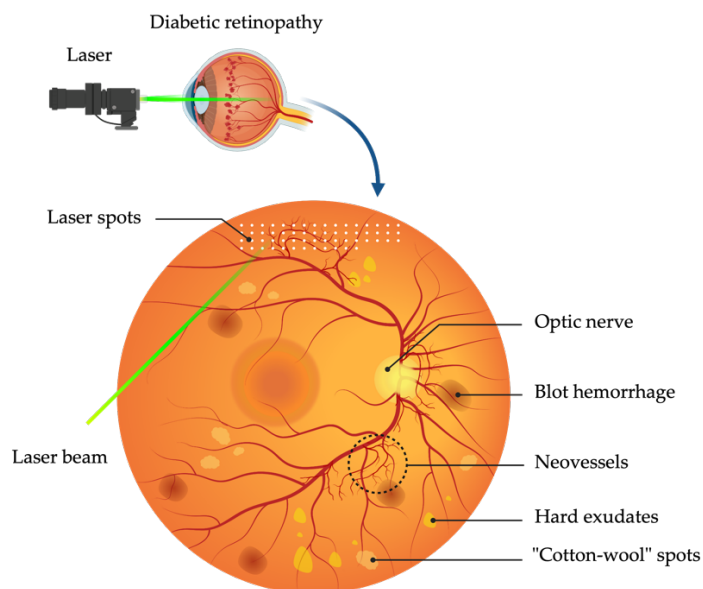


Figure 6. Laser photocoagulation treatment. Laser energy is precisely directed towards damaged areas of the retina in order to inhibit the growth of abnormal blood vessels or reduce the size of those already present in advanced stages of DR.

-Intravitreal anti-VEGF treatment: This group of agents target the largest promoter of angiogenesis during PDR, the growth factor VEGF. They act by inhibiting the molecule directly and/or by blocking its receptors. Available evidence suggests that there exist three classical anti-VEGF agents that may be useful in DR: ranibizumab, aflibercept and bevacizumab

(intravitreal injections of bevacizumab are “off-label”)¹¹². Recently, the US Food and Drug Administration (FDA) has approved a fourth anti-VEGF agent for the treatment of DME, faricimab, which also targets angiopoietin-2¹¹³. New brolocizumab and KSI 301 have also shown promising results¹¹⁴. Anti-VEGF agents, alone or in combination with PRP, are the current standard-of-care in the treatment of DME and PDR¹¹⁵. With different pharmacokinetics and binding targets and affinities, anti-VEGF agents have shown beneficial effects by regressing neovascularization, decreasing vascular permeability and reducing inflammation, resulting in visual acuity improvement. However, multiple injections are needed the long-term effectiveness is around 50%¹¹⁶. In addition, there also exist risks and limitations for the intravitreal use of anti-VEGF drugs, the most relevant being subconjunctival and vitreous hemorrhages, intraocular inflammation, endophthalmitis, transient floaters, uveitis, elevated intraocular pressure and retinal detachment^{109,112,115}. Long term-administrations could also inhibit the neuroprotective and neurotrophic effects of VEGF¹¹².

-Intravitreal corticosteroids: Corticosteroids are well-recognized anti-inflammatory drugs and exert their effect by inactivating multiple inflammatory genes that encode for cytokines, chemokines, inflammatory enzymes, adhesion molecules, receptors and proteins, while promoting the synthesis of anti-inflammatory proteins¹¹⁷. In the context of DR and DME, their oral administration has been associated with systemic adverse effects, such as exacerbation of diabetes, while intravitreal injections are the preferred route due to the protective effects observed in preclinical and clinical studies. These effects comprise anti-inflammatory properties, inhibition of leukocyte adhesion to vascular walls and preservation of tight junctions, inhibition of VEGF gene activation and decreased angiogenic capacity, reabsorption of the excess of extracellular fluid and reduction of vascular permeability, leading to the restoration of BRB breakdown^{118,119}. However, corticosteroids are not exempt from side effects; they have been linked to a high risk of cataract progression and glaucoma. Moreover, the beneficial effects are transient and recurrent injections may be necessary. Therefore, they are often considered as second-line agents for patients who do not respond adequately to anti-VEGF injections. Intravitreal injections of corticosteroids are mainly composed of triamcinolone acetonide, fluocinolone acetonide, or dexamethasone sodium phosphate¹²⁰.

-Vitreoretinal surgery: Vitreoretinal surgeries, such as vitrectomy, are a group of surgical procedures for patients suffering from the complications of PDR, which are mainly tractional retinal detachment and vitreous haemorrhages¹²¹. Vitrectomy has been associated with better visual outcome in patients with DME and/or PDR, including those patients who do not respond to PPR. This effect could be explained by the removal of hemorrhagic blood, decrease of the

vitreous reservoir of diffusible cytokines, better oxygenation and improved BRB integrity. This type of surgery always carries a high risk of intra- and post-operative complications, such as cataract formation, elevation of the intraocular pressure, intraoperative bleeding, postoperative vitreous hemorrhage, iatrogenic retinal breaks, corneal oedema, neovascular glaucoma or neovascularization of the iris (rubeosis)^{122,123}.

1.1.3.2. Potential treatments for early stages of DR

As regards the therapeutic approach to the earliest stages of the disease, at present there is no pharmacological treatment recognized by any scientific academic society. Current recommendations are to optimize blood glucose levels and lipid profile, and to maintain blood pressure under control. Nonetheless, the fact that proper control of these parameters does not guarantee the non-development of DR coupled with the aggressive nature, side effects and high cost of current treatments targeting late stages turn treatment of DR into an unmet medical need with an enormous associated economic burden¹²⁴. Therefore, new effective and personalized therapies against the early stages of DR are needed.

Emerging insights into the origin and progression of this complication enable the design and testing of new experimental approaches which are below summarized.

Targeting AGEs formation and/or RAGE activation

Inhibition of both AGEs formation and RAGE activation have demonstrated being effective in preventing leukostasis, pericyte loss, glial activation and neovascularization, while enhancing the antioxidant defenses^{125,126}. Despite this, preclinical protective results have not yet been translated to the clinical level^{127,128}.

Antioxidant treatment

In view of the important role that oxidative stress plays in the development of DR already at a very early stage, several antioxidant treatments have been proposed as well. Systemic administration of curcumin, green tea, cocoa, superoxide dismutase (SOD) mimetics, flavonoids, melatonin, vitamin E or nutritional supplements containing carotenoids, lipoic acid, or omega-3 fatty acids have been effective in preventing early microvascular impairment in animal models^{124,129,130}. Human studies, although controversial, show some promising results,

especially when administered in combination. However, none of these clinical studies exceeds 5 years in duration¹²⁹.

Anti-inflammatory treatment

Anti-inflammatory therapies are among the most tested experimental candidates, with corticosteroids being one of the most widely used drugs for advanced DR. In early DR, corticosteroids, non-steroidal anti-inflammatory drugs (NSAIDs), suppressors of cytokine signaling and specific blockers of TNF- α or other cytokines have been tested at preclinical level. Intravitreal corticosteroids are invasive and have been linked to adverse effects¹³¹, therefore its application cannot be justified at early stages when the damage does not affect vision¹³². Because of this, the usefulness of corticosteroids by topical route (eye drops) for treating human DME has been already tested with promising results¹³³. On the other hand, topical nepafenac, a NSAID, protected against DR vascular abnormalities while little or no effect was detected in neuronal survival¹³⁴. Nevertheless, the relative efficacy of NSAIDs observed in animal models lacks sufficient clinical data to support it¹³⁵. Subcutaneous etanercept and CNTO5048, two different TNF- α blockers, prevented inflammation, retinal leukostasis, apoptosis, formation of acellular capillary and BRB breakdown in diabetic rats^{136,137}, however controversial results have been found in clinical trials^{138,139}. Lastly, topical administration of suppressors of cytokine signaling has proved to be effective in preventing early vascular leakage and neurodegeneration by reducing microglial and macroglial activation and apoptosis, resulting in an improvement of retinal functionality¹⁴⁰. However, no clinical data have been reported.

Neuroprotective agents

One of the most explored experimental lines for the treatment of early DR is currently related to the use of neuroprotective treatments. Recent evidence of the high neurodegenerative component of the disease has allowed the design of new experimental therapies such as blocking the glutamate signaling pathway or the replacement of neurotrophic factors which are downregulated in the disease^{86,141}. Among the most extensively evaluated neurotrophic factors are PEDF, BDNF, NGF, SST and GLP-1. Both intravenous and topical PEDF were able to reduce oxidative stress, inflammation, glial activation, cell death and vascular leakage in diabetic rat and mouse retinas, respectively^{142,143}. In addition, intravenous administration of PEDF was accompanied by functional improvement¹⁴³. Topical treatment with NGF in diabetic mice prevented neurodegeneration and vascular dysfunction¹⁴⁴, while reduced inflammation and apoptosis in diabetic rats¹⁴⁵. BDNF administered via adeno-associated virus enhanced

retinal ganglion cell survival in diabetic rats¹⁴⁶, however high concentrations of BDNF can lead to a worsening of the inflammatory response. SST eye drops demonstrated the ability to inhibit microglial activation, reactive gliosis, neuronal death, glutamate excitotoxicity, and prevent functional impairment in the retinas of diabetic rats and mice^{141,147,148}. Similarly, SST showed effectiveness in mitigating the pro-inflammatory response in Bv.2 microglial cells¹⁴¹. Furthermore, the European Consortium for the Early Treatment of Diabetic (EUROCONDOR) clinical trial revealed the potential of topical administration of SST in preventing the progression of preexisting retinal neurodysfunction in individuals with T2DM⁶³.

Regarding the experimental results related to the direct or indirect activation of the pathway that triggers GLP-1 peptide, they will be presented in the following sections with greater detail and depth due to their significant relevance to the present thesis.

1.2. GLP-1 and DPP-4 inhibitors: a novel therapeutic approach for early diabetic retinopathy

1.2.1. GLP-1 peptide: an incretin with neuroprotective effects in the central nervous system

The GLP-1 peptide is a hormone involved in the regulation of glucose homeostasis. It is principally secreted by intestinal enteroendocrine L-cells in response to food intake and plays a role in lowering postprandial glucose levels. GLP-1 functions as an incretin, meaning it enhances the release of insulin in response to glucose. It also inhibits the absorption of glucose after food intake by delaying gastric emptying and reducing intestinal motility. Additionally, GLP-1 suppresses glucagon release and decreases hepatic glucose production¹⁴⁹. Through its receptors (GLP-1R) in the brainstem and hypothalamus, GLP-1 also promotes satiety, leading to a reduction in food and water intake¹⁵⁰. These glucoregulatory properties have positioned GLP-1-based therapies as a highly effective in type 2 diabetes. Furthermore, the major additional effect of these therapies on body weight loss has put them on center stage as anti-obesity drugs¹⁵¹.

The GLP-1 peptide is derived from the proglucagon gene and undergoes enzymatic cleavage and modifications to produce the biologically active forms of GLP-1, namely GLP-1 (7-36) amide and GLP-1 (7-37). These forms of GLP-1 are the primary circulating bioactive molecules in humans¹⁵². GLP-1 exerts its functions by binding to GLP-1R, leading to a

conformational change that activates the receptor. Briefly, this activation causes the dissociation of an inhibitory G-protein and the association of a stimulatory G-protein, which then interacts with adenylyl cyclase, an enzyme located in the cell membrane. This interaction results in the conversion of ATP into cyclic adenosine monophosphate (cAMP). Increased cAMP levels serve as a second messenger, triggering the activation of protein kinase A and the consequent intracellular signaling events¹⁵³.

To a lesser extent, GLP-1 is also synthesized from proglucagon by neurons located in the solitary tract nucleus of the brainstem, giving rise to two distinct sources of GLP-1 in the body¹⁵⁴. There exist evidences that suggest that GLP-1 released by the gut and GLP-1 produced within the brain constitute separate systems with distinct functions. While gut-derived GLP-1 contributes more to the functions previously mentioned, brain-derived GLP-1 acts more as a neurotransmitter or a neuromodulator. Nonetheless, the specific interplay between these two systems remains uncertain because the ability of GLP-1 to cross the blood-brain barrier (BBB) makes it difficult to distinguish which functions are attributable to which¹⁵⁵. However, the local production of GLP-1 in the brain emphasizes its relevance in the CNS, where its functions are mainly neuroprotective in nature, as it promotes neuronal differentiation, survival and proper functioning¹⁵⁶. It is also attributed a role in the regulation of synaptic plasticity and neurogenesis^{157,158}.

Low levels of GLP-1 or a malfunction of its signaling pathway have been associated with multiple CNS diseases where neurodegeneration plays an important role, such as Alzheimer's disease (AD) or Parkinson's disease (PD)¹⁵⁹. In these neurodegenerative disorders, administration of GLP-1R agonists rescues neuronal survival and functionality at preclinical level. Significant improvements have been observed in key pathological markers including motor impairment, loss of striatal-dopaminergic function and neuronal loss in PD, as well as loss of glutamatergic neurons and cognitive processes in AD. These positive outcomes have been observed in both preclinical studies and early clinical trials involving AD and PD patients¹⁶⁰. These promising findings highlight the considerable potential of GLP-1-based therapies as a pharmacological treatment option against neurodegenerative diseases.

1.2.1.1. The beneficial effects of GLP-1 in the diabetic retina

Given that the retina is ontogenetically derived from the brain, our group has hypothesized that GLP-1 could also be useful in preventing retinal neurodegeneration that occurs during DR¹³⁹. In fact, we and others have identified the presence of GLP-1 and GLP-1R

in the human retina^{86,161}. Additionally, some studies have revealed reduced levels of GLP-1 and GLP-1R in the retina of diabetic patients^{86,162}. These findings suggest that GLP-1/GLP-1R exerts a physiological role in maintaining retinal homeostasis, but its downregulation in the diabetic retina could be involved the development or early stages of DR.

GLP-1 and GLP-1R agonists administered through intravitreal injections or topical application have displayed neuroprotective properties in various experimental studies focusing on DR^{86,163,164}. They have exhibited positive effects on reactive gliosis, apoptosis, inflammation and functional abnormalities in the retina. Mechanistically, GLP-1 receptor activation inhibits the accumulation of glutamate, impedes the upregulation of proapoptotic markers, reduces the levels of ROS and proinflammatory cytokines and promotes the activation of survival pathways^{86,164–166}. The vasculotropic effects of GLP-1R activation encompass the protection of the BRB against diabetes-induced vascular leakage by maintaining the expression of tight junction proteins and regulating factors such as VEGF and IL-1 β ^{86,164}. Importantly, these effects have been attributed to the direct actions of GLP-1R activation within the retina, independent of blood glucose levels. Numerous additional studies have demonstrated the effectiveness of GLP-1 and GLP-1R agonists in the treatment of DR^{163,167–169}; however, when employing systemic administration routes that impact on systemic glucose levels, it becomes challenging to differentiate whether the observed effects are attributable to blood glucose control or a direct action within the eye.

1.2.2. DPP-4 inhibitors: an alternative therapeutic approach based on GLP-1R activation

The plasma half-life of the active forms of GLP-1 is relatively short, lasting approximately 1-2 minutes, due to their high susceptibility to the catalytic activity of the dipeptidyl peptidase-4 (DPP-4) enzyme. This enzyme cleaves off the first two N-terminal amino acids of the peptide, resulting in the formation of the GLP-1 metabolite 9-36 amide. However, this metabolite is unable to activate the GLP-1R receptor. Additional cleavages by neutral endopeptidase 24.1 give rise to smaller and also inactive metabolites¹⁷⁰. These observations led to hypothesize that DPP-4 enzyme inhibition, by mean of increasing half-life of GLP-1, could be a therapeutic alternative to improve glucose metabolism-related diseases. At present, there are five different DPP4 inhibitors (DPP-4i) on the market that have been approved by the FDA or the European Medicines Agency (EMA) for oral administration for the treatment of T2DM in adults¹⁷¹. The first DPP-4i, sitagliptin, was approved by the FDA in 2006 and the second, saxagliptin, was approved three years later. Later, linagliptin and

alogliptin were approved. Vildagliptin was approved in 2007 by the EMA, but not the FDA¹⁷¹. There exist some differences among them related to both molecular structure and mechanism of action. On one hand, alogliptin, linagliptin, and sitagliptin belong to the xanthine class, forming noncovalent bonds with DPP-4. On the other hand, saxagliptin and vildagliptin are cyanopyrrolidines that establish a covalent bond with the active site serine. However, despite these differences, all share the common ability to decrease the degradation of GLP-1¹⁷².

The well-established neuroprotective effects of GLP-1 in CNS diseases, together with the demonstrated safety of DPP-4i, have led to the emergence of DPP-4i as a promising new approach in preclinical studies for the treatment of CNS diseases. In experimental AD, they have shown promising results by reducing amyloid beta accumulation, neuronal cell apoptosis, tau hyperphosphorylation, mitochondrial dysfunction, oxidative stress and neuroinflammation, leading to a cognitive improvement^{173,174}. Additionally, in experimental PD, DPP-4i abrogated oxidative stress and the proinflammatory and proapoptotic environment of the substantia nigra, increased striatal dopamine levels and reduced nigral neuronal loss^{175,176}. Furthermore, in a model of premature aging, this group of drugs has exhibited the ability to prevent hippocampal neuronal cell death and mitigate impaired cognitive function¹⁷⁷.

1.2.2.1. The beneficial effects of DPP-4 inhibitors in the diabetic retina

Given the significant role of GLP-1 deficiencies in the pathophysiology of DR, the encouraging outcomes of experimental treatments involving local administration of GLP-1 and GLP-1R agonists in diabetic retinas, and the similarities between the retina and the CNS, where their beneficial effects have already been demonstrated, it is reasonable to consider a therapeutic approach for DR based on GLP-1 enhancement through DPP-4i.

On this basis, our research group found for the first time the presence of DPP-4 in the human retina, and in particular in RPE¹⁷⁸. In addition, a higher content of DPP-4 was found in the RPE of diabetic donors in comparison with non-diabetic patients (**Figure 7**)¹⁷⁸. High levels of DPP-4 in the RPE could reduce the effectiveness of topical GLP-1 administrations as all drugs that reach the retina via the transscleral route are first challenged by the choroid and the RPE¹⁷⁹. Therefore, the preservation of native GLP-1 synthesized by the retina by using topical administration of DPP-4i can be contemplated as a new approach for treating early stages of DR.

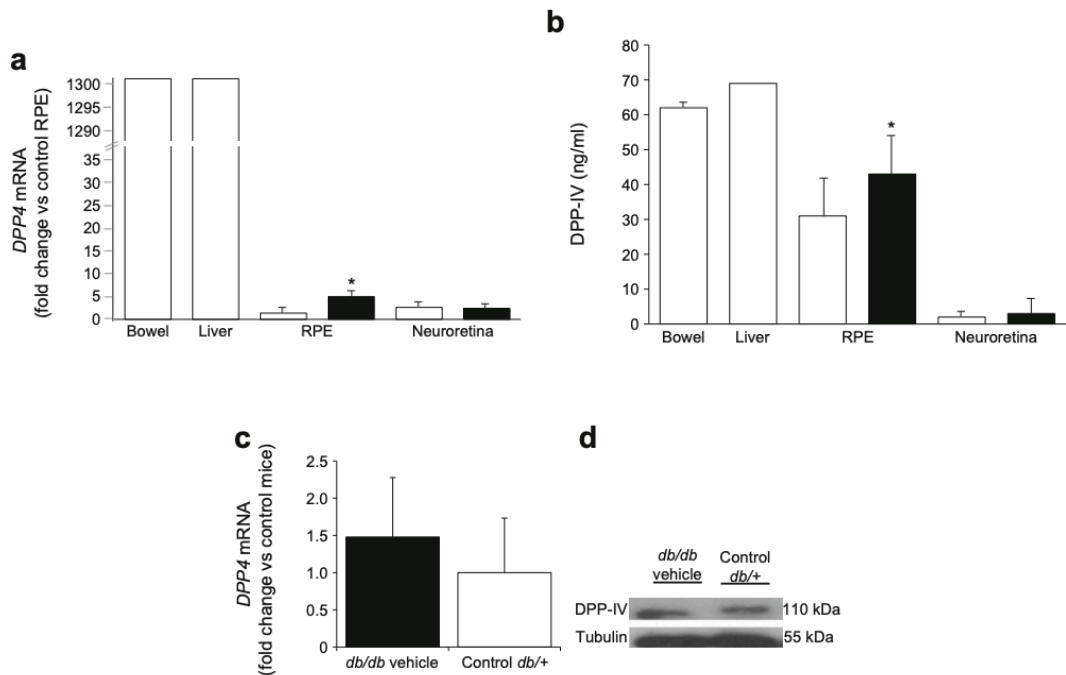


Figure 7. Previous evidence of DPP-4 content in healthy and diabetic human and mouse retinas (**A**) Real-time quantitative analysis of *Dpp4* mRNA and (**B**) DPP-IV concentration (ng/mL) in human retinas from diabetic ($n = 8$; black bars) and non-diabetic ($n = 8$; white bars) donors; * $p < 0.05$ between diabetic and non-diabetic donors. (**C**) Real-time quantitative analysis of *Dpp4* mRNA in mouse retinas expressed as the fold change relative to control ($n = 8$). (**D**) Western blotting bands of DPP-IV in mouse retina ($n = 4$). AU, arbitrary units. Adapted from Hernández *et al*¹⁷⁸.

The first experiments conducted to test the effectiveness of topical DPP-4i against early DR *in vivo* at preclinical level have shown promising results. Eye drops containing sitagliptin and saxagliptin increased GLP-1 levels in diabetic retinas while reducing glial activation, glutamate-mediated neuronal death, and vascular leakage. These results were accompanied by improvements in the ERG test, a technique to assess the cellular physiological status of different components of the retinal neurotransmission process, such as photoreceptors, bipolar cells or glial cells¹⁸⁰. Increased levels of exchange factor directly activated by cAMP 1 (EPAC-1), a downstream molecule of cAMP, were also detected, suggesting an increased GLP-1R activation¹⁷⁸.

It is worth mentioning that DPP-4i have other effects unrelated to the enhancement of GLP-1. In this regard, in absence of GLP-1, sitagliptin and linagliptin protected against TNF- α -mediated inflammation in cultures of retinal bovine endothelial cells and human endothelial cells, respectively^{181,182}. In addition, linagliptin displayed neuroprotective effects in a model of hyperglycemia-induced neurodegeneration in *Caenorhabditis elegans* in which GLP-1R is not

produced¹⁸³. Furthermore, DPP-4i also inhibit the degradation of other peptides, including neuropeptide Y (NPY), peptide YY (PYY), gastric inhibitory polypeptide (GIP), chemokine (C-C motif) ligand 5 (CCL5) and SDF-1¹⁸⁴. This is important because, for instance, NPY is downregulated in DR¹⁸⁵ and the rescue of the NPY levels by DPP-4i could exhibit potential neuroprotective effects, such as the attenuation of NMDA-induced apoptosis in retinal neurons and preservation of the integrity of inner retinal vasculature¹⁸⁶.

Another benefit of using DPP-4i is its superior stability and higher cost-effectiveness compared to GLP-1R agonists. Although the actual cost may differ based on variables such as insurance coverage and geographical location, DPP-4 inhibitors are frequently accessible in generic versions, rendering them more economically accessible when contrasted with branded GLP-1R agonists¹⁸⁷.

Nevertheless, a limiting factor to launch topical administration of DPP-4 inhibitors to the market is the limited preclinical mechanistic understanding in comparison to GLP-1R agonists. The main objective of this thesis is to address this limitation by trying to provide valuable insights into this area. The aims will be explained in more detail in the hypothesis and objectives section. However, to increase the likelihood of success in the clinical setting, it is crucial to select the most appropriate animal model that reproduces as closely as possible the main hallmarks of human DR.

1.3. Animal models for the study of diabetic retinopathy

Numerous animal models have been established to explore the causes and progression of DR, as well as to develop and evaluate potential treatments. Given the intricate nature of DR, which involves a combination of genetic and environmental factors, animal models are designed by induction or genetic modifications. Inducible models are generated by surgical procedures, drug administration, dietary adjustments, laser application or chemical damage. Genetic models, on the other hand, are created by selective breeding techniques and gene editing approaches¹⁸⁸. New advances in genome-wide technology have greatly facilitated the identification of genetic variants associated with the progression of DR, which can be induced or genetically engineered in animal models¹⁸⁹.

The selection of a suitable animal species to model DR *in vivo* involves careful consideration, given the diverse range of options available and the unique properties of each to investigate different aspects of the pathology. Among the most commonly used species are zebrafish, mice,

rats, rabbits, felines, canines, pigs and non-human primates. Rabbits, despite having larger eye globes than rodents, are not appropriate models for DR due to differences in their retinal circulation pattern. Non-human primates show structural similarities to humans, but do not exhibit advanced stages of DR. Larger animals like pigs, dogs, and cats present limitations in terms of cost, availability of reagents, genetic variations, and handling difficulties. In contrast, zebrafish possess a retina structure similar to humans and develop neovascularization, making them suitable for drug screening and genetic studies. Additionally, they exhibit short lifespan, rapid growth, and ability to breed in large numbers. Furthermore, zebrafish exhibit regenerative capabilities, allowing for neuroretinal regeneration through the reprogramming of Müller cells¹⁹⁰. Nonetheless, differences in retinal vascular structure and limited availability of molecular reagents hinder their use as a DR model¹⁹⁰.

Mouse and rat models are preferred because of their small size and ease of handling, low housing costs, short lifespan and short experimental turnover times, rapid reproduction rates, rapid development of the DR and all the genetic information available on them, including the identification of specific strains that exhibit inherited hyperglycemia or obesity. It is important to note that no single model fully encompasses the entire pathogenesis of DR observed in the human eye. These models do not comprehensively reproduce the full range of vascular and neural complications associated with the early and late stages of human DR^{188,189,191}.

1.3.1. Inducible rodent models

The main three approaches used to obtain inducible models of diabetes are administration of alloxan, administration of streptozotocin (STZ) and high-galactose diet. Although all of these induction methods are still being studied, STZ administration is the most widely used due to its rapid disease progression. Alloxan is considered less effective in inducing diabetes, while dietary approaches require more time for progression of the disease¹⁸⁸.

STZ is a highly selective cytotoxic agent of pancreatic islet β -cells that is used to induce T1DM in rodents, causing hyperglycemia in 1-4 weeks¹⁹². At a relative early age, both STZ-induced mice and rats exhibit DR-like features such as glial activation, retinal cell loss, microvascular abnormalities, BRB breakdown and increased vascular permeability, leukostasis and functional defects (ERG)¹⁹³. In this model both high levels of VEGF and even neovascularization have been reported^{194,195}. Rats are used more than mice because of their larger eyeball size and higher susceptibility to STZ toxicity, requiring only one administration whereas mice require 3-5. To minimize mortality rates, insulin supplementation may be given alongside STZ treatment. STZ

can also be used to induce T2DM through a variety of more complex methods, including combined administration of STZ and nicotinamide, high-fat diet feeding followed by multiple low-dose injections of STZ and administration of STZ during the neonatal period¹⁹¹. The main disadvantages of this model are the rapid onset of the disease and the lack of spontaneous development which results in the non-full replication of the human DR, especially when referring to the inflammatory and neurodegenerative processes¹⁹⁶. Additionally, diabetes induced by STZ has the inconvenience of the intrinsic neurotoxicity of STZ^{197,198}. This associated adverse effect makes extremely difficult to dissect whether retinal neurodegeneration is due to diabetic milieu or as a consequence of STZ itself. It is also important to note that the severity and manifestation of DR-related phenotypes in STZ-induced rodents is highly variable, making it difficult to obtain consistent and reproducible results¹⁹⁶.

On the other hand, the other most used chemical compound to induce DM and DR is the urea derivative alloxan. This agent causes pathological effects through two mechanisms, including selective inhibition of glucose-stimulated insulin secretion, and induced formation of ROS, both promoting selective necrosis of pancreatic β -cells¹⁹⁹. Most of the existing studies with alloxan have focused primarily on vascular damage, having reported loss of pericytes, vascular leakage, presence of acellular capillaries and neovascularization. Ganglion cell apoptosis and functional abnormalities (ERG) have also been detected¹⁹¹. One significant drawback of alloxan is its toxic effects on the liver and kidney, which limit its usefulness in research and clinical use. For this reason and the rapid degradation due to its high instability, STZ administration is increasingly used in place of alloxan¹⁹⁹.

DR can also be induced in rodents through the administration of a diet supplemented with 30-50% galactose. Rats and mice fed with galactose develop retinal microangiopathy, which closely resembles the initial stages of DR. This includes the loss of pericytes and endothelial cells, the presence of acellular capillaries, retinal thickening of the retinal capillary basement membrane, and the formation of intraretinal microvascular abnormalities²⁰⁰. Nonetheless, they do not display the exact microvascular damage observed in humans and frequently they can't reach the proliferative stage. On the other hand, the extended lifespan of this model enables observations for up to 26 months¹⁸⁸.

The main problem when using inducing diabetes in mice and rats is the lack of an anatomical macula and the difficulty of recapitulating PDR, thus making difficult to reproduce what occurs in advanced stages of DR.

1.3.2. Genetic rodent models

The development of DR is strongly influenced by genetic factors. Rodent genetic models have been widely used in DR research as they offer well-characterized genetic backgrounds and the possibility to manipulate their genes by knockout, knockdown and transgenic techniques. There are five major mouse genetic models [Ins2^{Akita}, Non-Obese Diabetic mouse (NOD), db/db mouse (Lepr^{db}), Kimba and Akimba] and six major rat genetic models [Zucker diabetic fatty (ZDF), Otsuka Long-Evans Tokushima fatty (OLETF), Biobreeding (BB), WBN/Kob, spontaneously diabetic Torii (SDT) and Goto-Kakizaki (GK)] designed specifically to study DR. Each genetic model has its own set of limitations and advantages, which can vary significantly^{188,189}.

T1DM genetic models

The Ins2^{Akita} mouse model presents a missense mutation in the insulin 2 gene causing hyperglycemia via a T1DM-like mechanism due to misfolded insulin accumulation and β -cell apoptosis²⁰¹. Although the model exhibits vascular, neural and glial abnormalities, it does not recapitulate the vascular changes observed in human DR¹⁸⁹. The spontaneous NOD mouse model develops DM due to destructive autoimmune pancreatic insulinitis that targets β -cells. It closely mimics the pathophysiology of T1DM in humans and shows damage to retinal vasculature, capillary basement membrane thickening and neovascularisation²⁰². The BB rat model is triggered by a frameshift mutation that leads to autoimmune-mediated β -cell apoptosis. This model displays pericyte dysfunction, microvascular degeneration and microaneurysms²⁰³.

T2DM genetic models

The ZDF rat and db/db mouse models are commonly used for the investigation of obesity-related T2DM, as mutations in the leptin receptor gene cause obesity and hyperglycaemia²⁰⁴. However, the ZDF rat model may not be suitable for studying DR due to the absence of retinal vascular damage²⁰⁵. The db/db mouse model closely mimics the pathophysiology of T2DM and exhibits retinal glial activation, neuronal death, thickening of the central retinal membrane, thinning of retinal layers, acellular capillaries and functional abnormalities^{206,207}. Rapid disease progression and short life expectancy are the main limitations of this model¹⁹¹. The OLETF rat model develops T2DM spontaneously through obesity, while the WBN/Kob rat model develops hyperglycemia through unknown mechanisms. Both models show retinal

microvascular changes, but may not fully reproduce all aspects of DR pathology¹⁸⁹. The SDT and GK rat models represent non-obese T2DM, and the SDT model closely resembles human pathophysiology. SDT rats exhibit intraretinal angiopathy, apoptosis in retinal layers and large gender differences in disease onset. The GK rat model shows reduced retinal blood flow, microcirculatory changes, increased blood-retinal barrier permeability and functional abnormalities^{208–210}.

[Non-diabetic/hybrid pathology models](#)

The Kimba mouse, a non-diabetic model, has been genetically modified to overexpress retinal VEGF, resulting in early retinal disease characterized by reduced ONL and INL, abnormal retinal microvasculature and loss of pericytes. By crossing Kimba and Ins2^{Akita} mice, the Akimba mouse model combines features of both parental strains, including hyperglycemia and neovascularization. The Kimba model has limitations such as early disease onset and rapid disease progression, whereas Akimba mice provide an effective model for studying DR with fewer common limitations seen in other animal models. The combined traits inherited from the parental strains significantly influence retinal disease progression in Akimba mice^{211,212}. These models are a valuable resource for DR research, in particular to elucidate VEGF-related mechanisms and develop interventions targeting neovascularization. However, the genetic overexpression of VEGF can be a problem to test the efficiency of drugs that inhibits VEGF by other pathways not directly related to its blockade.

1.3.2.1. The db/db mouse model

The db/db mouse (BKS.Cg-Dock7^{m/+}/Lepr^{db}) has been selected as the preferred model for this thesis among all the models presented in the previous sections. Originally generated by Jackson Laboratory, this congenic model presents a spontaneous recessive mutation in the leptin receptor (Lepr^{db}) which leads to a susceptibility to obesity, insulin resistance and T2DM²¹³. Leptin is released by adipose tissue and provides information about energy stores to the brain, leading to reduced food intake and increased energy expenditure. This mechanism helps maintain body fat stores in rodents and humans²¹⁴. Homozygous mice exhibit noticeable obesity by 3 to 4 weeks of age. Plasma insulin levels increase at 10 to 14 days, followed by elevated blood sugar levels at 4 to 8 weeks. These homozygous mutant mice display polyphagia, polydipsia, and polyuria. The disease progression is influenced by genetic background, with the C57BLKS background showing uncontrolled blood sugar rise, severe depletion of insulin-producing beta-cells, and mortality by 10 months. On the other hand,

heterozygous mice ($Lepr^{db/+}$) present normal body weight, blood glucose, and plasma insulin levels but exhibit increased metabolic efficiency and improved fasting tolerance. The misty ($Dock7^m$) mutation is introduced to maintain the diabetes mutation, causing coat color dilution and altered platelet function²¹³.

Regarding the use of the db/db mouse for the study of DR, the early neurodegenerative process has been well characterized in this model. At 8 weeks of age mice start exhibiting functional abnormalities (ERG studies) and GCL thickening, which can be attributed to glial activation, glutamate excitotoxicity and the consequent loss of ganglion cells. However, these damages are accentuated at 16 and 24 weeks of age²⁰⁶. ONL and INL thickenings also occur at 8 and 14 weeks of age respectively²¹⁵. At 12 weeks, activation of inflammatory pathways and antioxidant capacity failure have also been described^{60,164}. Pericyte loss, formation of acellular capillaries and neovascularization appear at 18 weeks of age. Controversy surrounds the occurrence of neovascularization in the model²⁰⁷. Furthermore, lowering blood glucose levels reduced the appearance of major DR abnormalities, demonstrating that NVU impairment in the db/db mouse is a consequence of hyperglycemia rather than genetic condition²⁰⁶. Nevertheless, the db/db mouse model has limitations due to the rapid progression of severe DM, characterized by escalating blood sugar levels and deteriorating cardiovascular health^{216,217}, which significantly shortens the lifespan to approximately 10 months, restricting the study of DR beyond that age²¹³. The main hallmarks of DR present in this model are summarized in **Figure 8**.

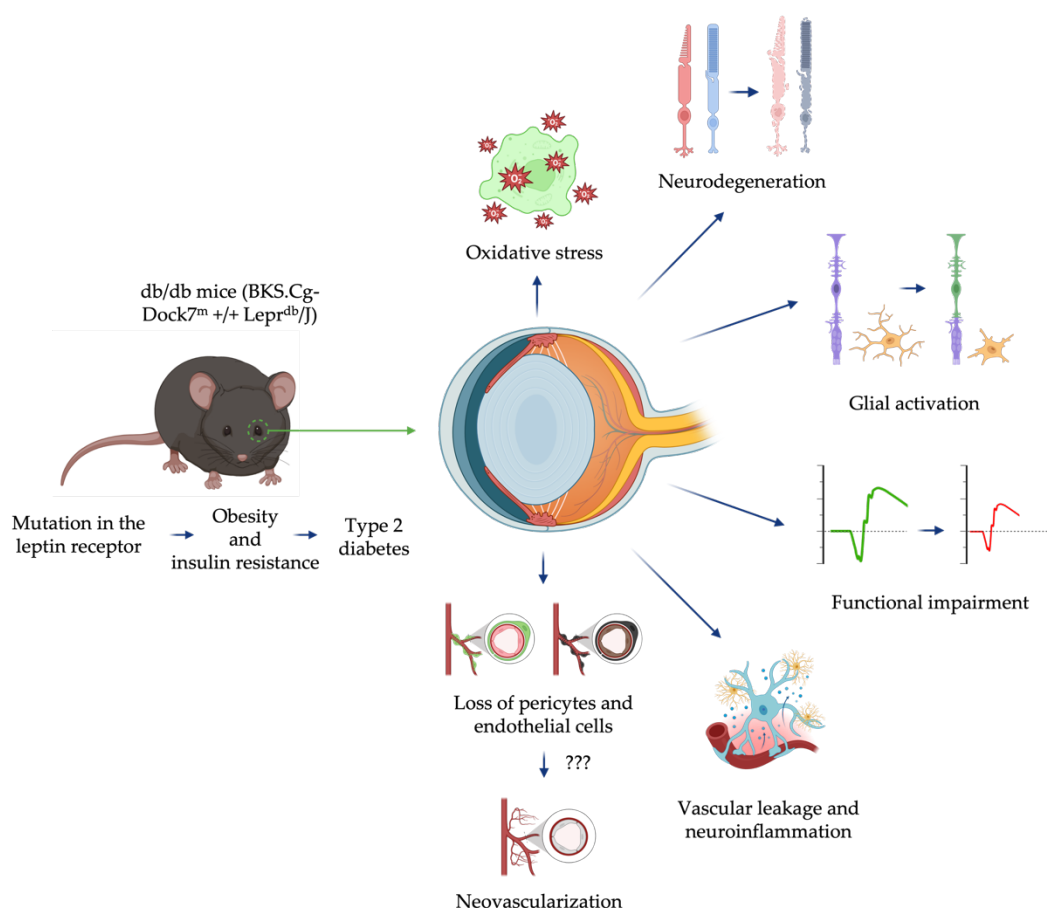


Figure 8. Main hallmarks of DR in the db/db mouse model.

Due to its modelling of the most common diabetes type today (T2DM) in a spontaneous manner and its development of the disease in a way that closely resembles early stages of human DR compared to chemically induced models that exhibit an extremely rapid onset of complications, the db/db mouse can be considered the best available rodent model for studying treatments particularly against early DR.

HYPOTHESIS AND OBJECTIVES

2.1. Hypothesis

In previous studies, it was demonstrated that topical administration of two DPP-4i, sitagliptin and saxagliptin, prevented the two main hallmarks of early DR (glial activation and neuronal death) in the experimental db/db mouse model. In addition, we detected that they were able to reduce vascular leakage and prevent neuronal functional impairment. The main hypothesis of this thesis is that topical administration (eye drops) of sitagliptin (the selected DPP-4i) could modulate key pathological processes involved in early stages of DR such as neuronal transmission, oxidative stress and inflammation. The confirmation of these mechanisms of action in the setting of experimental studies will be essential for the preclinical regulatory process needed before initiating the clinical development.

2.2. Objectives

In accordance with the outlined hypothesis and with the aim of facilitating the possible launch of this new therapeutic approach on the market, the specific objectives of this thesis were the following:

- 1) To perform a transcriptome comparison (microarrays and subsequent analysis) between retinas from db/db mice topically treated with vehicle, db/db mice topically treated with sitagliptin and non-diabetic db/+ mice in order to shed light on the mechanisms underlying the beneficial effects of DPP-4i in early stages of DR, with special emphasis in neuroprotection.
- 2) To validate the obtained results from the transcriptomic analysis through quantitative reverse transcription polymerase chain reaction (RT-qPCR) assays.
- 3) To evaluate the potential antioxidant properties of sitagliptin by analyzing NRF2 and antioxidant enzymes, ROS and macromolecule oxidative damage in the retinas of db/db mice after administering sitagliptin eye drops.
- 4) To study the potential anti-inflammatory effects of sitagliptin by analyzing NF- κ B pathway and the pathological overproduction of pro-inflammatory cytokines and adhesion molecules in db/db mice after topical treatment of sitagliptin.

HYPOTHESIS AND OBJECTIVES

- 5) To assess whether topical administration of sitagliptin is able to improve the low neuronal proliferation rate and reduced functionality of the diabetic retina.
- 6) To conduct a dose-effectiveness study with sitagliptin and saxagliptin eye drops to establish the minimum effective dose capable of reversing the main DR abnormalities (glial activation, neuronal death and vascular leakage).

MATERIALS AND METHODS

3.1. *In vivo* experimentation

3.1.1. Mice and housing conditions

A total of 24 diabetic male db/db (BKS.Cg-Dock7^m +/- Lepr^{db}/J) mice and 12 non-diabetic mice (db/+; (BKS.Cg-Dock7^m + Lepr^{db}/+)) aged 7 weeks were obtained from Charles River Laboratories Inc. (Calco, Italy) for the transcriptomic study and all the experiments performed to evaluate the properties of sitagliptin. Regarding the dose-effectiveness study, 63 diabetic male db/db mice and 14 non-diabetic mice db/+ were purchased. Animals were bred and kept in the animal facility of the Vall d'Hebrón Research Institute (VHIR). Animals were provided with unrestricted *ad libitum* feeding (ENVIGO Global Diet Complete Feed for Rodents, Mucedola, Milan, Italy) and filtered water. In order to minimize variability, animals were randomly housed (block randomization) in groups of 2 mice per cage in Tecniplast GM-500 cages (36×19×13.5cm) under standard laboratory conditions at 22 ± 2 °C, with a 12h light/dark cycle and relative humidity of 50–60%. Each cage contained absorbent bedding and nesting material (BioFresh Performance Bedding 1/800 Pelleted Cellulose, Absorption Corp, Ferndale, WA, USA). Both body weights and blood glucose levels were monitored weekly. Glycaemia measurements were performed by tail vein sampling (glucose assay kit, 170397, Abbott, IL, USA).

All animal experiments were conducted in accordance with the guidelines of the European Community (86/609/CEE) and the Association for Research in Vision and Ophthalmology (ARVO) for the use of laboratory animals. This research study received approval from the Animal Care and Use Committee of VHIR (CEEAA 75/15).

3.1.2. Interventional studies: topical treatments

3.1.2.1. Transcriptomic study and evaluation of the potential beneficial properties of sitagliptin

At the age of 10 weeks, sitagliptin (sitagliptin phosphate monohydrate, Y0001812, Merck KGaA, Darmstadt, Germany) eye drops (10 mg/mL; *n* = 12) and vehicle [phosphate-buffered saline (PBS)] eye drops (*n* = 12) were randomly administered twice per day directly onto the superior corneal surface of each eye of diabetic mice with the aid of a micropipette (5 µL). On day 15, animals (12 weeks of age) received one drop of sitagliptin or vehicle 1 hour (h)

before euthanasia. Twelve non-diabetic mice matched by age served as the control group. **Figure 9** shows a schematic view of the different experimental groups and the distribution of the samples for the different techniques that will be shown in the next sections.

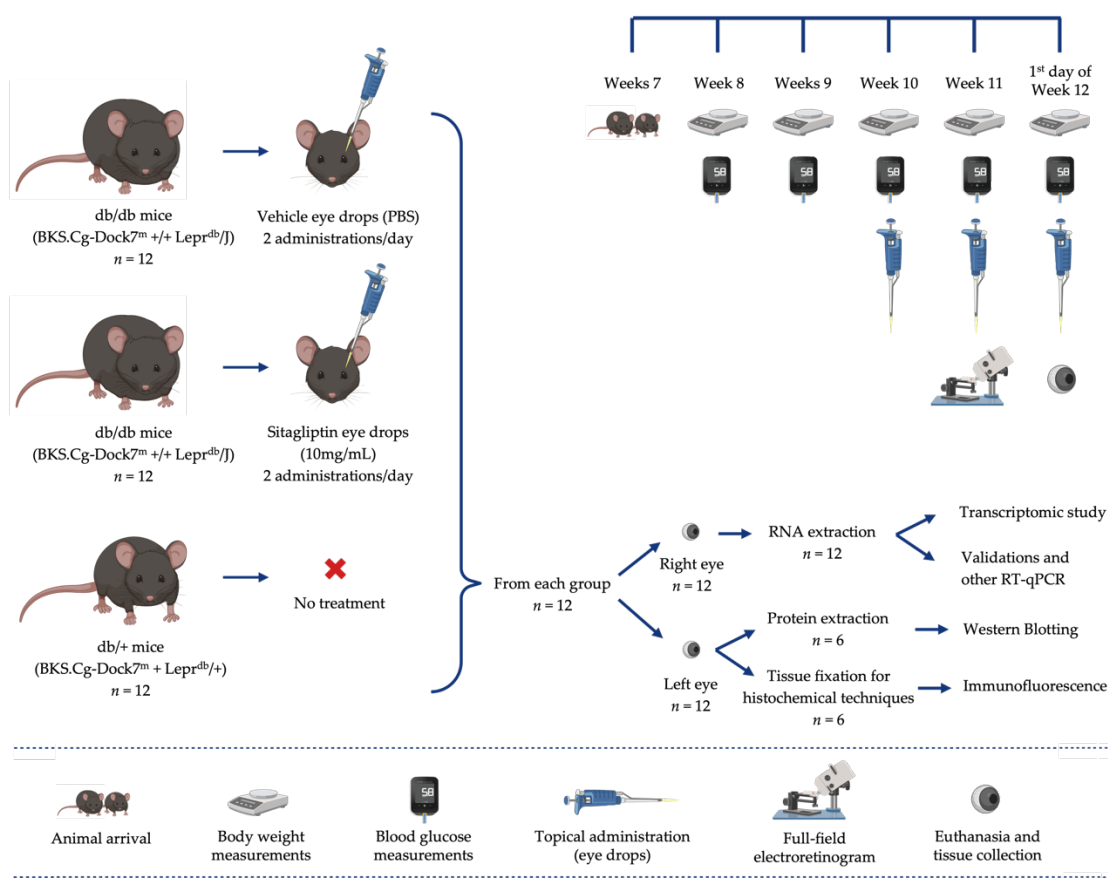


Figure 9. Schematic summary of the different experimental groups and the sample distribution for the transcriptomic study and the evaluation of the potential beneficial properties of sitagliptin.

3.1.2.2. Dose-effectiveness study with sitagliptin and saxagliptin

At the age of 10 weeks, sitagliptin 1 mg/mL (twice daily, $n = 7$), sitagliptin 5 mg/mL (twice daily, $n = 7$), sitagliptin 10 mg/mL (twice daily, $n = 7$), saxagliptin (saxagliptin hydrochloride, FS71931, Biosynth Carbosynth, Staad, Switzerland) 1 mg/mL ($n = 14$) (once and twice daily, $n = 7$ in each case), saxagliptin 10 mg/mL ($n = 14$) (once and twice daily, $n = 7$ in each case) and vehicle eye drops ($n = 14$) were randomly administered directly onto the superior corneal surface of each db/db eye using a micropipette (one drop: 5 μ L). Sitagliptin (1, 5 or 10 mg/mL), saxagliptin (1 or 10 mg/mL) or vehicle (5 μ L PBS, pH 7.4) was administrated for 15 days in each eye. On the last day (12 weeks of age), one drop of sitagliptin, saxagliptin or vehicle

was administered to each eye 1h before euthanasia. Fourteen non-diabetic mice (db/+) matched by age were used as control group.

3.1.3. Full-field electroretinogram

The ERG is a diagnostic methodology that measures the electrical activity of the retina in response to light stimulus, while maintaining non-invasiveness and physiological conditions. The ERG arises from currents produced directly by retinal neurons, coupled with inputs from retinal glial cells. As a result, it gives electrical wave patterns that through amplitude/timing measurements allows to test the functionality and therefore the health of certain groups of retinal cells²¹⁸. Within these patterns we can highlight the a-wave, which correlates with the response of photoreceptors (rods and cones), and the b-wave, which represents the functionality of bipolar neurons and Müller cells. It is also worth mentioning the high-frequency, low-voltage oscillations, known as oscillatory potentials, which are also frequently observed riding on the ascending limb of the b-wave. Although their origin is still debated, it has been suggested that they represent inner retinal potentials generated by neuronal interactions involving bipolar, amacrine and/or ganglion cells²¹⁹.

It has been reported in multiple studies that in early DR there are already functional alterations detectable with the ERG²²⁰. This anomaly extrapolates perfectly in the db/db mouse^{164,178}. All this enables to evaluate the possible effects that drugs may have on the functionality of the diabetic retina in its early stages.

Commencing in 1989, the International Society for Clinical Electrophysiology of Vision (ISCEV) introduced standardized fundamental ERG protocols with the aim of enabling consistent comparisons between different research facilities. These protocols are subject to periodic updates. The most recent ISCEV standard for clinical ERG consists of six protocols, named according to the stimulus (flash strength in candela-seconds per meter squared [cd/s/m^2]) and the adaptation state [dark-adaptation (scotopic ERG) or light-adaptation (photopic ERG)]²²¹. Briefly, dark-adapted ERG allows to obtain the data only from rods (only at very low intensity), the mixed data from both cones and rods and the data of the oscillatory potentials. On the other hand, light-adapted ERG enables to evaluate the cone-response without the mixed activity of the rods²²¹. **Figure 10** shows the wave patterns for each protocol and the different measures that can be obtained for each one. In this study the dark-adapted/scotopic ERG (A,B,C, and D from Figure 10) was performed using different intensities.

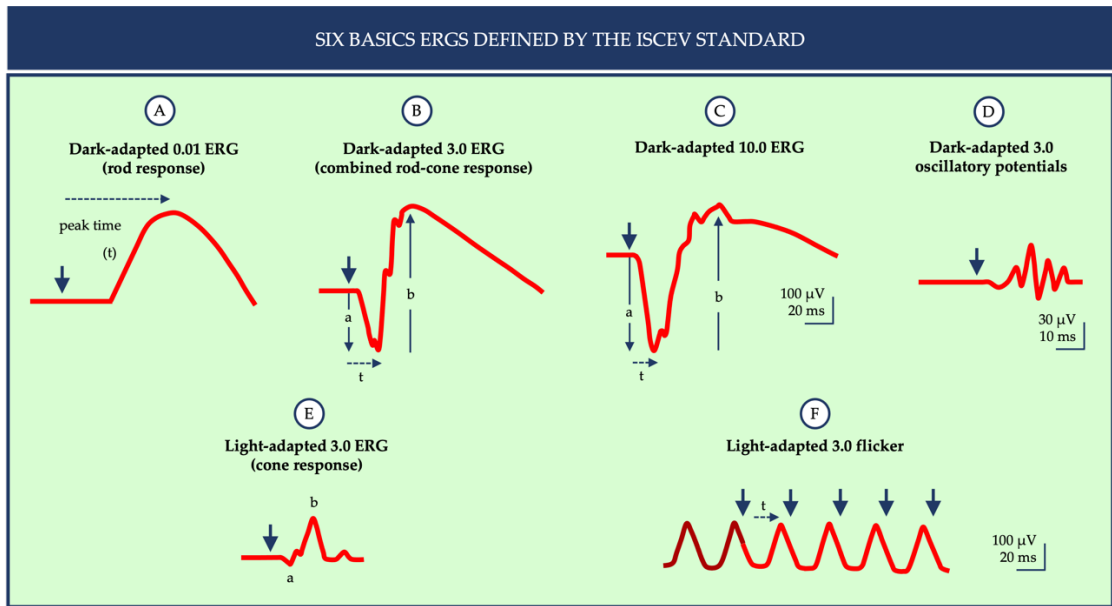


Figure 10. Normal full-field electroretinography (ERG) responses using the six International Society for Clinical Electrophysiology of Vision (ISCEV) protocols. Adapted from McCulloch *et al*²²¹.

ERG recordings were estimated using the Ganzfeld ERG platform (Phoenix Research Laboratories, Pleasanton, CA, USA) following the ISCEV guidelines^{221,222}. Animals were dark adapted for at least 8h prior to ERG recording and then anesthetized with isoflurane. An induction chamber (2% isoflurane and 4% oxygen) was used first and then animals was transferred to the temperature-controlled restraint platform to perform the ERG, which contains a buconasal mask to maintain anesthetic conditions. For proper pupil dilation, tropicamide 1.0% and phenylephrine 2.5% eye drops were topically administered to each eye prior to the test. A cutaneous ground electrode was placed near the base of the tail, a needle electrode was placed on the head between the two eyes, and a corneal electrode was placed near each eye. To prevent dehydration and corneal injury, carboxymethylcellulose 1.0% eye drops were applied to the inner surface of the contact lens electrodes before the eyes were placed in them.

For the recording of electrical activity, flashes of white light were emitted with gradually increasing intensity, starting with a baseline recording at 0 cd/s/m². Data were obtained for a- and b-wave amplitudes. In this thesis, only the recordings obtained at 1.25 cd/s/m² (low intensity) and 80 cd/s/m² (high intensity) are presented. It is important to note that while recording the electrical activity of one eye, the other eye was consistently maintained in a hydrated state through the application of artificial tears. Once the procedure was completed

and the inhalation anesthesia was withdrawn, in order to avoid hypothermia, the animal was placed on an electric blanket until full recovery. A summary of the employed methodology is depicted in **Figure 11**.

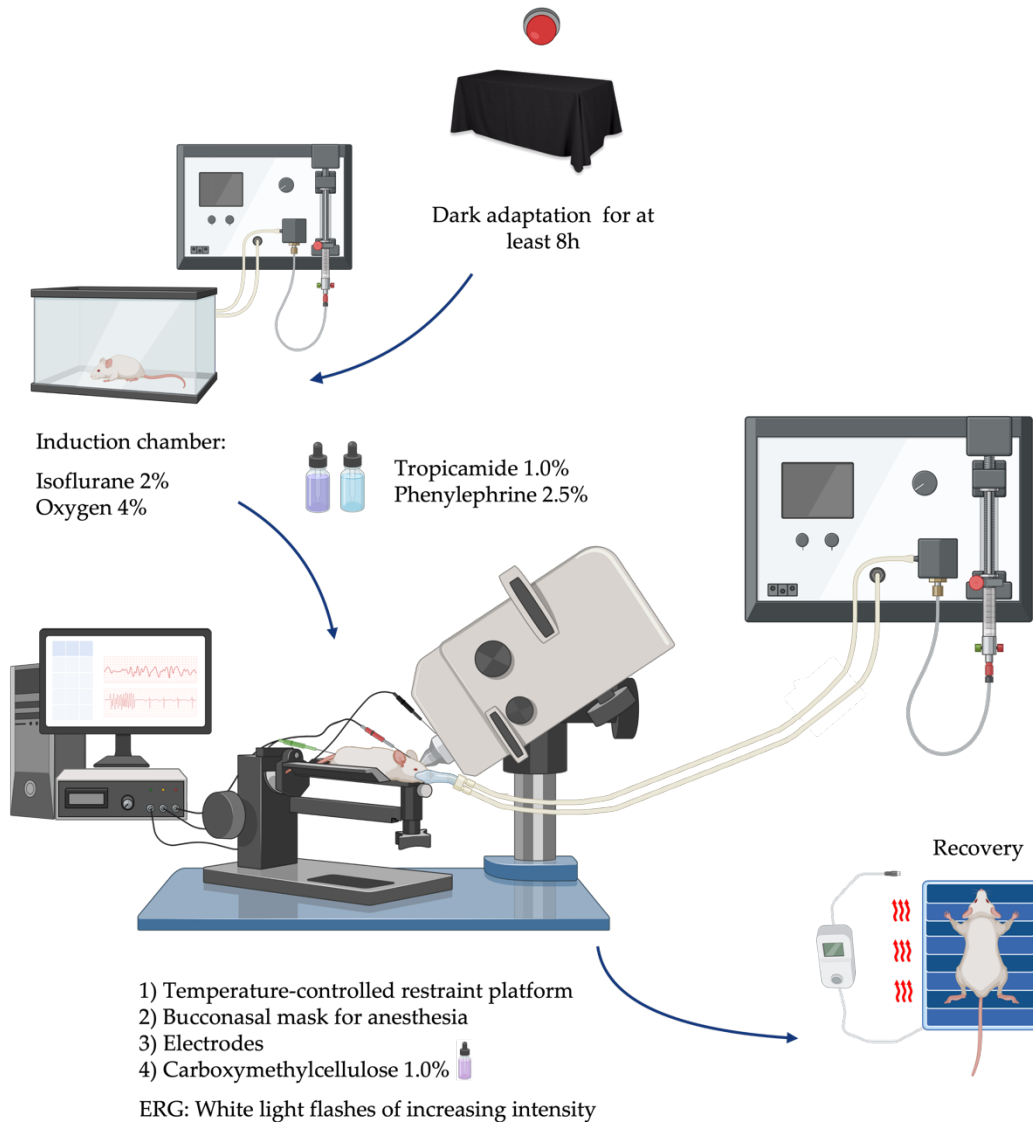


Figure 11. Overview of the dark-adapted ERG recording procedure.

3.1.4. Euthanasia and retinal tissue processing

On day 15, animals were euthanized through cervical dislocation. Eyes were rapidly enucleated, and the neuroretinas were dissected with the aid of a stereoscopic microscope

(SZB250, VWR, Radnor, PA, USA), two mirror finish forceps (11251-23, Fine Science Tools, Foster City, CA, USA), and a pair of vannas spring scissors (15000-08, Fine Science Tools, Foster City, CA, USA). In brief, the cornea was removed by cutting in a circular path along the *ora serrata* and the retina was detached by placing the forceps between the eyecup and the retina and moving the forceps slowly around the circumference. The second forceps was used to hold the sclera and stabilize the eyecup. The neuroretinas for the microarrays, the subsequent RT-qPCR validations and for the protein assessments were directly stored in an empty tube at -80°C . Regarding histochemical techniques, instead of dissecting the retinas, the whole eye was fixed in 4% paraformaldehyde (sc-281692, Santa Cruz Biotechnology, Dallas, TX, USA) for 5h and after overnight preservation in PBS, it was placed in a cassette for paraffinization and sectioning.

3.2. Nucleic acid analysis: genomic approaches

3.2.1. RNA extraction and quantification

The neuroretinas were introduced in individual tubes with 140 μL of TRIzol reagent (15596018, InvitrogenTM, Carlsbad, CA, USA) for RNA extraction. In order to remove genomic contamination, neuroretinas were treated with DNase (18068015, ThermoFisher Scientific, Waltham, MA, USA) and sequentially purified on RNeasy MinElute column (74106, Qiagen, Hilden, Germany). After supernatant elimination, RNA sediment was obtained and resuspended in 30 μL of RNase free water (AM9937, ThermoFisher Scientific, Waltham, MA, USA). An Agilent 2100 Bioanalyzer and a NanoDrop Spectrophotometer were used for sample integrity and quantity, respectively.

3.2.2. Transcriptomic study: microarrays and gene set enrichment analysis

The data for the analysis were obtained from the Genomic core facility of the High Technology Unit (UAT) at VHIR, where the microarrays were assessed. The research included 30 samples (comprising the top 10 RNA samples with the highest quality from each group) that were hybridized onto Clariom S Mouse Arrays (ThermoFisher Scientific, Waltham, MA, USA). Bioinformatics analysis was conducted in the Statistics and Bioinformatics Unit (UEB) at VHIR. Prior to normalization, quality assessments, such as principal component analysis (PCA), hierarchical clustering and HeatMaps depicting distances between arrays, were performed. No samples were excluded at this stage. Following the robust microchip average (RMA)

algorithm^{223,224}, all samples underwent normalization. Subsequent quality checks involving PCA and hierarchical clustering were carried out, leading to the exclusion of an outlier from the vehicle group. Using principal variance component analysis (PVCA), it was determined that the primary source of variance was the batch effect. The strategy for identifying differentially expressed genes (DEGs) involved adjusting a linear model with empirical Bayes moderation of the variance, which included a batch factor to adjust batch effects. This technique, similar to ANOVA, was specifically developed for microarray data analysis by Gordon K Smyth²²⁵. P-values underwent adjustment to ensure rigorous control over the false discovery rate, employing the Benjamini and Hochberg method. Statistical significance was set at 0.05 for adjusted p-values. The analysis of biological significance was relied on gene set enrichment analysis (GSEA) and was performed using the clusterProfiler package in R/Bioconductor²²⁶, which implements the GSEA algorithm proposed by Subramanian²²⁷. In GSEA, the genes can be ordered in a ranked list according to their differential expression between the classes using different annotation databases such as Gene Ontology (GO) or Reactome Pathway Knowledge base (RPD). The statistical analysis was assessed using the statistical language “R” (R, version 3.5.1 (2 July 2018), copyright (C) 2018, The R Foundation for Statistical Computing and the libraries developed for the microarray analysis in the Bioconductor Project (www.bioconductor.org) (accessed on 18 October 2021). Functional association networks were constructed and annotated using STRING version 11.5 (<https://string-db.org/>) (accessed on 18 October 2021). The *Mus musculus* genome was used as background genome. The data discussed in this publication were deposited in NCBI’s Gene Expression Omnibus²²⁸ and are accessible through GEO Series accession number GSE219084 (<https://www.ncbi.nlm.nih.gov/geo/query/acc.cgi?acc=GSE219084>).

3.2.3. cDNA reverse transcription and quantitative reverse transcription polymerase chain reaction assay

In accordance with manufacturer’s instructions, complementary DNA (cDNA) reverse transcription was performed in a T100 Thermal Cycler (Bio-Rad, Hercules, CA, USA) using a High-Capacity cDNA Reverse Transcription Kit (4368814, ThermoFisher Scientific, Waltham, MA, USA) and Oligo(dT)₁₈ Primer (SO131, ThermoFisher Scientific, Waltham, MA, USA). RT-qPCR was performed using SYBR Green PCR Master Mix (4309155, Applied Biosystems, Warrington, UK) and a 7.900 HT Sequence Detection System in 384-well optical plates with specific primers (**Table 1**). Relative quantifications were calculated using the ABI SDS 2.4 RQ software and displayed as a ratio between them and the endogenous controls [β -2 microglobulin (*B2m*) and actin beta (*Actb*)].

Primers	Gene ID	Nucleotide sequence	
<i>Actb</i>	11461	Forward (5'-3')	5' - CTAAGGCCAACCGTGAAAG - 3'
		Reverse (5'-3')	5' - CAGTATGTTCTCGGCTTCCCATTC - 3'
<i>Apha1</i>	319924	Forward (5'-3')	5' - GGTGCTGAGTCATCAAGCATAC - 3'
		Reverse (5'-3')	5' - GAACTTCAACGTAGGTTGGGAA - 3'
<i>B2m</i>	12010	Forward (5'-3')	5' - GTATGCTATCCAGAAAACCC - 3'
		Reverse (5'-3')	5' - CTGAAGGACATATCTGACATC - 3'
<i>C1ql1</i>	23829	Forward (5'-3')	5' - GGCACCTACTTTTTACCTACC - 3'
		Reverse (5'-3')	5' - AGTCGTAGTTCTGGTCTGCAT - 3'
<i>Cask</i>	12361	Forward (5'-3')	5' - TGAAGAAGTAGTCAAAGTCCAG - 3'
		Reverse (5'-3')	5' - TTTGTCCCGTACATTGCATCC - 3'
<i>Cat</i>	12359	Forward (5'-3')	5' - AGCGACCAGATGAAGCAGTG - 3'
		Reverse (5'-3')	5' - TCCGCTCTCTGTCAAAGTGTG - 3'
<i>Commd8</i>	27784	Forward (5'-3')	5' - AAATTCTCTGAGGAAGAGAC - 3'
		Reverse (5'-3')	5' - GCTTGATCTCATTTCTCCTAC - 3'
<i>Cplx1</i>	12889	Forward (5'-3')	5' - AGTTCGTGATGAAACAAGCCC - 3'
		Reverse (5'-3')	5' - TCTTCCTCCTCTTAGCAGCA - 3'
<i>Dlg2</i>	23859	Forward (5'-3')	5' - CTGTCACGAGGCAGGAAATAAA - 3'
		Reverse (5'-3')	5' - CGACTTCGTAGTCACGCTTTG - 3'
<i>Dlg4</i>	13385	Forward (5'-3')	5' - TGAGATCAGTCATAGCAGCTACT - 3'
		Reverse (5'-3')	5' - CTCCTCCCTAGCAGGTCC - 3'
<i>Gpx1</i>	14775	Forward (5'-3')	5' - CTCACCCGCTCTTTACCTTCCT - 3'
		Reverse (5'-3')	5' - ACACCGGAGACCAAATGATGTACT - 3'
<i>Gria1</i>	14799	Forward (5'-3')	5' - AAAGGAGTGTACGCCATCTTTG - 3'
		Reverse (5'-3')	5' - TGTCAACGGGAAACTTGGAG - 3'
<i>Grin1</i>	14810	Forward (5'-3')	5' - ATGCACCTGCTGACATTTCG - 3'
		Reverse (5'-3')	5' - TATTGGCCTGGTTTACTGCCT - 3'
<i>Grin2b</i>	14812	Forward (5'-3')	5' - GCCATGAACGAGACTGACCC - 3'
		Reverse (5'-3')	5' - GCTTCCTGGTCCGTGTCATC - 3'
<i>Grin2d</i>	14814	Forward (5'-3')	5' - GCTGCGAGACTATGGCTTCC - 3'
		Reverse (5'-3')	5' - CCAGTGACGGGTTTACCAGAAA - 3'
<i>Gsr</i>	14782	Forward (5'-3')	5' - GACACCTCTTCCTTCGACTACC - 3'
		Reverse (5'-3')	5' - CCCAGCTTGTGACTCTCCAC - 3'
<i>Il1b</i>	16176	Forward (5'-3')	5' - GCAACTGTTCTCTGAAGTCAACT - 3'
		Reverse (5'-3')	5' - ATCTTTGGGGTCCGTCAACT - 3'
<i>Kif1b</i>	16561	Forward (5'-3')	5' - GTCAATCGAATGAACGACCTGG - 3'
		Reverse (5'-3')	5' - GCCGATGCAAAAAGTTGAACTG - 3'

<i>Kif1bp</i>	72320	Forward (5'-3') Reverse (5'-3')	5' - TCTTGACCCGACTGAGCATTT - 3' 5' - ATAATGAGCGGCCTTCTCGAA - 3'
<i>Nrf2</i>	18024	Forward (5'-3') Reverse (5'-3')	5' - TCTTGGAGTAAGTCGAGAAGTGT - 3' 5' - GTTGAAACTGAGCGAAAAAGGC - 3'
<i>Slc17a7</i>	72961	Forward (5'-3') Reverse (5'-3')	5' - GGTGGAGGGGGTCACATAC - 3' 5' - AGATCCCCGAAGCTGCCATAGA - 3'
<i>Snap25</i>	20614	Forward (5'-3') Reverse (5'-3')	5' - CAACTGGAACGCATTGAGGAA - 3' 5' - GGCCACTACTCCATCCTGATTAT - 3'
<i>Sod1</i>	20655	Forward (5'-3') Reverse (5'-3')	5' - AACCAGTTGTGTTGTCAGGAC - 3' 5' - CCACCATGTTTCTTAGAGTGAGG - 3'
<i>Sod2</i>	20656	Forward (5'-3') Reverse (5'-3')	5' - CAGACCTGCCTTACGACTATG - 3' 5' - CTCGGTGGCGTTGAGATTGTT - 3'
<i>Stx1a</i>	20907	Forward (5'-3') Reverse (5'-3')	5' - CGCTGTCCCCGAAAGTTTGTG - 3' 5' - GTGTCTGGTCTCGATCTCACT - 3'
<i>Stxbp2</i>	20911	Forward (5'-3') Reverse (5'-3')	5' - AAGGCGGTGGTAGGGGAAA - 3' 5' - CAACAGGATGACAAGATTCGCA - 3'
<i>Stxbp4</i>	20913	Forward (5'-3') Reverse (5'-3')	5' - ACAGGTCTAGGTCTGAAGATCC - 3' 5' - CATCCTTGTAACAGTCACCTCC - 3'
<i>Stxbp6</i>	217517	Forward (5'-3') Reverse (5'-3')	5' - CTCTTGATGAAAGAATGCTGGGA - 3' 5' - TGACCTTCGTGATAGATGCCT - 3'
<i>Sv2b</i>	64176	Forward (5'-3') Reverse (5'-3')	5' - AGGTATCGGGACAACATATGAGG - 3' 5' - GCCTTCTGTAACATCGCTCTGT - 3'
<i>Syn1</i>	20964	Forward (5'-3') Reverse (5'-3')	5' - AATCACAAAGAGATGCTCAG - 3' 5' - GGACACGCACATCATATTTAG - 3'
<i>Syp</i>	20977	Forward (5'-3') Reverse (5'-3')	5' - TGCCAACAAGACGGAGAGTG - 3' 5' - TAGTGCCCCCTTTAACGCAG - 3'
<i>Syt1</i>	20979	Forward (5'-3') Reverse (5'-3')	5' - ACCCTGGGCTCTGTATCCC - 3' 5' - CCCTGACCACTGAGTGCAAA - 3'
<i>Tnfa</i>	21926	Forward (5'-3') Reverse (5'-3')	5' - CCCTCACACTCAGATCATCTTCT - 3' 5' - GCTACGACGTGGGCTACAG - 3'
<i>Unc13a</i>	382018	Forward (5'-3') Reverse (5'-3')	5' - GCTGTGCGTGAGGAGTCAAA - 3' 5' - CAGCTATGGTAGTGCTCTTCA - 3'
<i>Vamp2</i>	22318	Forward (5'-3') Reverse (5'-3')	5' - ATCATCGTTTACTTCAGCAC - 3' 5' - TGAAAGATATGGCTGAGAGG - 3'
<i>Vcam1</i>	22329	Forward (5'-3') Reverse (5'-3')	5' - TGGGAGCCTCAACGGTACTT - 3' 5' - ACAATGGTGACTCGCAGCCC - 3'

Table 1. Primers employed for the RT-qPCR experiments.

3.3. Analyses of protein levels

3.3.1. Protein extraction and quantification

Protein extraction consisted in a sonication of neuroretinas for 10–15 s in 80 μ L of lysis buffer [phenylmethanesulfonylfluoride (PMSF), 1mM; sodium fluoride (NaF), 100mM; sodium orthovanadate (Na_3VO_4) 2mM; RIPA buffer (R0278, Sigma-Aldrich, St Louis, MO, USA); 1x protease inhibitor cocktail (P8340, Sigma-Aldrich, St. Louis, MO, USA)]. Protein quantification was carried out by the Bicinchonine acid assay (BCA) method²²⁹, which allows the determination of the total protein concentration of a sample in a range of 0.5 μ g/mL to 1.5 mg/mL. For this purpose, a BCA kit (Pierce™ BCA Protein Assay Kit, 23225, ThermoFisher Scientific, Waltham, MA, USA) and a standard curve made with bovine serum albumin were used. Absorption spectra were obtained using a spectrophotometer (SpectraMax 340PC384 Microplate Reader, Molecular Devices, San José, CA, USA). Finally, total concentrations were calculated through the standard curve of known albumin concentrations.

3.3.2. Western Blotting assay

25 μ g of extracted protein were loaded in a 4–20% (vol./vol.) precast gels for sodium dodecyl sulfate polyacrylamide gel electrophoresis (SDS-PAGE) (4561096, Bio-Rad, Hercules, CA, USA), and electrophoresis was carried out at 100 V for 90 minutes (min). Proteins were then transferred to a polyvinylidene difluoride (PVDF) membrane (1620177, Bio-Rad Laboratories, Hercules, CA, USA) at 400 mA for 90 min and blocked in 5% powder milk (Central Lechera Asturiana, Spain) and 0.1% Tween in tris-buffered saline buffer. Primary antibodies ([Table 2](#)) were overnight incubated at 4 °C. On the next day, secondary antibodies ([Table 3](#)) were applied (1:10,000). Immunoreactive bands were detected using a WesternBright ECL horseradish peroxidase (HRP) substrate kit (K-12045-D50, Advansta, CA, USA). Vinculin and Cyclophilin A were used as housekeepings to normalize protein levels. The densitometric analysis was assessed with ImageJ software (version 1.8, National Institutes of Health, Bethesda, MD, USA).

Primary antibodies	Description
C1QL1	Rabbit polyclonal; 1:1000; orb1260; Biorbyt, Cambridge, UK
CAT	Rabbit polyclonal; 1:1000; GTX110704; GeneTex, Alton Pkwy Irvine, CA, USA

CuZnSOD	Rabbit polyclonal; 1:1000; GTX100554; GeneTex, Alton Pkwy Irvine, CA, USA
Cyclophilin A	Rabbit polyclonal; 1:10,000; BML-SA296; Enzo, NY, USA
GPX-1	Rabbit polyclonal; 1:1000; 55053-1-AP; Proteintech, Rosemont, IL, USA
GR	Mouse monoclonal; 1:1000; sc-133245; Santa Cruz, Dallas, TX, USA
I κ B α	Rabbit monoclonal; 1:1000; ab32518; Abcam, Cambridge, UK
MnSOD	Rabbit polyclonal; 1:1000; ab13533; Abcam, Cambridge, UK
NRF2	Rabbit polyclonal; 1:1000; 16396-1-AP; Proteintech, Rosemont, IL, USA
Phospho-I κ B α	Rabbit monoclonal; 1:1000; ab133462; Abcam, Cambridge, UK
SNAP-25	Rabbit polyclonal; 1:1000; 14903-1-AP; Proteintech, Rosemont, IL, USA
Synapsin I	Rabbit polyclonal; 1:2000; ab64581; Abcam, Cambridge, UK
Synaptophysin	Rabbit monoclonal; 1:200000; ab32127; Abcam, Cambridge, UK
Synaptotagmin	Mouse monoclonal; 1:1000; ab13259; Abcam, Cambridge, UK
Syntaxin 1A	Rabbit polyclonal; 1:100000; ab41453; Abcam, Cambridge, UK
VAMP-2	Rabbit polyclonal; 1:1000; 10135-1-AP; Proteintech, Rosemont, IL, USA
Vinculin	Mouse monoclonal; 1:7000; sc-73614; Santa Cruz, Dallas, TX, USA

Table 2. Primary antibodies employed for Western Blotting experiments.

Secondary antibodies	Description
Mouse Immunoglobulins/HRP	Rabbit polyclonal; 1:10000; P0260; Agilent, Santa Clara, CA, USA
Rabbit Immunoglobulins/HRP	Goat polyclonal; 1:10000; P0448; Agilent, Santa Clara, CA, USA

Table 3. Secondary antibodies employed for Western Blotting experiments.

3.3.2.1. Western Blot reproving: harsh stripping

In order to reuse PVDF membranes, it is necessary to remove primary and secondary antibodies through a process known as stripping. There exist different modalities depending on the intensity; in this case, the harsh stripping was performed. A buffer composed of 20 mL of 10% Sodium dodecyl sulfate (1610301, Bio-rad, Hercules, CA, USA), 12,5 mL of 0.5M Tris-Hydrochloride pH 6.8 and distilled water (made up to 100 mL) was prepared. This buffer and β -mercaptoethanol (M3148-250ML, Sigma-Aldrich, St Louis, MO, USA) (proportion of 0.8 mL/100 mL) were added under the fume hood in a sealable glass container. The container was heated to 50 °C and the membranes were placed inside for 20 minutes with agitation. Since traces of β -mercaptoethanol can damage antibodies, four 15-minute washes with 0.1% Tween

in tris-buffered saline buffer were performed for adequate removal. Once the fourth wash is finished, the PVDF membranes are ready for further blocking and incubation processes.

3.4. Histochemical techniques

3.4.1. Immunofluorescence staining

Paraffin-embedded ocular globes were sectioned (3 μ m) and mounted on 25.5 \times 75.5 \times 1.0 mm Poly-L-Lysine positive charged slides (S21.2113.A, Leica Biosystems, Wetzlar, Germany). Samples were deparaffinized in xylene, rehydrated in grade ethanol series, fixed in ice-cold acid methanol (−20 °C), and washed with PBS 0.01M at pH 7.4. Consecutively, eye sections were heated in a pressure cooker at 150 °C for 4 min in 250 mL of 1:10 diluted antigen retrieval with sodium citrate 10 mM, pH 6 (ab973, Abcam, Cambridge, UK). Then, sections were blocked with blocking solution (X0909, Dako Agilent, Santa Clara, CA, USA) for 1h at room temperature and then incubated overnight at 4 °C with specific primary antibodies (Table 4). The next day, after three washes in PBS, sections were incubated for 1h in the dark with secondary antibodies (Table 5). Samples were then washed with PBS three times, counterstained with Hoechst 33342 (bisbenzimidazole) (14533, ThermoFisher Scientific, Waltham, MA, USA), and mounted with Prolong Mounting Medium Fluorescence (P36930, Prolong, Invitrogen™, Thermo Fisher Scientific, Eugene, OR, USA) and a coverslip (15747592, ThermoFisher Scientific, Waltham, MA, USA). The images were obtained at 60X and a resolution of 1024 \times 1024 pixels using a laser confocal microscopy (Fluoview FV1000 Laser Scanning Confocal Microscope, Olympus Corporation, Shinjuku, Japan). Immunofluorescence intensities were quantified with ImageJ software (version 1.8, U. S. National Institutes of Health, Bethesda, MD, USA).

Primary antibodies	Description
8-Hydroxyguanosine	Mouse monoclonal; 1:100; ab62623; Abcam, Cambridge, UK
C1QL1	Rabbit polyclonal; 1:100; orb1260; Biorbyt, Cambridge, UK
Collagen IV	Rabbit monoclonal; 1:200; ab236640; Abcam, Cambridge, UK
CuZnSOD	Rabbit polyclonal; 1:100; GTX100554; GeneTex, Alton Pkwy Irvine, CA, USA
Dihydroethidium	D23107; ThermoFisher Scientific, Waltham, MA, USA
DPP-4	Rabbit polyclonal; 1:200; ab28340; Abcam, Cambridge, UK
GFAP	Rabbit monoclonal; 1:500; ab7260; Abcam, Cambridge, UK

IL-1 β	Rabbit polyclonal; 1:200; ab9722; Abcam, Cambridge, UK
Ki67	Rabbit polyclonal; 1:500; ab15580; Abcam, Cambridge, UK
MnSOD	Rabbit polyclonal; 1:100; ab13533; Abcam, Cambridge, UK
NeuN	Mouse monoclonal; 1:200; ab104224; Abcam, Cambridge, UK
NF- κ B	Mouse monoclonal; 1:100; sc-8008; Santa Cruz, Dallas, TX, USA
Nitrotyrosine	Mouse monoclonal; 1:100; ab7048; Abcam, Cambridge, UK
NRF2	Rabbit polyclonal; 1:100; 16396-1-AP; Proteintech, Rosemont, IL, USA
PKC- β	Rabbit polyclonal; 1:100; ab189782; Abcam, Cambridge, UK
PKC- δ	Rabbit monoclonal; 1:100; ab182126; Abcam, Cambridge, UK
SNAP-25	Rabbit polyclonal; 1:100; 14903-1-AP; Proteintech, Rosemont, IL, USA
Synapsin I	Rabbit polyclonal; 1:100; ab64581; Abcam, Cambridge, UK
Synaptophysin	Rabbit monoclonal; 1:100; ab32127; Abcam, Cambridge, UK
Synaptotagmin	Mouse monoclonal; 1:200; ab13259; Abcam, Cambridge, UK
Syntaxin 1A	Rabbit polyclonal; 1:200; ab41453; Abcam, Cambridge, UK
TNF- α	Mouse monoclonal; 1:100; ab1793; Abcam, Cambridge, UK
TXNIP	Rabbit monoclonal; 1:200; ab188865; Abcam, Cambridge, UK
VAMP-2	Rabbit polyclonal; 1:100; 10135-1-AP; Proteintech, Rosemont, IL, USA
VCAM-1	Rabbit monoclonal; 1:100; ab134047; Abcam, Cambridge, UK

Table 4. Primary antibodies used for immunofluorescence experiments.

Secondary antibodies	Description
Alexa Fluor 488 Goat anti-mouse	Goat polyclonal; 1:600; ab150113; Abcam, Cambridge, UK
Alexa Fluor 488 Goat anti-rabbit	Goat polyclonal; 1:600; ab150081; Abcam, Cambridge, UK
Alexa Fluor 594 Goat anti-mouse	Goat polyclonal; 1:600; A-11032; ThermoFisher Scientific, Waltham, MA, USA
Alexa Fluor 594 Goat anti-rabbit	Goat polyclonal; 1:600; A-11012; ThermoFisher Scientific, Waltham, MA, USA

Table 5. Secondary antibodies used for immunofluorescence experiments.

3.4.1.1. Measurements of glial activation

Glial activation was evaluated by laser scanning confocal microscopy (Fluoview FV1000 Laser Scanning Confocal Microscope, Olympus Corporation, Shinjuku, Japan) at a magnification of 60× using specific staining antibodies against GFAP. To evaluate the degree of glial activation, we used a scoring system based on the extent of GFAP staining, following the methodology described²³⁰. This scoring system (previously used by our group) was as follows: Müller cell endfeet region/GCL only (score 1); Müller cell endfeet region/GCL plus a few proximal processes (score 2); Müller cell endfeet plus many processes, but not extending to ONL (score 3); Müller cell endfeet plus processes throughout with some in the ONL (score 4); and Müller cell endfeet plus many dark processes from GCL to the outer margin of ONL (score 5). For statistical purposes, the GFAP extent score was categorized as “normal” (scores 1 and 2) and “pathological” (scores 3, 4 and 5), and for comparisons between groups, Fisher’s exact test was used. Statistical significance was set at $p < 0.05$. A summary of the method is illustrated in **Figure 12**.

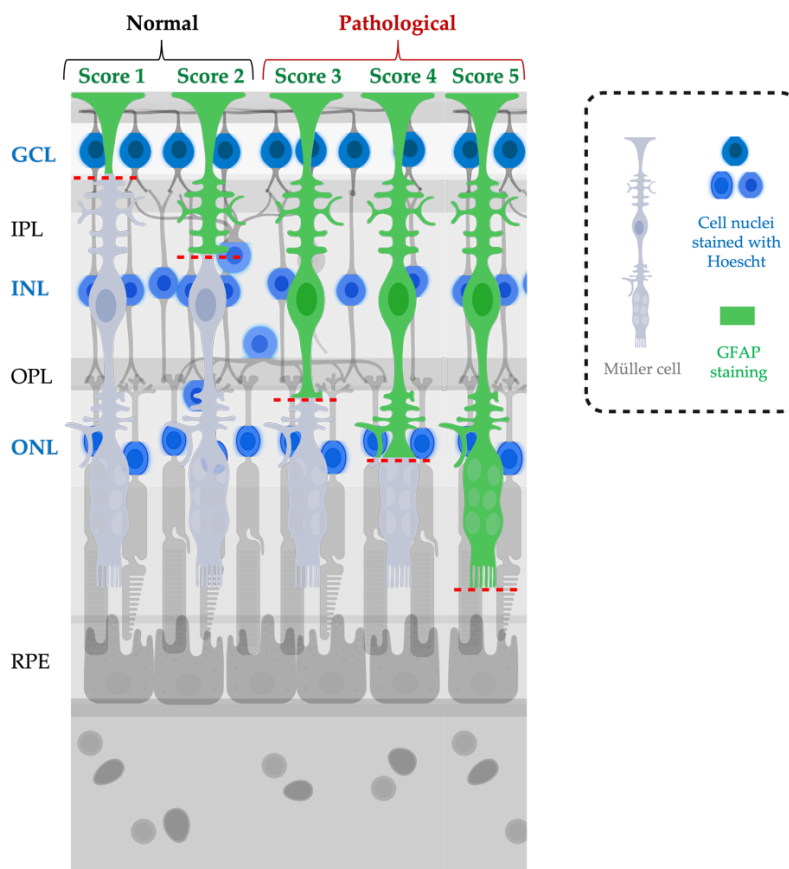


Figure 12. Criteria employed for the measurement of glial activation (GFAP protein expression).

3.4.1.2. Evaluation of the nuclear translocation of NF- κ B

For the NF- κ B nuclear translocation assay, different slices along the Z-axis of retinal sections were acquired at 60X and a resolution of 1024x1024 pixels. Orthogonal projections of the sections were obtained (Fluoview FV1000 Laser Scanning Confocal Microscope, Olympus Corporation, Shinjuku, Japan) and analyzed with the FV10-ASW Viewer software (version 4.2b, Olympus Corporation, Shinjuku, Japan) to detect NF- κ B colocalization events with the cell nuclei.

3.4.2. Hematoxylin-eosin staining

After paraffin embedding, retinas were cross-sectioned (3 μ m) and a hematoxylin and eosin (H&E) staining was performed for a systematic morphometric analysis of retinal layers. Images of H&E-stained sections were captured with a microscope (FSX100 Inverted Microscope Olympus, Hamburg, Germany) at a magnification of 35 \times and quantified using the software ImageJ (version 1.8, U. S. National Institutes of Health, Bethesda, MD, USA).

3.4.2.1. Cell counting of the ganglion cell layer and the inner nuclear layer

Measurements were taken in three different regions of the central retina. Similar and comparative locations for all studied retinas were determined using the same demarcation, which consists in selecting regions close to the optic nerve but with a minimum extension of 300 μ m from both sides of the optic nerve head rim (posterior pole of the eye). Cell counts of GCL and INL were averaged and compared among all the experimental groups.

3.4.2.2. Analysis of retinal thickness

Total and INL thicknesses were measured using the ImageJ software. Five distinct images of each retina were analyzed, quantified, and averaged for obtaining both thicknesses. Imaged regions were selected according to the demarcation described in the cell-counting section, and for each region, a representative value was obtained through the arithmetical mean of ten different measures.

3.4.3. Evans Blue assay

The permeability of the retinal vasculature was evaluated using the *ex vivo* Evans blue albumin method. Evans Blue is a tetrasodium diazo dye with high affinity to serum albumin (10:1 molar ratio), whose intravenous or intraperitoneal injection has been extensively used to study the permeability of the BBB and the BRB²³¹. Under physiological conditions, the endothelium restricts the presence of macromolecules to the inside of blood vessels, while a pathological environment can promote the loss of endothelial junctions causing the leakage of small proteins such as albumin²³². As Evans Blue is a fluorescent dye (excitation at 620 nm, emission at 680 nm), its binding to albumin allows the detection and the quantification of plasma albumin extravasation which is a direct indicator of vascular permeability^{231,233}.

A pH 7.4 solution of Evans blue (E2129, Millipore Sigma, Burlington, MA, USA), concentrated 5 mg/mL and dissolved in PBS, was intraperitoneally injected in 3 mice per experimental group (17 mg/kg). After 2h, animals turned blue, confirming the absorption and distribution of the dye. Mice were subsequently euthanized by cervical dislocation and the eyes were enucleated. For tissue fixation, ocular globes were immersed in a 2 mL tube with 4% paraformaldehyde (sc-281692, Santa Cruz Biotechnology, Dallas, TX, USA) for 30 min and rapidly moved into tubes containing pH 7.4 PBS. During all this process eyes were kept ice. Both retinas of each animal were dissected and flat-mounted in $25.5 \times 75.5 \times 1.0$ mm³ poly-L-Lysine positively charged microscopic slides (S21.2113.A, Leica Biosystems, Wetzlar, Germany) with ProLong™ Gold Antifade Mountant (P36930, Invitrogen™, ThermoFisher Scientific, Eugene, OR, USA) and coverslips (15747592, ThermoFisher Scientific, Waltham, MA, USA). Flat-mounting, also known as whole-mounting, consists in flattening the cup-shaped retina through four radial cuts within two drops of pH 7.4 PBS on a slide. The PBS is then carefully removed and the samples can be mounted as conventional sections. Images of different fields were acquired at 60X using a 561 nm laser line on a confocal laser-scanning microscope (Fluoview FV1000 Laser Scanning Confocal Microscope, Olympus Corporation, Shinjuku, Japan). All images were recorded with identical beam intensity at a resolution of 1024×1024 pixels. The number of extravasations per 60X field was counted for the quantitative analysis using ImageJ software (version 1.8, U. S. National Institutes of Health, Bethesda, MD, USA). A schematic illustration of the procedure is shown in **Figure 13**.

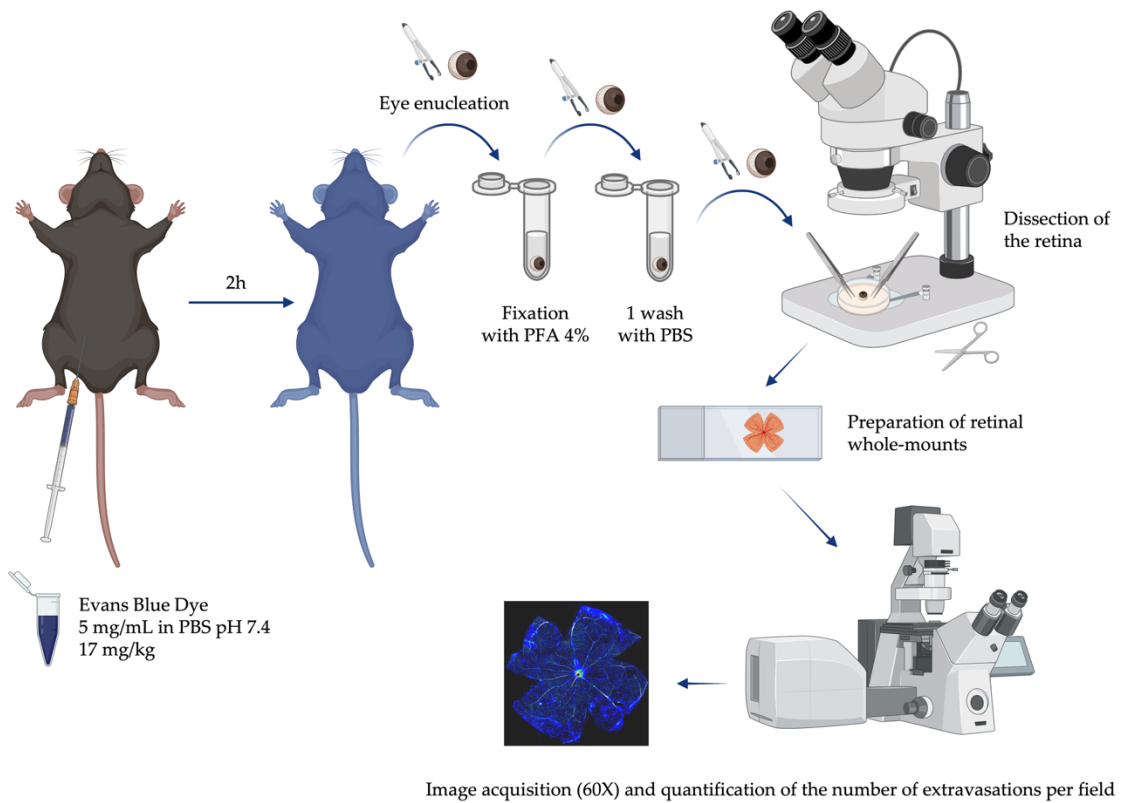


Figure 13. Schematic diagram illustrating the procedure for conducting the Evans Blue Assay.

3.5. Statistical analysis

Data are expressed as the mean \pm standard error of the mean (SEM). For multiple comparisons, a one-way ANOVA followed by the Bonferroni post-hoc test was carried out. Statistical significance was set at a p value of < 0.05 . The analysis was performed with the IBM SPSS statistics software (version 18, IBM, Armonk, NY, USA).

RESULTS

4.1. Study of the mechanisms underlying the beneficial effects of sitagliptin eye drops during early diabetic retinopathy in the db/db model

4.1.1. Monitoring of body weight and systemic blood glucose levels

Db/db mice exhibited significantly elevated blood glucose levels compared to nondiabetic mice (**Figure 14A**), confirming their diabetic condition. There were no differences in body weight or blood glucose levels between diabetic mice treated with sitagliptin or vehicle eye drops (**Figure 14A,B**). These findings suggest that the observed effects that will be described in the next sections can only be attributed to the direct impact of the drug on the retina, rather than any systemic metabolic improvement.

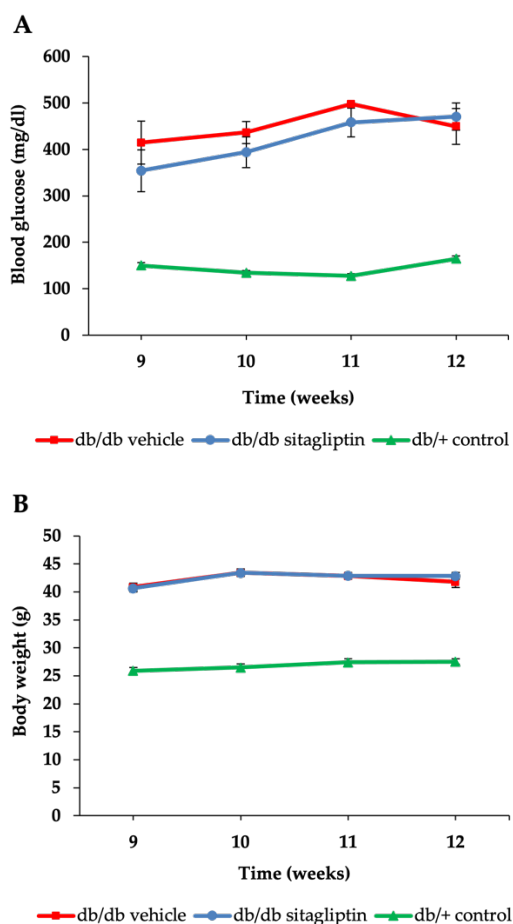


Figure 14. Monitoring of body weight and systemic blood glucose levels. (A) Blood glucose measurements during the course of the experiment in db/db mice treated with sitagliptin (blue circles) or vehicle (red squares),

RESULTS

as well as in db/+ mice (green triangles). **(B)** Body weight course of db/db mice treated with sitagliptin (blue circles) or vehicle (red squares) and db/+ mice (green triangles); $n = 10$.

4.1.2. Transcriptomic study to identify the mechanisms mediating the protective effects of sitagliptin eye drops

4.1.2.1. Multiple transcriptome comparison between all groups

Under an adjusted p-value (Adj.P.Val) of less than 0.05, the comparison between vehicle-treated db/db mice (eye drops) and control db/+ mice, representing the effect of the diabetic condition itself, revealed 19 differential expressed genes (DEGs), with 10 genes up-regulated and 9 genes down-regulated. Furthermore, in the comparison between sitagliptin-treated db/db mice and vehicle-treated db/db mice (effect of sitagliptin administration in diabetic mice), 20 DEGs were identified, with 17 up-regulated genes and 3 down-regulated genes, all at the same level of significance (**Table 6**).

	db/db sitagliptin vs. db/+ control	db/db vehicle vs. db/+ control	db/db sitagliptin vs. db/db vehicle
UpReg_B	65	15	33
DownReg_B	20	13	9
UpRegAdj0.01	18	5	0
DownRegAdj0.01	6	3	0
UpRegAdj0.05	108	10	17
DownRegAdj0.05	33	9	3
UpRegAdj0.15	369	16	185
DownRegAdj0.15	122	14	65
UpRegAdj0.25	728	24	494
DownRegAdj0.25	291	19	195
UpRegP0.01	363	71	275
DownRegP0.01	116	56	96
UpRegP0.05	852	218	82
DownRegP0.01	376	223	329

Table 6. Summary table of the DEGs acquired for each comparison at distinct significance thresholds. $n = 10$.

4.1.2.2. Comparison of retinal expression patterns between diabetic animals treated with sitagliptin and vehicle

To focus on the effect of topical treatment with sitagliptin, a detailed analysis was conducted on the "db/db sitagliptin vs. db/db vehicle" comparison. A HeatMap clustering was performed using transcripts that had an absolute logarithmic fold change (AbsLogFC) greater than or equal to 0.3 and an adjusted p-value (Adj.P.Val) less than 0.05. This analysis revealed two distinct clusters with different expression patterns (**Figure 15**). All samples from each condition were grouped together within their respective clusters, except for the sample "Db/db vehicle_15_1".

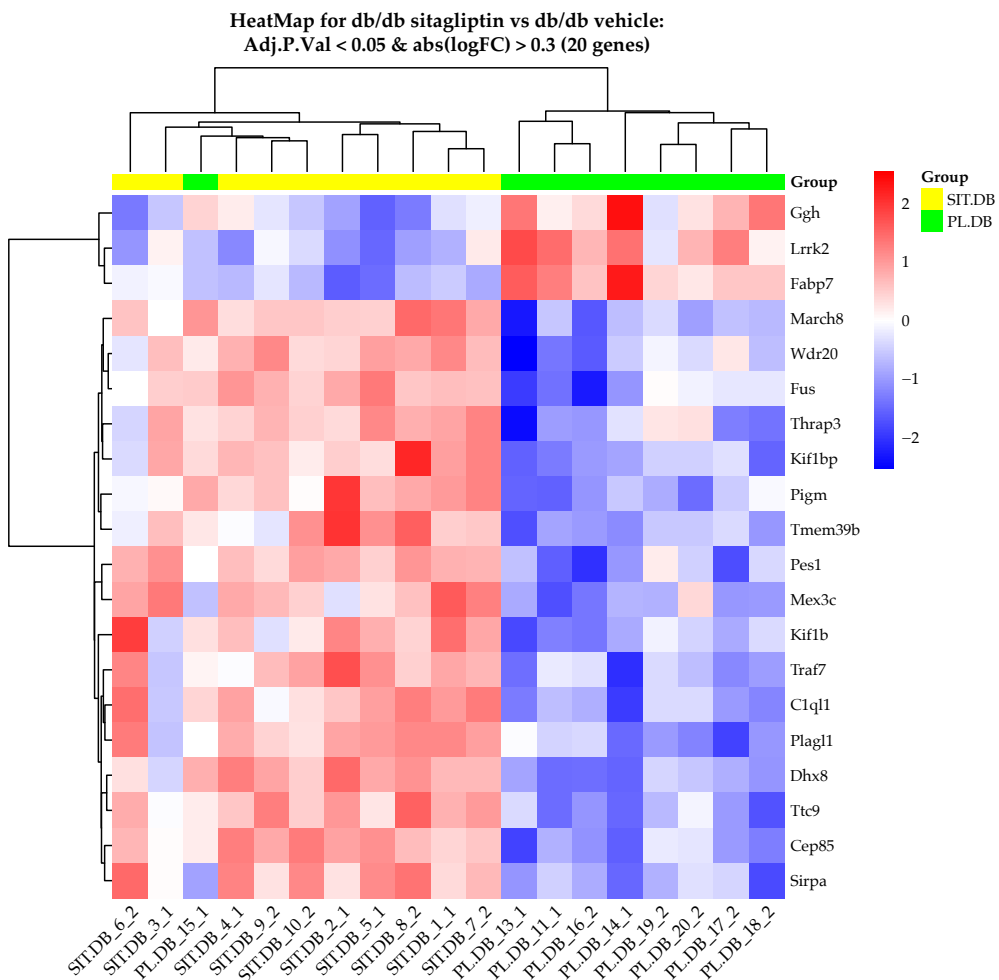


Figure 15. Comparison of retinal expression patterns between db/db mice treated with sitagliptin or vehicle. HeatMap for the comparison between sitagliptin-treated db/db mice and vehicle-treated db/db mice, using genes with an adjusted p-value of less than 0.05 and an absolute LogFC greater than 0.3 (20 genes). High and low row z-scores are represented in red and blue, respectively. $n = 10$.

RESULTS

To highlight the genes with the highest differential expression, a summary table of the top 10 genes and a volcano plot displaying the top 20 genes were generated (Figure 16A,B). A table with the 200 most differentiated genes can be found in the annexes section (Supplementary table 1). These visualizations provide a concise overview of the most significant gene expression changes observed between the "db/db sitagliptin" and "db/db vehicle" groups.

A

Affymetrix.ID	Gene Symbol	Entrez	logFC	AveExpr	t	P.Value	adj.P.Val	B
TC1100003858.mm.2	C1ql1	23,829	0.51	8.46	5.24	0.00	0.04	3.57
TC1000002262.mm.2	Kif1bp	72,320	0.74	7.9	5.07	0.00	0.04	3.12
TC100000093.mm.2	Plagl1	22,634	0.33	8.41	4.73	0.00	0.04	2.2
TC0400003726.mm.2	Cep85	70,012	0.3	9.95	4.71	0.00	0.04	2.15
TC0400004035.mm.2	Kif1b	16,561	0.48	9.05	4.69	0.00	0.04	2.11
TC0400000169.mm.2	Ggh	14,590	-0.46	8.88	-4.69	0.00	0.04	2.1
TC1100000028.mm.2	Pes1	64,934	0.32	10.1	4.67	0.00	0.04	2.04
TC1100001959.mm.2	Sirpa	19,261	0.3	10.66	4.65	0.00	0.04	2
TC1100001296.mm.2	March8	71,779	0.41	8.85	4.63	0.00	0.04	1.95
TC1100003530.mm.2	Thrap3	230,753	0.47	9.15	4.49	0.00	0.04	1.58

B

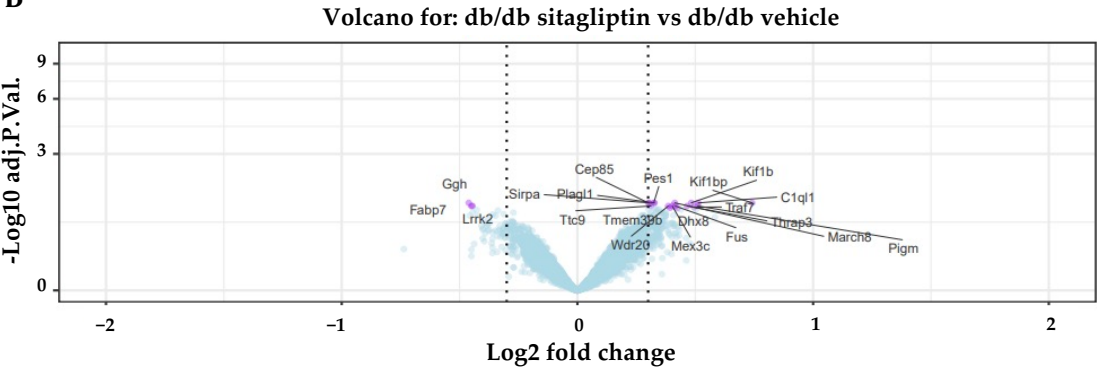


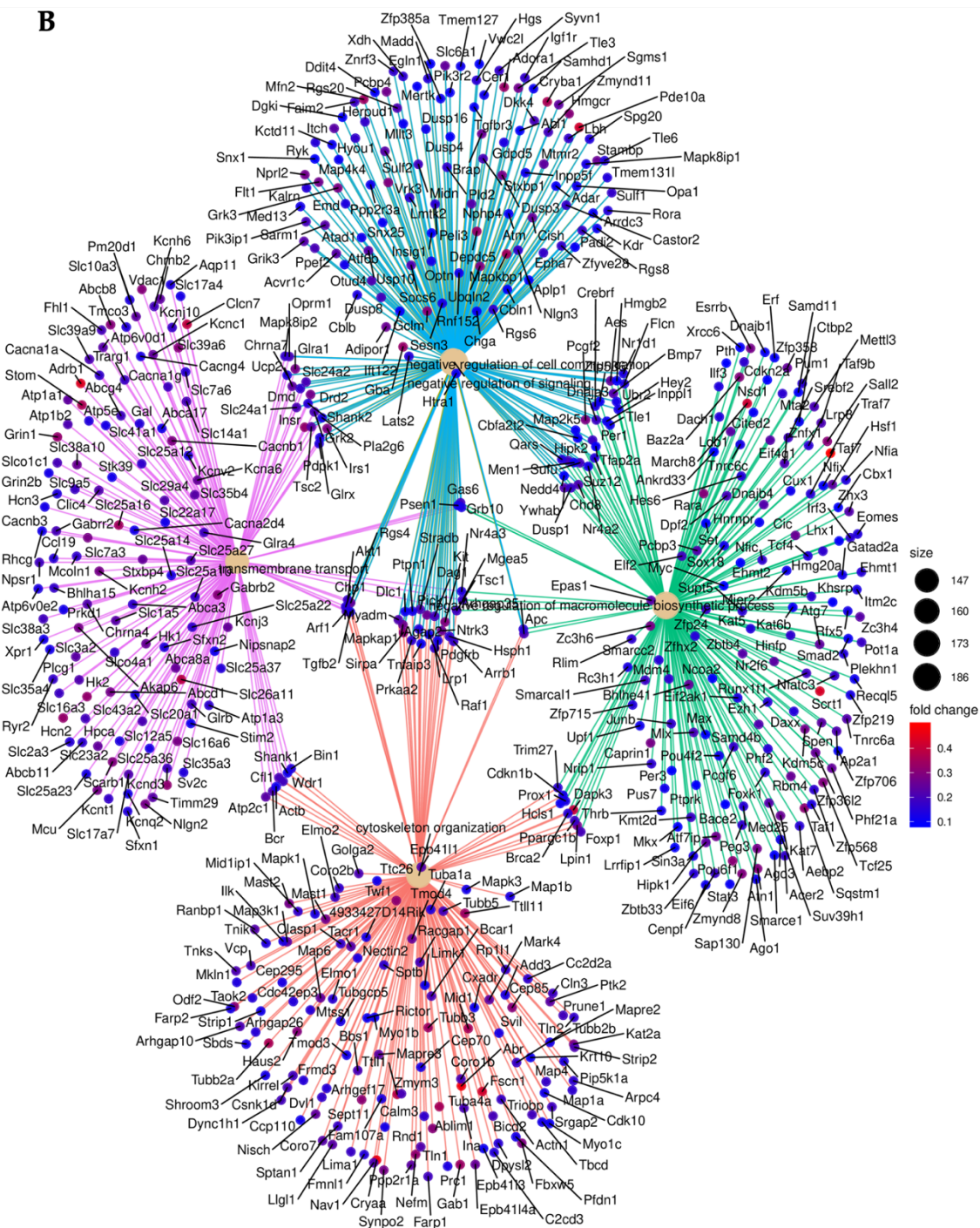
Figure 16. Most differentiated genes. **(A)** Table of the top 10 genes more differentially expressed when comparing mice treated with the vehicle versus those treated with sitagliptin. AveExpr denotes the average gene expression across all arrays on a logarithmic scale (log2), while the "t" statistic represents a moderated-t statistic resembling the conventional Student's t statistic. **(B)** Volcano plot depicting the comparison between db/db mice treated with sitagliptin and db/db mice treated with the vehicle is presented. Genes meeting the criteria of an adjusted p-value below 0.05 and an absolute logarithmic fold change above 0.3 are highlighted in purple. The top 20 most significant genes are labelled with their respective gene symbols.

4.1.2.3. Assessment of the biological significance of the obtained results: gene set enrichment analysis

Gene set enrichment analyses (GSEA), a robust method for interpreting gene expression data, was employed to assess the biological significance²²⁷. The analysis utilized two distinct annotation databases: the GO database with a focus on the Biological Process (BP) subcategory, and the Reactome Pathway Database (RPD). The results from both analyses consistently highlighted neurotransmission as the most distinctive biological process between the transcriptomes of sitagliptin-treated db/db mice and vehicle-treated mice. In the Gene Ontology (GO) analysis, enriched terms encompassed more general and non-cell-type-specific categories such as transmembrane transport, cytoskeleton organization, secretion, negative regulation of cell communication, and others (Figure 17A–C). A positive normalized enrichment score (NES) indicates that the enriched term is mainly composed of up-regulated genes, whereas a negative score indicates the opposite.

A

ID	Description	Set Size	Enrichment Score	NES	P.Value	adj.P.Val
GO:0055085	transmembrane transport	466	0.33	1.46	0.00	0.07
GO:0007010	cytoskeleton organization	483	0.34	1.51	0.00	0.07
GO:0010558	negative regulation of macromolecule biosynthetic process	468	0.33	1.47	0.00	0.07
GO:0010648	negative regulation of cell communication	477	0.34	1.52	0.00	0.07
GO:0023057	negative regulation of signaling	477	0.34	1.52	0.00	0.07
GO:0033043	regulation of organelle organization	485	0.31	1.39	0.00	0.07
GO:0045934	negative regulation of nucleobase-containing compound metabolic process	467	0.31	1.39	0.00	0.07
GO:0046903	secretion	418	0.32	1.45	0.00	0.07
GO:0051253	negative regulation of RNA metabolic process	415	0.33	1.47	0.00	0.07
GO:2000113	negative regulation of cellular macromolecule biosynthetic process	458	0.33	1.48	0.00	0.07

B

- cytoskeleton organization
- negative regulation of cell communication
- negative regulation of macromolecule biosynthetic process
- negative regulation of signaling
- transmembrane transport

C

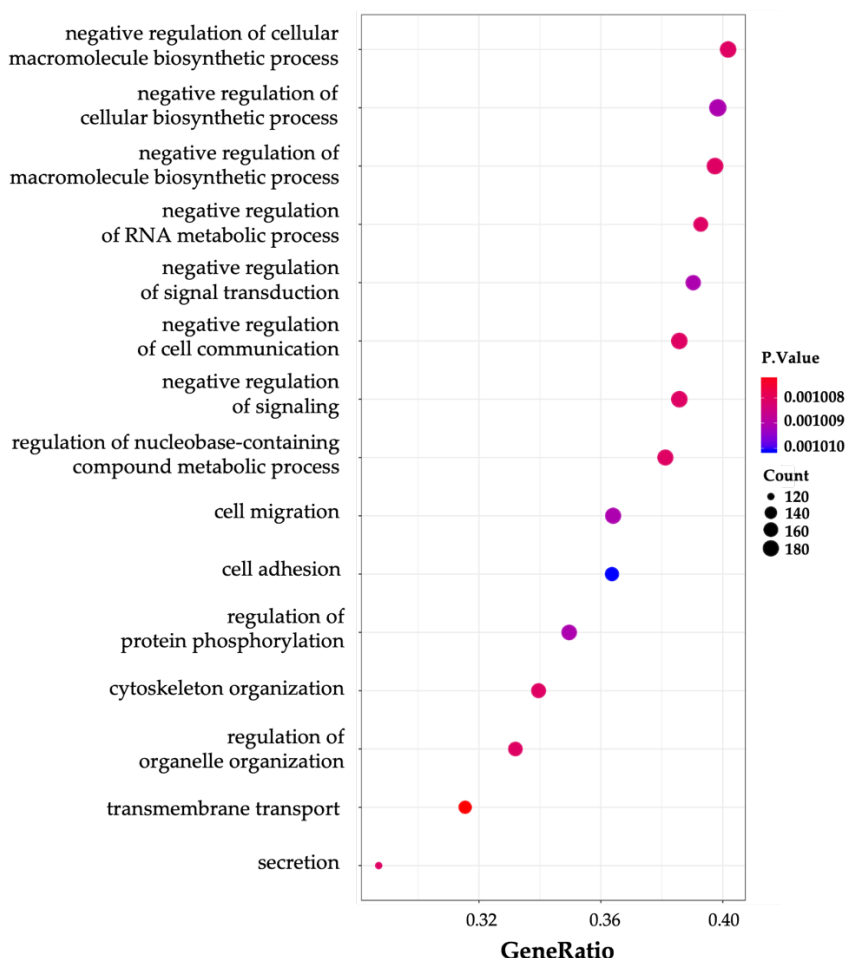


Figure 17. Enrichment analysis of the transcriptome study between db/db mice treated with vehicle and db/db mice treated with sitagliptin using the GO Database (BP subcategory). (A) Table of top 10 enriched GO terms (BP) for the comparison “db/db sitagliptin vs. db/db vehicle”. (B) Network plot of the top five enriched GO term (BP) for “db/db sitagliptin vs. db/db vehicle”. (C) Dot plot of the top 15 enriched GO terms (BP) for the “db/db sitagliptin vs. db/db vehicle” comparison. Results were adjusted with a p-value less than 0.25. The results shown correspond to the top enriched terms with an adjusted p-value < 0.07.

The RPD analysis showed the influence of sitagliptin in the neuronal components of the retina through terms such as: neuronal system, transmission across chemical synapses, neurotransmitters receptors and postsynaptic signal transmission, membrane trafficking, vesicle-mediated transport, etc. (Figure 18A–C). A table with the 50 most enriched pathways obtained with the RPD analysis can be found in the annexes section (Supplementary table 2). In relation to the most enriched biological pathways, the specific HeatMaps related to

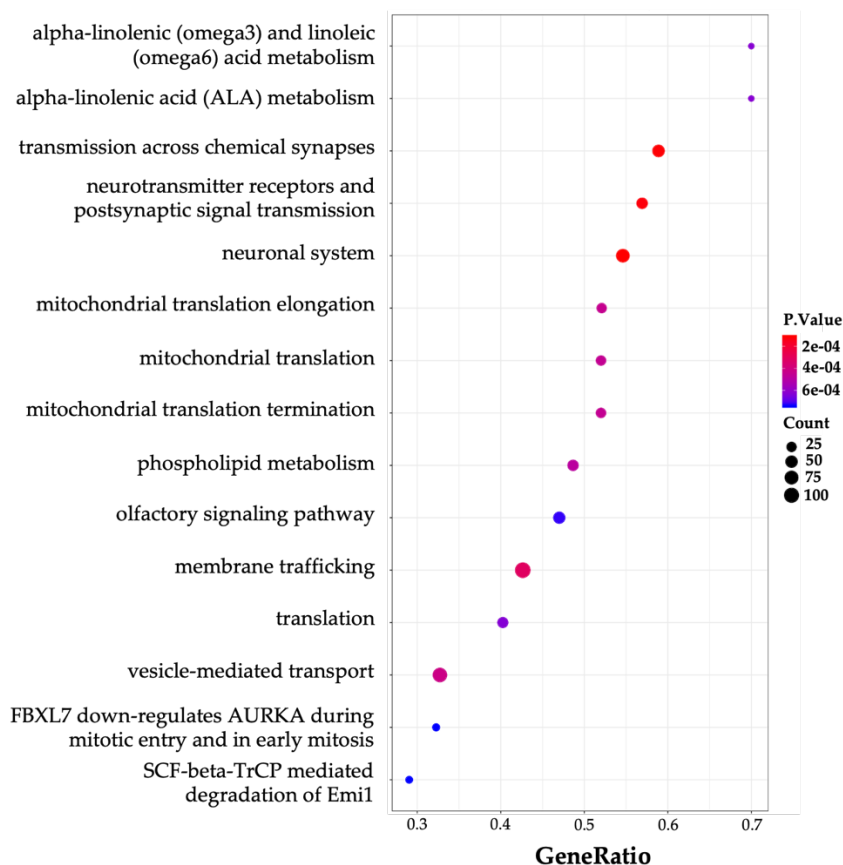
RESULTS

neurotransmission show clear differential expression patterns between both groups and also expose which genes belong to these pathways (**Figure 19A–C**).

A

ID	Description	Set Size	Enrichment Score	NES	P.Value	adj.P.Val
R-MMU-112316	neuronal system	130	0.52	2.13	0.00	0.03
R-MMU-112315	transmission across chemical synapses	90	0.58	2.27	0.00	0.03
R-MMU-112314	neurotransmitter receptors and postsynaptic signal transmission	65	0.58	2.16	0.00	0.03
R-MMU-199991	membrane trafficking	258	0.37	1.61	0.00	0.03
R-MMU-5653656	vesicle-mediated transport	269	0.36	1.59	0.00	0.03
R-MMU-5389840	mitochondrial translation elongation	48	−0.51	−2.17	0.00	0.03
R-MMU-5368287	mitochondrial translation	50	−0.48	−2.05	0.00	0.03
R-MMU-5419276	mitochondrial translation termination	50	−0.48	−2.05	0.00	0.03
R-MMU-1483257	phospholipid metabolism	74	0.48	1.81	0.00	0.03
R-MMU-2046104	alpha-linolenic (omega3) and linoleic (omega6) acid metabolism	10	0.78	1.89	0.00	0.03

B



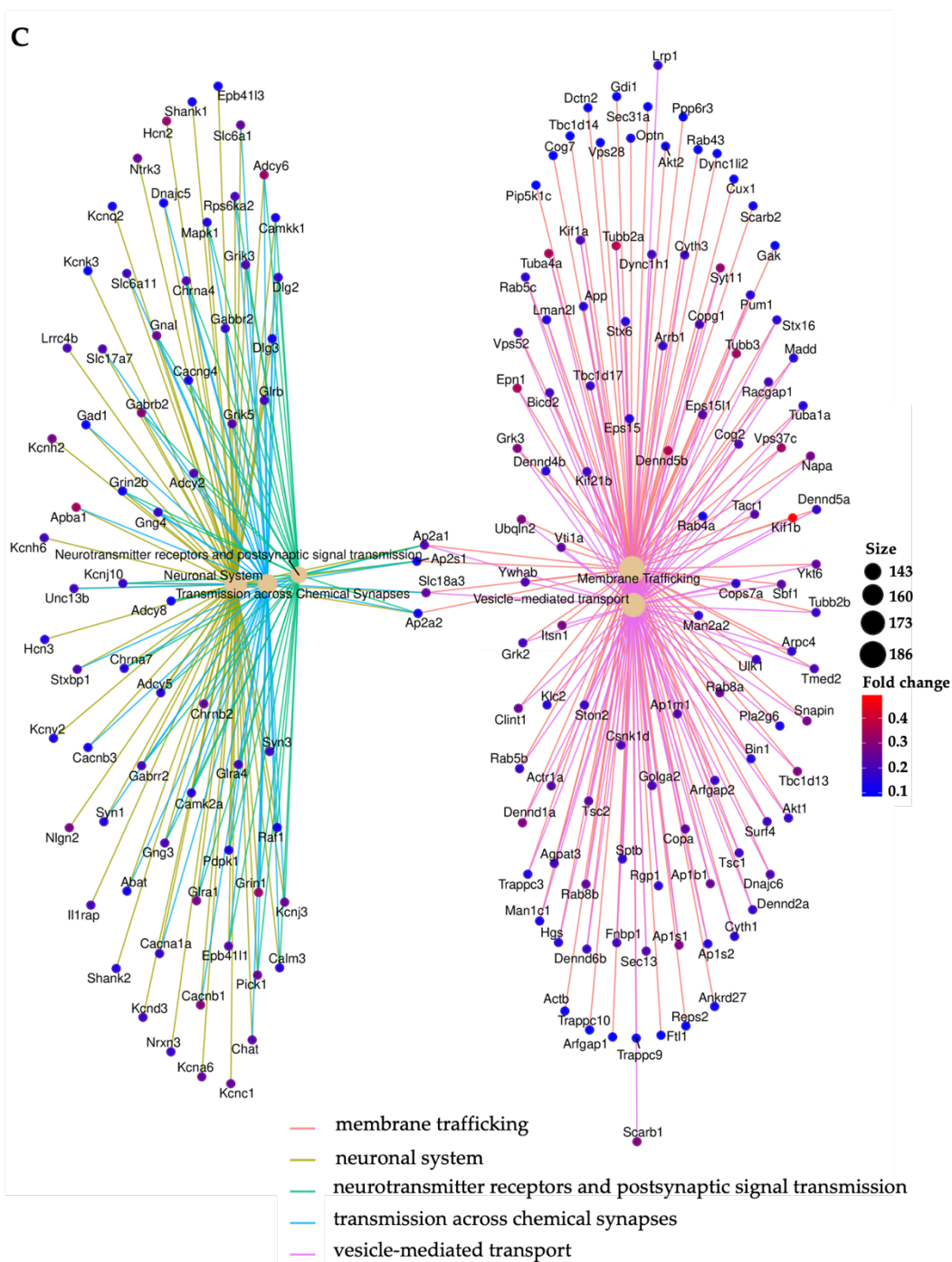


Figure 18. Enrichment analysis of the transcriptome comparison between vehicle-treated db/db mice and db/db mice treated with sitagliptin using the RPD. (A) Table of the top 10 enriched pathways (RPD) for the comparative study “db/db sitagliptin vs. db/db vehicle”. (B) Dot plot of the top 15 enriched pathways (RPD). (C) Network plot of the top five enriched pathways for the comparison between db/db sitagliptin and db/db vehicle conditions (RPD). The results shown correspond to the top enriched terms with an adjusted p-value < 0.05.

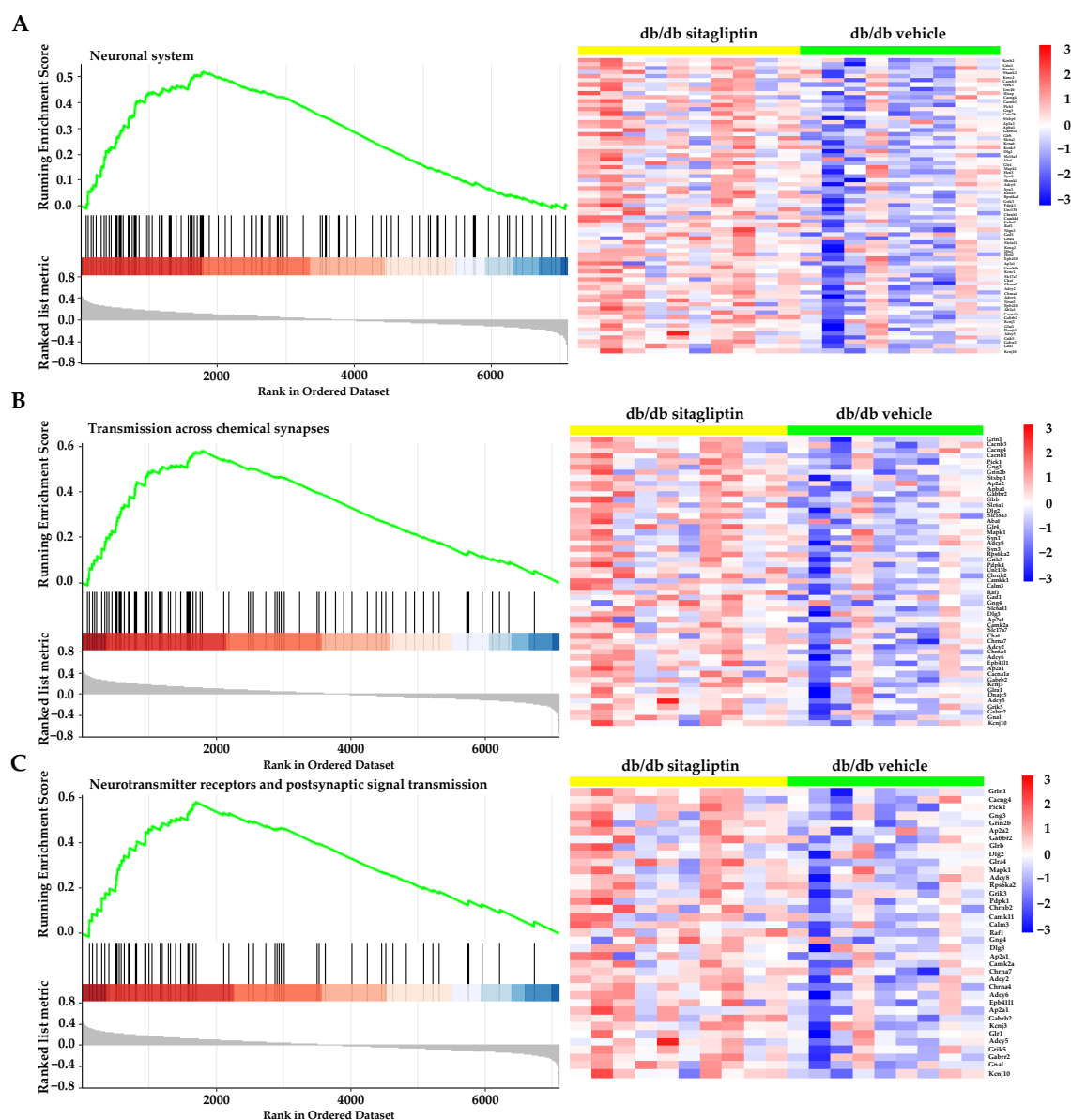
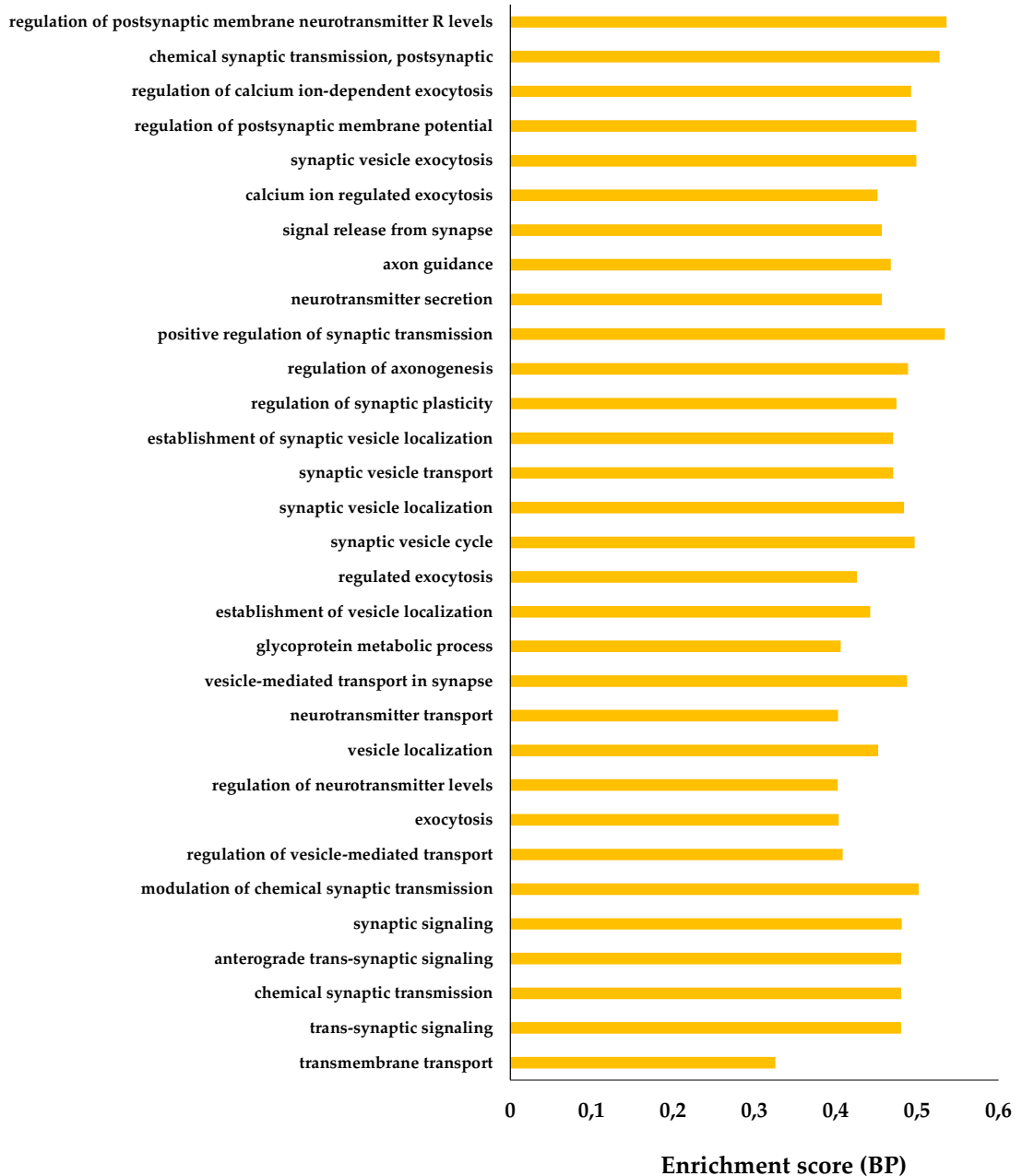


Figure 19. Gene set enrichment analysis (GSEA). (A–C) HeatMaps of the most enriched neurotransmission-related pathways between vehicle-treated db/db mice and sitagliptin-treated db/db mice.

Upon refining the GO study by narrowing the search to neuronal terms, we performed a reanalysis that verified the findings of the RPD analysis (Figure 20A). Furthermore, Figure 20B illustrates an enrichment map depicting the most distinctive gene sets linked to synaptic transmission within the sitagliptin vs. vehicle comparison.

A



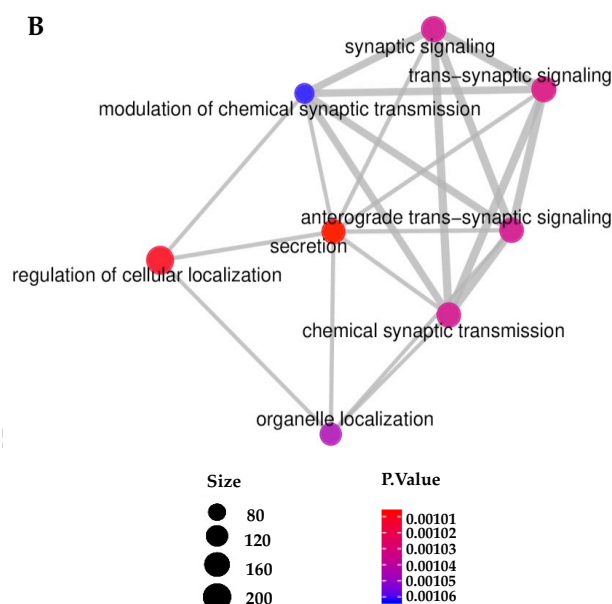


Figure 20. Sitagliptin-enhanced pathways linked to synaptic transmission. **(A)** Most enriched terms involved in neurotransmission between db/db mice treated with sitagliptin and vehicle-treated db/db mice using the GO database and the Biological Process (BP) subcategory (p-value < 0.005). X-axis represents the enrichment score for each category. **(B)** Cluster related to synaptic transmission from the GO enrichment map of the top 60 enriched terms (BP) between db/db sitagliptin and db/db vehicle.

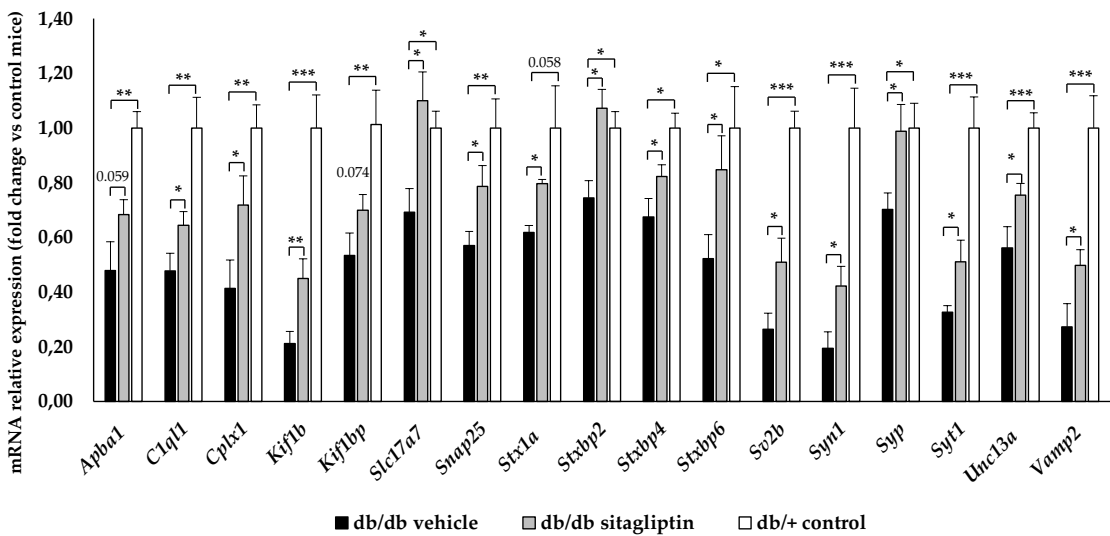
4.1.2.4. Evaluation of retinal gene expression of proteins related to synapse formation, maintenance and synaptic transmission

To validate the findings obtained from the individual gene studies and the GSEA, a comprehensive approach was taken. Apart from the genes identified in these analyses, other genes with significant roles in the obtained enriched pathways were also included. This comprehensive gene selection aimed to strengthen the validity of the results and capture a broader understanding of the underlying mechanisms involved in the observed pathways.

In contrast to db/+ control mice, diabetic mice exhibited a notable decrease in the expression of several genes associated with the formation and maintenance of synapses [complement C1q-like 1 (*C1ql1*); kinesin family member 1B (*Kif1b*); KIF-1 binding protein (*Kif1bp*)], synaptic transmission at presynaptic level [amyloid beta precursor protein-binding family A member 1 (*Apha1*); complexin 1 (*Cplx1*); solute carrier family 17 member 7 (*Slc17a7*); synaptosome-associated protein 25 (*Snapt25*); syntaxin-1A (*Stx1a*); syntaxin-binding protein 2, 4 and 6 (*Stxbp2*, *Stxbp4* and *Stxbp6*); synaptic vesicle glycoprotein 2B (*Sv2b*); synapsin I (*Syn1*); synaptophysin (*Syp*); synaptotagmin (*Syt1*); Unc-13 homolog A (*Unc13A*); vesicle-associated membrane

protein 2 (*Vamp2*)] and postsynaptic level [calcium/calmodulin-dependent serine protein kinase (*Cask*); discs large MAGUK scaffold protein 2 and 4 (*Dlg2* and *Dlg4*); glutamate ionotropic receptor AMPA-type subunit 1 (*Gria1*); glutamate ionotropic receptor NMDA-type subunit 1, 2B and 2D (*Grin1*, *Grin2b* and *Grin2d*)] (**Figure 21A,B**). Topical administration of sitagliptin in db/db mice effectively prevented these abnormal expression patterns. Sitagliptin treatment led to a significant rescue of down-regulated genes involved in synapse-related processes (**Figure 21A,B**).

A



B

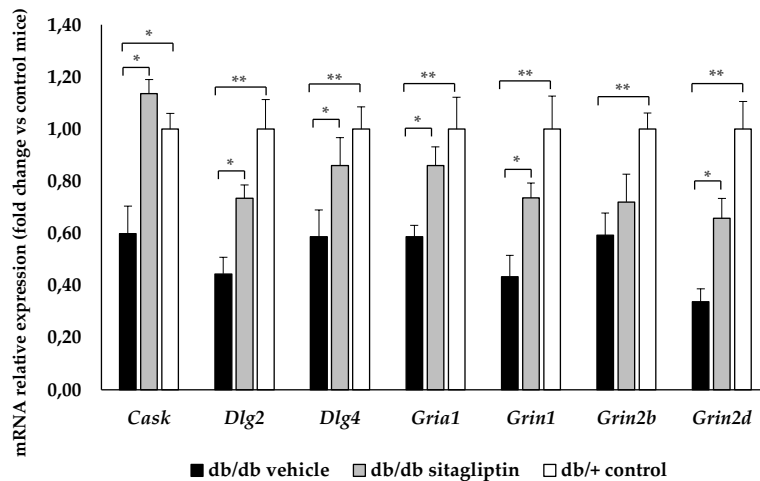


Figure 21. Evaluation of gene expression. **(A)** RT-PCR analysis of genes related to synapse formation and neurotransmission at presynaptic level in vehicle-treated db/db mice (black bars), sitagliptin-treated db/db mice (grey bars) and in non-diabetic mice (white bars) **(B)** RT-PCR analysis of genes associated with neurotransmission at postsynaptic level in vehicle-treated db/db mice (black bars), sitagliptin-treated db/db mice (grey bars) and in control mice (white bars). $n = 4$; * $p < 0.05$, ** $p < 0.01$.

RESULTS

Furthermore, the STRING interactions analysis revealed a close relationship and interconnectedness between all the analyzed genes, emphasizing their collective importance in synaptic function and regulation (Figure 22).

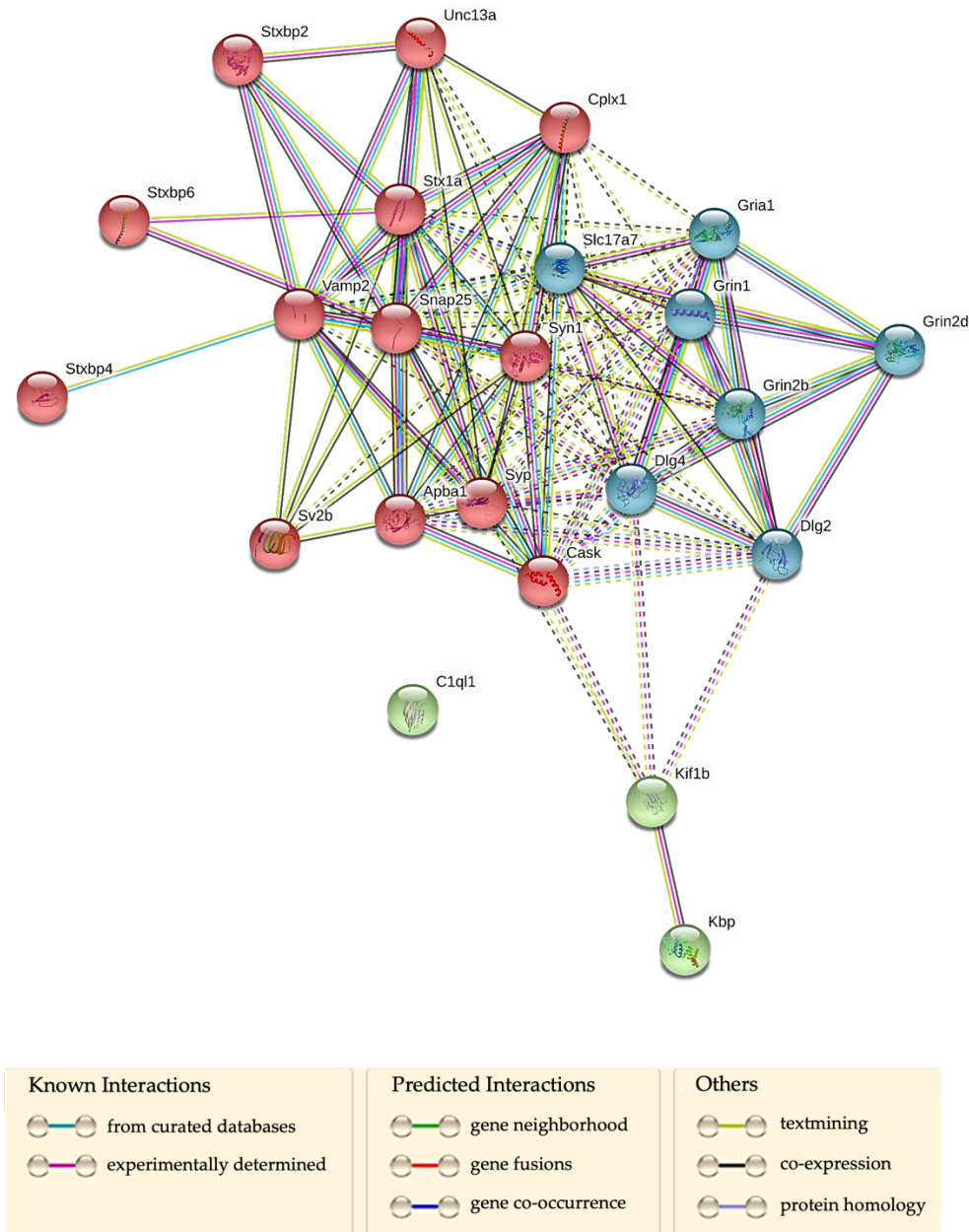


Figure 22. Gene interactions of studied genes (STRING version 11.5). The red cluster represents genes associated with presynaptic proteins, the blue cluster exhibits genes linked to postsynaptic proteins and the green cluster illustrates genes associated with synaptic formation. Dashed lines indicate interactions between genes from different clusters, while solid lines indicate interactions of genes from the same cluster.

4.1.2.5. Examination of presynaptic protein content in the retina

Consistent with previous literature findings²³⁴, diabetic mice exhibited reduced levels of presynaptic proteins compared to control mice. Topical (eye drops) administration of sitagliptin prevented this abnormality and restored the expression of presynaptic proteins in the retina. Similar results were obtained for the protein encoded by the most differentially expressed gene identified in the transcriptomic analysis (*C1ql1*) (Figure 23 and Figure 24).

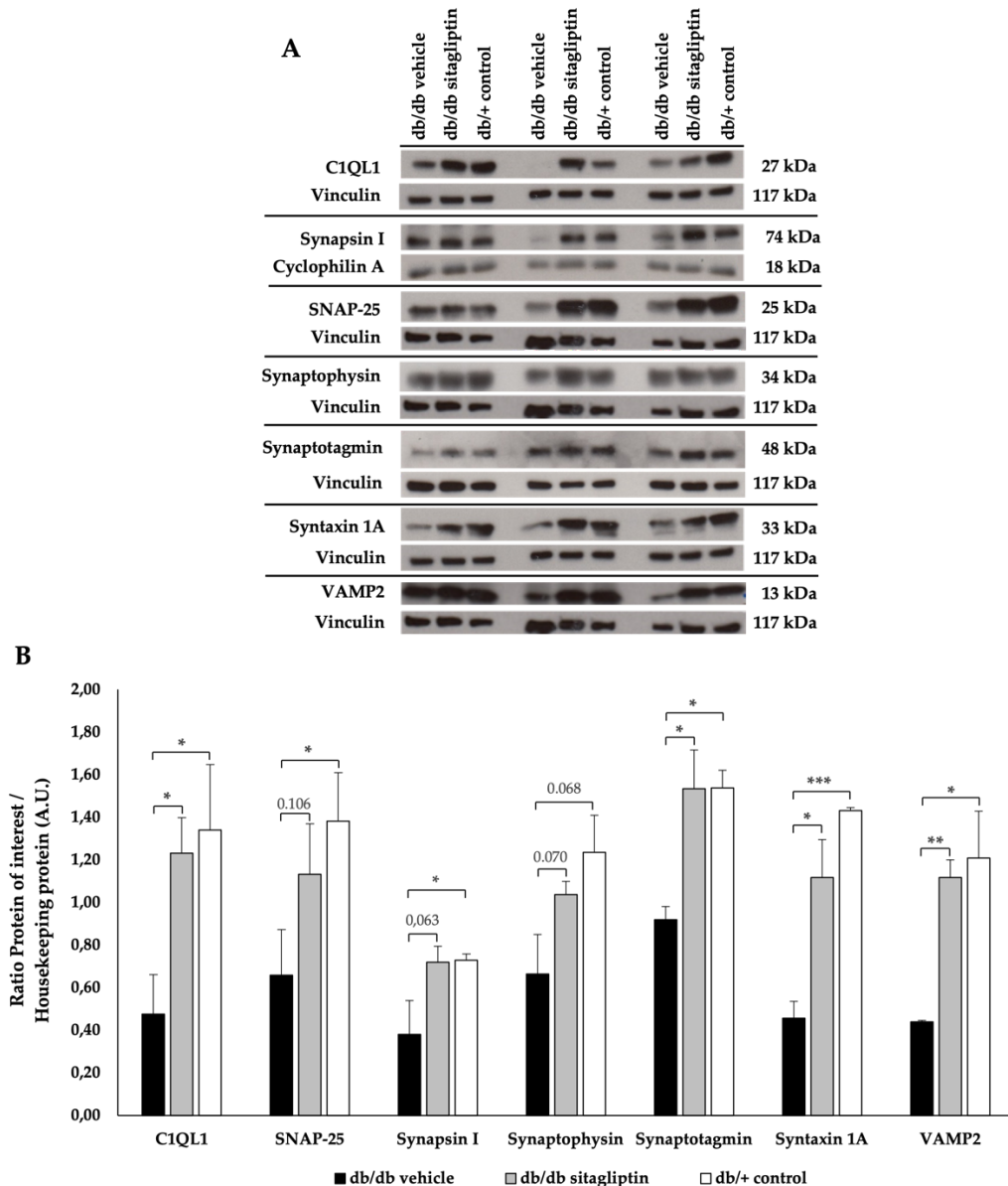
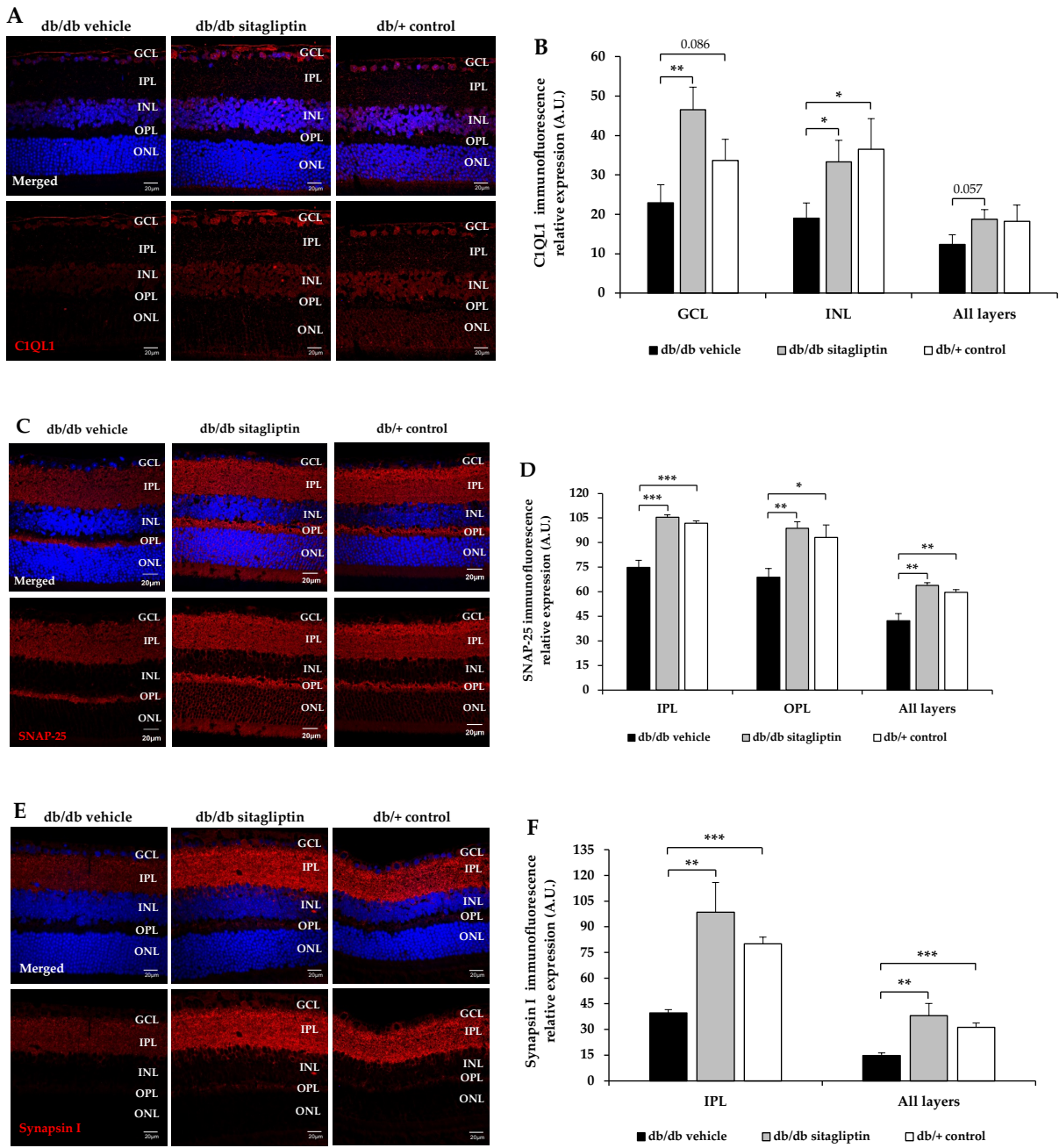


Figure 23. Protein levels of C1ql1 and presynaptic proteins. (A,B) Western Blot bands and densitometric analysis of C1ql1 and presynaptic proteins corresponding to retinas of db/db mice treated with vehicle eye drops (black

RESULTS

bars), sitagliptin eye drops (grey bars) and to non-diabetic mice retinas (white bars). Protein levels were normalized with vinculin. $n = 3$; * $p < 0.05$, ** $p < 0.01$, *** $p < 0.001$.



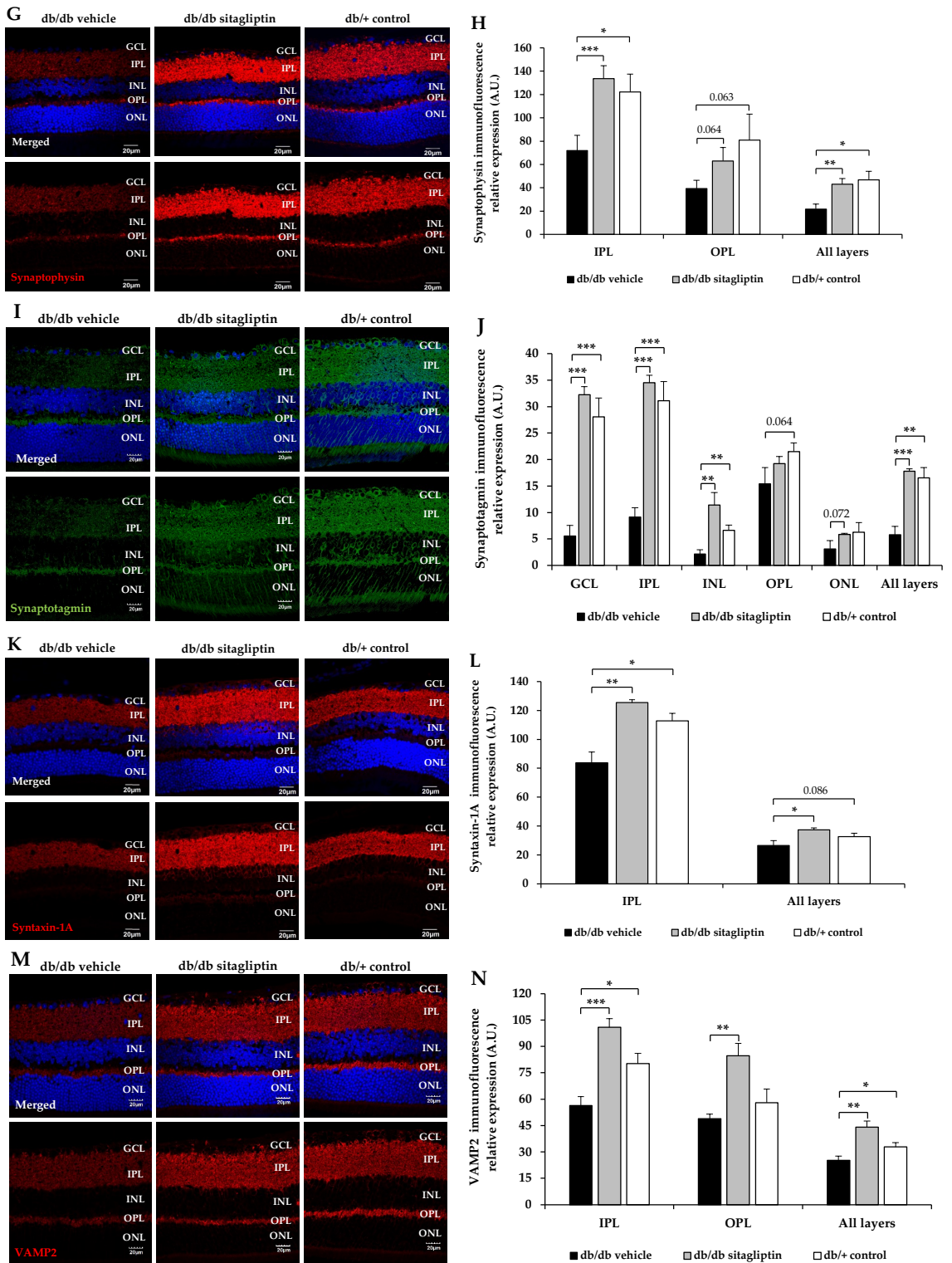


Figure 24. Immunofluorescence analysis of C1QL1 and presynaptic proteins. (A,C,E,G,I,K,M) Comparison of immunofluorescence intensities between representative samples from the respective experimental groups.

RESULTS

Proteins studied are: C1QL1 (red), SNAP-25 (red), synapsin I (red), synaptophysin (red), synaptotagmin (green), syntaxin-1A (red), and VAMP-2 (red). Relative fluorescence intensities are displayed both alone and in combination with Hoechst nuclei staining (blue). Scale bars, 20 μ m. GCL: ganglion cell layer; IPL: inner plexiform layer; INL: inner nuclear layer; OPL: outer plexiform layer; ONL: outer nuclear layer. (B,D,F,H,J,L,N) Quantification of immunofluorescence intensities. Db/db vehicle group is represented with black bars, while db/db sitagliptin group and control group are represented with grey and white bars respectively. $n = 4$; * $p < 0.05$, ** $p < 0.01$, *** $p < 0.001$.

4.1.3. Study of the effect of sitagliptin eye drops on oxidative stress and inflammation

4.1.3.1. Evaluation of antioxidant defenses

NRF2 is a transcription factor that is sensitive to changes in cellular redox state. It plays a crucial role in NVU by regulating the expression of antioxidant enzymes, modulating microglial dynamics, and providing protection to neurons and astrocytes against toxic substances²³⁵. NRF2 binds to specific DNA sequences called AREs, which are located in the promoter regions of genes encoding various antioxidant enzymes such as CuZnSOD, MnSOD, CAT, GPX, and GR²³⁶. In db/db mice, both messenger RNA (mRNA) and protein levels of NRF2 were found to be decreased. However, treatment with topical sitagliptin prevented the decline in protein levels across all retinal layers (Figure 25A–D). Similarly, the mRNA and protein levels of antioxidant enzymes, including CuZnSOD, MnSOD, CAT, GPX, and GR, were downregulated in the retinas of db/db mice. Sitagliptin administration effectively prevented these reductions in most enzymes, except for catalase, where it had a neutral effect (Figure 26A–E). Notably, sitagliptin administration significantly prevented the downregulation of MnSOD in all retinal layers (Figure 26F,G) and CuZnSOD specifically in the GCL (Figure 26D,E).

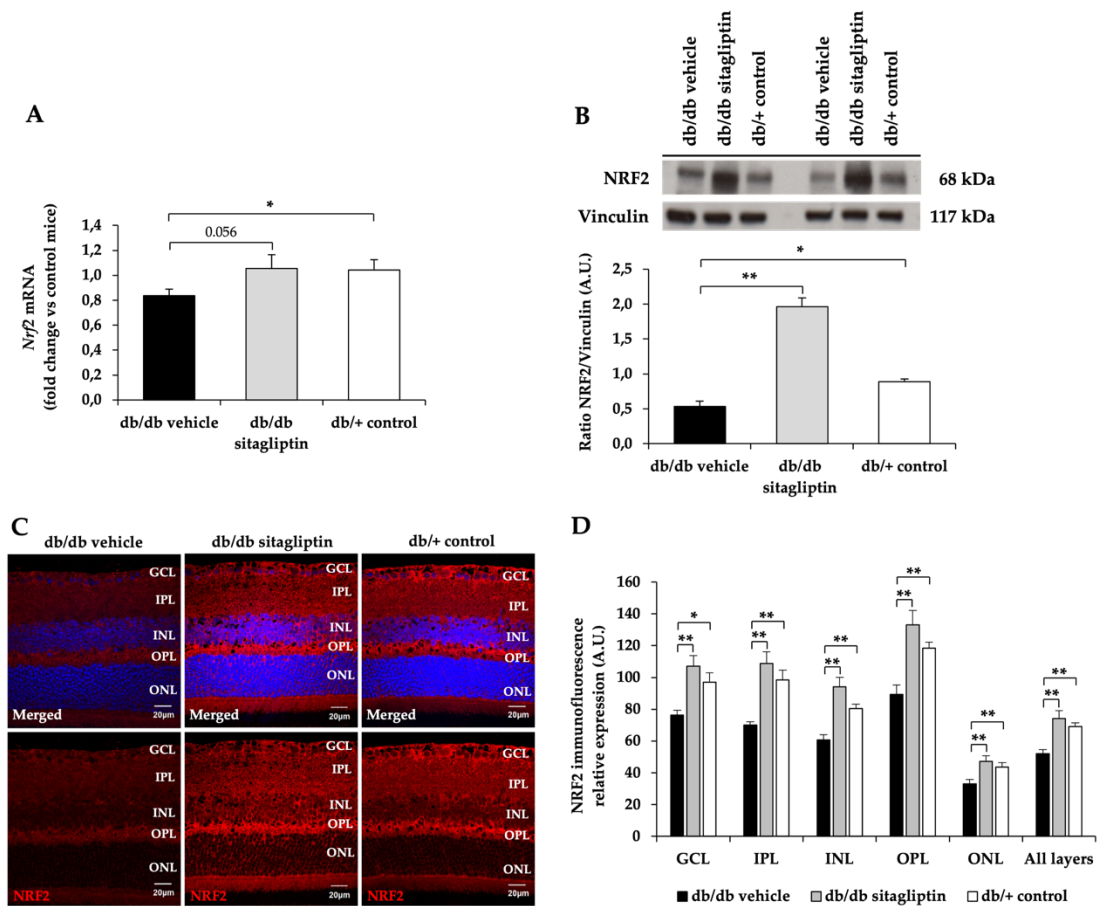


Figure 25. Examination of the mRNA and protein levels of NRF2. **(A)** RT-PCR analysis of the gene that codifies for NRF2 (*Nrf2*) in vehicle-treated db/db mice (black bars), sitagliptin-treated db/db mice (grey bars), and in db/+ mice (white bars). Results are presented as fold change vs. control mice. $n = 4$. **(B)** Western Blot bands and densitometric analysis of NRF2 protein levels in retinas of db/db mice treated with vehicle (black bars) or sitagliptin (grey bars), and in retinas of nondiabetic mice (white bars); $n = 3$. **(C,D)** Representative images and quantifications of retinal immunofluorescence staining for NRF2 (red) in diabetic mice treated with vehicle eye drops (black bars), sitagliptin eye drops (grey bars), and control mice (white bars). Relative fluorescence intensities are displayed both alone and in combination with Hoechst nuclei staining (blue). GCL (ganglion cell layer), IPL (inner plexiform layer), INL (inner nuclear layer), OPL (outer plexiform layer), ONL (outer nuclear layer). Scale bars, 20 μm ; $n = 4$; * $p < 0.05$; ** $p < 0.01$.

RESULTS

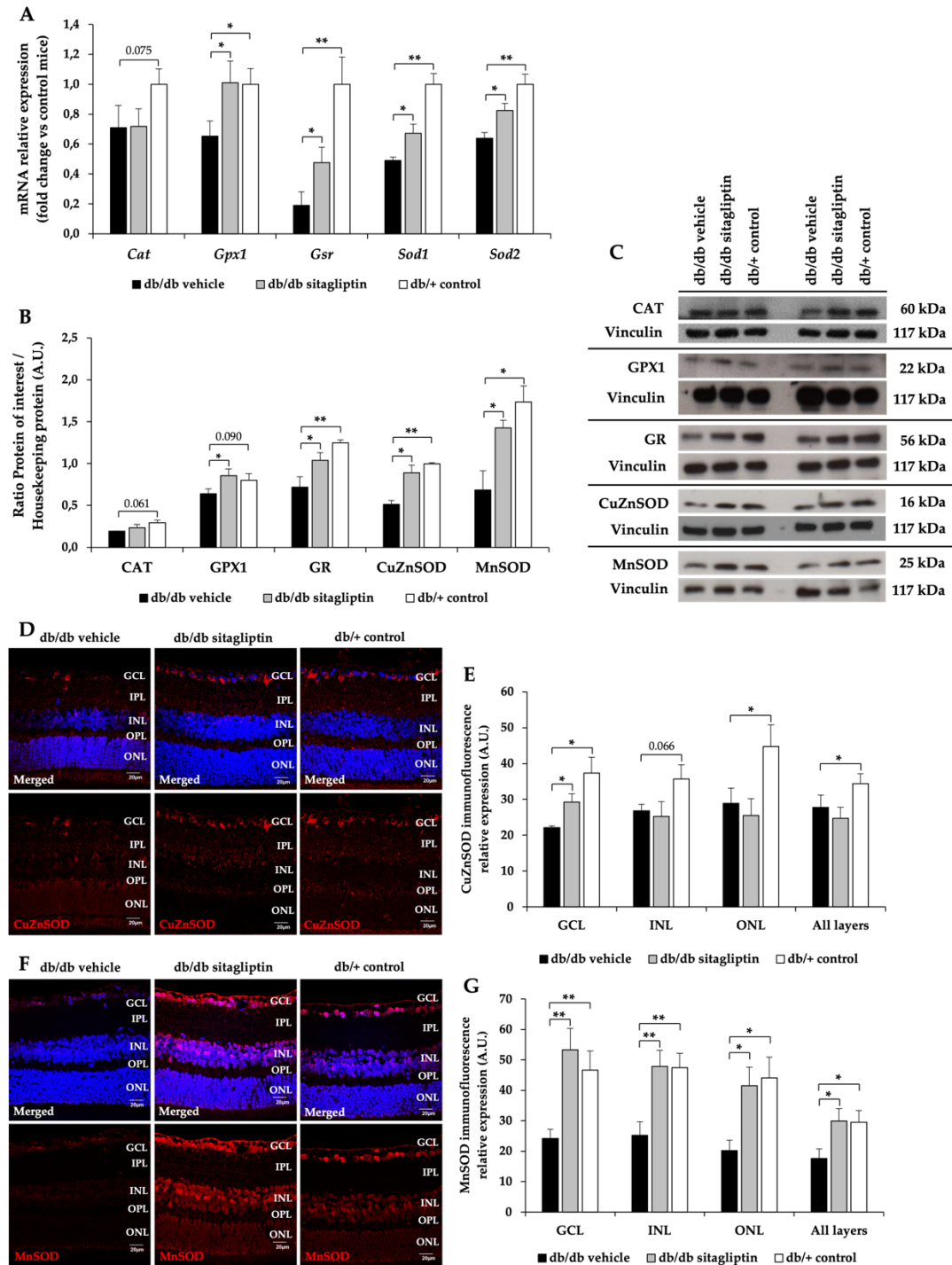


Figure 26. Study of the mRNA and protein levels of the most relevant antioxidant enzymes. (A) RT-PCR analysis of the genes that codify for CAT (*Cat*), GPX isoform 1 (*Gpx1*), GR (*Gsr*), CuZnSOD (*Sod1*) and MnSOD (*Sod2*) in vehicle-treated db/db mice (black bars), sitagliptin-treated db/db mice (grey bars) and in db/+ mice (white bars). Results are presented as fold change vs control mice; $n = 4$. (B,C) Densitometric analysis and Western Blot bands of CAT, GPX isoform 1 (GPX1), GR, CuZnSOD and MnSOD protein levels in retinas of db/db mice treated with vehicle (black bars)

or sitagliptin (grey bars) and in retinas of control mice (white bars); $n = 3$. (D-G) Representative images and quantifications of the retinal immunofluorescences of CuZnSOD (red) (D,E) and MnSOD (red) (F,G) in vehicle-treated db/db mice (black bars), sitagliptin-treated db/db mice (grey bars) and in db/+ mice (white bars). Relative fluorescence intensities are displayed both alone and in combination with Hoechst nuclei staining (blue). GCL (ganglion cell layer), IPL (inner plexiform layer), INL (inner nuclear layer), OPL (outer plexiform layer), ONL (outer nuclear layer). Scale bars, 20 μm ; $n = 4$; * $p < 0.05$; ** $p < 0.01$.

NRF2 regulates the transcription of other genes whose physiological expression is disrupted by high glucose levels and oxidative stress, such as the gene encoding thioredoxin interacting protein (TXNIP)^{237,238}. TXNIP expression has been extensively associated with hyperglycemia in retinal cell cultures, and its persistent expression over time contributes to oxidative stress, inflammation, and premature cell death²³⁷. In db/db mice treated with vehicle, there was a notable increase in the number of TXNIP-positive cells compared to control mice. However, in sitagliptin-treated db/db mice, the levels of TXNIP-positive cells were comparable to those observed in control mice, indicating a potential protective effect of sitagliptin against TXNIP-mediated cellular effects. (Figure 27A-C)

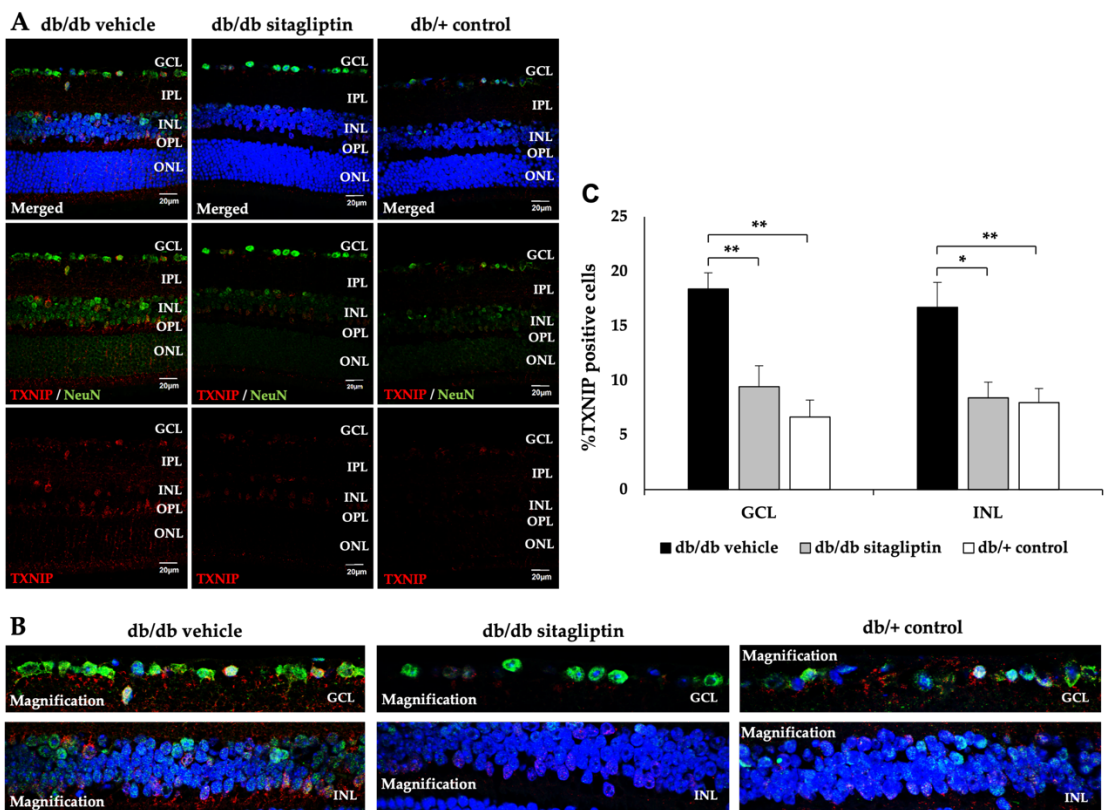


Figure 27. TXNIP immunofluorescence analysis. (A-C) Representative images (A), with a magnification of the GCL and INL layers (B), and positive cell count (C) of TXNIP (red) retinal immunofluorescences in vehicle-treated db/db mice (black bars), sitagliptin-treated db/db mice (grey bars) and db/+ mice (white bars). NeuN (green) and Hoechst staining (blue) are used as neuronal and nuclei markers respectively. GCL (ganglion cell layer), IPL (inner plexiform

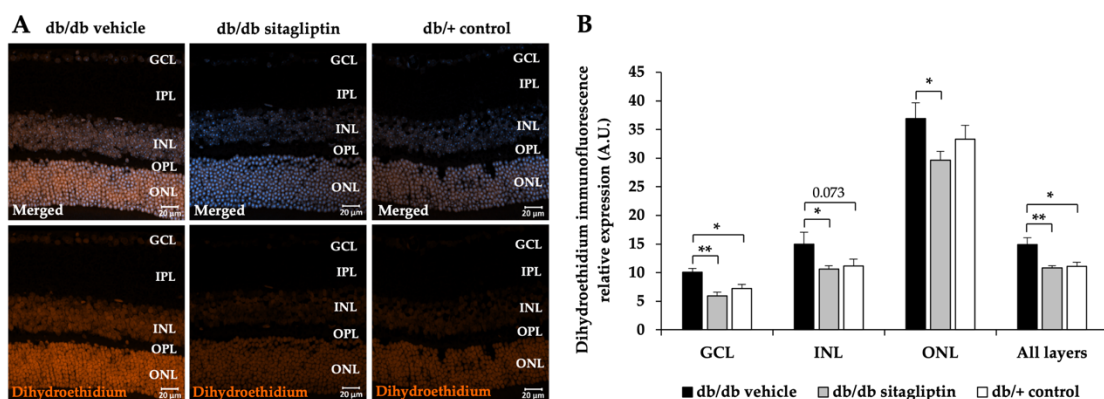
RESULTS

layer), INL (inner nuclear layer), OPL (outer plexiform layer), ONL (outer nuclear layer). Scale bars, 20 μm . $n = 4$; * $p < 0.05$; ** $p < 0.01$.

4.1.3.2. Assessment of superoxide anion levels and nitro-oxidative damage to biological macromolecules

The diabetic retina experiences increased oxidative stress due to the excessive generation of superoxide radicals, which is primarily associated with hyperglycemia. To detect and quantify superoxide production, a hydrophobic and uncharged molecule called dihydroethidium (5-ethyl-5,6-dihydro-6-phenyl-3,8-diaminophe-nanthridine, hydroethidine) (DHE) is commonly used. DHE has the unique property of crossing both extracellular and intracellular membranes, where it undergoes oxidation by superoxide radicals, resulting in the formation of two distinct fluorescent products: ethidium and 2-hydroxyethidium²³⁹. This staining technique utilizing DHE enables the detection and assessment of superoxide levels within the retinal tissue. DHE IF intensity was higher in the nuclear layers of diabetic mice compared to non-diabetic mice and we observed that topical administration of sitagliptin reduced hyperglycemia-related superoxide overproduction. (Figure 28A, B).

Elevated levels of ROS and reactive nitrogen species can lead to binding with DNA, proteins, and lipids, causing cellular damage and dysfunction²⁴⁰. Markers such as 8-hydroxyguanosine (the predominant product of DNA/RNA oxidative damage) and nitrotyrosine are commonly used to assess oxidative stress-induced DNA/RNA damage and protein nitration, respectively^{241,242}. In our study, both markers were significantly higher in the nuclear layers of diabetic retinas treated with vehicle compared to non-diabetic retinas. Notably, sitagliptin treatment effectively prevented these diabetic retinopathy-related abnormalities (Figure 28C-F).



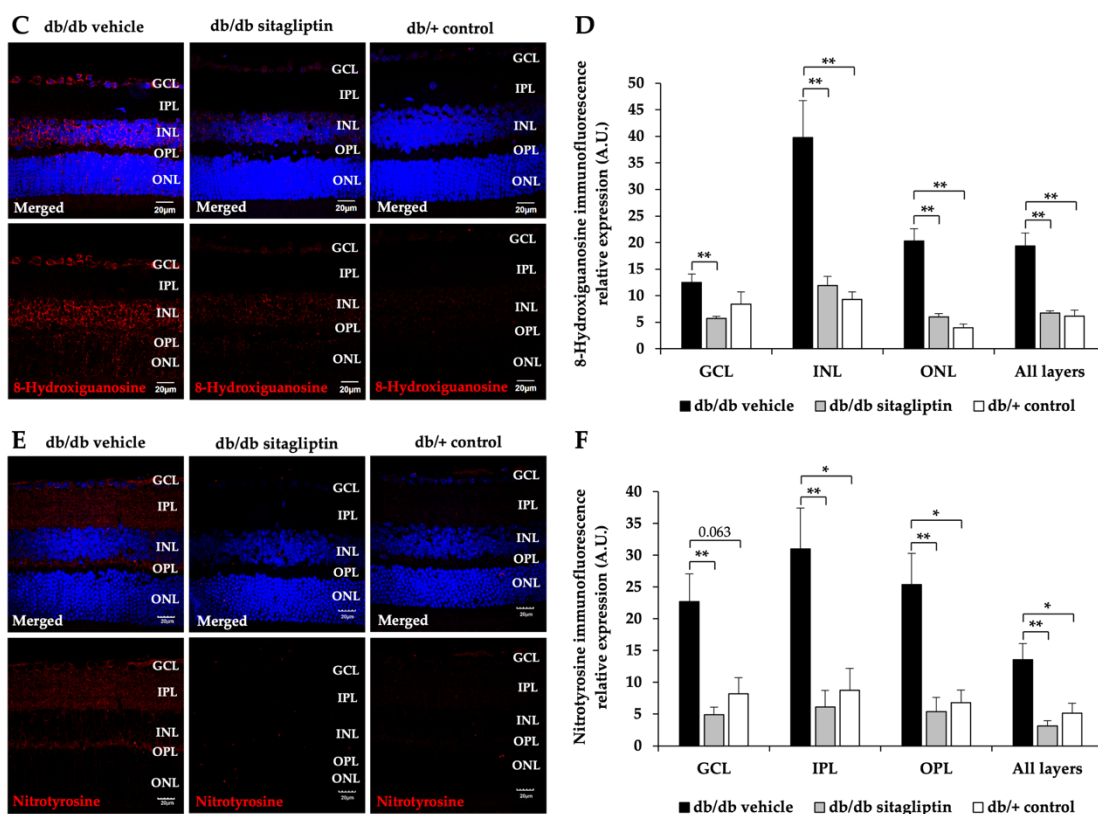


Figure 28. Evaluation of superoxide anion levels and nitro-oxidative damage to biological macromolecules. (A-F) Representative images and quantifications of the retinal immunofluorescences of dihydroethidium (orange) (A,B), 8-hydroxiguanosine (red) (C,D) and nitrotyrosine (red) (E,F) in vehicle-treated db/db mice (black bars), sitagliptin-treated db/db mice (grey bars) and in db/+ mice (white bars). Relative fluorescence intensities are displayed both alone and in combination with Hoechst nuclei staining (blue). GCL (ganglion cell layer), IPL (inner plexiform layer), INL (inner nuclear layer), OPL (outer plexiform layer), ONL (outer nuclear layer). Scale bars, 20 µm. $n = 4$; * $p < 0.05$; ** $p < 0.01$.

4.1.3.3. Examination of the PKC content

The PKC family is composed of 12 isoforms, in which PKC- α , - β , - δ , and - ϵ activation play a key role in the development of DR⁴⁴. The results show a significant increase in the relative IF expression of PKC- β and the number of PKC- δ positive cells in db/db mice treated with vehicle when compared to control mice. However, topical administration of sitagliptin prevented this abnormal increase of both PKC isoforms. (Figure 29A,B).

RESULTS

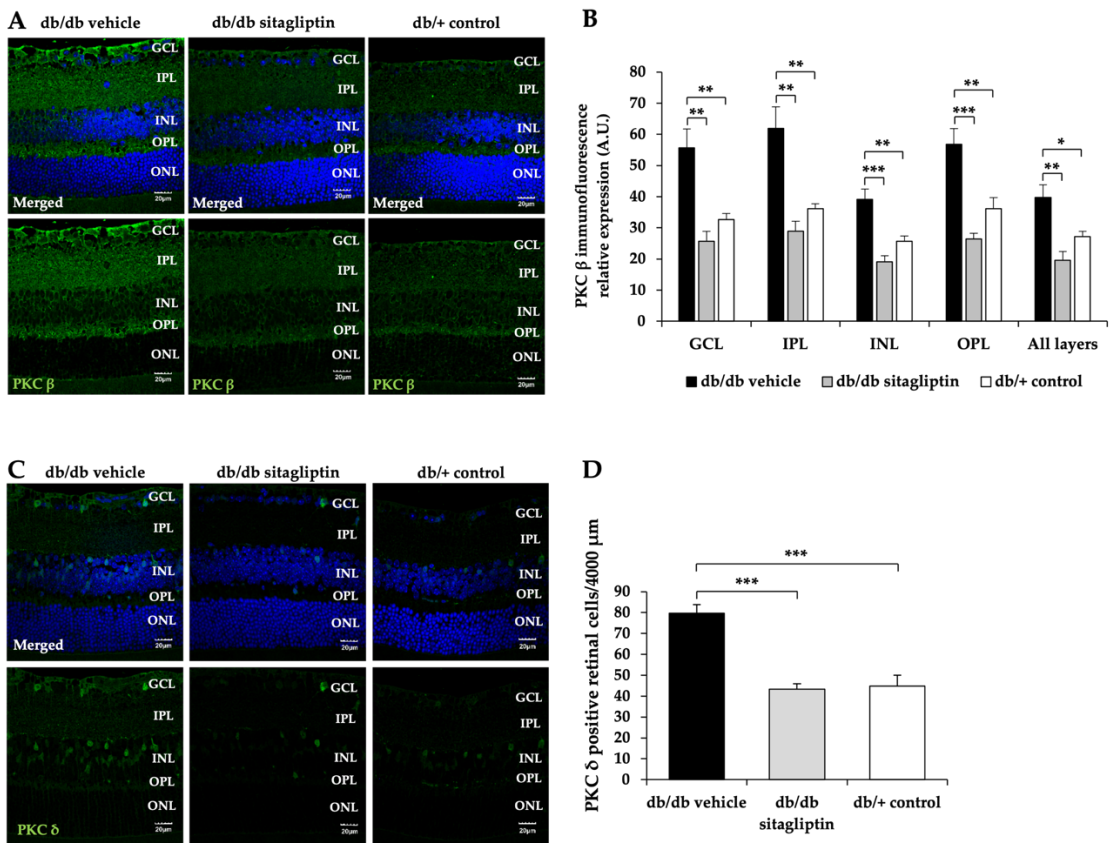


Figure 29. Study of the PKC content. (A-D) Representative images and quantifications of the retinal immunofluorescences of PKC- β (green) (A-B) and PKC- δ (green) (C,D) in vehicle-treated db/db (black bars), sitagliptin-treated db/db mice (grey bars) and in db/+ mice (white bars). Relative fluorescence intensities are displayed both alone and in combination with Hoechst nuclei staining (blue). GCL (ganglion cell layer), IPL (inner plexiform layer), INL (inner nuclear layer), OPL (outer plexiform layer), ONL (outer nuclear layer). Scale bars, 20 μm . $n = 4$; * $p < 0.05$; ** $p < 0.01$; *** $p < 0.001$.

4.1.3.4. Evaluation of the NF- κ B pathway and the pro-inflammatory cytokine production

Activation of the PKC pathway not only leads to increased production of ROS, but also promotes the activation of nuclear factor NF- κ B. Normally, NF- κ B is inactive and located in the cytosol, forming a complex with the inhibitory protein nuclear factor of kappa light polypeptide gene enhancer in B-cells inhibitor alpha (I κ B α). Various factors, such as hyperglycemia or oxidized proteins, can stimulate the enzyme I κ B kinase (IKK) which phosphorylates I κ B α . This results in the phosphorylation of I κ B α , its ubiquitination, dissociation from the NF- κ B complex, and subsequent degradation by the proteasome. As a consequence, NF- κ B is activated and translocated to the cell nucleus, where it regulates inflammatory responses (i.e., cytokine production)²⁴³.

Topical administration of sitagliptin in db/db mice resulted in a reduction of I κ B α phosphorylation and NF- κ B translocation compared to db/db mice treated with vehicle. These findings were comparable to the levels observed in the nondiabetic condition. (Figure 30A-C). In addition, mRNA and protein levels of IL-1 β and TNF α were higher in vehicle-treated diabetic mice in comparison with control mice. Notably, abnormal levels of both cytokines were attenuated by sitagliptin (Figure 31A-E).

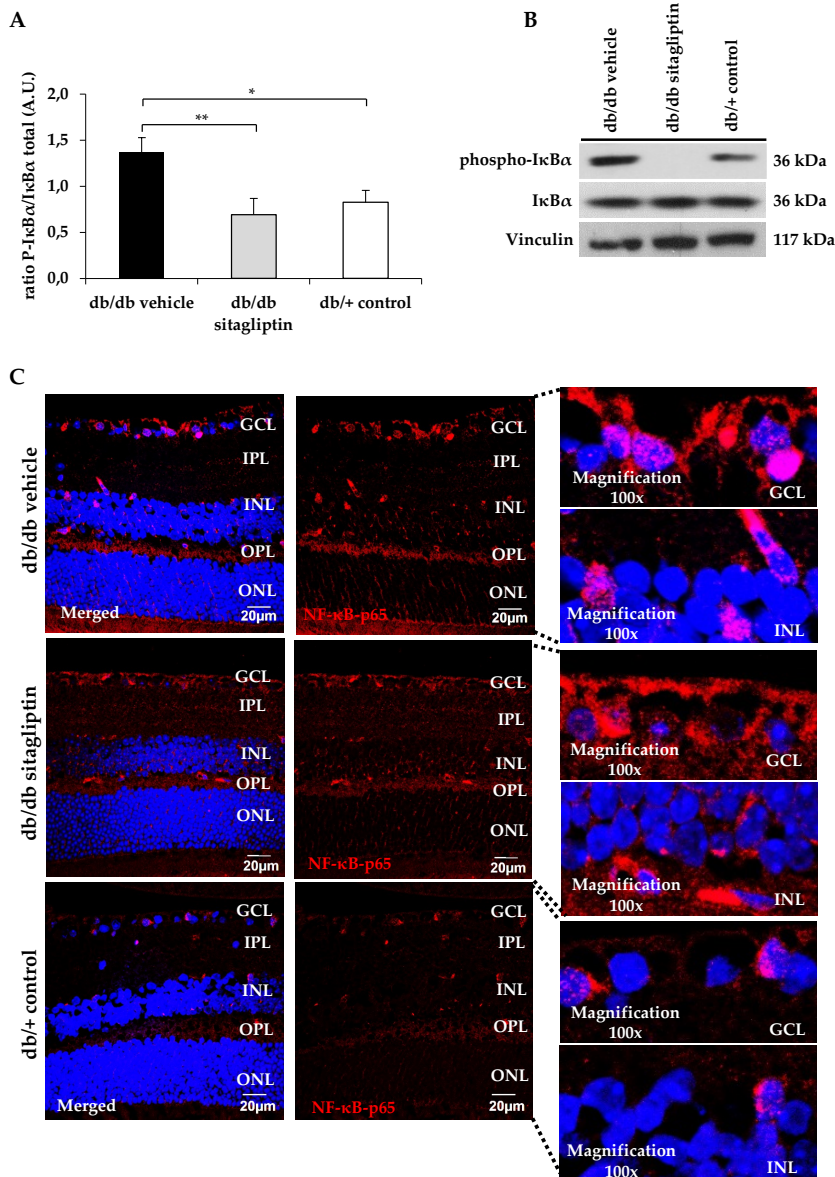


Figure 30. Comparison of NF- κ B translocated cells (red) through immunofluorescence. NF- κ B relative fluorescence intensity is displayed alone and merged with Hoechst nuclei staining (blue). A 100 \times magnification of merged images for each group is attached. Scale bars, 20 μ m; $n = 4$. GCL (ganglion cell layer), IPL (inner plexiform layer), INL (inner nuclear layer), OPL (outer plexiform layer), ONL (outer nuclear layer).

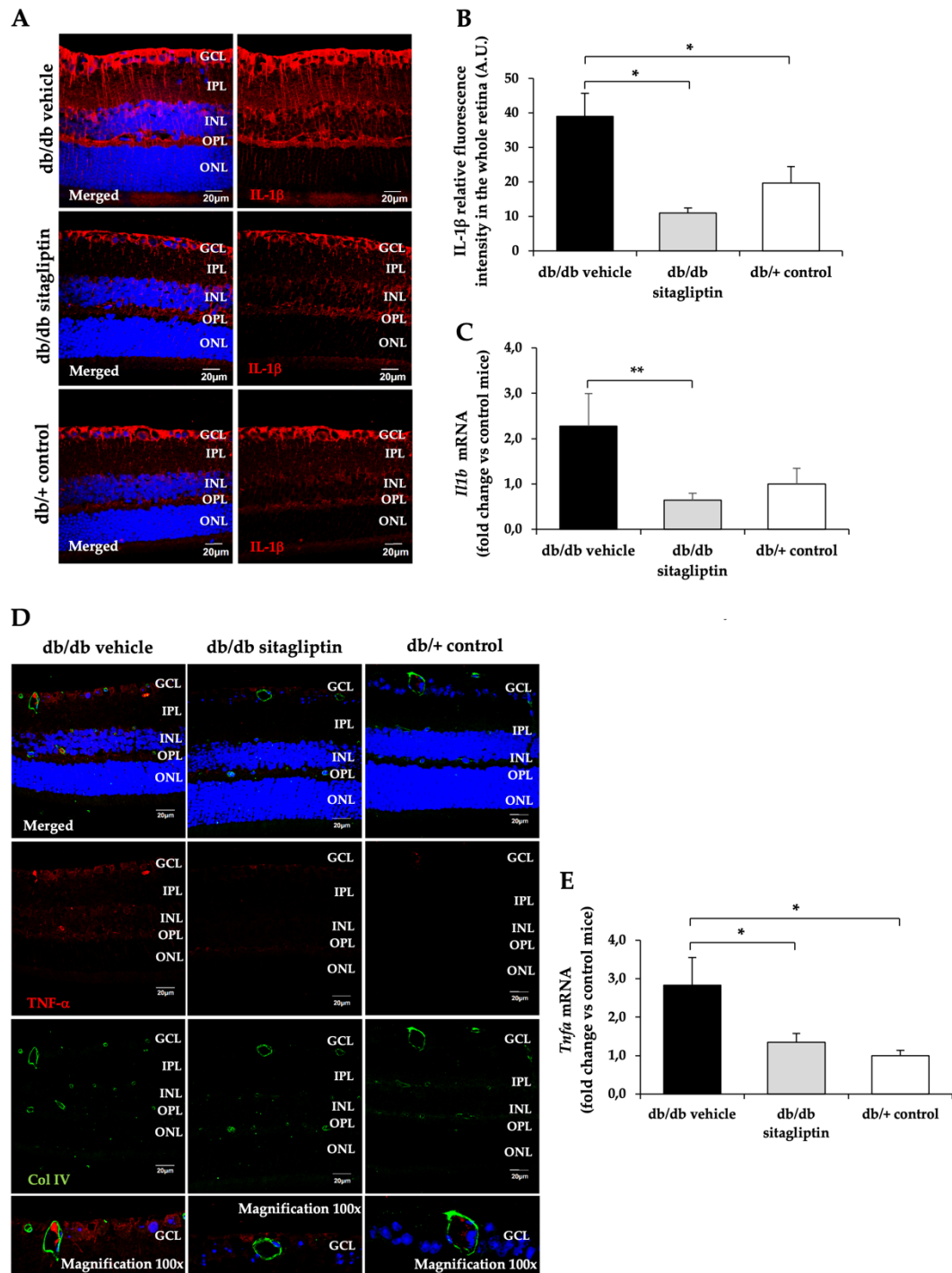


Figure 31. Evaluation of cytokine expression. **(A,B)** Representative images and quantifications of IL-1 β protein levels (red) through immunofluorescence among vehicle-treated db/db mice (black bars), sitagliptin-treated db/db mice (grey bars) and db/+ mice. Relative fluorescence intensity is displayed alone and merged with Hoechst nuclei staining (blue). GCL (ganglion cell layer), IPL (inner plexiform layer), INL (inner nuclear layer), OPL (outer plexiform layer), ONL

(outer nuclear layer). Scale bars, 20 μm . $n = 4$. (C) Comparison of IL-1 β mRNA levels between vehicle-treated db/db mice (black bars), sitagliptin-treated group (grey bars) and db/+ mice (white bars). Results are presented as fold change vs control mice. $n = 4$ (D) Comparison of the immuno-histochemical reactivities of TNF- α (red)/ Collagen IV (Col IV) (green) colabelling among representative samples. TNF- α /Col IV relative fluorescence intensities are displayed isolated and both merged with Hoechst nuclei staining (blue). Magnifications are also displayed in the figure. Scale bars, 20 μm ; $n = 4$. (E) Comparison of TNF- α mRNA levels between vehicle-treated db/db mice (black bars), sitagliptin-treated group (grey bars) and db/+ mice (white bars). Results are presented as fold change vs control mice. $n = 4$; * $p < 0.05$; ** $p < 0.01$.

Interestingly, in the transcriptomic study described in section 4.1.2., we observe the presence of the *Commf8* gene among the top 30 most differentiated genes. This gene encodes a protein called copper metabolism Murr1 domain-containing 8 (COMMD8), which has been implicated in the regulation of I κ B turnover and NF- κ B activation. It has been suggested that COMMD8, in association with coiled-coil domain-containing protein 22 (CCDC22), facilitates the degradation of I κ B, leading to the activation of NF- κ B²⁴⁴. Hence, the mRNA expression levels of the COMMD8 protein were investigated, showing a decrease in diabetic animals treated with sitagliptin compared to those treated with the vehicle, approaching statistical significance (Figure 32). Unfortunately, due to the unavailability of a suitable antibody, we were unable to assess the protein levels of COMMD8.

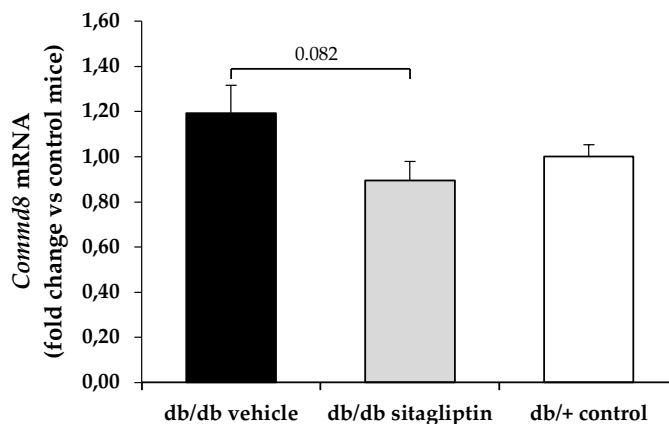


Figure 32. Comparison of COMMD8 mRNA levels between vehicle-treated db/db mice (black bars), sitagliptin-treated group (grey bars) and db/+ mice (white bars). Results are presented as fold change vs control mice. $n = 4$; * $p < 0.05$; ** $p < 0.01$.

4.1.3.5. Analysis of the content of VCAM-1

The activation of VCAM-1 expression is induced by pro-inflammatory cytokines such as TNF α , as well as by various factors including ROS, oxidized low density lipoprotein or high glucose levels^{245–247}. VCAM-1 plays a crucial role in promoting leukocyte recruitment and

RESULTS

adhesion to the retinal blood vessels during the inflammatory process of diabetic retinopathy. It contributes to the disruption of endothelial barrier function and facilitates the infiltration of immune cells into the retina, ultimately exacerbating retinal inflammation and contributing to the progression of the disease²⁴⁸.

In the retinas of diabetic animals that received vehicle treatment, elevated levels of this protein were detected in comparison to control animals, which was prevented by topical administration of sitagliptin (**Figure 33A-C**).

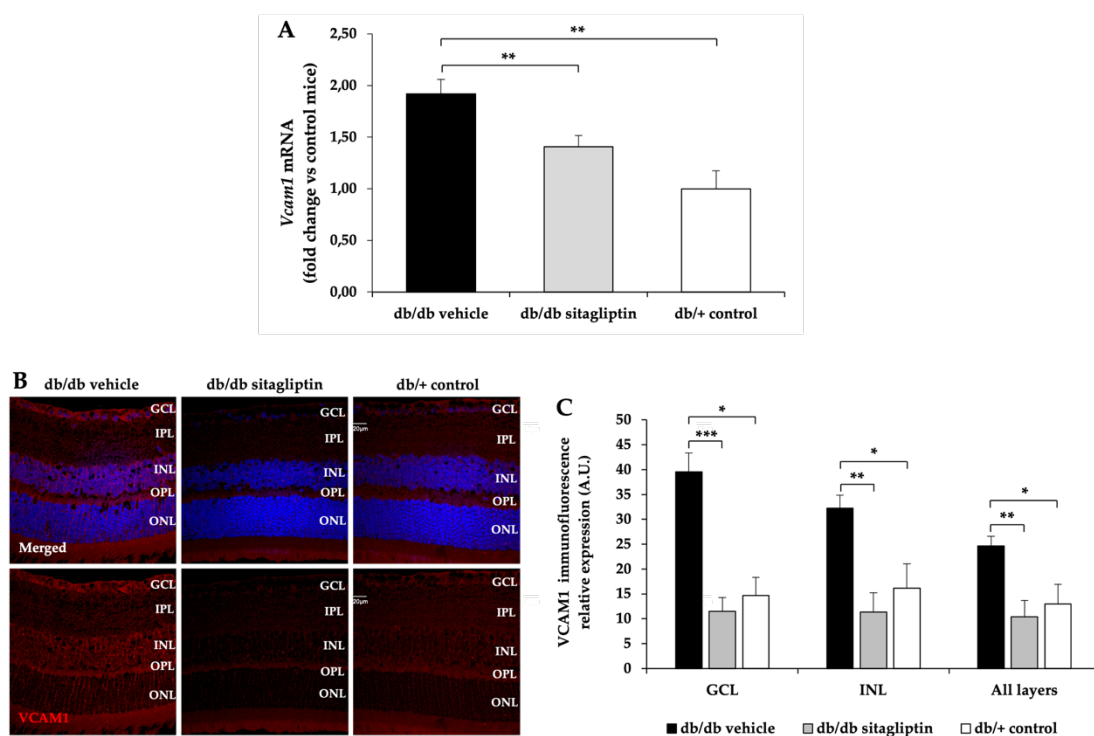


Figure 33. Examination of the mRNA and protein levels of VCAM-1. **(A)** RT-PCR analysis of the gene that codifies for VCAM-1 (*Vcam1*) in vehicle-treated db/db mice (black bars), sitagliptin-treated db/db mice (grey bars), and in db/+ mice (white bars). Results are presented as fold change vs. control mice. $n = 4$. **(B,C)** Representative images and quantifications of retinal immunofluorescence staining for VCAM-1 (red) in diabetic mice treated with vehicle eye drops (black bars), sitagliptin eye drops (grey bars) and non-diabetic mice (white bars). Relative fluorescence intensities are displayed both alone and in combination with Hoechst nuclei staining (blue). GCL (ganglion cell layer), IPL (inner plexiform layer), INL (inner nuclear layer), OPL (outer plexiform layer), ONL (outer nuclear layer). Scale bars, 20 μm . $n = 4$; * $p < 0.05$; ** $p < 0.01$; *** $p < 0.001$.

4.1.4. Study of neuronal proliferation

The Ki67 marker is commonly used to assess cell proliferation. It is a nuclear protein that is expressed during active phases of the cell cycle, specifically in the G1, S, G2, and M phases, but not in the resting (G0) phase²⁴⁹. Ki67 is considered a reliable marker for measuring cell proliferation because it is absent in non-dividing cells and its presence indicates active cell division. By quantifying the percentage of Ki67-positive cells through immunohistochemically staining, the proliferative activity of a cell population can be estimated²⁵⁰. We observed that the proportion of Ki67-positive cells, indicating the ability of neuronal cells to proliferate, is reduced in retinas of db/db mice in comparison with non-diabetic mice. The application of sitagliptin eye drops abrogated the down-regulation of Ki67-positive cells induced by diabetes, thus indicating a potential promotion of neurogenesis in the diabetic retina (**Figure 34A-B**).

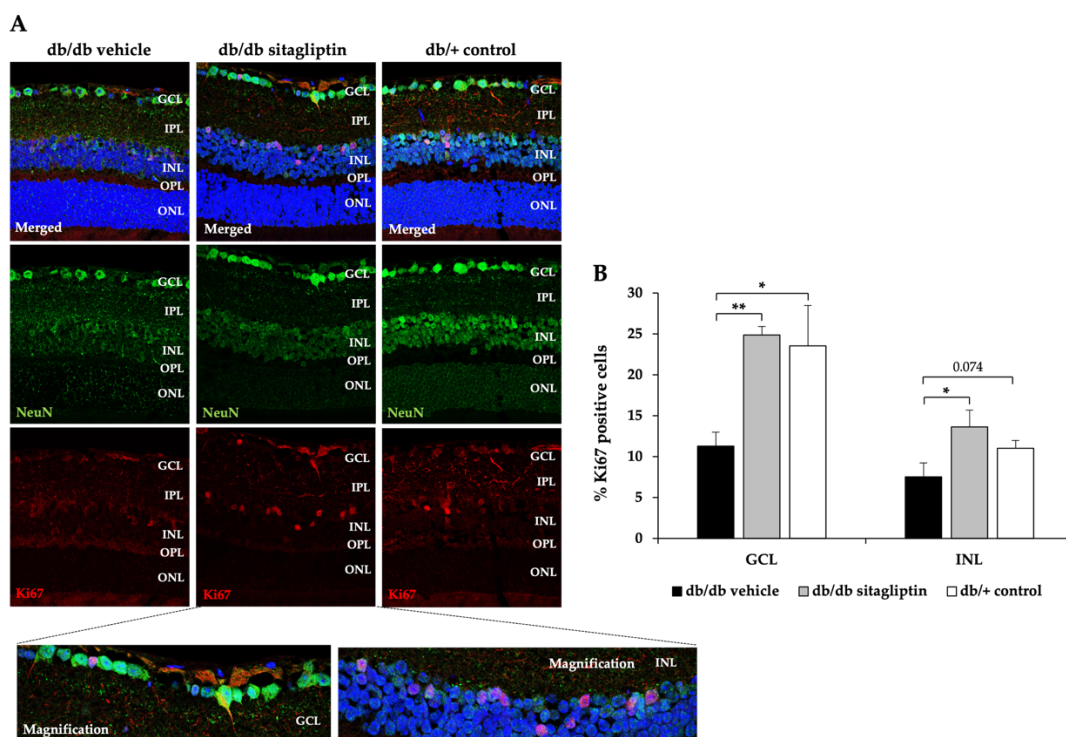


Figure 34. Assessment of retinal cell proliferation. **(A)** Comparison of Ki67 (red) protein levels through immunofluorescence among representative samples of db/db mice treated with vehicle or sitagliptin and db/+ mice. Ki67 is colabelled with NeuN (neuronal specific marker) (green) and Hoechst staining (nuclei specific marker) (blue). Optical magnifications of GCL and INL are also presented in this figure. **(B)** Quantification and comparison of the percentages of Ki67 positive cells among diabetic mice treated with vehicle (black bars) or sitagliptin (grey bars) and non-diabetic mice (white bars). $n = 4$; * $p < 0.05$; ** $p < 0.01$.

4.1.5. *In vivo* assessment of retinal functionality

The functionality of the retina among the different groups studied was assessed by ERG. **Figure 35A** and **Figure 35B** show that diabetic animals treated with vehicle, compared to control animals, show delayed responses and lower a- and b-wave amplitudes, especially when stimulated with high intensity (80 cd/s/m^2). In contrast, and in accordance with the preservation of synaptic proteins, sitagliptin-treated animals show patterns similar to control animals, indicating a functional enhancement of the retina. Statistical analysis reveals a significant improvement in a-wave amplitudes when comparing the data (**Figure 35C**).

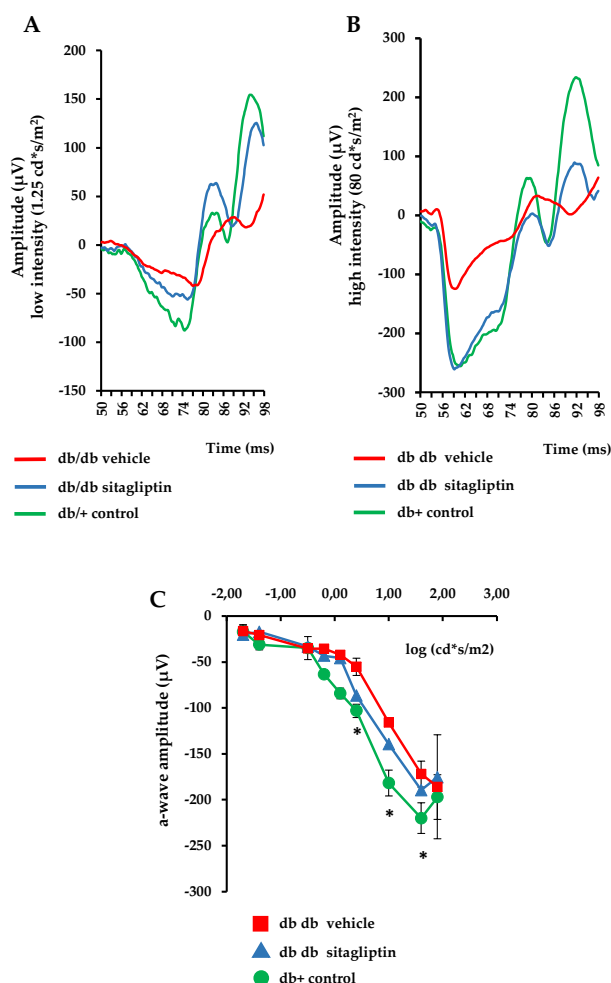
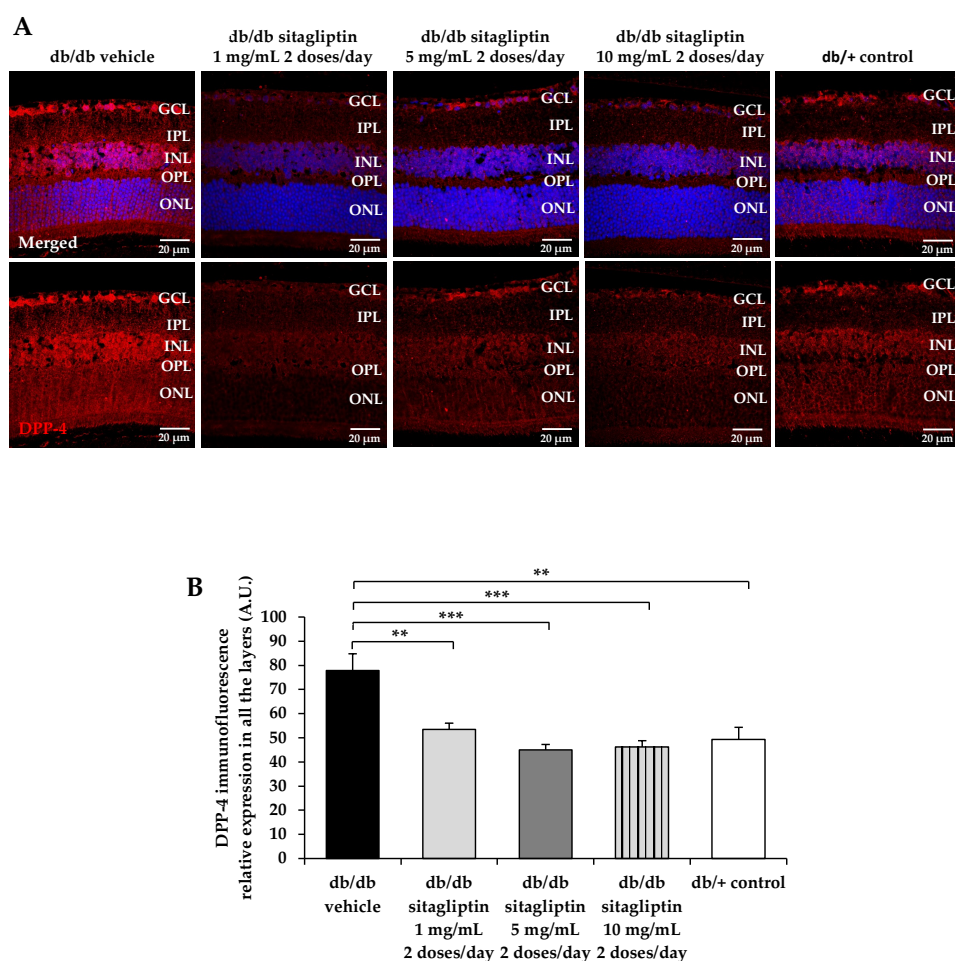


Figure 35. Assessment of retinal functionality. (A) Electroretinogram traces in response to low and high stimulus intensities ($25 \text{ cd}^{\circ}/\text{s/m}^2$ and $80 \text{ cd}^{\circ}/\text{s/m}^2$) in non-diabetic mouse (green), db/db mouse treated with vehicle (red), and a db/db mouse treated with sitagliptin (blue). (B) Quantitative analyses of a wave amplitude in db/db mice treated with vehicle (red squares), db/db mice treated with sitagliptin (blue triangles), and non-diabetic mice (green circles). $n = 4$; * $p < 0.05$.

4.2. Minimum effective dose study of sitagliptin and saxagliptin for the early treatment of diabetic retinopathy

4.2.1. Dose-response effect on DPP-4 levels

Both DPP-4i (sitagliptin and saxagliptin) lowered the protein content of DPP-4 within the diabetic retina (**Figure 36**). For sitagliptin, all the tested concentrations significantly reduced DPP-4 levels in a similar way, with no differences among them. Regarding saxagliptin, twice-daily administration was more effective in reducing DPP-4 levels than once-daily administration. In fact, saxagliptin 1 mg/mL did not reduce the DPP-4 content (**Figure 36**).



RESULTS

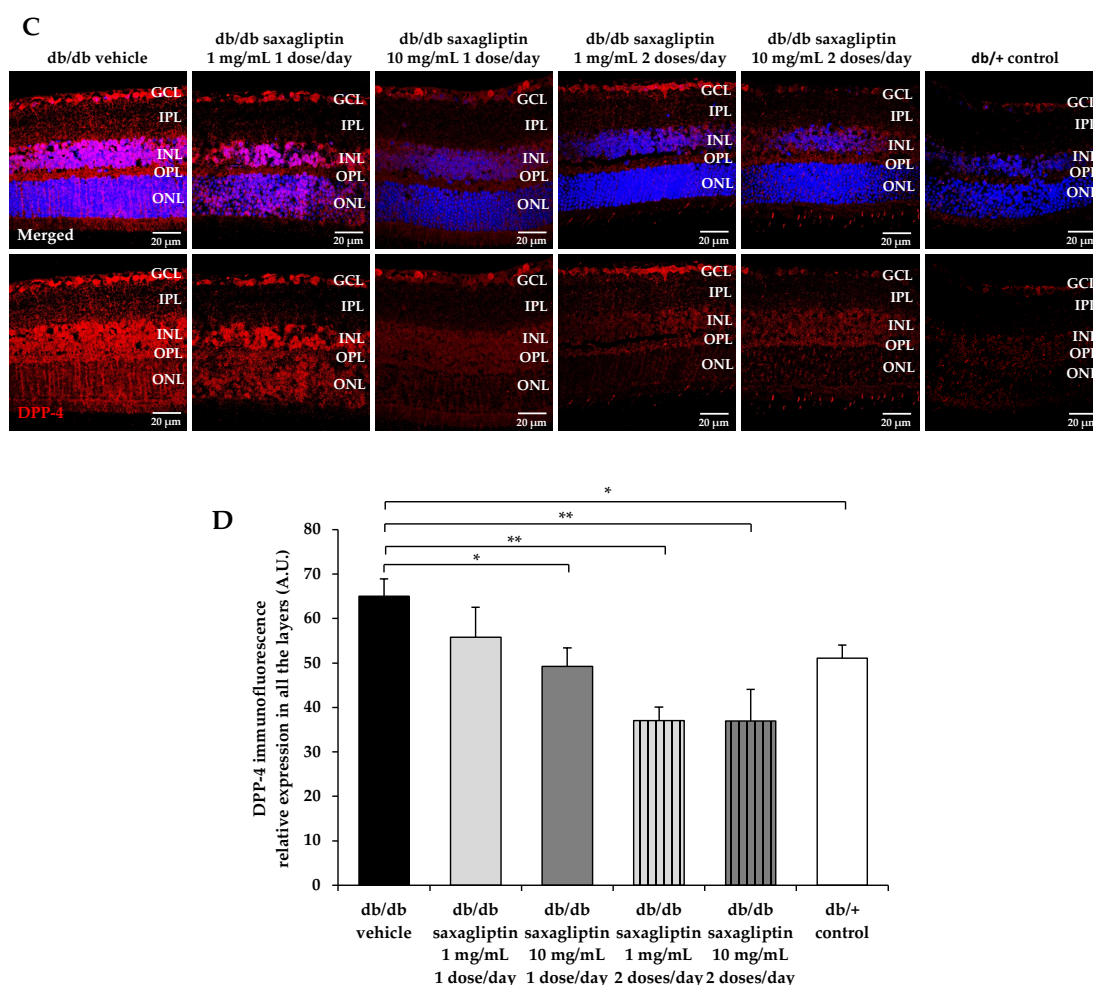
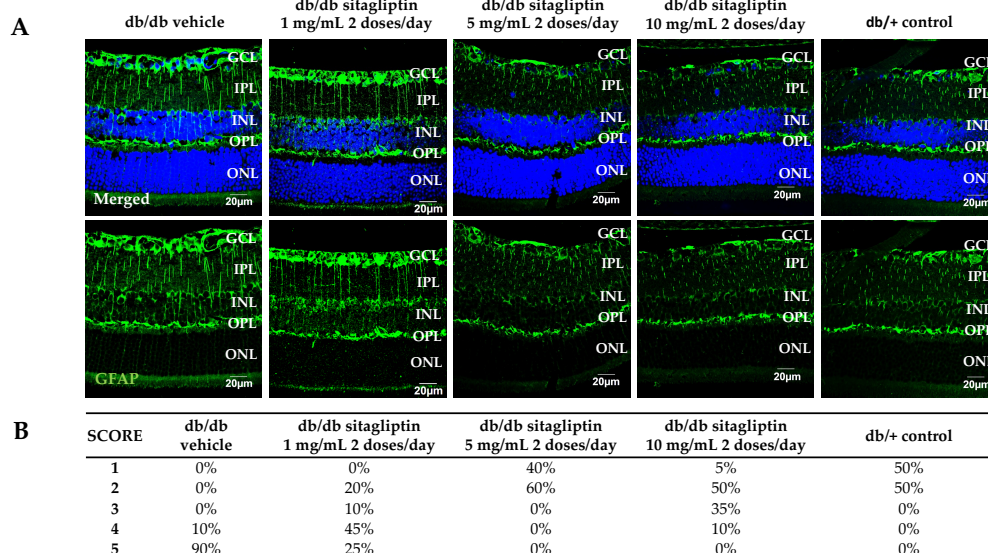


Figure 36. Examination of DPP-4 protein levels. **(A,C)** Retinal DPP-4 immunofluorescence reactivity comparison (red) between representative samples from the respective experimental groups. Relative DPP-4 fluorescence intensities are displayed both alone and in combination with Hoechst nuclei staining (blue). Scale bars, 20 μ m. GCL: ganglion cell layer; IPL: inner plexiform layer; INL: inner nuclear layer; OPL: outer plexiform layer; ONL: outer nuclear layer. **(B,D)** Quantification of the DPP-4 immunofluorescence levels. Treatments with sitagliptin and saxagliptin are compared in panel **(B)** and **(D)** respectively. In graph **(B)** vehicle group is represented with black bars, sitagliptin 5 mg/mL 2 doses/day group with grey bars, sitagliptin 10 mg/mL 2 doses/day group with dark grey bars and control group with white bars. In graph **(D)** vehicle is displayed with black bars, saxagliptin 1 mg/mL 1 dose/day with white bars with diagonal lines, saxagliptin 10 mg/mL 1 dose/day with white bars with horizontal lines, saxagliptin 1 mg/mL 2 doses/day with grey bars, saxagliptin 10 mg/mL 2 doses/day with dark grey bars and control mice with white bars $n = 4$; * $p < 0.05$; ** $p < 0.01$; *** $p < 0.001$.

4.2.2. Dose-response effect on glial activation

During the early stages of DR, glial activation occurs, one of the main hallmarks of the disease. Müller cells experience reactive gliosis, which is marked by the unusual expression of GFAP. Gliosis is a process that encompasses various changes on a biochemical, physiological, and structural level³⁸.

According to the quantification method presented in Section 3.4.1.1, mice without diabetes presented GFAP scores below 3, as illustrated in **Figure 37A-D**. In contrast, vehicle-treated diabetic mice exhibited a score of four or higher due to aberrant GFAP overexpression (**Figure 37A-D**). Sitagliptin, except at the lowest concentration (1 mg/mL), effectively prevented reactive gliosis, with 5 mg/mL being the most potent concentration (**Figure 37A,B**). For saxagliptin, the highest concentration (10 mg/mL) demonstrated the greatest reduction in glial activation (**Figure 37C,D**), regardless of whether it was administered once or twice daily.



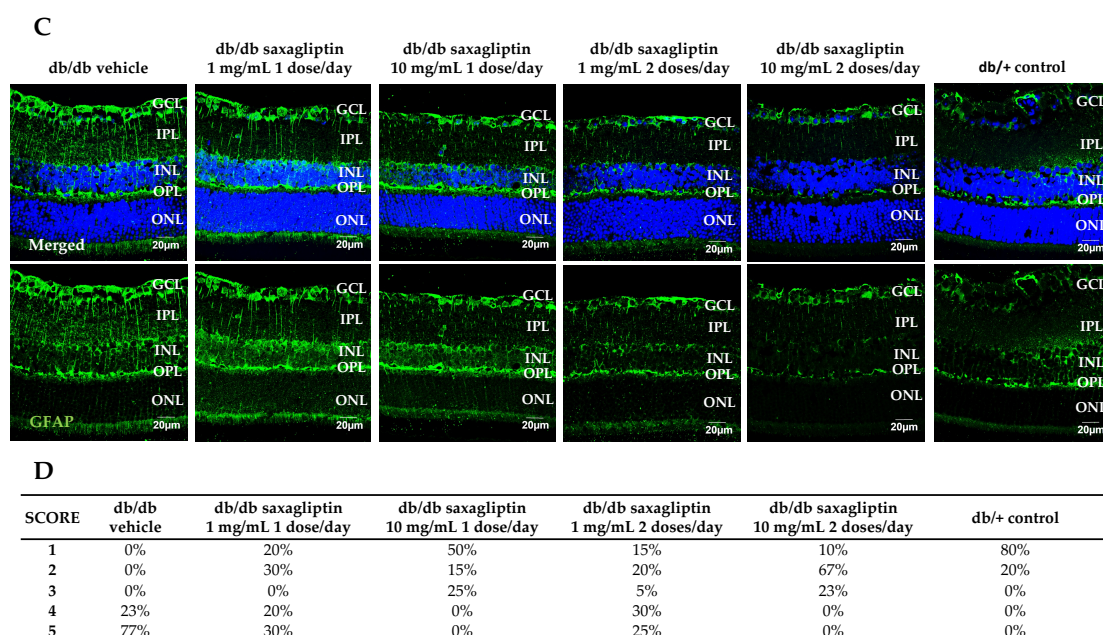


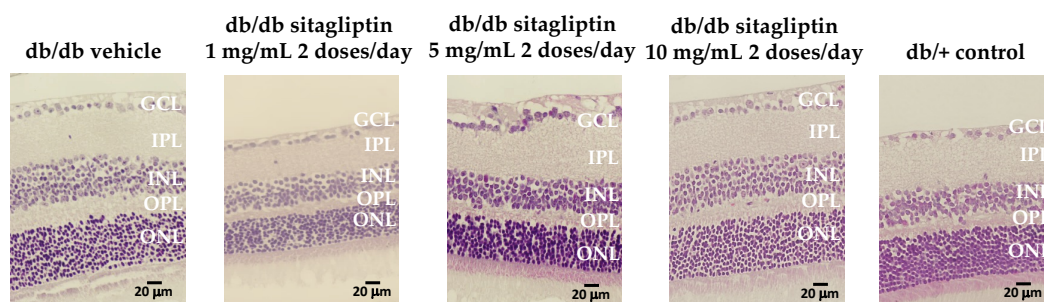
Figure 37. Glial activation. (A,C) Comparison of GFAP immunofluorescence reactivity (green) among experimental groups to assess the dose-efficacy effect of sitagliptin (A), and saxagliptin (C). GFAP relative fluorescence intensity is exhibited isolated and merged with Hoechst nuclei staining (blue). GCL: ganglion cell layer; IPL: inner plexiform layer; INL: inner nuclear layer; OPL: outer plexiform layer; ONL: outer nuclear layer. Scale bars, 20 μ m. (B,D) Quantification of the percentage of reactive gliosis present in the samples based on the GFAP staining extent. $n = 4$.

4.2.3. Dose-response effect on cell death and retinal thinning

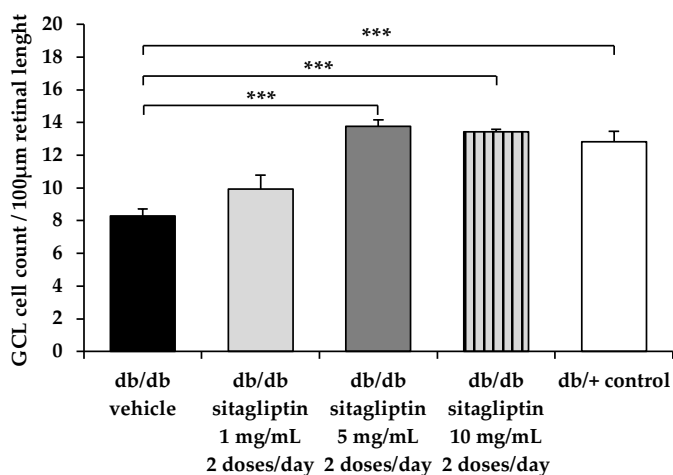
Diabetes-induced neuroglial degeneration includes reactive gliosis, decreased retinal neuronal function and neuronal cell apoptosis. Retinal ganglion cells and amacrine cells are the first neurons in which diabetes-induced apoptosis is detected, but photoreceptors also show a higher apoptotic rate. The structural consequence of this apoptotic death is a reduction in the thickness of the inner retinal layers²⁵¹.

Diabetic mice treated with vehicle demonstrated a significant decrease in GCL and INL cell counts, as well as retinal thickness measurements, in comparison with control mice (Figure 38A–F). Sitagliptin eye drops administered at 5 mg/mL and 10 mg/mL, effectively promoted cell survival and preserved retinal thinning. However, the results obtained with the 1 mg/mL concentration were similar to those observed in diabetic mice treated with the vehicle (Figure 38A–C). With regard to saxagliptin, both concentrations reduced neuronal cell death in the GCL and INL. Nonetheless, only when saxagliptin was administered twice daily did it have a significant impact on INL and overall retinal thicknesses.

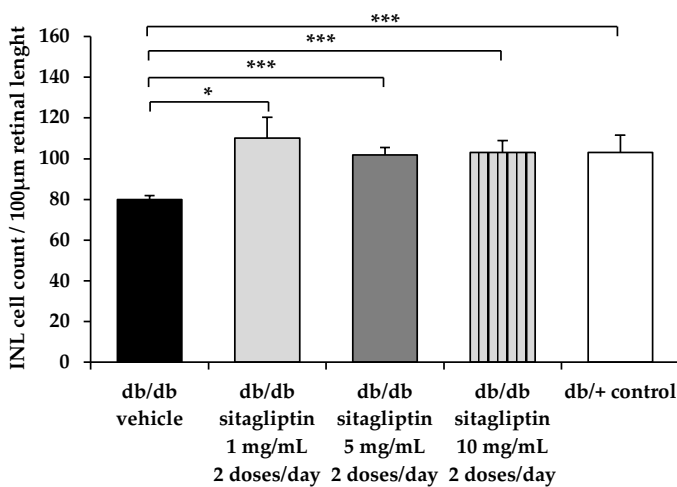
A



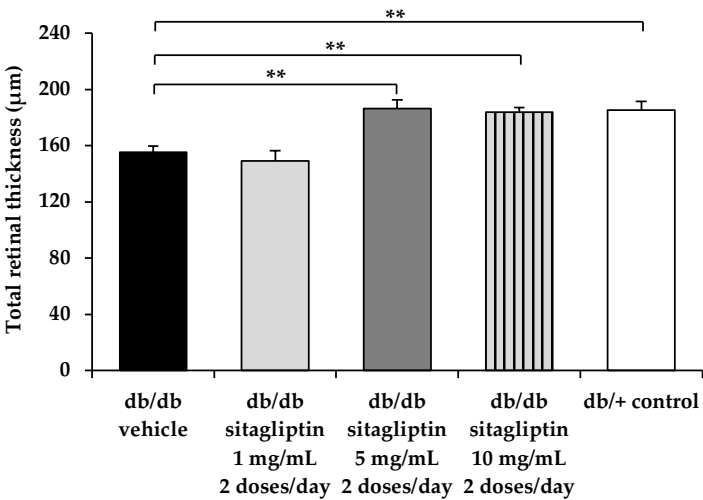
B



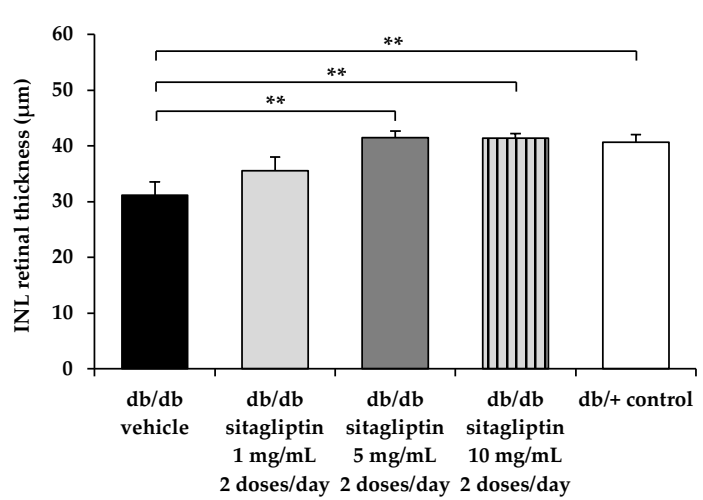
C



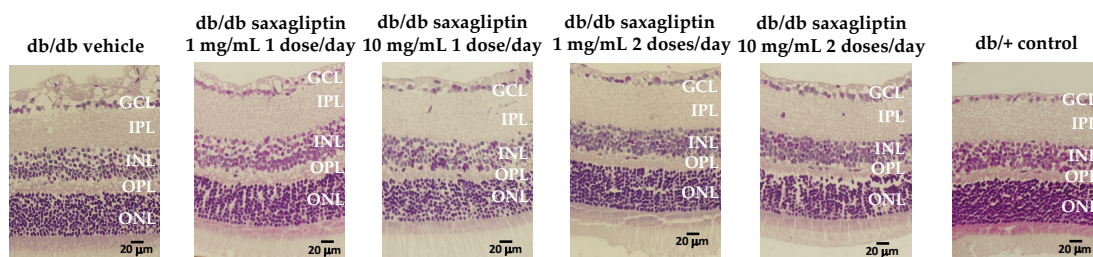
D



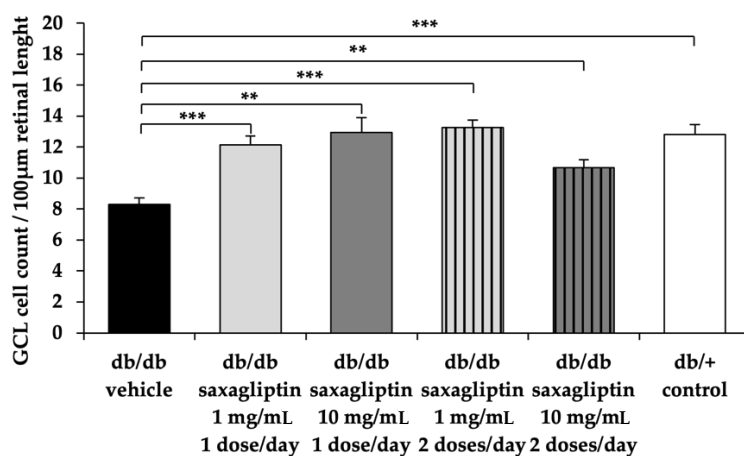
E



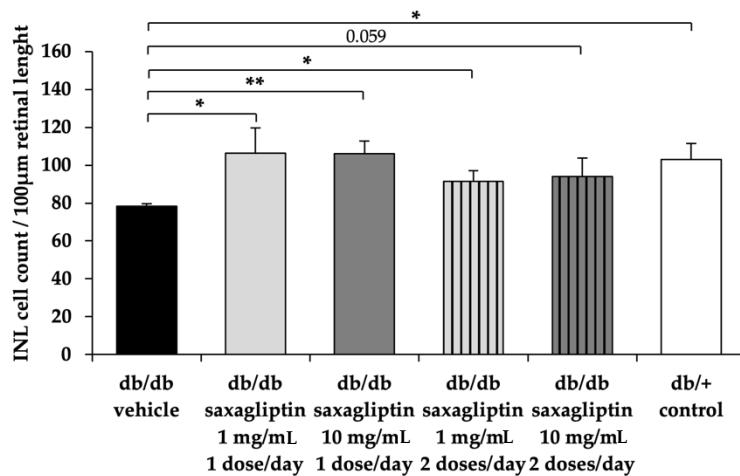
F



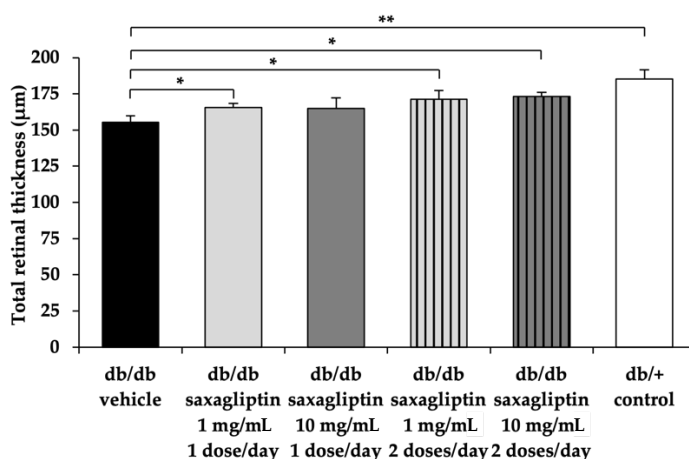
G



H



I



J

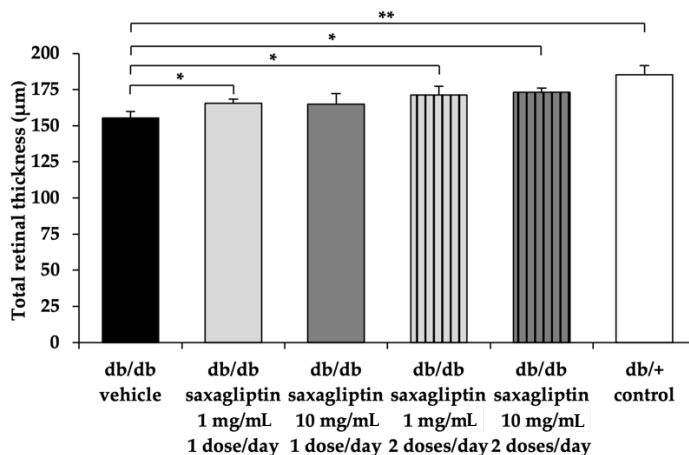
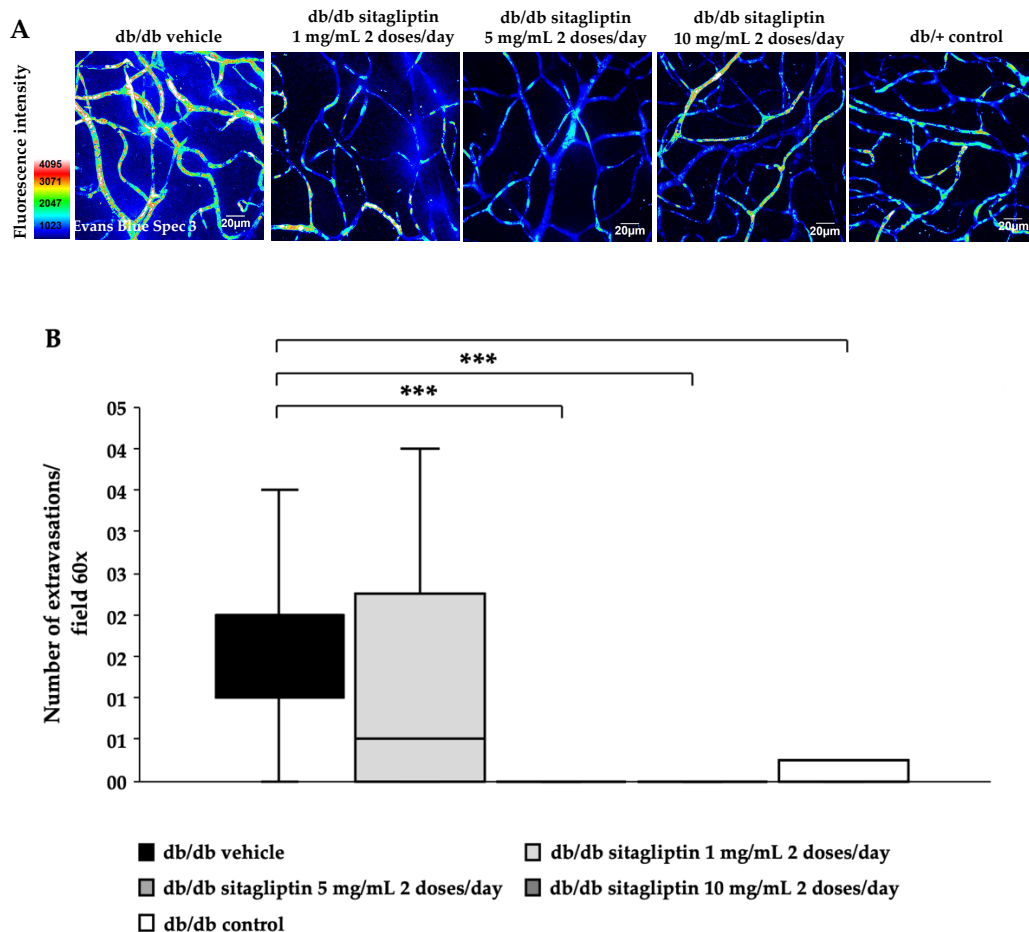


Figure 38. Assessment of cell death and retinal thinning. (A,F) Comparison of H&E-stained retinas among representative samples of each experimental group. GCL: ganglion cell layer; IPL: inner plexiform layer; INL: inner nuclear layer; OPL: outer plexiform layer; ONL: outer nuclear layer. Scale bars, 20 μ m. (B, C, G, H) Cell count of GCL and INL layers. (D,E,I,J) Quantification of INL and whole retina thicknesses. For sitagliptin comparison, vehicle group is represented with black bars, sitagliptin 5 mg/mL 2 doses/day group with grey bars, sitagliptin 10 mg/mL 2 doses/day group with dark grey bars and control group with white bars. For saxagliptin comparison, vehicle group is displayed with black bars, saxagliptin 1 mg/mL 1 dose/day group with white bars with diagonal lines, saxagliptin 10 mg/mL 1 dose/day group with white bars with horizontal lines, saxagliptin 1 mg/mL 2 doses/day group with grey bars, saxagliptin 10 mg/mL 2 doses/day group with dark grey bars and control mice with white bars $n = 4$; * $p < 0.05$; ** $p < 0.01$; *** $p < 0.001$.

4.2.4. Dose-response effect on vascular leakage

Both iBRB and oBRB control the passage of proteins and other macromolecules into the retina from the bloodstream via tight junctions and adherens junctions between adjacent cells, which effectively block paracellular permeability. Disruption of BRB, in particular iBRB, leads to vascular leakage, which is essential in the pathogenesis of DR²⁵².

As a result of multiple extravasation sites, diabetic mice exposed to vehicle showed increased Evans blue fluorescence outside blood vessels compared to control mice (Figure 39A,C). The higher concentrations of sitagliptin (5 and 10 mg/mL) significantly inhibited these vascular abnormalities, while the 1 mg/mL concentration did not prevent vascular leakage (Figure 39A,B). Similarly, saxagliptin effectively prevented vascular leakage, being more effective when administered twice per day, independently of the concentration (Figure 39C,D).



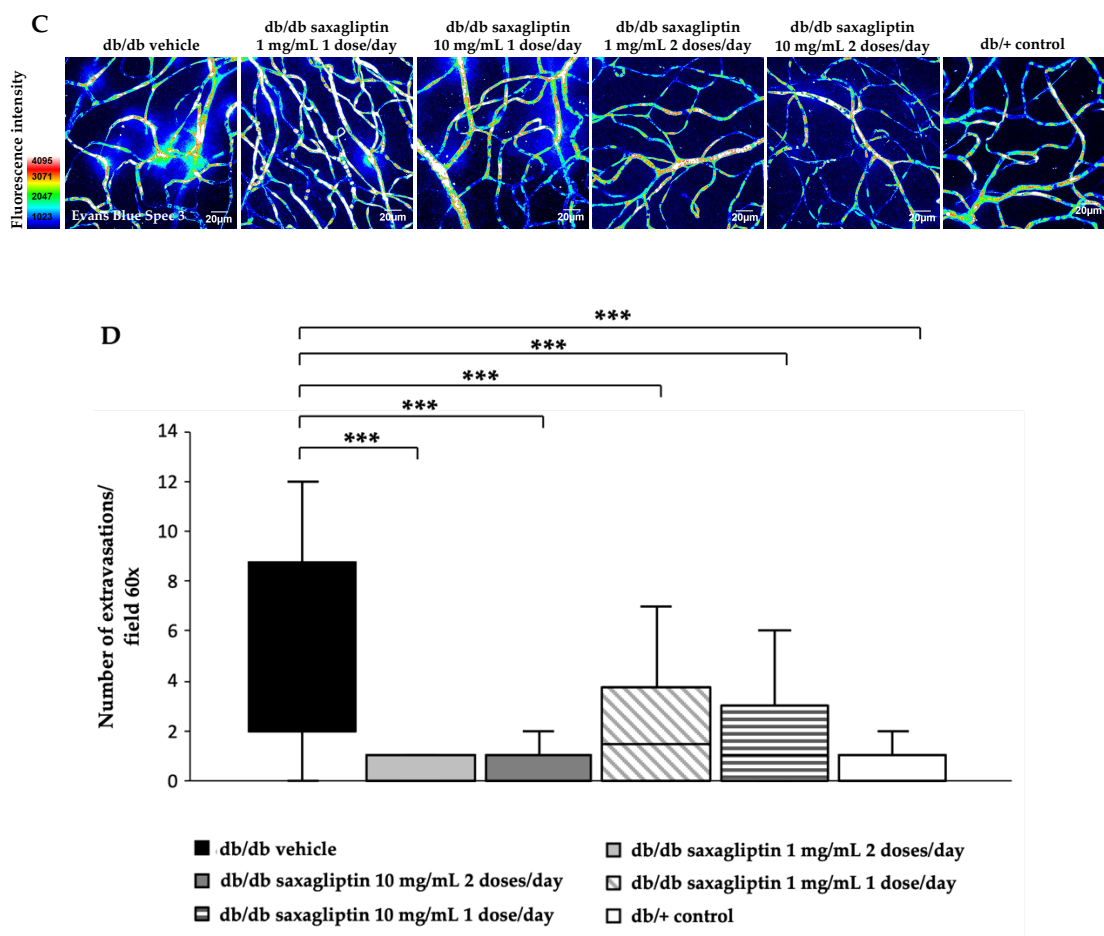


Figure 39. Examination of retinal vascular leakage. (A,C) Confocal images of retinal whole mounts stained with Evans blue dye to evaluate vascular permeability. Sitagliptin treatments are compared in panel (A) while treatments with saxagliptin are displayed in panel (C). Spec3, fluorescent spectral signature 3. Scale bars, 20 μ m. (B,D) Quantification of extravasations per 60 \times field of the retina. Treatments with sitagliptin and saxagliptin are compared in panel (B) and (D) respectively. In graph (B) vehicle group is represented with black bars, sitagliptin 5 mg/mL 2 doses/day group with grey bars, sitagliptin 10 mg/mL 2 doses/day group with dark grey bars and control group with white bars. In graph (D) vehicle is displayed with black bars, saxagliptin 1 mg/mL 1 dose/day with white bars with diagonal lines, saxagliptin 10 mg/mL 1 dose/day with white bars with horizontal lines, saxagliptin 1 mg/mL 2 doses/day with grey bars, saxagliptin 10 mg/mL 2 doses/day with dark grey bars and control mice with white bars. $n = 3$, 25–30 fields per animal were analyzed; *** $p < 0.001$

DISCUSSION

5.1. Preservation of retinal neurotransmission: a primary mechanism of neuroprotection of sitagliptin in early stages of diabetic retinopathy

In order to address the lack of information regarding the mechanisms of action through which DPP-4i exert beneficial effects in experimental models of early DR, a study was performed comparing the transcriptomic retinal profiles of db/db mice topically treated with vehicle, db/db mice topically treated with sitagliptin (10 mg/mL) and non-diabetic mice. This transcriptomic study consisted in a multi-step approach including microarray assay, subsequent GSEA and validation of the results. Microarrays allow to study the expression levels of thousands of genes simultaneously and are widely employed to gain insights into the gene expression patterns of diseases. Additionally, they are utilized to investigate how these pathological gene expression patterns change under different conditions, such as when treatments are applied or modified. On the other hand, GSEA facilitates the integration of biological knowledge into the analysis and interpretation of microarray data by comparing gene expression patterns with emerging pathways, systems, and phenotypes²⁵³. Thanks to this combination of techniques and the subsequent validation by RT-qPCR, we could evidence that the primary mechanism through which sitagliptin eye drops confer its beneficial effects against early DR is by preserving the biological process of neurotransmission. Furthermore, they facilitated the characterization of the genes responsible for this enhancement.

The first evidence we obtained was when comparing the microarray results between diabetic animals treated with vehicle or sitagliptin, where three of the five most differentiated genes are associated with crucial functions of the neuronal system. *C1ql1*, the most differentiated gene, encodes for a secreted protein that interacts with hippocampal receptors facilitating spinogenesis, synaptogenesis and constitution of the synaptic territory, fundamental processes for achieving a functional neuronal connectivity²⁵⁴. On the other hand, *Kif1b* and *Kif1bp* genes (top five and two) conform the KIF1B-KBP complex, necessary for proper axon elongation²⁵⁵. Mutations in kinesin proteins have been associated with numerous neurological disorders, and the loss of KIF1B or KBP has been specifically linked to axonal degeneration²⁵⁶. Although no general conclusions can be drawn from studying only 3 individual genes, the fact that sitagliptin up-regulates these genes in such a significant manner is already an indication of its neuroprotective capabilities.

Employing two distinct annotations databases (GO and RPD) and subject to stringent statistical criteria, the retinal GSEA also unveiled significant positive enrichments after sitagliptin treatment of multiple terms related to synaptic transmission (mostly in the RPD), including: “neuronal system”, “transmission across chemical synapses”, “neurotransmitter transport”, “neurotransmitters receptors and postsynaptic signal transmission”, “regulation of postsynaptic membrane potential”, membrane trafficking”, “vesicle-mediated transport in synapse”, “axon guidance”, etc. Prominently, within these biological processes, there is a significant up-regulation by sitagliptin of genes associated with neurotransmitter uptake and release (*Apha1*, *Cplx1*, *Slc17a7*, *Stxbp2*, *Stxbp4*, *Stxbp6*, *Sv2b* and *Unc13a*) and postsynaptic processing (*Cask*, *Dlg2*, *Dlg4*, *Gria1*, *Grin1*, *Grin2b*, *Grin2d*).

The proteins encoded by the presynaptic genes play vital roles in vesicle biogenesis, mobilization, docking, fusion, and recycling processes²⁵⁷. Despite not being the most extensively characterized proteins within these biological pathways, we also examined the mRNA levels of *Snap25*, *Stx1a*, *Syn1*, *Syp*, *Syt1*, and *Vamp2* during our RT-qPCR validation. The core machinery responsible for neurotransmitter release consists of N-ethylmaleimide-sensitive factor attachment protein (SNAP) receptors (SNAREs), namely syntaxin-1 (*Stx1a*), SNAP-25 (*Snap25*), and synaptobrevin (*Vamp2*). Together, they form the SNARE complex, a four-helix bundle that brings the vesicle and plasma membrane into close proximity, facilitating proper vesicle docking and fusion²⁵⁸. Mammalian uncoordinated-18 (Munc-18) (*Stxbp2*, *Stxbp4*, *Stxbp6*) and Mammalian uncoordinated-13 (Munc-13) (*Unc13a*) proteins regulate the formation of the SNARE complex. Munc-18 binds to a “closed” conformation of syntaxin-1 and to synaptobrevin to stabilize the assembly of the SNARE complex, thus preventing its dissociation and probably affecting vesicle docking²⁵⁹. Munc-13 is responsible for syntaxin-1 “opening” and permits vesicle binding to the plasma membrane²⁶⁰. Amyloid beta precursor protein-binding family A member 1 (APBA1) (*Apha1*) facilitates the function of Munc-18²⁶¹. Synaptotagmin 1 (*Syt1*) is a transmembrane protein located in synaptic vesicles, and it serves as a sensor to detect and synchronize neurotransmitter release in response to Ca^{2+} influx²⁶². As for complexin I (*Cplx1*), its precise role is not fully elucidated, but it has been associated with vesicle fusion²⁶³. Synaptic vesicle glycoprotein 2B (SV2B) (*Sv2b*) plays a crucial role in stabilizing vesicle content, maintaining and orienting the releasable pool of vesicles, and modulating vesicular calcium sensitivity to facilitate efficient neurotransmitter release²⁶⁴. Additionally, vesicular glutamate transporter 1 (VGLUT1) (*Slc17a7*) enables the refill of presynaptic recycling vesicles with glutamate, the primary excitatory transmitter in the retina, whose excitotoxicity is a hallmark of DR²⁶⁵. Synaptophysin (*Syp*) and synapsin (*Syn1*) are the most abundant synaptic proteins and are the most widely used markers for presynaptic

terminals²⁶⁶. Synaptophysin modulates the kinetics of synaptic vesicles endocytosis²⁶⁷, while synapsin orchestrates the reserve pool of synaptic vesicles available for exocytosis and organizes the abundance of vesicles at presynaptic terminals^{268,269}.

Regarding postsynaptic processing, our transcriptomic study revealed that sitagliptin promotes up-regulation of genes that encode for three distinct subunits of the glutamate ionotropic receptor (N-methyl-D-aspartate) NMDA (*Grin1*, *Grin2b*, *Grin2d*), one subunit of the glutamate α -amino-3-hydroxy-5-methyl-4-isoxazolepropionic acid (AMPA) receptor (*Gria1*), two different postsynaptic density proteins (PSD) (*Dlg2*, *Dlg4*) and the calcium/calmodulin-dependent serine protein kinase (CASK) (*Cask*). The interaction of glutamate with both metabotropic and ionotropic receptors activates and mediates postsynaptic responses. NMDA and AMPA receptors are crucial modulators of synaptic plasticity, the dysregulation of which can lead to neurodegenerative events, including DR^{270,271}. PSD-93, PSD-95 and CASK, codified by *Dlg2*, *Dlg4* and *Cask* respectively, serve as postsynaptic scaffolding proteins, regulating the synaptic localization of numerous receptors, channels, and signaling proteins^{272,273}.

The proper functioning of retinal synapses is crucial for the neural processing of visual perception and any morphological alterations in synaptic terminals or changes in the content of all the synaptic proteins mentioned above (among others) have the potential to disrupt neuronal behavior, thus affecting the retinal capacity to sense and process light stimuli efficiently²⁷⁴. As was mentioned in the introduction section, DR has been widely related to synaptic loss and deficiencies in neurotransmitter release and uptake systems, which result in altered synaptic activity and electrophysiological abnormalities in the retina^{79,84}. Masser *et al.* observed that diabetes reduces retinal synaptophysin content in STZ-induced diabetic rats. Early insulin treatment corrects this abnormality, while delayed treatment fails to restore synaptic protein levels²⁷⁵. In both RT-qPCR validation and protein assessments through Western Blotting and immunofluorescence assay (IF), where non-diabetic animals were included, we confirmed the downregulation of these proteins in the retinas of db/db mice at the age of 12 weeks. This finding aligns with previous studies conducted on the same model or other diabetic models at comparable ages^{276–278}, being synaptophysin, synapsin I and PSD-95 the most studied synaptic markers²³⁴. To our knowledge, our analyses also provide the first evidences regarding the downregulation that diabetes exerts on synaptic proteins that have received less attention such as Munc-13, Munc-18, APBA1, or complexin-1.

It should be noted that topical administration of sitagliptin effectively preserved their mRNA and protein levels, demonstrating its positive and meaningful influence on the retinal neuronal

system. Nagamatsu *et al.* already reported that oral sitagliptin was able to increase syntaxin 1 clusters in the plasma membranes of pancreatic beta cells from db/db mice, promoting vesicle docking and insulin exocytosis²⁷⁹, while Kutsyr *et al.* showed the capacity of oral sitagliptin to preserve presynaptic and postsynaptic elements in experimental retinitis pigmentosa²⁸⁰. However, our study represents the first demonstration of the neuroprotective effects of sitagliptin on synaptic transmission in the context of experimental DR when administered topically. Furthermore, given the essential role of synaptic proteins in retinal functionality, their preservation could explain the beneficial effects of sitagliptin observed in the ERG.

It is noteworthy that IF assays, in addition to confirming the Western Blotting results at the protein level, provided valuable insights into the specific retinal areas where these changes occur. These improvements were observed in both IPL and OPL layers, suggesting a widespread effect on all retinal synapses rather than being limited to a specific group. However, syntaxin-1A and synapsin I levels could not be verified in the OPL due to the scarcity of these isoforms in that particular group of synapses, where syntaxin-3 and Synapsin III prevail²⁸¹.

The C1QL1 protein and the KIF1B-KBP complex could be playing a fundamental role behind these improvements in synaptic transmission, as demonstrated by the high significance obtained in the microarray assay. Notably, the RPD analysis revealed several pathways related to neurotransmission that involved the *Kif1b* gene. Consequently, we incorporated these three genes into our RT-qPCR validation and the most differentiated gene (*C1ql1*) into our protein assessments. Our findings indicated that diabetes led to downregulation of all these proteins, whereas topical sitagliptin treatment also preserved their levels. Additionally, IF results revealed that the primary producers of C1QL1 are ganglion neurons and INL neurons. KIF1B protein was initially linked to mitochondrial transport and a motor role in axon elongation, however, subsequent findings have associated it with synaptic vesicles containing synaptophysin, synaptotagmin, and SV2²⁸². In addition, Mok *et al.* demonstrated that KIF1B can bind PSD-95 and regulate the transport of several PSD-95-associated membrane or signaling proteins like some NMDA receptor subunits²⁸³. These findings suggest that it may have an involvement in synaptic transmission at both pre- and post-synaptic levels. Regarding C1QL1 protein, it has been demonstrated that it not necessary for proper presynaptic structures development in adult cochlear inner hair cells, nonetheless, its deletion leads to loss of afferent synapse maintenance, impaired neuronal transmission and finally hearing loss, thus suggesting its high impact on the organ functionality²⁸⁴. Possibly, a similar phenomenon could be occurring in diabetic retinas.

The primary mediator of all these neuroprotective effects appears to be the retinal GLP-1/GLP-1R axis. Its activation has demonstrated to be essential for enhancing sitagliptin-induced GABAergic transmission²⁸⁵. Furthermore, there exist evidences that support that GLP-1R activation can modulate glutamatergic synapses²⁸⁶. In addition, our previous studies with GLP-1 eye drops showed its own capacity of protecting retinal functionality while they share common neuroprotective effects with DPP-4i treatments, including inhibition of glutamate excitotoxicity through GLAST downregulation^{86,178}. Although the main actions of sitagliptin seem mediated by an increase of retinal GLP-1 levels, the simultaneous activation of other mechanisms unrelated to GLP-1/GLP-1R cannot be ruled out¹⁸³. The DPP4 enzyme is expressed in neurons and recent data demonstrates its colocalization with presynaptic proteins, such as synaptophysin, in axonal terminals, suggesting a possible role in synaptic physiology²⁸⁷, which may be independent of GLP-1. Additionally, other DPP-4 substrates such as CCL5, NPY, PPY or SDF-1 have been related with synapse transmission. CCL5 facilitates excitatory aminoacid release²⁸⁸, NPY and PYY inhibit excitatory synaptic transmission²⁸⁹, and SDF-1 can modulate GABAergic synapses²⁹⁰. The evidence indicates that there exist intricate interactions between the effects of GLP-1 on neurotransmission and those of other DPP-4 substrates. Despite this complexity, the overarching perspective reveals a clear and positive impact, suggesting a beneficial effect overall.

It is worth mentioning that one of the main lessons of the EUROCONDOR clinical trial was that neurodegeneration (at least when assessed by multifocal electroretinography) was not detected in a significant proportion (35%) of patients presenting early microvascular impairment^{63,291}. Hence, neurodegeneration could be the herald of DR only in a subset of subjects with diabetes. These findings revealed that the screening retinal neurodysfunction is a critical issue for identifying those patients in whom neuroprotective treatment might be of particular benefit in early stages of DR⁷.

In conclusion, the administration of topical sitagliptin (eye drops) has neuroprotective effects in an experimental model of DR. One of the main mechanisms of action rely in the preservation of pre- and postsynaptic proteins and other crucial molecules involved in synapse formation and maintenance (**Figure 40**). This evidence supports the concept that sitagliptin can be envisaged as a new strategy for treating not only early stages of DR but also other retinal diseases in which neurodegeneration/synaptic abnormalities play a key role.

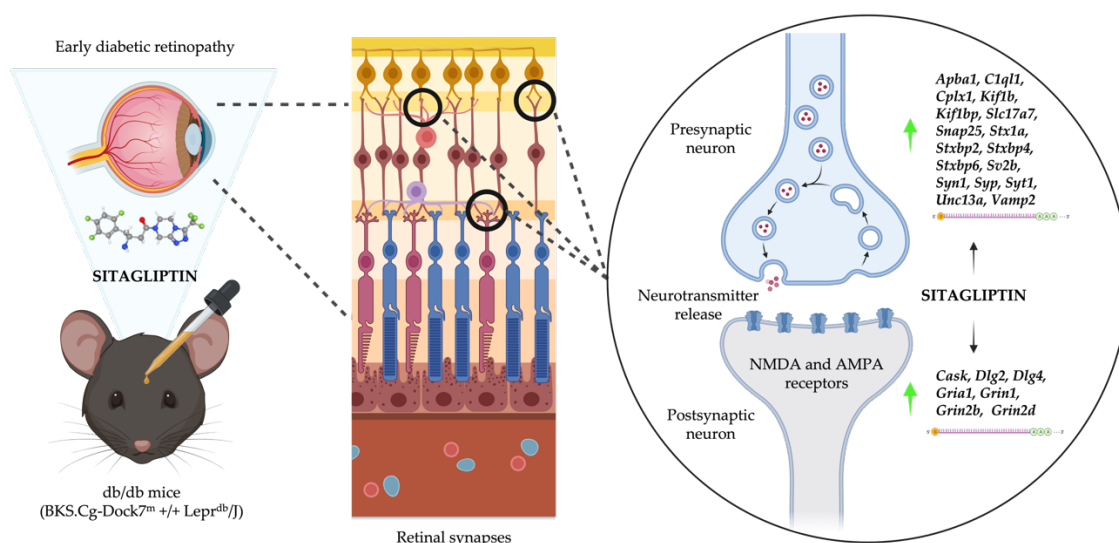


Figure 40. Overview of the main mechanisms of action of sitagliptin eye drops related to synaptic transmission.

5.2. The antioxidant properties of sitagliptin

Oxidative stress plays a pivotal role in the earliest stages of the disease as it is directly altered by hyperglycemia and by the hexosamine, polyol, PKC and AGEs pathways⁴³. This, together with the high susceptibility of the retina to this type of damage, makes oxidative stress one of the main therapeutic targets in terms of new experimental strategies^{53,54}. For all these reasons, we wanted to evaluate the antioxidant capacity of sitagliptin in early DR in the db/db mouse model.

The results of the present study provide evidence that in 12 weeks-aged db/db mice there exists a significant increase in $O_2^{\bullet-}$ levels and oxidative damage to DNA/RNA and proteins. Additionally, there is a notable down-regulation of NRF2 and antioxidant enzymes such as CAT, GPX, GR, CuZnSOD, and MnSOD when compared to db/+ nondiabetic control mice. Moreover, we also provide evidence that sitagliptin eye drops are able to reduce oxidative damage by preserving crucial antioxidant enzymes and decreasing superoxide levels.

The ability of sitagliptin to stimulate the NRF2/ARE pathway and improve the unfavorable effects of conditions driven by oxidative stress has been previously demonstrated. An instance of this is observed in a rat model of Alzheimer's disease induced by β -amyloid, where sitagliptin enhanced cognitive function through its antioxidant properties, brought about by activating NRF2²⁹². Sitagliptin demonstrated also to be able to increase the activities of some

antioxidant enzymes, such as SOD, independently of their glucose-lowering abilities²⁹³. In the present study, we found that sitagliptin eye drops preserved mRNA and protein production by the murine retina of both antioxidant elements: the NRF2/ARE pathway and the enzymatic defenses GPX, GR, CuZnSOD, and MnSOD (with the exception of CAT and CuZnSOD in the ONL). In addition, we found that sitagliptin reduced the number of TXNIP positive cells. TXNIP is a prooxidant and proapoptotic protein that inhibits thioredoxin, another important antioxidant enzyme crucial for retinal homeostasis^{294,295}. Remarkably, we further detected that the topical administration of sitagliptin also reduced the RNA/DNA oxidative damage induced by RNS and ROS in the retinas of db/db mice. All these findings are in agreement with other studies where sitagliptin was administered systemically^{296,297}. However, in these studies it is not possible to know whether the observed effects are due to a direct antioxidative action of the drug or as a consequence of the reduction of systemic oxidative stress due to the improvement of hyperglycemia. Overall, to the best of our knowledge, this is the first evidence of antioxidant effects of sitagliptin in the diabetic retina when administered topically to the eye.

Limited understanding exists regarding the mechanisms underlying the antioxidant and intrinsic functions of DPP-4i. Given that the elevation of GLP-1 availability stands as a primary outcome of administering DPP-4i, it could be hypothesized that the antioxidant impact is primarily driven by GLP-1 rather than DPP-4i itself. Indeed, previous research has shown that GLP-1 applied topically also possesses the ability to decrease oxidative damage in the same experimental DR model⁶⁰. Nonetheless, the antioxidant effects of DPP-4i have also been observed in *in vitro* models without GLP-1²⁹⁸. Furthermore, our study has revealed that sitagliptin, unlike GLP-1 eye drops, is able to ameliorate the deficiencies of GPX and GR at protein level and improve the downregulation of CuZnSOD protein levels in the GCL layer⁶⁰. These findings reinforce our hypothesis about the relevance of GLP-1-independent mechanisms of sitagliptin in the context of treating early stages of DR.

We also evaluated PKC hyperactivation, which is one of the mechanisms that has been postulated as a possible link between hyperglycemia and oxidative stress in DR²⁹⁹. It is not still clear whether PKC activation contributes more to oxidative stress than oxidative stress contributes to its enhancement⁴³. Gerald *et al.* reported that hyperglycemia promotes through PKC- δ two different fundamental DR pathways: cumulative ROS production and NF- κ B activation⁴⁴. Notably, we have found that sitagliptin eye drops prevented diabetic up-regulation of PKC- δ . We also obtained similar results for PKC- β , an isoform that has been strongly associated to the vascular dysfunction³⁰⁰. In the same line, Koyani *et al.* proved that saxagliptin was able to reduce PKC hyperactivation in cardiomyocytes³⁰¹.

To summarize, the topical use of sitagliptin demonstrates strong antioxidant efficacy by maintaining the equilibrium between prooxidant and antioxidant mediators, which are disrupted in DR. This therapeutic approach could also be suitable for other retinal diseases linked to oxidative stress apart from DR.

5.3. The anti-inflammatory effects of sitagliptin

DR is considered a chronic low-grade inflammatory condition that involves several inflammatory mediators and adhesion molecules, which play a key role in both early and late stages of the disease⁷⁵. Our results evidenced that sitagliptin eye drops are able to reduce I κ B α phosphorylation and the subsequent NF- κ B translocation while diminishing the production of crucial pro-inflammatory cytokines (IL-1 β and TNF- α), thus demonstrating the anti-inflammatory capacity of sitagliptin in early DR. In the same line, Hasegawa, *et al.* reported in human endothelial cells stimulated with lipopolysaccharide a significant reduction of NF- κ B after sitagliptin treatment³⁰². Additionally, Li *et al.* demonstrated that linagliptin reduces TNF- α accumulation and NF- κ B activation in retinal endothelial cells¹⁸². These *in vitro* results support the beneficial effects of sitagliptin independently of GLP-1 enhancement. In addition, Gonçalves *et al.* also proved sitagliptin's capability to reduce IL-1 β in the retinas of ZDF rats²⁹⁷. However, in this case, since sitagliptin was administered by the oral route, the beneficial effects could be attributed to the increase of systemic GLP-1 and/or the improvement of glucose control.

Behind these anti-inflammatory properties could be the modulation that the drug exerts on the *Commd8* gene, one of the most differentiated genes between vehicle-treated and sitagliptin-treated animals in the microarray study. As this gene is closely related to the I κ B α /NF- κ B pathway, through its role in I κ B α turnover²⁴⁴, it could be a genuine mechanism by which sitagliptin reduces inflammation. At the protein level, it was not possible to study COMMD8 because it has aroused little scientific interest till now and, consequently, there are not antibodies working properly. Recently, Nakai *et al.* reported that COMMD8 is crucial for B cell migration and humoral immune responses³⁰³, suggesting that the anti-inflammatory action associated with the downregulation of this protein extends beyond the NF- κ B pathway.

Regarding VCAM-1, an important player in leukocyte recruitment and adhesion to retinal blood vessels during the inflammatory process of DR²⁴⁸, we found an abnormal up-regulation of its levels in db/db mice treated with vehicle. Similar results were obtained by Gustavsson *et*

al. in STZ mice³⁰⁴, and Qong *et al.*³⁰⁵. Interestingly, sitagliptin eye drops effectively lowered VCAM-1 protein and mRNA levels, providing further evidence of its anti-inflammatory properties. The reduction of VCAM-1 could be mediated by GLP-1, as GLP-1R agonists can cause this effect by themselves in retinal cells³⁰⁶. Furthermore, regarding other GLP-1R-independent mechanisms, only SDF-1, a substrate of DPP-4, has been related to VCAM-1, raising VCAM-1 expression³⁰⁷. This increase contributes to the reported proangiogenic effects of SDF-1. However these effects may occur only during the late stages of DR (PDR and DME)^{307,308}, while during early stages SDF-1 have a protective role^{309,310}, specially on retinal ganglion cells and the optic nerve³¹¹. Despite all this, the overall balance of the VCAM-1 content showed a reduction, thus it could be hypothesized that the reducing and beneficial effects of GLP-1 on VCAM-1 levels are greater than the ability of SDF-1 to increase them.

Therefore, topical administration of sitagliptin, in addition to its neuroprotective and antioxidant effects, has anti-inflammatory properties, further increasing the spectrum of retinal diseases that could benefit from this new therapeutic strategy. All these beneficial effects could be involved in the functional recovery (ERG) and the preservation of the rate of proliferation (Ki67 positive cells) (**Figure 41**).

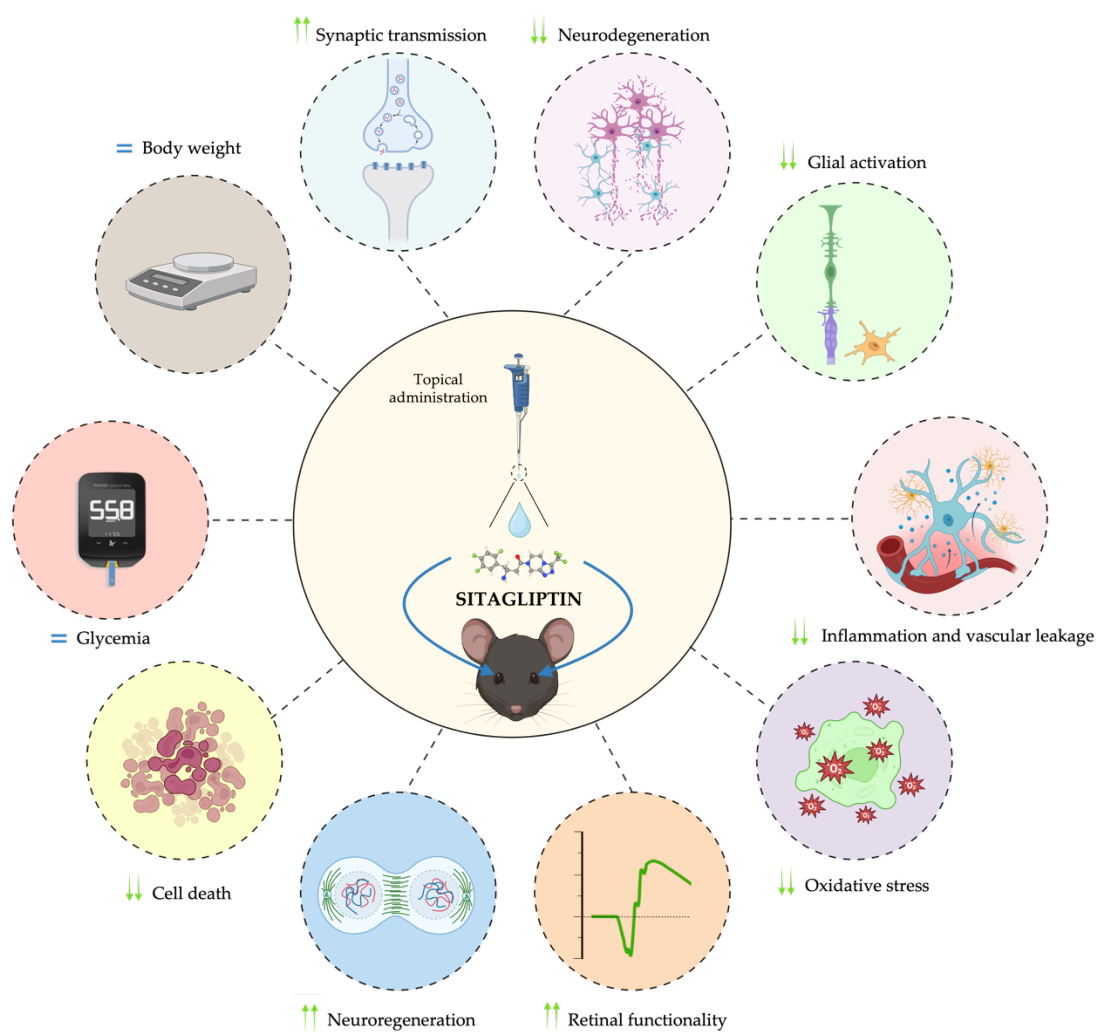


Figure 41. The main effects of sitagliptin eye drops in the db/db mouse model after two weeks of twice-daily administration.

5.4. The relevance of the topical administration

One of the innovative strengths of this therapeutic approach, sitagliptin eye drops, is the type of administration used. Unlike current treatments that use invasive intravitreal injections¹⁰⁸, this approach allows the drug to be delivered in a much safer way without losing efficacy³¹². In addition, it allows self-administration of the drug to patients, reducing visits and medical interventions, thus minimizing the costs involved. However, errors in self-administration of eye drops may occur, increasing the risk of therapeutic failure³¹³. Despite this, with proper patient education in long-term administration of eye drops³¹³, maximum benefit of

DPP-4i can be gained by using this highly safe route of administration. Furthermore, to treat early diabetic retinopathy where vision is not yet compromised, such an invasive route as intravitreal injections can hardly be justified.

Another safe route of administration of DPP-4i, which has been tested several times in experimental DR, is oral administration, which is precisely the one approved by the FDA and the EMA for the treatment of T2DM³¹⁴. Nevertheless, current evidence does not indicate any beneficial effect of neither oral nor any other type of systemic administration of DPP-4i on DR in addition to their improvement of blood glucose levels. Indeed, systematic reviews and meta-analyses reported a neutral effect of DPP-4i on DR^{315–317}. This may be explained by the fact that most DPP-4i, including sitagliptin, are unable to cross the BRB^{318,319}. For this reason, we examined the effect of topical administration of sitagliptin. It is worth mentioning again that the ability of antidiabetic drugs to lower blood glucose levels is a confounding factor in studies aimed at assessing their potential effect on the development or progression of DR.

In our study, neither body weight nor blood glucose levels were altered after topical sitagliptin treatment, indicating that all the neuroprotective, antioxidant and anti-inflammatory effects described previously can only be attributed to the direct effect of the drug on the retina and not to a systemic improvement. Hence, the results presented in the present thesis, to our knowledge, represent one of the first evidences of the direct beneficial effects of DPP-4i for the treatment of early DR.

5.5. Translational implications: minimum effective dose study

The results of the present thesis provide further insights into the mechanisms of action behind the prevention of the main hallmarks of the disease in the db/db mouse model, which were previously published by our group¹⁷⁸. This resolves the lack of preclinical evidence on the topical use of DPP-4i, more specifically sitagliptin, bringing them one step closer to market launch. In addition, we decided to perform a dose-effectiveness study where we tested two low concentrations of sitagliptin, 1 and 5 mg/mL, to see if they were equally capable of reversing the main hallmarks of the NVU impairment (glial activation, neuronal cell death and vascular leakage). We also decided to include saxagliptin, which belongs to the other type of DPP-4i, the cyanopyrrolidines, and was the first of this subgroup to be marketed for the treatment of T2DM. In this case, we decided to test 1 mg/mL and 10 mg/mL, both administered twice daily. Whereas sitagliptin inhibits DPP-4 enzyme by forming non-covalent bonds with its catalytic site, saxagliptin forms a covalent enzyme–inhibitor complex with slow rates of dissociation and

DISCUSSION

consequently longer durations of action³²⁰. For this reason, we also wanted to examine whether saxagliptin could be administered once per day instead of twice per day.

Our findings indicated that the minimum effective concentrations for inhibiting all studied retinal abnormalities were 5 mg/mL for sitagliptin and 10 mg/mL for saxagliptin when both were administered twice daily. It was observed that while glial activation could be abrogated by using saxagliptin once daily, there was no significant reduction in neuroretinal thinning and vascular leakage. Similarly, to achieve complete neurovascular protection with saxagliptin twice-daily administration was needed.

In this dose-effectiveness study we also wanted to see if DPP-4 inhibition could have any effect on the retinal content of the enzyme. Interestingly, sitagliptin and saxagliptin (with the exception of the administration at 1 mg/mL once per day) down-regulated the DPP-4 content in the diabetic retina. Although we do not have any reliable explanation for this finding, it could be related to the reported GLP-1 enhancement that occurs after topical ocular administration of DPP-4i in the same experimental model¹⁷⁸.

Finally, it is important to mention that sitagliptin eye drops for the treatment of early stages of DR are currently in the process of finishing preclinical regulatory studies. Furthermore, the first human clinical trial is expected to start in 2024.

5.6. Limitations of the study

The first limitation refers to what has been mentioned throughout this discussion section, which is the challenge of distinguishing the exclusive effects mediated by GLP-1, those mediated by other DPP-4 substrates, and the synergistic effects between both. To address this, the use of a diabetic model that is also a knockout for GLP-1R would be necessary. This would allow to observe whether sitagliptin is able to prevent damage to diabetic retinas without the protective actions of GLP-1, similar to what Dietrich *et al.* did using linagliptin (a DPP-4i) in the *Caenorhabditis elegans* model of hyperglycemia-induced neurodegeneration in which GLP-1R is not produced¹⁸³. However, to the best of our knowledge there is only one viable model of GLP-1R to date^{321,322}.

Another constraint is that it is difficult to speak of prevention or reversal, as we do not know to what extent the various abnormalities observed in the retinas of the 12-week-old diabetic animals were already present at 10 weeks and have therefore been reversed by the drug, or

whether they have appeared over the weeks of treatment in a manner in which sitagliptin has prevented their appearance. Perhaps both events, prevention and reversal, may occur at the same time.

Another potential limiting factor to consider is the relatively short treatment duration of 2 weeks. Nevertheless, all the published studies testing the effectiveness of DPP-4i and other molecules addressed to treat early stages of DR using topical administration have been performed using similar treatment duration^{178,323,324}. Despite this, the effects of sitagliptin after long-term administration should be evaluated.

Finally, this model recapitulates most of the human DR abnormalities, however, several differences between both species have been described^{188,200,325}. In addition, the db/db mouse is a model of T2DM, and although it could be hypothesized that the beneficial effects of sitagliptin eye drops would be useful in T1DM patients, specific research to confirm this issue is needed.

CONCLUSIONS

1. Transcriptomes comparison (microarrays and GSEA) between sitagliptin-treated and vehicle-treated db/db mice, revealed that **topical** administration of **sitagliptin positively modulates** pathways related **neurotransmission**.
2. **Presynaptic proteins** involved in vesicle biogenesis, mobilization, docking, fusion and recycling, **are down-regulated in db/db mice retinas** at mRNA and protein levels
3. **Postsynaptic glutamate receptors and scaffolding proteins** that regulate the synaptic localization of many receptors, channels and signaling proteins **are down-regulated in db/db mice retinas** at mRNA levels
4. **Topical** administration (eye drops) of **sitagliptin preserves presynaptic and postsynaptic elements** in db/db mice. Up -regulation of *C1ql1* gene may potentially exert a significant role in mediating these effects.
5. **Topical** administration (eye drops) of sitagliptin **preserve** the **physiological oxidative balance** between ROS and antioxidant defenses. The treatment reduces ROS, preserves the levels of NRF2 and crucial antioxidant enzymes (MnSOD, CuZnSOD, GR and GPX), and abrogates oxidative damage to macromolecules in the diabetic retina.
6. **Topical** administration (eye drops) of **sitagliptin diminishes the inflammatory response** within diabetic retinas. It inhibits the activation of the NF- κ B pathway by avoiding I κ B α phosphorylation and the consequent NF- κ B translocation to the nucleus. Furthermore, it reduces the levels of pro-inflammatory cytokines and adhesion molecules (IL-1 β , TNF- α , VCAM-1). The down-regulation of *Commf8* gene by sitagliptin could play a relevant role on these beneficial effects.
7. **Topical** administration of **sitagliptin preserves** the physiological **proliferation** rate of retinal neurons in db/db diabetic mice.
8. **Sitagliptin eye drops improve** the **functionality** of the diabetic retina.
9. The **minimum effective concentrations** for **sitagliptin** and **saxagliptin** are **5 mg/mL** and **10 mg/mL** respectively, administered twice per day.

These **findings could pave the way for clinical trials** to test this new approach in the treatment of early stages of DR or even other retinal diseases.

REFERENCES

1. Cole, J. B. & Florez, J. C. Genetics of diabetes mellitus and diabetes complications. *Nat Rev Nephrol* **16**, 377–390 (2020).
2. Classification and diagnosis of diabetes: standards of medical care in diabetes—2018. *Diabetes Care* **41**, S13–S27 (2018).
3. Sun, H. *et al.* IDF Diabetes Atlas: Global, regional and country-level diabetes prevalence estimates for 2021 and projections for 2045. *Diabetes Res Clin Pract* **183**, 109119 (2022).
4. Ding, J. & Wong, T. Y. Current epidemiology of diabetic retinopathy and diabetic macular edema. *Curr Diab Rep* **12**, 346–354 (2012).
5. Wong, T. Y., Cheung, C. M. G., Larsen, M., Sharma, S. & Simó, R. Diabetic retinopathy. *Nat Rev Dis Primers* **2**, 16012 (2016).
6. Solomon, S. D. *et al.* Diabetic retinopathy: A position statement by the american diabetes association. *Diabetes Care* **40**, 412–418 (2017).
7. Simó, R., Stitt, A. W. & Gardner, T. W. Neurodegeneration in diabetic retinopathy: Does it really matter? *Diabetologia* **61**, 1902–1912 (2018).
8. Zhang, J. *et al.* Diabetic macular edema: Current understanding, molecular mechanisms and therapeutic implications. *Cells* **11**, 3362 (2022).
9. Simó, R. & Hernández, C. Neurodegeneration is an early event in diabetic retinopathy: therapeutic implications. *British Journal of Ophthalmology* **96**, 1285–1290 (2012).
10. Leasher, J. L. *et al.* Global estimates on the number of people blind or visually impaired by diabetic retinopathy: A meta-analysis from 1990 to 2010. *Diabetes Care* **39**, 1643–1649 (2016).
11. Lee, R., Wong, T. Y. & Sabanayagam, C. Epidemiology of diabetic retinopathy, diabetic macular edema and related vision loss. *Eye and Vision* **2**, 17 (2015).
12. Teo, Z. L. *et al.* Global prevalence of diabetic retinopathy and projection of burden through 2045. *Ophthalmology* **128**, 1580–1591 (2021).
13. Simó, R. & Hernández, C. What else can we do to prevent diabetic retinopathy? *Diabetologia* (2023) doi:10.1007/s00125-023-05940-5.
14. Keenan, H. A. *et al.* Clinical factors associated with resistance to microvascular complications in diabetic patients of extreme disease duration. *Diabetes Care* **30**, 1995–1997 (2007).
15. Zhang, L., Krzentowski, G., Albert, A. & Lefebvre, P. J. Risk of developing retinopathy in diabetes control and complications trial type 1 diabetic patients with good or poor metabolic control. *Diabetes Care* **24**, 1275–1279 (2001).
16. Trott, M., Driscoll, R. & Pardhan, S. Associations between diabetic retinopathy and modifiable risk factors: An umbrella review of meta-analyses. *Diabetic Medicine* **39**, (2022).

REFERENCES

17. Shah, J. *et al.* Dietary intake and diabetic retinopathy: A systematic review of the literature. *Nutrients* **14**, 5021 (2022).
18. Sasongko, M. B. *et al.* Novel versus traditional risk markers for diabetic retinopathy. *Diabetologia* **55**, 666–670 (2012).
19. Cheung, N. & Wong, T. Y. Obesity and eye diseases. *Surv Ophthalmol* **52**, 180–195 (2007).
20. Conway, B. N. Prediction of proliferative diabetic retinopathy with hemoglobin level. *Archives of Ophthalmology* **127**, 1494 (2009).
21. Donaghue, K. C. *et al.* Do all prepubertal years of diabetes duration contribute equally to diabetes complications? *Diabetes Care* **26**, 1224–1229 (2003).
22. Chandrasekaran, P., Madanagopalan, V. & Narayanan, R. Diabetic retinopathy in pregnancy - A review. *Indian J Ophthalmol* **69**, 3015 (2021).
23. Hietala, K., Forsblom, C., Summanen, P. & Groop, P.-H. Heritability of proliferative diabetic retinopathy. *Diabetes* **57**, 2176–2180 (2008).
24. Iadecola, C. The neurovascular unit coming of age: A journey through neurovascular coupling in health and disease. *Neuron* **96**, 17–42 (2017).
25. London, A., Benhar, I. & Schwartz, M. The retina as a window to the brain—from eye research to CNS disorders. *Nat Rev Neurol* **9**, 44–53 (2013).
26. Meng, C. *et al.* Pyroptosis in the retinal neurovascular unit: New insights into diabetic retinopathy. *Front Immunol* **12**, (2021).
27. Simó, R., Simó-Servat, O., Bogdanov, P. & Hernández, C. Neurovascular unit: A new target for treating early stages of diabetic retinopathy. *Pharmaceutics* **13**, 1320 (2021).
28. Brown, L. S. *et al.* Pericytes and Neurovascular Function in the Healthy and Diseased Brain. *Front Cell Neurosci* **13**, (2019).
29. Holmes, D. Reconstructing the retina. *Nature* **561**, S2–S3 (2018).
30. Chaya, T. *et al.* Versatile functional roles of horizontal cells in the retinal circuit. *Sci Rep* **7**, 5540 (2017).
31. Masland, R. H. The tasks of amacrine cells. *Vis Neurosci* **29**, 3–9 (2012).
32. Huang, H. Pericyte-endothelial interactions in the retinal microvasculature. *Int J Mol Sci* **21**, 7413 (2020).
33. Ornelas, S. *et al.* Three-dimensional ultrastructure of the brain pericyte-endothelial interface. *Journal of Cerebral Blood Flow & Metabolism* **41**, 2185–2200 (2021).
34. Díaz-Coránguez, M., Ramos, C. & Antonetti, D. A. The inner blood-retinal barrier: Cellular basis and development. *Vision Res* **139**, 123–137 (2017).
35. Metea, M. R. & Newman, E. A. Signalling within the neurovascular unit in the mammalian retina. *Exp Physiol* **92**, 635–640 (2007).

36. Simó, R. & Hernández, C. Neurodegeneration in the diabetic eye: new insights and therapeutic perspectives. *Trends in Endocrinology & Metabolism* **25**, 23–33 (2014).
37. Metea, M. R. & Newman, E. A. Calcium signaling in specialized glial cells. *Glia* **54**, 650–655 (2006).
38. Kugler, E. C., Greenwood, J. & MacDonald, R. B. The “neuro-glial-vascular” unit: The role of glia in neurovascular unit formation and dysfunction. *Front Cell Dev Biol* **9**, (2021).
39. Nian, S., Lo, A. C. Y., Mi, Y., Ren, K. & Yang, D. Neurovascular unit in diabetic retinopathy: Pathophysiological roles and potential therapeutical targets. *Eye and Vision* **8**, 15 (2021).
40. Fernández-Sánchez, L., Lax, P., Campello, L., Pinilla, I. & Cuenca, N. Astrocytes and Müller cell alterations during retinal degeneration in a transgenic rat model of retinitis pigmentosa. *Front Cell Neurosci* **9**, (2015).
41. Zeng, Y. *et al.* Early retinal neurovascular impairment in patients with diabetes without clinically detectable retinopathy. *British Journal of Ophthalmology* **103**, 1747–1752 (2019).
42. Yumnamcha, T., Guerra, M., Singh, L. P. & Ibrahim, A. S. Metabolic dysregulation and neurovascular dysfunction in diabetic retinopathy. *Antioxidants* **9**, 1244 (2020).
43. Kang, Q. & Yang, C. Oxidative stress and diabetic retinopathy: Molecular mechanisms, pathogenetic role and therapeutic implications. *Redox Biol* **37**, 101799 (2020).
44. Geraldles, P. & King, G. L. Activation of protein kinase C isoforms and its impact on diabetic complications. *Circ Res* **106**, 1319–1331 (2010).
45. Mathebula, S. D. Biochemical changes in diabetic retinopathy triggered by hyperglycaemia: A review. *African Vision and Eye Health* **77**, (2018).
46. Safi, S. Z., Qvist, R., Kumar, S., Batumalaie, K. & Ismail, I. S. Bin. Molecular mechanisms of diabetic retinopathy, general preventive strategies, and novel therapeutic targets. *Biomed Res Int* **2014**, 1–18 (2014).
47. Lorenzi, M. The polyol pathway as a mechanism for diabetic retinopathy: attractive, elusive, and resilient. *Exp Diabetes Res* **2007**, 1–10 (2007).
48. Brownlee, M. Biochemistry and molecular cell biology of diabetic complications. *Nature* **414**, 813–820 (2001).
49. Singh, V. P., Bali, A., Singh, N. & Jaggi, A. S. Advanced glycation end products and diabetic complications. *The Korean Journal of Physiology & Pharmacology* **18**, 1 (2014).
50. Ott, C. *et al.* Role of advanced glycation end products in cellular signaling. *Redox Biol* **2**, 411–429 (2014).
51. Zong, H., Ward, M. & Stitt, A. W. AGEs, RAGE, and diabetic retinopathy. *Curr Diab Rep* **11**, 244–252 (2011).
52. Betteridge, D. J. What is oxidative stress? *Metabolism* **49**, 3–8 (2000).

REFERENCES

53. Dammak, A. *et al.* From oxidative stress to inflammation in the posterior ocular diseases: Diagnosis and treatment. *Pharmaceutics* **13**, 1376 (2021).
54. Pinazo-duran, M. *et al.* Oxidative stress and its downstream signaling in aging eyes. *Clin Interv Aging* 637 (2014) doi:10.2147/CIA.S52662.
55. Al-Shabrawey, M. & Smith, S. Prediction of diabetic retinopathy: role of oxidative stress and relevance of apoptotic biomarkers. *EPMA Journal* **1**, 56–72 (2010).
56. Pacher, P., Nivorozhkin, A. & Szabó, C. Therapeutic effects of xanthine oxidase inhibitors: Renaissance half a century after the discovery of allopurinol. *Pharmacol Rev* **58**, 87–114 (2006).
57. Gubitosi-Klug, R. A., Talahalli, R., Du, Y., Nadler, J. L. & Kern, T. S. 5-lipoxygenase, but not 12/15-lipoxygenase, contributes to degeneration of retinal capillaries in a mouse model of diabetic retinopathy. *Diabetes* **57**, 1387–1393 (2008).
58. Madonna, R. *et al.* High glucose-induced hyperosmolarity contributes to COX-2 expression and angiogenesis: implications for diabetic retinopathy. *Cardiovasc Diabetol* **15**, 18 (2016).
59. Deliyanti, D. *et al.* Nox (NADPH oxidase) 1, Nox4, and Nox5 promote vascular permeability and neovascularization in retinopathy. *Hypertension* **75**, 1091–1101 (2020).
60. Ramos, H. *et al.* Beneficial effects of glucagon-like peptide-1 (GLP-1) in diabetes-induced retinal abnormalities: Involvement of oxidative stress. *Antioxidants* **9**, 846 (2020).
61. Kansanen, E., Kuosmanen, S. M., Leinonen, H. & Levonen, A.-L. The Keap1-Nrf2 pathway: Mechanisms of activation and dysregulation in cancer. *Redox Biol* **1**, 45–49 (2013).
62. Albert-Garay, J. S., Riesgo-Escovar, J. R. & Salceda, R. High glucose concentrations induce oxidative stress by inhibiting Nrf2 expression in rat Müller retinal cells in vitro. *Sci Rep* **12**, 1261 (2022).
63. Simó, R. *et al.* Effects of topically administered neuroprotective drugs in early stages of diabetic retinopathy: Results of the EUROCONDOR clinical trial. *Diabetes* **68**, 457–463 (2019).
64. Yang, S., Zhang, J. & Chen, L. The cells involved in the pathological process of diabetic retinopathy. *Biomedicine & Pharmacotherapy* **132**, 110818 (2020).
65. Sorrentino, F. S., Allkabet, M., Salsini, G., Bonifazzi, C. & Perri, P. The importance of glial cells in the homeostasis of the retinal microenvironment and their pivotal role in the course of diabetic retinopathy. *Life Sci* **162**, 54–59 (2016).
66. Arroba, A. I. & Valverde, Á. M. Modulation of microglia in the retina: new insights into diabetic retinopathy. *Acta Diabetol* **54**, 527–533 (2017).

67. Coorey, N. J., Shen, W., Chung, S. H., Zhu, L. & Gillies, M. C. The role of glia in retinal vascular disease. *Clin Exp Optom* **95**, 266–281 (2012).
68. Wang, J., Xu, X., Elliott, M. H., Zhu, M. & Le, Y.-Z. Müller cell-derived VEGF is essential for diabetes-induced retinal inflammation and vascular leakage. *Diabetes* **59**, 2297–2305 (2010).
69. Shin, E. S., Huang, Q., Gurel, Z., Sorenson, C. M. & Sheibani, N. High glucose alters retinal astrocytes phenotype through increased production of inflammatory cytokines and oxidative stress. *PLoS One* **9**, e103148 (2014).
70. Zeng, H. Microglial activation in human diabetic retinopathy. *Archives of Ophthalmology* **126**, 227 (2008).
71. Rübsam, A., Parikh, S. & Fort, P. Role of inflammation in diabetic retinopathy. *Int J Mol Sci* **19**, 942 (2018).
72. Altmann, C. & Schmidt, M. The role of microglia in diabetic retinopathy: Inflammation, microvasculature defects and neurodegeneration. *Int J Mol Sci* **19**, 110 (2018).
73. Tonade, D., Liu, H., Palczewski, K. & Kern, T. S. Photoreceptor cells produce inflammatory products that contribute to retinal vascular permeability in a mouse model of diabetes. *Diabetologia* **60**, 2111–2120 (2017).
74. Tang, J. & Kern, T. S. Inflammation in diabetic retinopathy. *Prog Retin Eye Res* **30**, 343–358 (2011).
75. Vujosevic, S. & Toma, C. Diabetic retinopathy: An inflammatory disease. *Ann Eye Sci* **3**, 52–52 (2018).
76. Du, Y., Veenstra, A., Palczewski, K. & Kern, T. S. Photoreceptor cells are major contributors to diabetes-induced oxidative stress and local inflammation in the retina. *Proceedings of the National Academy of Sciences* **110**, 16586–16591 (2013).
77. Simão, S., Costa, M. Â., Sun, J. K., Cunha-Vaz, J. & Simó, R. Development of a normative database for multifocal electroretinography in the context of a multicenter clinical trial. *Ophthalmic Res* **57**, 107–117 (2017).
78. Ishikawa, M. Abnormalities in glutamate metabolism and excitotoxicity in the retinal diseases. *Scientifica (Cairo)* **2013**, 1–13 (2013).
79. VanGuilder, H. D. *et al.* Diabetes downregulates presynaptic proteins and reduces basal synapsin I phosphorylation in rat retina. *European Journal of Neuroscience* **28**, 1–11 (2008).
80. Zhang, L., Ino-ue, M., Dong, K. & Yamamoto, M. Retrograde axonal transport impairment of large- and medium-sized retinal ganglion cells in diabetic rat. *Curr Eye Res* **20**, 131–6 (2000).
81. Li, Q. & Puro, D. G. Diabetes-induced dysfunction of the glutamate transporter in retinal Müller cells. *Invest Ophthalmol Vis Sci* **43**, 3109–16 (2002).

REFERENCES

82. Lau, J. C. M., Kroes, R. A., Moskal, J. R. & Linsenmeier, R. A. Diabetes changes expression of genes related to glutamate neurotransmission and transport in the Long-Evans rat retina. *Mol Vis* **19**, 1538–53 (2013).
83. Christensen, I. *et al.* The susceptibility of retinal ganglion cells to glutamatergic excitotoxicity is type-specific. *Front Neurosci* **13**, (2019).
84. Ly, A. *et al.* Retinal proteome alterations in a mouse model of type 2 diabetes. *Diabetologia* **57**, 192–203 (2014).
85. Robinson, W. F., VanGuilder, H. D., D’Cruz, T. S., El-Remessy, A. B. & Barber, A. J. Synapsin 1 protein expression and phosphorylation are compromised by diabetes in rodent and human retinas. *Investigative Ophthalmology & Visual Science May* **49**, 4920 (2008).
86. Hernández, C. *et al.* Topical administration of GLP-1 receptor agonists prevents retinal neurodegeneration in experimental diabetes. *Diabetes* **65**, 172–187 (2016).
87. Garcia-Ramírez, M. *et al.* Interphotoreceptor retinoid-binding protein (IRBP) is downregulated at early stages of diabetic retinopathy. *Diabetologia* **52**, 2633–41 (2009).
88. Barnstable, C. Neuroprotective and antiangiogenic actions of PEDF in the eye: molecular targets and therapeutic potential. *Prog Retin Eye Res* **23**, 561–577 (2004).
89. Carrasco, E. *et al.* Lower somatostatin expression is an early event in diabetic retinopathy and is associated with retinal neurodegeneration. *Diabetes Care* **30**, 2902–2908 (2007).
90. Gonzalez-Fernandez, F. & Ghosh, D. Focus on molecules: Interphotoreceptor retinoid-binding protein (IRBP). *Exp Eye Res* **86**, 169–170 (2008).
91. den Hollander, A. I. *et al.* A homozygous missense mutation in the IRBP gene (RBP3) associated with autosomal recessive retinitis pigmentosa. *Investigative Ophthalmology & Visual Science* **50**, 1864 (2009).
92. Roy, S., Bae, E., Amin, S. & Kim, D. Extracellular matrix, gap junctions, and retinal vascular homeostasis in diabetic retinopathy. *Exp Eye Res* **133**, 58–68 (2015).
93. Oshitari, T. *et al.* Effect of combined antisense oligonucleotides against high-glucose- and diabetes-induced overexpression of extracellular matrix components and increased vascular permeability. *Diabetes* **55**, 86–92 (2006).
94. Pfister, F. *et al.* Pericyte migration. *Diabetes* **57**, 2495–2502 (2008).
95. Korn, C. & Augustin, H. G. Mechanisms of vessel pruning and regression. *Dev Cell* **34**, 5–17 (2015).
96. Hammes, H.-P., Feng, Y., Pfister, F. & Brownlee, M. Diabetic retinopathy: Targeting vasoregression. *Diabetes* **60**, 9–16 (2011).

97. Xu, Y. *et al.* Increased sCD200 levels in vitreous of patients with proliferative diabetic retinopathy and its correlation with VEGF and proinflammatory cytokines. *Investigative Ophthalmology & Visual Science* **56**, 6565 (2015).
98. Karan, B. M., Little, K., Augustine, J., Stitt, A. W. & Curtis, T. M. Aldehyde dehydrogenase and aldo-keto reductase enzymes: Basic concepts and emerging roles in diabetic retinopathy. *Antioxidants* **12**, 1466 (2023).
99. dell'Omo, R. *et al.* Vitreous mediators in retinal hypoxic diseases. *Mediators Inflamm* **2013**, 1–16 (2013).
100. Abu El-Asrar, A. M. *et al.* Angiogenesis regulatory factors in the vitreous from patients with proliferative diabetic retinopathy. *Acta Diabetol* **50**, 545–551 (2013).
101. Wang, X., Bove, A. M., Simone, G. & Ma, B. Molecular bases of VEGFR-2-mediated physiological function and pathological role. *Front Cell Dev Biol* **8**, (2020).
102. Gucciardo, E., Loukovaara, S., Salven, P. & Lehti, K. Lymphatic vascular structures: A new aspect in proliferative diabetic retinopathy. *Int J Mol Sci* **19**, 4034 (2018).
103. Loukovaara, S. *et al.* Quantitative proteomics analysis of vitreous humor from diabetic retinopathy patients. *J Proteome Res* **14**, 5131–5143 (2015).
104. Simó-Servat, O., Hernández, C. & Simó, R. Usefulness of the vitreous fluid analysis in the translational research of diabetic retinopathy. *Mediators Inflamm* **2012**, 1–11 (2012).
105. Daruich, A. *et al.* Mechanisms of macular edema: Beyond the surface. *Prog Retin Eye Res* **63**, 20–68 (2018).
106. Simó, R., Villarroel, M., Corraliza, L., Hernández, C. & Garcia-Ramírez, M. The retinal pigment epithelium: Something more than a constituent of the blood-retinal barrier-implications for the pathogenesis of diabetic retinopathy. *J Biomed Biotechnol* **2010**, 1–15 (2010).
107. Reichenbach, A. *et al.* Müller cells as players in retinal degeneration and edema. *Graefes Archive for Clinical and Experimental Ophthalmology* **245**, 627–636 (2007).
108. Tomita, Y., Lee, D., Tsubota, K., Negishi, K. & Kurihara, T. Updates on the current treatments for diabetic retinopathy and possibility of future oral therapy. *J Clin Med* **10**, 4666 (2021).
109. Zhao, Y. & Singh, R. P. The role of anti-vascular endothelial growth factor (anti-VEGF) in the management of proliferative diabetic retinopathy. *Drugs Context* **7**, 1–10 (2018).
110. Fong, D. S., Girach, A. & Boney, A. Visual side effects of successful scatter laser photocoagulation surgery for proliferative diabetic retinopathy. *Retina* **27**, 816–824 (2007).
111. Deschler, E. K., Sun, J. K. & Silva, P. S. Side-effects and complications of laser treatment in diabetic retinal disease. *Semin Ophthalmol* **29**, 290–300 (2014).

REFERENCES

112. Simó, R., Sundstrom, J. M. & Antonetti, D. A. Ocular anti-VEGF therapy for diabetic retinopathy: The role of VEGF in the pathogenesis of diabetic retinopathy. *Diabetes Care* **37**, 893–899 (2014).
113. Wykoff, C. C. *et al.* Efficacy, durability, and safety of intravitreal faricimab with extended dosing up to every 16 weeks in patients with diabetic macular oedema (YOSEMITE and RHINE): two randomised, double-masked, phase 3 trials. *The Lancet* **399**, 741–755 (2022).
114. Uludag, G. *et al.* Efficacy and safety of intravitreal anti-VEGF therapy in diabetic retinopathy: what we have learned and what should we learn further? *Expert Opin Biol Ther* **22**, 1275–1291 (2022).
115. Zehden, J. A., Mortensen, X. M., Reddy, A. & Zhang, A. Y. Systemic and ocular adverse events with intravitreal anti-VEGF therapy used in the treatment of diabetic retinopathy: a review. *Curr Diab Rep* **22**, 525–536 (2022).
116. Yorston, D. Anti-VEGF drugs in the prevention of blindness. *Community Eye Health* **27**, 44–6 (2014).
117. Barnes, P. J. How corticosteroids control inflammation: Quintiles Prize Lecture 2005. *Br J Pharmacol* **148**, 245–254 (2006).
118. Dugel, P. U., Bandello, F. & Loewenstein, A. Dexamethasone intravitreal implant in the treatment of diabetic macular edema. *Clinical Ophthalmology* **1321** (2015) doi:10.2147/OPTH.S79948.
119. Zhang, W., Liu, H., Rojas, M., Caldwell, R. W. & Caldwell, R. B. Anti-inflammatory therapy for diabetic retinopathy. *Immunotherapy* **3**, 609–628 (2011).
120. Kirk, J. & Fraser-Bell, S. Steroids for diabetic macular oedema – A brief review of the data. *European Ophthalmic Review* **13**, 44 (2019).
121. Abdelhadi, A. M., Helaly, H. A. & Abuelkeir, A. Evaluation of retinal detachment after diabetic vitrectomy: causes and ways of management. *Clinical Ophthalmology* **Volume 14**, 53–60 (2020).
122. Gupta, V. & Arevalo, Jf. Surgical management of diabetic retinopathy. *Middle East Afr J Ophthalmol* **20**, 283 (2013).
123. Al-Hinai, A. Vitrectomy versus Phaco-vitrectomy. *Oman J Ophthalmol* **12**, 71 (2019).
124. Simó, R. & Hernández, C. New Insights into treating early and advanced stage diabetic retinopathy. *Int J Mol Sci* **23**, 8513 (2022).
125. Saleh, I., Maritska, Z., Parisa, N. & Hidayat, R. Inhibition of receptor for advanced glycation end products as new promising strategy treatment in diabetic retinopathy. *Open Access Maced J Med Sci* **7**, 3921–3924 (2019).

126. Ren, X. *et al.* Protective function of pyridoxamine on retinal photoreceptor cells via activation of the p-Erk1/2/Nrf2/Trx/ASK1 signalling pathway in diabetic mice. *Mol Med Rep* **14**, 420–424 (2016).
127. Jakus, V. & Rietbrock, N. Advanced glycation end-products and the progress of diabetic vascular complications. *Physiol Res* **53**, 131–42 (2004).
128. Lewis, E. J. *et al.* Pyridorin in type 2 diabetic nephropathy. *Journal of the American Society of Nephrology* **23**, 131–136 (2012).
129. Garcia-Medina, J. J. *et al.* Update on the effects of antioxidants on diabetic retinopathy: In vitro experiments, animal studies and clinical trials. *Antioxidants* **9**, 561 (2020).
130. Filippelli, M. *et al.* Anti-inflammatory effect of curcumin, homotaurine, and vitamin D3 on human vitreous in patients with diabetic retinopathy. *Front Neurol* **11**, (2021).
131. Gao, L., Zhao, X., Jiao, L. & Tang, L. Intravitreal corticosteroids for diabetic macular edema: a network meta-analysis of randomized controlled trials. *Eye and Vision* **8**, 35 (2021).
132. Ramos, H., Hernández, C., Simó, R. & Simó-Servat, O. Inflammation: The link between neural and vascular impairment in the diabetic retina and therapeutic implications. *Int J Mol Sci* **24**, 8796 (2023).
133. Ohira, A. *et al.* Topical dexamethasone γ -cyclodextrin nanoparticle eye drops increase visual acuity and decrease macular thickness in diabetic macular oedema. *Acta Ophthalmol* **93**, 610–615 (2015).
134. Kern, T. S. *et al.* Topical administration of nepafenac inhibits diabetes-induced retinal microvascular disease and underlying abnormalities of retinal metabolism and physiology. *Diabetes* **56**, 373–379 (2007).
135. Schoenberger, S. D. & Kim, S. J. Nonsteroidal anti-inflammatory drugs for retinal disease. *Int J Inflam* **2013**, 1–8 (2013).
136. Wen Li, H. H. Blockade of tumor necrosis factor alpha prevents complications of diabetic retinopathy. *J Clin Exp Ophthalmol* **05**, (2014).
137. Ye, Q. Effects of etanercept on the apoptosis of ganglion cells and expression of Fas, TNF- α , caspase-8 in the retina of diabetic rats. *Int J Ophthalmol* **12**, (2019).
138. Wu, L. *et al.* Intravitreal tumor necrosis factor inhibitors in the treatment of refractory diabetic macular edema. *Retina* **31**, 298–303 (2011).
139. Sfikakis, P. P. *et al.* Regression of sight-threatening macular edema in type 2 diabetes following treatment with the anti-tumor necrosis factor monoclonal antibody infliximab. *Diabetes Care* **28**, 445–447 (2005).

REFERENCES

140. Hernández, C. *et al.* SOCS1-derived peptide administered by eye drops prevents retinal neuroinflammation and vascular leakage in experimental diabetes. *Int J Mol Sci* **20**, 3615 (2019).
141. Hernández, C. *et al.* Effect of topical administration of somatostatin on retinal inflammation and neurodegeneration in an experimental model of diabetes. *J Clin Med* **9**, 2579 (2020).
142. Liu, Y. *et al.* Pigment epithelium-derived factor (PEDF) peptide eye drops reduce inflammation, cell death and vascular leakage in diabetic retinopathy in Ins2Akita mice. *Molecular Medicine* **18**, 1387–1401 (2012).
143. Yoshida, Y. *et al.* Protective role of pigment epithelium-derived factor (PEDF) in early phase of experimental diabetic retinopathy. *Diabetes Metab Res Rev* **25**, 678–686 (2009).
144. Zerbini, G. *et al.* Topical nerve growth factor prevents neurodegenerative and vascular stages of diabetic retinopathy. *Front Pharmacol* **13**, (2022).
145. Park, J. H., Kang, S.-S., Kim, J. Y. & Tchah, H. Nerve growth factor attenuates apoptosis and inflammation in the diabetic cornea. *Investigative Ophthalmology & Visual Science* **57**, 6767 (2016).
146. Gong, Y. *et al.* Protective effects of adeno-associated virus mediated brain-derived neurotrophic factor expression on retinal ganglion cells in diabetic rats. *Cell Mol Neurobiol* **32**, 467–475 (2012).
147. Hernández, C. *et al.* Topical administration of somatostatin prevents retinal neurodegeneration in experimental diabetes. *Diabetes* **62**, 2569–2578 (2013).
148. Arroba, A. I. *et al.* Somatostatin protects photoreceptor cells against high glucose-induced apoptosis. *Mol Vis* **22**, 1522–1531 (2016).
149. Kuhre, R. E., Deacon, C. F., Holst, J. J. & Petersen, N. What is an L-cell and how do we study the secretory mechanisms of the L-cell? *Front Endocrinol (Lausanne)* **12**, (2021).
150. Seino, Y., Fukushima, M. & Yabe, D. GIP and GLP-1, the two incretin hormones: Similarities and differences. *J Diabetes Investig* **1**, 8–23 (2010).
151. Knudsen, L. B. Inventing liraglutide, a glucagon-like peptide-1 analogue, for the treatment of diabetes and obesity. *ACS Pharmacol Transl Sci* **2**, 468–484 (2019).
152. Bethea, M., Bozadjieva-Kramer, N. & Sandoval, D. A. Preproglucagon products and their respective roles regulating insulin secretion. *Endocrinology* **162**, (2021).
153. Marzook, A., Tomas, A. & Jones, B. The interplay of glucagon-like peptide-1 receptor trafficking and signalling in pancreatic beta cells. *Front Endocrinol (Lausanne)* **12**, (2021).
154. Alhadeff, A. L., Rupprecht, L. E. & Hayes, M. R. GLP-1 neurons in the nucleus of the solitary tract project directly to the ventral tegmental area and nucleus accumbens to control for food intake. *Endocrinology* **153**, 647–658 (2012).

155. Trapp, S. & Brierley, D. I. Brain GLP-1 and the regulation of food intake: GLP-1 action in the brain and its implications for GLP-1 receptor agonists in obesity treatment. *Br J Pharmacol* **179**, 557–570 (2022).
156. Siddiqui, E. M., Mehan, S., Bhalla, S. & Shandilya, A. Potential role of IGF-1/GLP-1 signaling activation in intracerebral hemorrhage. *Current Research in Neurobiology* **3**, 100055 (2022).
157. Kim, Y.-K., Kim, O. Y. & Song, J. Alleviation of depression by glucagon-like peptide 1 through the regulation of neuroinflammation, neurotransmitters, neurogenesis, and synaptic function. *Front Pharmacol* **11**, (2020).
158. Abbas, T., Faivre, E. & Hölscher, C. Impairment of synaptic plasticity and memory formation in GLP-1 receptor KO mice: Interaction between type 2 diabetes and Alzheimer's disease. *Behavioural Brain Research* **205**, 265–271 (2009).
159. Grieco, M. *et al.* Glucagon-like peptide-1: A focus on neurodegenerative diseases. *Front Neurosci* **13**, (2019).
160. Reich, N. & Hölscher, C. The neuroprotective effects of glucagon-like peptide 1 in Alzheimer's and Parkinson's disease: An in-depth review. *Front Neurosci* **16**, (2022).
161. Puddu, A., Sanguineti, R., Montecucco, F. & Viviani, G. L. Retinal pigment epithelial cells express a functional receptor for glucagon-like peptide-1 (GLP-1). *Mediators Inflamm* **2013**, 1–10 (2013).
162. Chen, H. *et al.* Decreased expression of glucagon-like peptide-1 receptor and sodium-glucose co-transporter 2 in patients with proliferative diabetic retinopathy. *Front Endocrinol (Lausanne)* **13**, (2022).
163. Wei, L. *et al.* GLP-1 RA improves diabetic retinopathy by protecting the blood-retinal barrier through GLP-1R-ROCK-p-MLC signaling pathway. *J Diabetes Res* **2022**, 1–14 (2022).
164. Sampedro, J. *et al.* New insights into the mechanisms of action of topical administration of GLP-1 in an experimental model of diabetic retinopathy. *J Clin Med* **8**, 339 (2019).
165. Lawrence, E. C. N. *et al.* Topical and systemic GLP-1R agonist administration both rescue retinal ganglion cells in hypertensive glaucoma. *Front Cell Neurosci* **17**, (2023).
166. Shu, X. *et al.* Topical ocular administration of the GLP-1 receptor agonist liraglutide arrests hyperphosphorylated tau-triggered diabetic retinal neurodegeneration via activation of GLP-1R/Akt/GSK3 β signaling. *Neuropharmacology* **153**, 1–12 (2019).
167. Zhang, Y. *et al.* Protection of exendin-4 analogue in early experimental diabetic retinopathy. *Graefes's Archive for Clinical and Experimental Ophthalmology* **247**, 699–706 (2009).

REFERENCES

168. Zeng, Y. *et al.* The glucagon like peptide 1 analogue, exendin-4, attenuates oxidative stress-induced retinal cell death in early diabetic rats through promoting Sirt1 and Sirt3 expression. *Exp Eye Res* **151**, 203–211 (2016).
169. Fan, Y. *et al.* Exendin-4 alleviates retinal vascular leakage by protecting the blood–retinal barrier and reducing retinal vascular permeability in diabetic Goto-Kakizaki rats. *Exp Eye Res* **127**, 104–116 (2014).
170. Holst, J. J. The physiology of glucagon-like peptide 1. *Physiol Rev* **87**, 1409–1439 (2007).
171. Kasina, S. V. S. K. & Baradhi, K. M. *Dipeptidyl peptidase IV (DPP IV) inhibitors*. (2023). [Updated 2023 May 22]. In: StatPearls [Internet]. Treasure Island (FL): StatPearls Publishing; 2023 Jan-. Available from: <https://www.ncbi.nlm.nih.gov/books/NBK542331/>
172. Gwaltney II, S. Medicinal chemistry approaches to the inhibition of dipeptidyl peptidase IV. *Curr Top Med Chem* **8**, 1545–1552 (2008).
173. Angelopoulou, E. & Piperi, C. DPP-4 inhibitors: A promising therapeutic approach against Alzheimer’s disease. *Ann Transl Med* **6**, 255–255 (2018).
174. Dong, Q. *et al.* Sitagliptin protects the cognition function of the Alzheimer’s disease mice through activating glucagon-like peptide-1 and BDNF-TrkB signalings. *Neurosci Lett* **696**, 184–190 (2019).
175. Nassar, N. N., Al-Shorbagy, M. Y., Arab, H. H. & Abdallah, D. M. Saxagliptin: A novel antiparkinsonian approach. *Neuropharmacology* **89**, 308–317 (2015).
176. Badawi, G. A., Abd El Fattah, M. A., Zaki, H. F. & El Sayed, M. I. Sitagliptin and liraglutide reversed nigrostriatal degeneration of rodent brain in rotenone-induced Parkinson’s disease. *Inflammopharmacology* **25**, 369–382 (2017).
177. Hasegawa, Y. *et al.* DPP-4 inhibition with linagliptin ameliorates the progression of premature aging in klotho^{-/-} mice. *Cardiovasc Diabetol* **16**, 154 (2017).
178. Hernández, C. *et al.* Topical administration of DPP-IV inhibitors prevents retinal neurodegeneration in experimental diabetes. *Diabetologia* **60**, 2285–2298 (2017).
179. Boddu, S., Gupta, H. & Patel, S. Drug delivery to the back of the eye following topical administration: An update on research and patenting activity. *Recent Pat Drug Deliv Formul* **8**, 27–36 (2014).
180. Bhatt, Y., Hunt, D. M. & Carvalho, L. S. The origins of the full-field flash electroretinogram b-wave. *Front Mol Neurosci* **16**, (2023).
181. Gonçalves, A. *et al.* The dipeptidyl peptidase-4 (DPP-4) inhibitor sitagliptin ameliorates retinal endothelial cell dysfunction triggered by inflammation. *Biomedicine & Pharmacotherapy* **102**, 833–838 (2018).

182. Li, H., Zhang, J., Lin, L. & Xu, L. Vascular protection of DPP-4 inhibitors in retinal endothelial cells in in vitro culture. *Int Immunopharmacol* **66**, 162–168 (2019).
183. Dietrich, N. *et al.* The DPP4 inhibitor linagliptin protects from experimental diabetic retinopathy. *PLoS One* **11**, e0167853 (2016).
184. Deacon, C. F. Physiology and pharmacology of DPP-4 in glucose homeostasis and the treatment of type 2 diabetes. *Front Endocrinol (Lausanne)* **10**, (2019).
185. Campos, E. J. *et al.* Impact of type 1 diabetes mellitus and sitagliptin treatment on the neuropeptide Y system of rat retina. *Clin Exp Ophthalmol* **46**, 783–795 (2018).
186. Ou, K. *et al.* Treatment of diabetic retinopathy through neuropeptide Y-mediated enhancement of neurovascular microenvironment. *J Cell Mol Med* **24**, 3958–3970 (2020).
187. Alogliptin (Nesina) for type 2 Diabetes Mellitus [Internet]. Ottawa (ON): Canadian Agency for Drugs and Technologies in Health; 2015 Aug. Table 1, Cost Comparison Table for DPP-4 Inhibitors and Other Second-Line Oral Drugs. Available from: <https://www.ncbi.nlm.nih.gov/books/NBK349203/table/T58/>.
188. Olivares, A. M. *et al.* Animal models of diabetic retinopathy. *Curr Diab Rep* **17**, 93 (2017).
189. Quiroz, J. & Yazdanyar, A. Animal models of diabetic retinopathy. *Ann Transl Med* **9**, 1272–1272 (2021).
190. Simó, R., Simó-Servat, O., Bogdanov, P. & Hernández, C. Diabetic retinopathy: Role of neurodegeneration and therapeutic perspectives. *Asia-Pacific Journal of Ophthalmology* **11**, 160–167 (2022).
191. Lai, A. K. W. & Lo, A. C. Y. Animal models of diabetic retinopathy: summary and comparison. *J Diabetes Res* **2013**, 1–29 (2013).
192. Furman, B. L. Streptozotocin-induced diabetic models in mice and rats. *Curr Protoc* **1**, (2021).
193. Lelyte, I., Ahmed, Z., Kaja, S. & Kalesnykas, G. Structure–function relationships in the rodent streptozotocin-induced model for diabetic retinopathy: a systematic review. *Journal of Ocular Pharmacology and Therapeutics* **38**, 271–286 (2022).
194. Gong, C.-Y., Lu, B., Hu, Q.-W. & Ji, L.-L. Streptozotocin induced diabetic retinopathy in rat and the expression of vascular endothelial growth factor and its receptor. *Int J Ophthalmol* **6**, 573–7 (2013).
195. Naderi, A., Zahed, R., Aghajani, L., Amoli, F. A. & Lashay, A. Long term features of diabetic retinopathy in streptozotocin-induced diabetic Wistar rats. *Exp Eye Res* **184**, 213–220 (2019).
196. Pitale, P. M. & Gorbatyuk, M. S. Diabetic retinopathy: from animal models to cellular signaling. *Int J Mol Sci* **23**, 1487 (2022).

REFERENCES

197. Phipps, J. A., Fletcher, E. L. & Vingrys, A. J. Paired-flash identification of rod and cone dysfunction in the diabetic rat. *Investigative Ophthalmology & Visual Science* **45**, 4592 (2004).
198. Genrikhs, E. E., Stelmashook, E. V., Golyshev, S. A., Aleksandrova, O. P. & Isaev, N. K. Streptozotocin causes neurotoxic effect in cultured cerebellar granule neurons. *Brain Res Bull* **130**, 90–94 (2017).
199. Ighodaro, O. M., Adeosun, A. M. & Akinloye, O. A. Alloxan-induced diabetes, a common model for evaluating the glycemic-control potential of therapeutic compounds and plants extracts in experimental studies. *Medicina (B Aires)* **53**, 365–374 (2017).
200. Robinson, R., Barathi, V. A., Chaurasia, S. S., Wong, T. Y. & Kern, T. S. Update on animal models of diabetic retinopathy: from molecular approaches to mice and higher mammals. *Dis Model Mech* **5**, 444–456 (2012).
201. Barber, A. J. *et al.* The Ins2(Akita) mouse as a model of early retinal complications in diabetes. *Investigative Ophthalmology & Visual Science* **46**, 2210 (2005).
202. Pearson, J. A., Wong, F. S. & Wen, L. The importance of the Non Obese Diabetic (NOD) mouse model in autoimmune diabetes. *J Autoimmun* **66**, 76–88 (2016).
203. Sima, A. A. F., Chakrabarti, S., Garcia-Salinas, R. & Basu, P. K. The BB-rat-an authentic model of human diabetic retinopathy. *Curr Eye Res* **4**, 1087–1092 (1985).
204. Li, C.-R. & Sun, S.-G. Spontaneous rodent models of diabetes and diabetic retinopathy. *Int J Ophthalmol* **3**, 1–4 (2010).
205. Caolo, V. *et al.* Resistance to retinopathy development in obese, diabetic and hypertensive ZSF1 rats: an exciting model to identify protective genes. *Sci Rep* **8**, 11922 (2018).
206. Bogdanov, P. *et al.* The db/db mouse: a useful model for the study of diabetic retinal neurodegeneration. *PLoS One* **9**, e97302 (2014).
207. Kang, M.-K. *et al.* Dietary compound chrysin inhibits retinal neovascularization with abnormal capillaries in db/db mice. *Nutrients* **8**, 782 (2016).
208. Matsubara, H. *et al.* Time-dependent course of electroretinograms in the spontaneous diabetic Goto-Kakizaki rat. *Jpn J Ophthalmol* **50**, 211–216 (2006).
209. Kakehashi, A. *et al.* Characteristics of diabetic retinopathy in SDT rats. *Diabetes Metab Res Rev* **22**, 455–461 (2006).
210. Gong, C.-Y. The development of diabetic retinopathy in Goto-Kakizaki rat and the expression of angiogenesis-related signals. *Chin J Physiol* 預刊文章, 1–9 (2016).
211. Wisniewska-Kruk, J. *et al.* Molecular analysis of blood–retinal barrier loss in the Akimba mouse, a model of advanced diabetic retinopathy. *Exp Eye Res* **122**, 123–131 (2014).
212. Rakoczy, E. P. *et al.* Characterization of a mouse model of hyperglycemia and retinal neovascularization. *Am J Pathol* **177**, 2659–2670 (2010).

213. BKS.Cg-Dock7m +/+ Leprdb/J. <https://www.jax.org/strain/000642>.
214. Klok, M. D., Jakobsdottir, S. & Drent, M. L. The role of leptin and ghrelin in the regulation of food intake and body weight in humans: a review. *Obesity Reviews* **8**, 21–34 (2007).
215. Tang, L. *et al.* Dietary wolfberry ameliorates retinal structure abnormalities in db/db mice at the early stage of diabetes. *Exp Biol Med* **236**, 1051–1063 (2011).
216. Wang, S. *et al.* Zinc Prevents the Development of Diabetic Cardiomyopathy in db/db Mice. *Int J Mol Sci* **18**, 580 (2017).
217. Sukumaran, V., Tsuchimochi, H., Tatsumi, E., Shirai, M. & Pearson, J. T. Azilsartan ameliorates diabetic cardiomyopathy in young db/db mice through the modulation of ACE-2/ANG 1–7/Mas receptor cascade. *Biochem Pharmacol* **144**, 90–99 (2017).
218. Cornish, E. E., Vaze, A., Jamieson, R. V. & Grigg, J. R. The electroretinogram in the genomics era: outer retinal disorders. *Eye* **35**, 2406–2418 (2021).
219. Dong, C.-J., Agey, P. & Hare, W. A. Origins of the electroretinogram oscillatory potentials in the rabbit retina. *Vis Neurosci* **21**, 533–543 (2004).
220. McAnany, J. J., Persidina, O. S. & Park, J. C. Clinical electroretinography in diabetic retinopathy: a review. *Surv Ophthalmol* **67**, 712–722 (2022).
221. McCulloch, D. L. *et al.* ISCEV Standard for full-field clinical electroretinography (2015 update). *Documenta Ophthalmologica* **130**, 1–12 (2015).
222. Marmor, M. F., Holder, G. E., Seeliger, M. W. & Yamamoto, S. Standard for clinical electroretinography (2004 update). *Documenta Ophthalmologica* **108**, 107–114 (2004).
223. Gentleman, R., Carey, V. J., Wolfgang, H., Irizarry, R. A. & Dudoit, S. *Bioinformatics and computational biology solutions using R and Bioconductor*. (Springer, 2005).
224. Irizarry, R. A. *et al.* Exploration, normalization, and summaries of high density oligonucleotide array probe level data. *Biostatistics* **4**, 249–264 (2003).
225. Smyth, G. K. Linear models and empirical Bayes methods for assessing differential expression in microarray experiments. *Stat Appl Genet Mol Biol* **3**, 1–25 (2004).
226. Wu, T. *et al.* clusterProfiler 4.0: A universal enrichment tool for interpreting omics data. *The Innovation* **2**, 100141 (2021).
227. Subramanian, A. *et al.* Gene set enrichment analysis: A knowledge-based approach for interpreting genome-wide expression profiles. *Proceedings of the National Academy of Sciences* **102**, 15545–15550 (2005).
228. Edgar, R. Gene Expression Omnibus: NCBI gene expression and hybridization array data repository. *Nucleic Acids Res* **30**, 207–210 (2002).
229. Smith, P. K. *et al.* Measurement of protein using bicinchoninic acid. *Anal Biochem* **150**, 76–85 (1985).

REFERENCES

230. Anderson, P. Glial and endothelial blood-retinal barrier responses to amyloid-beta in the neural retina of the rat. *Clinical Ophthalmology* 801 (2008) doi:10.2147/OPTH.S3967.
231. Xu, Q., Qaum, T. & Adamis, A. P. Sensitive blood-retinal barrier breakdown quantitation using Evans blue. *Invest Ophthalmol Vis Sci* **42**, 789–794 (2001).
232. Radu, M. & Chernoff, J. An in vivo assay to test blood vessel permeability. *J Vis Exp* e50062 (2013) doi:10.3791/50062.
233. Saria, A. & Lundberg, J. M. Evans blue fluorescence: Quantitative and morphological evaluation of vascular permeability in animal tissues. *J Neurosci Methods* **8**, 41–9 (1983).
234. Jadhav, S., Berendschot, T. T. J. M., Kumaramanickavel, G., De Clerck, E. E. B. & Webers, C. A. B. Diabetic retinal neurodegeneration associated with synaptic proteins and functional defects: A systematic review. *Endocrine and Metabolic Science* **11**, 100127 (2023).
235. Carvalho, C. & Moreira, P. I. Oxidative stress: A major player in cerebrovascular alterations associated to neurodegenerative events. *Front Physiol* **9**, (2018).
236. Bajpai, V. K. *et al.* Antioxidant efficacy and the upregulation of Nrf2-mediated HO-1 expression by (+)-lariciresinol, a lignan isolated from *Rubia philippinensis*, through the activation of p38. *Sci Rep* **7**, 46035 (2017).
237. Singh, L. P. Thioredoxin interacting protein (TXNIP) and pathogenesis of diabetic retinopathy. *J Clin Exp Ophthalmol* **04**, (2013).
238. He, X. & Ma, Q. Redox regulation by nuclear factor erythroid 2-related factor 2: Gatekeeping for the basal and diabetes-induced expression of thioredoxin-interacting protein. *Mol Pharmacol* **82**, 887–897 (2012).
239. Peshavariya, H. M., Dusting, G. J. & Selemidis, S. Analysis of dihydroethidium fluorescence for the detection of intracellular and extracellular superoxide produced by NADPH oxidase. *Free Radic Res* **41**, 699–712 (2007).
240. Juan, C. A., Pérez de la Lastra, J. M., Plou, F. J. & Pérez-Lebeña, E. The chemistry of reactive oxygen species (ROS) revisited: Outlining their role in biological macromolecules (DNA, lipids and proteins) and induced pathologies. *Int J Mol Sci* **22**, 4642 (2021).
241. Guo, C. *et al.* 8-Hydroxyguanosine as a possible RNA oxidative modification marker in urine from colorectal cancer patients: Evaluation by ultra performance liquid chromatography-tandem mass spectrometry. *Journal of Chromatography B* **1136**, 121931 (2020).
242. Bandookwala, M. & Sengupta, P. 3-Nitrotyrosine: a versatile oxidative stress biomarker for major neurodegenerative diseases. *International Journal of Neuroscience* **130**, 1047–1062 (2020).

243. Liu, T., Zhang, L., Joo, D. & Sun, S.-C. NF- κ B signaling in inflammation. *Signal Transduct Target Ther* **2**, 17023 (2017).
244. Starokadomskyy, P. *et al.* CCDC22 deficiency in humans blunts activation of proinflammatory NF- κ B signaling. *Journal of Clinical Investigation* **123**, 2244–2256 (2013).
245. Quagliaro, L. *et al.* Intermittent high glucose enhances ICAM-1, VCAM-1 and E-selectin expression in human umbilical vein endothelial cells in culture: The distinct role of protein kinase C and mitochondrial superoxide production. *Atherosclerosis* **183**, 259–267 (2005).
246. Lin, C.-C. *et al.* Tumor necrosis factor- α induces VCAM-1-mediated inflammation via c-Src-dependent transactivation of EGF receptors in human cardiac fibroblasts. *J Biomed Sci* **22**, 53 (2015).
247. Deem, T. L. & Cook-Mills, J. M. Vascular cell adhesion molecule 1 (VCAM-1) activation of endothelial cell matrix metalloproteinases: role of reactive oxygen species. *Blood* **104**, 2385–2393 (2004).
248. Kong, D.-H., Kim, Y., Kim, M., Jang, J. & Lee, S. Emerging roles of vascular cell adhesion molecule-1 (VCAM-1) in immunological disorders and cancer. *Int J Mol Sci* **19**, 1057 (2018).
249. Lopez, F. *et al.* Modalities of synthesis of Ki67 antigen during the stimulation of lymphocytes. *Cytometry* **12**, 42–49 (1991).
250. Sun, X. & Kaufman, P. D. Ki-67: more than a proliferation marker. *Chromosoma* **127**, 175–186 (2018).
251. Barber, A. J. *et al.* Neural apoptosis in the retina during experimental and human diabetes. Early onset and effect of insulin. *Journal of Clinical Investigation* **102**, 783–791 (1998).
252. Klaassen, I., Van Noorden, C. J. F. & Schlingemann, R. O. Molecular basis of the inner blood-retinal barrier and its breakdown in diabetic macular edema and other pathological conditions. *Prog Retin Eye Res* **34**, 19–48 (2013).
253. Oprescu, S., Horzmann, K., Yue, F., Freeman, J. & Kuang, S. Microarray, IPA and GSEA analysis in mice models. *Bio Protoc* **8**, (2018).
254. Sigoillot, S. M. *et al.* The secreted protein C1QL1 and its receptor BAI3 control the synaptic connectivity of excitatory inputs converging on cerebellar Purkinje cells. *Cell Rep* **10**, 820–832 (2015).
255. Drerup, C. M., Lusk, S. & Nechiporuk, A. Kif1B interacts with KBP to promote axon elongation by localizing a microtubule regulator to growth cones. *Journal of Neuroscience* **36**, 7014–7026 (2016).

REFERENCES

256. Campbell, P. D. *et al.* Unique function of kinesin Kif5A in localization of mitochondria in axons. *The Journal of Neuroscience* **34**, 14717–14732 (2014).
257. Becherer, U. & Rettig, J. Vesicle pools, docking, priming, and release. *Cell Tissue Res* **326**, 393–407 (2006).
258. Han, J., Pluhackova, K. & Böckmann, R. A. The multifaceted role of SNARE proteins in membrane fusion. *Front Physiol* **8**, (2017).
259. Stepien, K. P., Prinslow, E. A. & Rizo, J. Munc18-1 is crucial to overcome the inhibition of synaptic vesicle fusion by α SNAP. *Nat Commun* **10**, 4326 (2019).
260. Lipstein, N. *et al.* Munc13-1 is a Ca²⁺-phospholipid-dependent vesicle priming hub that shapes synaptic short-term plasticity and enables sustained neurotransmission. *Neuron* **109**, 3980–4000.e7 (2021).
261. Okamoto, M. & Südhof, T. C. Mints, Munc18-interacting proteins in synaptic vesicle exocytosis. *Journal of Biological Chemistry* **272**, 31459–31464 (1997).
262. He, R., Li, C., Liu, Y. & Yu, H. Reconstitution and biochemical studies of extended synaptotagmin-mediated lipid transport. in 33–62 (2022). doi:10.1016/bs.mie.2022.07.003.
263. Courtney, N. A., Bao, H., Briguglio, J. S. & Chapman, E. R. Synaptotagmin 1 clamps synaptic vesicle fusion in mammalian neurons independent of complexin. *Nat Commun* **10**, 4076 (2019).
264. Stout, K. A., Dunn, A. R., Hoffman, C. & Miller, G. W. The synaptic vesicle glycoprotein 2: Structure, function, and disease relevance. *ACS Chem Neurosci* **10**, 3927–3938 (2019).
265. Martineau, M., Guzman, R. E., Fahlke, C. & Klingauf, J. VGLUT1 functions as a glutamate/proton exchanger with chloride channel activity in hippocampal glutamatergic synapses. *Nat Commun* **8**, 2279 (2017).
266. Micheva, K. D., Busse, B., Weiler, N. C., O'Rourke, N. & Smith, S. J. Single-synapse analysis of a diverse synapse population: Proteomic imaging methods and markers. *Neuron* **68**, 639–653 (2010).
267. Kwon, S. E. & Chapman, E. R. Synaptophysin regulates the kinetics of synaptic vesicle endocytosis in central neurons. *Neuron* **70**, 847–854 (2011).
268. Böhler, M., Benfenati, F., Valtorta, F. & Greengard, P. The synapsins and the regulation of synaptic function. *BioEssays* **12**, 259–263 (1990).
269. Bykhovskaia, M. Synapsin regulation of vesicle organization and functional pools. *Semin Cell Dev Biol* **22**, 387–392 (2011).
270. Huang, S., Chen, L., Bladen, C., Stys, P. K. & Zamponi, G. W. Differential modulation of NMDA and AMPA receptors by cellular prion protein and copper ions. *Mol Brain* **11**, 62 (2018).

271. Smith, S. B. Diabetic retinopathy and the NMDA receptor. *Drug News Perspect* **15**, 226 (2002).
272. Hsueh, Y.-P. The role of the MAGUK protein CASK in neural development and synaptic function. *Curr Med Chem* **13**, 1915–1927 (2006).
273. Jeong, J. *et al.* PSD-95 binding dynamically regulates NLGN1 trafficking and function. *Proceedings of the National Academy of Sciences* **116**, 12035–12044 (2019).
274. Barber, A. J. & Baccouche, B. Neurodegeneration in diabetic retinopathy: Potential for novel therapies. *Vision Res* **139**, 82–92 (2017).
275. Masser, D. R. *et al.* Insulin treatment normalizes retinal neuroinflammation but not markers of synapse loss in diabetic rats. *Exp Eye Res* **125**, 95–106 (2014).
276. Ying, Y. *et al.* Neuroprotective effects of ginsenoside Rg1 against hyperphosphorylated Tau-induced diabetic retinal neurodegeneration via activation of IRS-1/Akt/GSK3 β signaling. *J Agric Food Chem* **67**, 8348–8360 (2019).
277. Pavlou, S. *et al.* Attenuating diabetic vascular and neuronal defects by targeting P2rx7. *Int J Mol Sci* **20**, 2101 (2019).
278. Bogdanov, P. *et al.* Effects of liposomal formulation of citicoline in experimental diabetes-induced retinal neurodegeneration. *Int J Mol Sci* **19**, 2458 (2018).
279. Nagamatsu, S., Ohara-Imaizumi, M., Nakamichi, Y., Aoyagi, K. & Nishiwaki, C. DPP-4 inhibitor des-F-sitagliptin treatment increased insulin exocytosis from db/db mice β cells. *Biochem Biophys Res Commun* **412**, 556–560 (2011).
280. Kutsyr, O. *et al.* Sitagliptin, a dipeptidyl peptidase-IV inhibitor, attenuates retinal neurodegeneration in rd10 mice. *Acta Ophthalmol* **96**, 68–68 (2018).
281. Sherry, D. M., Mitchell, R., Standifer, K. M. & du Plessis, B. Distribution of plasma membrane-associated syntaxins 1 through 4 indicates distinct trafficking functions in the synaptic layers of the mouse retina. *BMC Neurosci* **7**, 54 (2006).
282. Zhao, C. *et al.* Charcot-Marie-tooth disease Type 2A caused by mutation in a microtubule motor KIF1B β . *Cell* **105**, 587–597 (2001).
283. Mok, H. *et al.* Association of the kinesin superfamily motor protein KIF1B α with postsynaptic density-95 (PSD-95), synapse-associated protein-97, and synaptic scaffolding molecule PSD-95/discs large/zona occludens-1 proteins. *The Journal of Neuroscience* **22**, 5253–5258 (2002).
284. Qi, Y. *et al.* Deletion of C1ql1 causes hearing loss and abnormal auditory nerve fibers in the mouse cochlea. *Front Cell Neurosci* **15**, (2021).
285. Zhang, Y. *et al.* Inhibition of DPP4 enhances inhibitory synaptic transmission through activating the GLP-1/GLP-1R signaling pathway in a rat model of febrile seizures. *Biochem Pharmacol* **156**, 78–85 (2018).

REFERENCES

286. Mietlicki-Baase, E. G. *et al.* The food intake-suppressive effects of glucagon-like peptide-1 receptor signaling in the ventral tegmental area are mediated by AMPA/kainate receptors. *American Journal of Physiology-Endocrinology and Metabolism* **305**, E1367–E1374 (2013).
287. Király, K. *et al.* Glial cell type-specific changes in spinal dipeptidyl peptidase 4 expression and effects of its inhibitors in inflammatory and neuropathic pain. *Sci Rep* **8**, 3490 (2018).
288. Di Prisco, S., Summa, M., Chellakudam, V., Rossi, P. I. A. & Pittaluga, A. RANTES-mediated control of excitatory amino acid release in mouse spinal cord. *J Neurochem* **121**, 428–437 (2012).
289. Browning, K. N. & Travagli, R. A. Neuropeptide Y and Peptide YY inhibit excitatory synaptic transmission in the rat dorsal motor nucleus of the vagus. *J Physiol* **549**, 775–785 (2003).
290. Bhattacharyya, B. J. *et al.* The Chemokine stromal cell-derived factor-1 regulates GABAergic inputs to neural progenitors in the postnatal dentate gyrus. *Journal of Neuroscience* **28**, 6720–6730 (2008).
291. Santos, A. R. *et al.* Functional and structural findings of neurodegeneration in early stages of diabetic retinopathy: Cross-sectional analyses of baseline data of the EUROCONDOR project. *Diabetes* **66**, 2503–2510 (2017).
292. Li, Y. *et al.* Activation of Nrf2 signaling by sitagliptin and quercetin combination against β -amyloid induced Alzheimer's disease in rats. *Drug Dev Res* **80**, 837–845 (2019).
293. Kawanami, D., Takashi, Y., Takahashi, H., Motonaga, R. & Tanabe, M. Renoprotective effects of DPP-4 inhibitors. *Antioxidants* **10**, 246 (2021).
294. Holubiec, M. I. *et al.* Thioredoxin 1 plays a protective role in retinas exposed to perinatal hypoxia-ischemia. *Neuroscience* **425**, 235–250 (2020).
295. Gimeno-Hernández, R. *et al.* Thioredoxin delays photoreceptor degeneration, oxidative and inflammation alterations in retinitis pigmentosa. *Front Pharmacol* **11**, (2020).
296. Civantos, E. *et al.* Sitagliptin ameliorates oxidative stress in experimental diabetic nephropathy by diminishing the miR-200a/Keap-1/Nrf2 antioxidant pathway. *Diabetes Metab Syndr Obes* **Volume 10**, 207–222 (2017).
297. Gonçalves, A. *et al.* Protective effects of the dipeptidyl peptidase IV inhibitor sitagliptin in the blood-retinal barrier in a type 2 diabetes animal model. *Diabetes Obes Metab* **14**, 454–463 (2012).
298. Wang, C. *et al.* Sitagliptin, an anti-diabetic drug, suppresses estrogen deficiency-induced osteoporosis in vivo and inhibits RANKL-induced osteoclast formation and bone resorption in vitro. *Front Pharmacol* **8**, (2017).

299. Giacco, F. & Brownlee, M. Oxidative stress and diabetic complications. *Circ Res* **107**, 1058–1070 (2010).
300. Kim, J.-H., Kim, J. H., Jun, H.-O., Yu, Y. S. & Kim, K.-W. Inhibition of protein kinase C δ attenuates blood-retinal barrier breakdown in diabetic retinopathy. *Am J Pathol* **176**, 1517–1524 (2010).
301. Koyani, C. N. *et al.* Saxagliptin but not sitagliptin inhibits CaMKII and PKC via DPP9 inhibition in cardiomyocytes. *Front Physiol* **9**, (2018).
302. Hasegawa, H. & Nakamura, Y. Sitagliptin inhibits the lipopolysaccharide-induced inflammation. *J Pharm Drug Deliv Res* **5**, (2016).
303. Nakai, A. *et al.* The COMMD3/8 complex determines GRK6 specificity for chemoattractant receptors. *Journal of Experimental Medicine* **216**, 1630–1647 (2019).
304. Gustavsson, C. *et al.* Vascular cellular adhesion molecule-1 (VCAM-1) expression in mice retinal vessels is affected by both hyperglycemia and hyperlipidemia. *PLoS One* **5**, e12699 (2010).
305. Gong, Q. *et al.* SGLT2 inhibitor-empagliflozin treatment ameliorates diabetic retinopathy manifestations and exerts protective effects associated with augmenting branched chain amino acids catabolism and transportation in db/db mice. *Biomedicine & Pharmacotherapy* **152**, 113222 (2022).
306. Dorecka, M. *et al.* Exendin-4 and GLP-1 decreases induced expression of ICAM-1, VCAM-1 and RAGE in human retinal pigment epithelial cells. *Pharmacological Reports* **65**, 884–890 (2013).
307. Butler, J. M. *et al.* SDF-1 is both necessary and sufficient to promote proliferative retinopathy. *Journal of Clinical Investigation* **115**, 86–93 (2005).
308. You, J.-J., Yang, C.-H., Huang, J.-S., Chen, M.-S. & Yang, C.-M. Fractalkine, a CX3C chemokine, as a mediator of ocular angiogenesis. *Investigative Ophthalmology & Visual Science* **48**, 5290 (2007).
309. Otsuka, H. *et al.* Stromal cell-derived factor-1 is essential for photoreceptor cell protection in retinal detachment. *Am J Pathol* **177**, 2268–2277 (2010).
310. Deng, L., Jia, J., Yao, J. & Xu, Z. Stromal cell-derived factor 1 (SDF-1) and its receptor CXCR4 improves diabetic retinopathy. *Biosci Biotechnol Biochem* **83**, 1072–1076 (2019).
311. Xie, L. *et al.* Monocyte-derived SDF1 supports optic nerve regeneration and alters retinal ganglion cells' response to Pten deletion. *Proceedings of the National Academy of Sciences* **119**, (2022).
312. Khatun, A. & Hu, V. H. Safety around medicines for eye care. *Community Eye Health* **34**, 19–21 (2021).

REFERENCES

313. Lampert, A., Bruckner, T., Haefeli, W. E. & Seidling, H. M. Improving eye-drop administration skills of patients – A multicenter parallel-group cluster-randomized controlled trial. *PLoS One* **14**, e0212007 (2019).
314. Srinivasa Venkata Siva Kumar Kasina, K. M. B. Dipeptidyl peptidase IV (DPP IV) Inhibitors.
315. Chung, Y.-R. *et al.* Dipeptidyl peptidase-4 inhibitors versus other antidiabetic drugs added to metformin monotherapy in diabetic retinopathy progression: A real World-based cohort study. *Diabetes Metab J* **43**, 640 (2019).
316. Taylor, O. M. & Lam, C. The effect of dipeptidyl peptidase-4 inhibitors on macrovascular and microvascular complications of diabetes mellitus: A systematic review. *Current Therapeutic Research* **93**, 100596 (2020).
317. Tang, H. *et al.* Comparisons of diabetic retinopathy events associated with glucose-lowering drugs in patients with type 2 diabetes mellitus: A network meta-analysis. *Diabetes Obes Metab* **20**, 1262–1279 (2018).
318. Fuchs, H., Binder, R. & Greischel, A. Tissue distribution of the novel DPP-4 inhibitor BI 1356 is dominated by saturable binding to its target in rats. *Biopharm Drug Dispos* **30**, 229–240 (2009).
319. Fura, A. *et al.* Pharmacokinetics of the dipeptidyl peptidase 4 inhibitor saxagliptin in rats, dogs, and monkeys and clinical projections. *Drug Metabolism and Disposition* **37**, 1164–1171 (2009).
320. Golightly, L. K., Drayna, C. C. & McDermott, M. T. Comparative clinical pharmacokinetics of dipeptidyl peptidase-4 inhibitors. *Clin Pharmacokinet* **51**, 501–514 (2012).
321. Ayala, J. E. *et al.* Glucagon-like peptide-1 receptor knockout mice are protected from high-fat diet-induced insulin resistance. *Endocrinology* **151**, 4678–4687 (2010).
322. Lamont, B. J. *et al.* Pancreatic GLP-1 receptor activation is sufficient for incretin control of glucose metabolism in mice. *Journal of Clinical Investigation* **122**, 388–402 (2012).
323. Huang, L. *et al.* Therapeutic effects of fenofibrate nano-emulsion eye drops on retinal vascular leakage and neovascularization. *Biology (Basel)* **10**, 1328 (2021).
324. Ibán-Arias, R. *et al.* Effect of topical administration of the microneurotrophin BNN27 in the diabetic rat retina. *Graefe's Archive for Clinical and Experimental Ophthalmology* **257**, 2429–2436 (2019).
325. Kern, T. S., Antonetti, D. A. & Smith, L. E. H. Pathophysiology of diabetic retinopathy: contribution and limitations of laboratory research. *Ophthalmic Res* **62**, 196–202 (2019).

ANNEXES

8.1. Fundings

This research was funded by grants from the Ministerio de Economía y Competitividad (PID2019-104225RB-I00) and the Instituto de Salud Carlos III (DTS18/0163, PI19/01215 and ICI20/00129). The study funder was not involved in the design of the study.

8.2. Supplementary data

Most differentiated genes

Affymetrix ID	Gene Symbol	Entrez	logFC	AveExpr	t	adj.P.Val	B
TC1100003858.mm.2	C1ql1	23829	0,51	8,46	5,24	0,04	3,57
TC1000002262.mm.2	Kif1bp	72320	0,74	7,90	5,07	0,04	3,12
TC1000000093.mm.2	Plagl1	22634	0,33	8,41	4,73	0,04	2,20
TC0400003726.mm.2	Cep85	70012	0,30	9,95	4,71	0,04	2,15
TC0400004035.mm.2	Kif1b	16561	0,48	9,05	4,69	0,04	2,11
TC0400000169.mm.2	Ggh	14590	-0,46	8,88	-4,69	0,04	2,10
TC1100000028.mm.2	Pes1	64934	0,32	10,10	4,67	0,04	2,04
TC0200001959.mm.2	Sirpa	19261	0,30	10,66	4,65	0,04	2,00
TC0600001296.mm.2	March8	71779	0,41	8,85	4,63	0,04	1,95
TC0400003530.mm.2	Thrap3	230753	0,47	9,15	4,49	0,04	1,58
TC1800000771.mm.2	Mex3c	240396	0,40	8,83	4,49	0,04	1,57
TC0700001871.mm.2	Fus	233908	0,42	10,03	4,47	0,04	1,52
TC1000000508.mm.2	Fabp7	12140	-0,45	7,27	-4,45	0,04	1,47
TC0100001613.mm.2	Pigm	67556	0,51	6,52	4,39	0,04	1,31
TC1200001215.mm.2	Wdr20	69641	0,39	8,45	4,38	0,04	1,29
TC1500000897.mm.2	Lrrk2	66725	-0,44	7,15	-4,38	0,04	1,28
TC1200000760.mm.2	Ttc9	69480	0,31	7,99	4,36	0,04	1,24
TC1700002797.mm.2	Traf7	224619	0,50	9,76	4,32	0,05	1,13
TC0400003611.mm.2	Tmem39b	230770	0,39	8,24	4,29	0,05	1,05
TC1100001670.mm.2	Dhx8	217207	0,43	9,24	4,27	0,05	0,99
TC0300000750.mm.2	Gba	14466	0,33	8,85	4,25	0,05	0,93
TC0800001522.mm.2	Tubb3	22152	0,34	9,06	4,19	0,05	0,79
TC1800001083.mm.2	Slc39a6	106957	0,30	9,81	4,18	0,05	0,77
TC1900000806.mm.2	Adrb1	11554	0,44	7,74	4,17	0,05	0,74
TC1100003821.mm.2	Mpp2	50997	0,50	7,50	4,16	0,05	0,71
TC1000000590.mm.2	Slc25a16	73132	0,35	8,33	4,15	0,05	0,69
TC0500002567.mm.2	Commd8	27784	-0,43	8,80	-4,14	0,05	0,65
TC1300001927.mm.2	Tpmt	22017	-0,34	8,61	-4,11	0,06	0,59
TC1900000386.mm.2	Apba1	319924	0,34	8,90	4,09	0,06	0,53
TC0700001916.mm.2	5430419D17Rik	71395	0,36	9,39	4,06	0,06	0,45
TC1000000386.mm.2	Sec63	140740	-0,27	9,74	-4,02	0,06	0,35
TC0500001087.mm.2	Rpl5	1,01E+08	-0,44	11,20	-4,02	0,06	0,35

ANNEXES

TC0400001715.mm.2	Eif4g3	230861	0,37	8,10	4,01	0,06	0,32
TC0800002935.mm.2	Ddx19b	234733	0,35	8,75	4,00	0,06	0,29
TC1900001095.mm.2	Fads2	56473	0,33	10,34	3,99	0,06	0,28
TC0X00002084.mm.2	Tmem255a	245386	0,36	8,51	3,98	0,06	0,26
TC1100002664.mm.2	Sqstm1	18412	0,31	10,09	3,98	0,06	0,24
TC1600001005.mm.2	Ifnar1	15975	0,38	7,93	3,94	0,07	0,15
TC0100002604.mm.2	Tuba4a	22145	0,35	7,73	3,94	0,07	0,15
TC1300000969.mm.2	Cetn3	12626	-0,31	11,03	-3,93	0,07	0,11
TC0600001636.mm.2	Strap	20901	-0,36	9,40	-3,91	0,07	0,08
TC1000002943.mm.2	Slc35e3	215436	0,28	8,11	3,88	0,07	0,01
TC0400003888.mm.2	Plekhm2	69582	0,41	9,21	3,88	0,07	-0,02
TC0500001586.mm.2	Mdh2	17448	0,31	10,05	3,87	0,07	-0,02
TC0700002037.mm.2	B4galnt4	330671	0,32	7,74	3,86	0,07	-0,06
TC0600003412.mm.2	Bcat1	12035	0,29	9,88	3,85	0,07	-0,09
TC0800002428.mm.2	Ano8	382014	0,37	5,90	3,83	0,07	-0,12
TC0500001302.mm.2	Fbxo21	231670	0,27	8,42	3,83	0,07	-0,14
TC1700001194.mm.2	Qpct	70536	-0,35	8,65	-3,82	0,07	-0,16
TC1100000284.mm.2	Efemp1	216616	-0,42	10,17	-3,80	0,07	-0,20
TC0400002007.mm.2	Dnajc11	230935	0,28	8,41	3,80	0,07	-0,21
TC0300000878.mm.2	Pogz	229584	0,38	8,96	3,79	0,07	-0,23
TC1500001717.mm.2	Lynx1	23936	0,38	9,33	3,79	0,07	-0,23
TC0900000863.mm.2	Ciao2a	68250	-0,46	9,52	-3,79	0,07	-0,23
TC0700000024.mm.2	Leng8	232798	0,58	9,44	3,76	0,08	-0,31
TC0300002324.mm.2	Syt11	229521	0,32	9,19	3,75	0,08	-0,33
TC0500001355.mm.2	Hectd4	269700	0,37	10,13	3,75	0,08	-0,34
TC0400001934.mm.2	Srm	20810	0,33	8,40	3,72	0,08	-0,40
TC0800001608.mm.2	Insr	16337	0,32	9,81	3,72	0,08	-0,42
TC0100001944.mm.2	Vcpip1	70675	-0,38	10,52	-3,71	0,08	-0,43
TC0400003383.mm.2	St3gal3	20441	0,37	9,53	3,65	0,09	-0,58
TC0X00001796.mm.2	Wdr13	73447	0,25	8,66	3,64	0,09	-0,59
TC1000002374.mm.2	Gucd1	68778	0,30	8,81	3,64	0,09	-0,61
TC1000001149.mm.2	Tmcc3	319880	0,28	7,36	3,64	0,09	-0,61
TC1900001035.mm.2	Otub1	107260	0,29	10,87	3,63	0,09	-0,62
TC0900001441.mm.2	Nme6	54369	0,32	6,79	3,62	0,09	-0,64
TC1300001779.mm.2	Tubb2a	22151	0,36	10,19	3,62	0,09	-0,65
TC0200005155.mm.2	Zmynd8	228880	0,29	9,50	3,61	0,09	-0,68
TC0500003629.mm.2	Flt1	14254	0,27	8,78	3,61	0,09	-0,68
TC1600002139.mm.2	Hmgn1	15312	-0,28	10,41	-3,61	0,09	-0,68
TC0700002492.mm.2	Clptm1	56457	0,29	10,45	3,60	0,09	-0,70
TC1700000705.mm.2	Mdc1	240087	0,36	8,22	3,60	0,09	-0,70
TC0100001228.mm.2	Adipor1	72674	0,26	9,89	3,59	0,09	-0,72
TC1100003245.mm.2	Abr	109934	0,47	9,00	3,59	0,09	-0,73
TC1200001460.mm.2	Lpin1	14245	0,27	8,63	3,59	0,09	-0,73
TC1500002243.mm.2	Pou6f1	19009	0,31	7,47	3,57	0,10	-0,78
TC0700004413.mm.2	Fam53b	77938	0,34	8,14	3,57	0,10	-0,78
TC0600003475.mm.2	Dennd5b	320560	0,36	8,27	3,56	0,10	-0,79
TC0200001786.mm.2	Mapkbp1	26390	0,35	8,05	3,56	0,10	-0,81

TC1300000670.mm.2	Caml	12328	-0,27	9,64	-3,55	0,10	-0,84
TC0400000725.mm.2	Atp6v1g1	66290	-0,29	9,97	-3,54	0,10	-0,84
TC0200003142.mm.2	Grin1	14810	0,32	9,06	3,53	0,10	-0,86
TC0X00003098.mm.2	Acsl4	50790	-0,28	8,81	-3,52	0,10	-0,90
TC0900002325.mm.2	Wdr61	66317	-0,27	9,44	-3,52	0,10	-0,90
TC1200001269.mm.2	Cep170b	217882	0,40	8,05	3,51	0,10	-0,93
TC0700003775.mm.2	Acer3	66190	-0,37	7,85	-3,51	0,10	-0,93
TC1300000998.mm.2	Edil3	13612	-0,39	10,76	-3,50	0,10	-0,95
TC0200002032.mm.2	Cds2	110911	0,27	10,85	3,49	0,10	-0,97
TC0800000732.mm.2	Sugp1	70616	0,26	9,60	3,48	0,10	-0,99
TC0200003373.mm.2	Ttll11	74410	0,34	8,50	3,48	0,10	-0,99
TC0100000129.mm.2	Paqr8	74229	0,31	6,62	3,48	0,10	-1,00
TC0700001580.mm.2	Olfml1	244198	-0,30	5,55	-3,48	0,10	-1,01
TC0700001827.mm.2	Cdipt	52858	0,34	8,09	3,47	0,10	-1,02
TC0900001927.mm.2	Herpud2	80517	0,40	7,74	3,47	0,10	-1,02
TC1000000886.mm.2	Dapk3	13144	0,39	7,93	3,46	0,11	-1,05
TC1200001814.mm.2	Trappc6b	78232	-0,27	9,90	-3,45	0,11	-1,06
TC1100003609.mm.2	Ube2z	268470	0,32	9,50	3,45	0,11	-1,07
TC1400000263.mm.2	Arf4	11843	-0,38	9,98	-3,45	0,11	-1,08
TC1500001967.mm.2	Cyb5r3	109754	0,32	9,09	3,44	0,11	-1,09
TC0600002024.mm.2	Plxna4	243743	0,27	7,35	3,44	0,11	-1,09
TC1100002851.mm.2	Snap47	67826	0,35	8,61	3,43	0,11	-1,12
TC1000002586.mm.2	Appl2	216190	0,29	9,92	3,43	0,11	-1,13
TC1500001171.mm.2	Egflam	268780	0,33	9,26	3,42	0,11	-1,14
TC0500001734.mm.2	Daglb	231871	0,29	9,15	3,42	0,11	-1,14
TC0500000213.mm.2	Abcb8	74610	0,30	8,93	3,42	0,11	-1,15
TC1100003780.mm.2	Kat2a	14534	0,29	8,30	3,41	0,11	-1,16
TC1100000459.mm.2	Clint1	216705	0,26	9,12	3,41	0,11	-1,17
TC0500001390.mm.2	Gpn3	68080	-0,30	7,09	-3,40	0,11	-1,19
TC0700004629.mm.2	Setd1a	233904	0,27	8,32	3,40	0,11	-1,19
TC0400004157.mm.2	Tas1r3	83771	0,26	7,96	3,39	0,11	-1,21
TC0400001107.mm.2	Dhcr24	74754	0,28	8,70	3,39	0,11	-1,21
TC1000000813.mm.2	Hcn2	15166	0,32	6,32	3,39	0,11	-1,21
TC0200002517.mm.2	Pigt	78928	0,41	9,55	3,39	0,11	-1,22
TC0200000525.mm.2	Tbc1d13	70296	0,29	7,24	3,38	0,11	-1,23
TC0400001712.mm.2	Rap1gap	110351	0,30	9,17	3,38	0,11	-1,23
TC0200000515.mm.2	Odf2	18286	0,31	8,53	3,37	0,11	-1,25
TC1100002126.mm.2	Ewsr1	14030	0,27	11,24	3,37	0,11	-1,27
TC1300002474.mm.2	Hmgcr	15357	0,30	9,77	3,36	0,11	-1,29
TC1000001822.mm.2	Pex7	18634	-0,30	8,35	-3,34	0,12	-1,33
TC0100003104.mm.2	Adora1	11539	0,33	9,23	3,33	0,12	-1,34
TC1100002550.mm.2	Ccng1	12450	-0,38	9,94	-3,33	0,12	-1,35
TC1900000940.mm.2	Bbs1	52028	0,21	9,05	3,33	0,12	-1,35
TC1500001022.mm.2	Smarcd1	83797	0,27	8,24	3,33	0,12	-1,36
TC0X00003429.mm.2	L1cam	16728	0,29	9,49	3,32	0,12	-1,38
TC0300002325.mm.2	1500004A13Rik	319830	0,32	7,48	3,32	0,12	-1,38
TC0200004454.mm.2	Ehd4	98878	0,36	7,67	3,32	0,12	-1,39

ANNEXES

TC0100002189.mm.2	Actr1b	226977	0,26	9,48	3,32	0,12	-1,39
TC0800003034.mm.2	Zdhhc7	102193	0,41	6,51	3,31	0,12	-1,40
TC1700002804.mm.2	Pigq	14755	0,33	7,92	3,31	0,12	-1,41
TC0100000957.mm.2	Fam174a	67698	-0,41	9,98	-3,30	0,12	-1,42
TC0800002529.mm.2	Gab1	14388	0,34	7,54	3,30	0,12	-1,43
TC1200001974.mm.2	Tmem229b	268567	0,42	8,08	3,30	0,12	-1,44
TC1500000351.mm.2	Eny2	223527	-0,24	9,00	-3,29	0,12	-1,45
TC1300001318.mm.2	Mocs2	17434	-0,28	9,12	-3,29	0,12	-1,45
TC0600001268.mm.2	Slc6a1	232333	0,25	9,18	3,29	0,12	-1,46
TC1000003163.mm.2	Tmem198b	73827	0,28	8,01	3,28	0,12	-1,47
TC0700000219.mm.2	Napa	108124	0,27	10,39	3,28	0,12	-1,47
TC0700003702.mm.2	Tyr	22173	-0,30	5,44	-3,28	0,12	-1,47
TC1100001704.mm.2	Nmt1	18107	0,24	9,00	3,28	0,12	-1,47
TC1100003041.mm.2	Cyb5d1	327951	0,31	7,12	3,28	0,12	-1,48
TC0500003709.mm.2	Babam2	107976	0,26	9,88	3,27	0,12	-1,49
TC1100000125.mm.2	Vwc2	319922	-0,25	8,37	-3,27	0,12	-1,50
TC1600001011.mm.2	Itsn1	16443	0,28	9,97	3,27	0,12	-1,50
TC1100000417.mm.2	Gabrb2	14401	0,30	9,81	3,26	0,12	-1,51
TC0300002355.mm.2	Chrn2	11444	0,24	8,69	3,26	0,12	-1,53
TC1100003588.mm.2	Kat7	217127	0,26	8,75	3,25	0,12	-1,54
TC0900001371.mm.2	Nprl2	56032	0,27	9,12	3,25	0,12	-1,54
TC0100002405.mm.2	Sumo1	22218	-0,33	9,21	-3,25	0,12	-1,55
TC1500001977.mm.2	Till1	319953	0,38	8,48	3,25	0,12	-1,55
TC1100001999.mm.2	Gaa	14387	0,37	10,01	3,24	0,12	-1,56
TC0400003776.mm.2	Pithd1	66193	0,41	7,24	3,24	0,12	-1,56
TC0400000353.mm.2	Chmp5	76959	-0,26	9,01	-3,24	0,12	-1,57
TC1100000085.mm.2	Ykt6	56418	0,25	8,83	3,24	0,12	-1,57
TC0800000017.mm.2	Stxbp2	20911	0,33	9,33	3,24	0,12	-1,57
TC0500003024.mm.2	Grk3	320129	0,28	7,57	3,24	0,12	-1,57
TC1700001860.mm.2	Zfp763	73451	-0,29	8,15	-3,24	0,12	-1,57
TC0500002486.mm.2	Ugdh	22235	-0,23	8,89	-3,22	0,12	-1,61
TC0800001058.mm.2	Fto	26383	0,35	8,42	3,22	0,12	-1,62
TC0800000965.mm.2	Farsa	66590	0,28	8,54	3,22	0,12	-1,62
TC1400002368.mm.2	Fndc3a	319448	0,27	9,47	3,22	0,12	-1,62
TC0800001520.mm.2	Tcf25	66855	0,29	9,60	3,21	0,12	-1,63
TC1200002359.mm.2	Wars	22375	0,43	8,78	3,21	0,12	-1,64
TC0600000456.mm.2	Casp2	12366	0,27	8,45	3,21	0,12	-1,65
TC1900001711.mm.2	Ablim1	226251	0,30	10,79	3,20	0,13	-1,66
TC1300000050.mm.2	Larp4b	217980	-0,23	9,54	-3,20	0,13	-1,67
TC0300002444.mm.2	Riad1	66353	-0,21	8,05	-3,19	0,13	-1,69
TC0100001853.mm.2	Ints7	77065	0,32	7,98	3,19	0,13	-1,69
TC0700004657.mm.2	Sec11a	56529	-0,27	10,11	-3,19	0,13	-1,69
TC0300000730.mm.2	Ubqln4	94232	0,27	8,64	3,18	0,13	-1,71
TC1900000208.mm.2	Vps37c	107305	0,33	8,89	3,17	0,13	-1,72
TC1400001103.mm.2	Kbtbd7	211255	-0,31	9,59	-3,17	0,13	-1,73
TC1100002592.mm.2	Lsm11	72290	0,28	6,82	3,17	0,13	-1,74
TC1100003817.mm.2	Dusp3	72349	0,28	7,91	3,17	0,13	-1,74

TC0200003362.mm.2	Stom	13830	0,36	9,37	3,16	0,13	-1,75
TC1400000304.mm.2	Dcp1a	75901	0,28	6,99	3,16	0,13	-1,75
TC0400002471.mm.2	Fam219a	71901	0,28	7,71	3,16	0,13	-1,75
TC1100000763.mm.2	Smcr8	237782	0,33	8,85	3,16	0,13	-1,76
TC0600001281.mm.2	Tsen2	381802	0,28	6,58	3,15	0,13	-1,77
TC0900000040.mm.2	Dcun1d5	76863	-0,30	9,09	-3,15	0,13	-1,77
TC0200001797.mm.2	Haus2	66296	0,30	7,96	3,15	0,13	-1,78
TC0900000593.mm.2	Drd2	13489	0,27	9,15	3,15	0,13	-1,78
TC0200000547.mm.2	Gpr107	277463	0,25	8,21	3,15	0,13	-1,78
TC1000001802.mm.2	Abrac1	73112	-0,40	7,39	-3,13	0,13	-1,81
TC1200000741.mm.2	Slc39a9	328133	0,21	9,47	3,13	0,13	-1,82
TC0800000847.mm.2	Rasd2	75141	0,36	6,13	3,13	0,13	-1,82
TC0100002495.mm.2	Acadl	11363	-0,28	5,71	-3,13	0,13	-1,83
TC0300000396.mm.2	Proser1	212127	0,30	9,67	3,13	0,13	-1,83
TC1200000432.mm.2	Akap6	238161	0,28	9,03	3,12	0,14	-1,86
TC0200001586.mm.2	Immp1l	66541	-0,31	10,62	-3,11	0,14	-1,86
TC0700000816.mm.2	Vrk3	101568	0,29	9,11	3,11	0,14	-1,86
TC0200002453.mm.2	Plcg1	18803	0,22	9,15	3,10	0,14	-1,88
TC0800002700.mm.2	Ces1b	382044	-0,28	5,67	-3,10	0,14	-1,89
TC0700003590.mm.2	Rccd1	269955	0,33	7,17	3,10	0,14	-1,89
TC1100002451.mm.2	Chac2	68044	-0,27	8,85	-3,09	0,14	-1,91
TC0100002163.mm.2	Fam168b	214469	0,26	9,65	3,09	0,14	-1,92
TC1400000298.mm.2	Selenok	80795	-0,21	10,78	-3,09	0,14	-1,92
TC0X00001277.mm.2	Drp2	13497	0,23	7,72	3,09	0,14	-1,92
TC0100000233.mm.2	Plekhhb2	226971	0,24	10,08	3,09	0,14	-1,92
TC0700001727.mm.2	Abca16	233810	-0,24	4,88	-3,09	0,14	-1,92
TC1100000923.mm.2	Zbtb4	75580	0,23	9,51	3,09	0,14	-1,92

Supplementary table 1. Most differentiated genes. Table of the top 200 genes more differentially expressed when comparing mice treated with the vehicle versus those treated with sitagliptin. AveExpr denotes the average gene expression across all arrays on a logarithmic scale (\log_2), while the "t" statistic represents a moderated-t statistic resembling the conventional Student's t statistic.

Most enriched pathways obtained with the RPD analysis

ID	Description	Set Size	Enrichment score	NES	adj.P.Val
R-MMU-112316	Neuronal System	130	0,52	2,13	0,03
R-MMU-112315	Transmission across Chemical Synapses	90	0,58	2,27	0,03
R-MMU-112314	Neurotransmitter receptors and postsynaptic signal transmission	65	0,58	2,16	0,03
R-MMU-199991	Membrane Trafficking	258	0,37	1,61	0,03
R-MMU-5653656	Vesicle-mediated transport	269	0,36	1,59	0,03
R-MMU-5389840	Mitochondrial translation elongation	48	-0,51	-2,17	0,03
R-MMU-5368287	Mitochondrial translation	50	-0,48	-2,05	0,03
R-MMU-5419276	Mitochondrial translation termination	50	-0,48	-2,05	0,03
R-MMU-1483257	Phospholipid metabolism	74	0,48	1,81	0,03
R-MMU-2046104	alpha-linolenic (omega3) and linoleic (omega6) acid metabolism	10	0,78	1,89	0,03
R-MMU-2046106	alpha-linolenic acid (ALA) metabolism	10	0,78	1,89	0,03
R-MMU-72766	Translation	82	-0,39	-1,87	0,03
R-MMU-381753	Olfactory Signaling Pathway	100	-0,36	-1,76	0,03
R-MMU-174113	SCF-beta-TrCP mediated degradation of Emi1	31	-0,51	-1,96	0,03
R-MMU-8854050	FBXL7 down-regulates AURKA during mitotic entry and in early mitosis	31	-0,51	-1,95	0,03
R-MMU-5607761	Dectin-1 mediated noncanonical NF-kB signaling	32	-0,50	-1,94	0,03
R-MMU-5676590	NIK-->noncanonical NF-kB signaling	32	-0,50	-1,94	0,03
R-MMU-68949	Orc1 removal from chromatin	34	-0,49	-1,93	0,03
R-MMU-174184	Cdc20:Phospho-APC/C mediated degradation of Cyclin A	35	-0,47	-1,86	0,03
R-MMU-179419	APC:Cdc20 mediated degradation of cell cycle proteins prior to satisfaction of the cell cycle checkpoint	35	-0,47	-1,86	0,03
R-MMU-6799198	Complex I biogenesis	36	-0,48	-1,89	0,03
R-MMU-1236975	Antigen processing-Cross presentation	36	-0,48	-1,91	0,03
R-MMU-176409	APC/C:Cdc20 mediated degradation of mitotic proteins	36	-0,47	-1,86	0,03
R-MMU-176814	Activation of APC/C and APC/C:Cdc20 mediated degradation of mitotic proteins	36	-0,47	-1,86	0,03
R-MMU-5658442	Regulation of RAS by GAPs	37	-0,48	-1,91	0,03
R-MMU-422475	Axon guidance	119	0,42	1,68	0,03
R-MMU-176408	Regulation of APC/C activators between G1/S and early anaphase	40	-0,48	-1,93	0,03
R-MMU-174143	APC/C-mediated degradation of cell cycle proteins	42	-0,46	-1,91	0,03

R-MMU-453276	Regulation of mitotic cell cycle	42	-0,46	-1,91	0,03
R-MMU-112040	G-protein mediated events	16	0,67	1,86	0,03
R-MMU-69239	Synthesis of DNA	50	-0,45	-1,93	0,03
R-MMU-983231	Factors involved in megakaryocyte development and platelet production	38	0,53	1,80	0,03
R-MMU-6811438	Intra-Golgi traffic	17	0,67	1,88	0,04
R-MMU-373760	L1CAM interactions	34	0,54	1,77	0,04
R-MMU-6811442	Intra-Golgi and retrograde Golgi-to-ER traffic	84	0,44	1,70	0,04
R-MMU-983189	Kinesins	19	0,65	1,88	0,04
R-MMU-69306	DNA Replication	52	-0,44	-1,88	0,04
R-MMU-350562	Regulation of ornithine decarboxylase (ODC)	28	-0,53	-1,98	0,04
R-MMU-68827	CDT1 association with the CDC6:ORC:origin complex	30	-0,51	-1,92	0,04
R-MMU-5610780	Degradation of GLI1 by the proteasome	34	-0,47	-1,83	0,05
R-MMU-4608870	Asymmetric localization of PCP proteins	31	-0,49	-1,85	0,05
R-MMU-5610785	GLI3 is processed to GLI3R by the proteasome	35	-0,46	-1,81	0,05
R-MMU-977443	GABA receptor activation	24	0,60	1,82	0,05
R-MMU-425407	SLC-mediated transmembrane transport	86	0,42	1,65	0,05
R-MMU-69242	S Phase	61	-0,39	-1,73	0,05
R-MMU-438064	Post NMDA receptor activation events	17	0,65	1,81	0,05
R-MMU-8878166	Transcriptional regulation by RUNX2	30	-0,50	-1,88	0,05
R-MMU-383280	Nuclear Receptor transcription pathway	25	0,59	1,80	0,06
R-MMU-112043	PLC beta mediated events	15	0,66	1,80	0,06
R-MMU-8939902	Regulation of RUNX2 expression and activity	29	-0,50	-1,87	0,07

Supplementary table 2. Table of the top 50 enriched pathways (RPD) for the comparative study “db/db sitagliptin vs. db/db vehicle”.

8.3. Licenses



49 Spadina Ave. Suite 200
Toronto ON M5V 2J1 Canada
www.biorender.com

Confirmation of Publication and Licensing Rights

August 30th, 2023
Science Suite Inc.

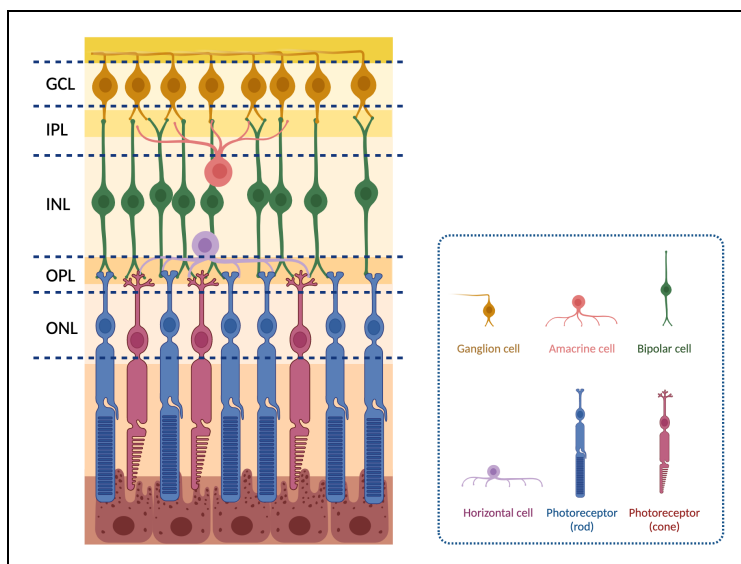
Subscription: Student Plan
Agreement number: SV25SLP0C5
Journal name: Tesis Doctorales en Red

To whom this may concern,

This document is to confirm that Hugo Ramos Abellan has been granted a license to use the BioRender content, including icons, templates and other original artwork, appearing in the attached completed graphic pursuant to BioRender's [Academic License Terms](#). This license permits BioRender content to be sublicensed for use in journal publications.

All rights and ownership of BioRender content are reserved by BioRender. All completed graphics must be accompanied by the following citation: "Created with BioRender.com".

BioRender content included in the completed graphic is not licensed for any commercial uses beyond publication in a journal. For any commercial use of this figure, users may, if allowed, recreate it in BioRender under an Industry BioRender Plan.



For any questions regarding this document, or other questions about publishing with BioRender refer to our [BioRender Publication Guide](#), or contact BioRender Support at support@biorender.com.

Confirmation of Publication and Licensing Rights

September 9th, 2023

Science Suite Inc.

Subscription:

Student Plan

Agreement number:

HT25U20AZT

Journal name:

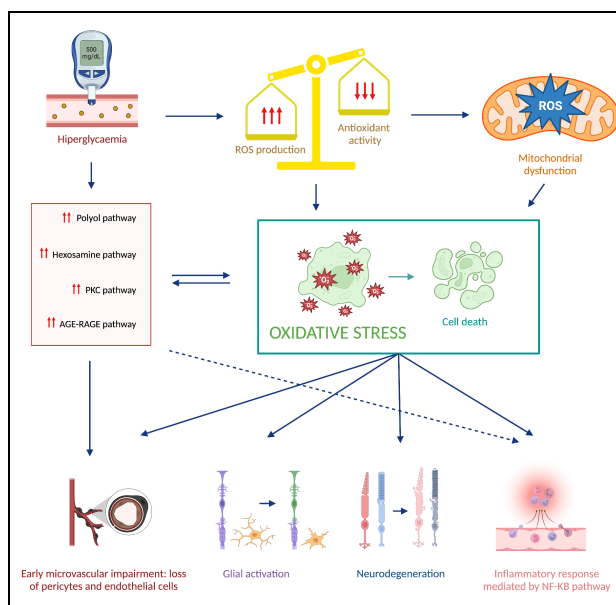
Tesis Doctorales en Red

To whom this may concern,

This document is to confirm that Hugo Ramos Abellan has been granted a license to use the BioRender content, including icons, templates and other original artwork, appearing in the attached completed graphic pursuant to BioRender's [Academic License Terms](#). This license permits BioRender content to be sublicensed for use in journal publications.

All rights and ownership of BioRender content are reserved by BioRender. All completed graphics must be accompanied by the following citation: "Created with BioRender.com".

BioRender content included in the completed graphic is not licensed for any commercial uses beyond publication in a journal. For any commercial use of this figure, users may, if allowed, recreate it in BioRender under an Industry BioRender Plan.



For any questions regarding this document, or other questions about publishing with BioRender refer to our [BioRender Publication Guide](#), or contact BioRender Support at support@biorender.com.

Confirmation of Publication and Licensing Rights

September 10th, 2023
Science Suite Inc.

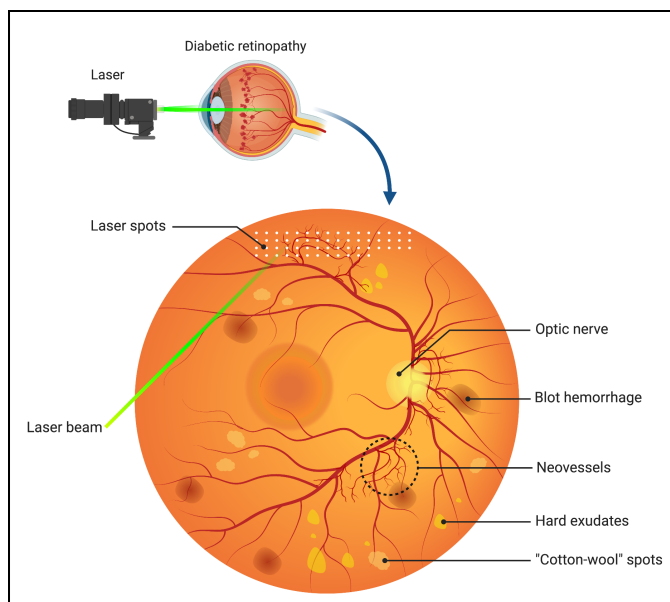
Subscription: *Student Plan*
Agreement number: *UQ25U5TS71*
Journal name: *Tesis Doctorales en Red*

To whom this may concern,

This document is to confirm that Hugo Ramos Abellan has been granted a license to use the BioRender content, including icons, templates and other original artwork, appearing in the attached completed graphic pursuant to BioRender's [Academic License Terms](#). This license permits BioRender content to be sublicensed for use in journal publications.

All rights and ownership of BioRender content are reserved by BioRender. All completed graphics must be accompanied by the following citation: "Created with BioRender.com".

BioRender content included in the completed graphic is not licensed for any commercial uses beyond publication in a journal. For any commercial use of this figure, users may, if allowed, recreate it in BioRender under an Industry BioRender Plan.



For any questions regarding this document, or other questions about publishing with BioRender refer to our [BioRender Publication Guide](#), or contact BioRender Support at support@biorender.com.

Confirmation of Publication and Licensing Rights

September 5th, 2023
Science Suite Inc.

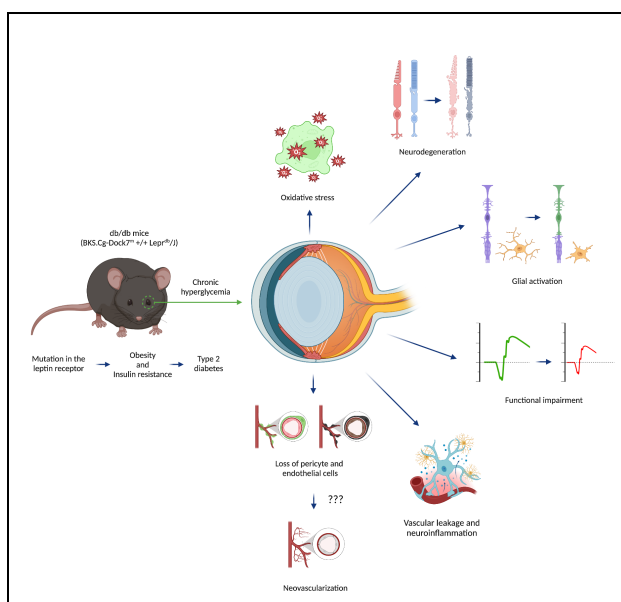
Subscription: Student Plan
Agreement number: YH25TES8XL
Journal name: Tesis Doctorales en Red

To whom this may concern,

This document is to confirm that Hugo Ramos Abellan has been granted a license to use the BioRender content, including icons, templates and other original artwork, appearing in the attached completed graphic pursuant to BioRender's [Academic License Terms](#). This license permits BioRender content to be sublicensed for use in journal publications.

All rights and ownership of BioRender content are reserved by BioRender. All completed graphics must be accompanied by the following citation: "Created with BioRender.com".

BioRender content included in the completed graphic is not licensed for any commercial uses beyond publication in a journal. For any commercial use of this figure, users may, if allowed, recreate it in BioRender under an Industry BioRender Plan.



For any questions regarding this document, or other questions about publishing with BioRender refer to our [BioRender Publication Guide](#), or contact BioRender Support at support@biorender.com.

Confirmation of Publication and Licensing Rights

August 28th, 2023

Science Suite Inc.

Subscription:

Student Plan

Agreement number:

CU25SB3H3J

Journal name:

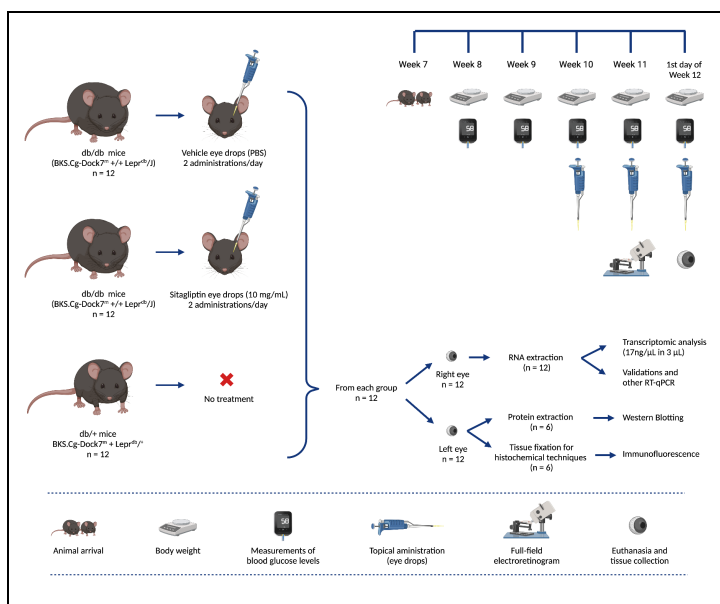
Tesis Doctorales en Red

To whom this may concern,

This document is to confirm that Hugo Ramos Abellan has been granted a license to use the BioRender content, including icons, templates and other original artwork, appearing in the attached completed graphic pursuant to BioRender's [Academic License Terms](#). This license permits BioRender content to be sublicensed for use in journal publications.

All rights and ownership of BioRender content are reserved by BioRender. All completed graphics must be accompanied by the following citation: "Created with BioRender.com".

BioRender content included in the completed graphic is not licensed for any commercial uses beyond publication in a journal. For any commercial use of this figure, users may, if allowed, recreate it in BioRender under an Industry BioRender Plan.



For any questions regarding this document, or other questions about publishing with BioRender refer to our [BioRender Publication Guide](#), or contact BioRender Support at support@biorender.com.

Confirmation of Publication and Licensing Rights

August 28th, 2023
Science Suite Inc.

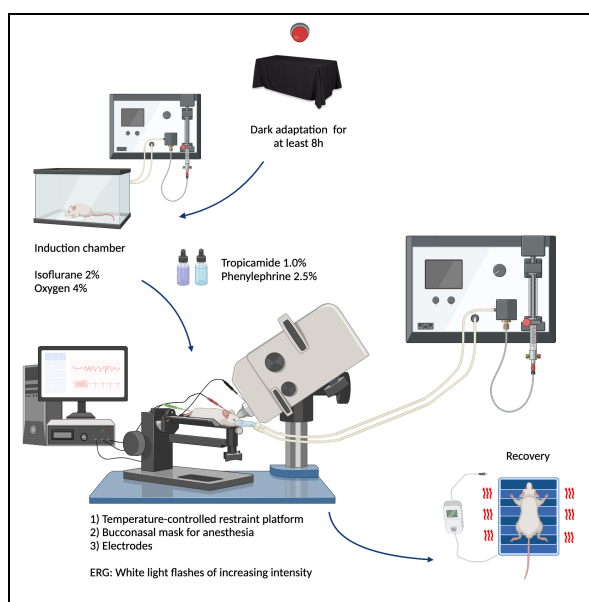
Subscription: *Student Plan*
Agreement number: *BV25S7ET4S*
Journal name: *Tesis Doctorales en Red*

To whom this may concern,

This document is to confirm that Hugo Ramos Abellan has been granted a license to use the BioRender content, including icons, templates and other original artwork, appearing in the attached completed graphic pursuant to BioRender's [Academic License Terms](#). This license permits BioRender content to be sublicensed for use in journal publications.

All rights and ownership of BioRender content are reserved by BioRender. All completed graphics must be accompanied by the following citation: "Created with BioRender.com".

BioRender content included in the completed graphic is not licensed for any commercial uses beyond publication in a journal. For any commercial use of this figure, users may, if allowed, recreate it in BioRender under an Industry BioRender Plan.



For any questions regarding this document, or other questions about publishing with BioRender refer to our [BioRender Publication Guide](#), or contact BioRender Support at support@biorender.com.

Confirmation of Publication and Licensing Rights

August 29th, 2023
Science Suite Inc.

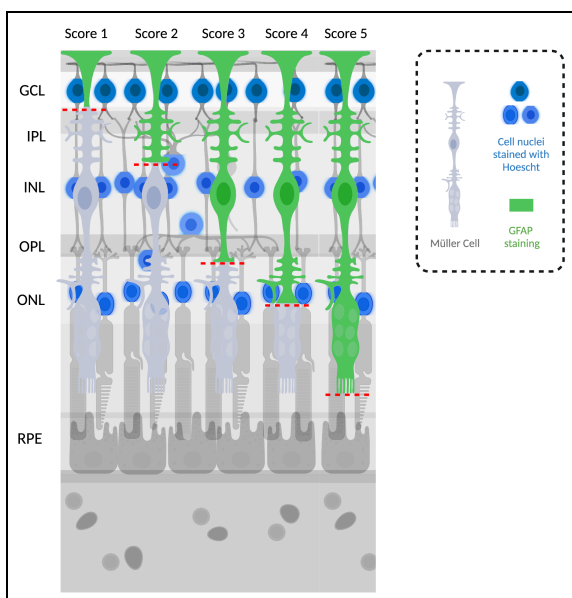
Subscription: *Student Plan*
Agreement number: *SU25SCI53E*
Journal name: *Tesis Doctorales en Red*

To whom this may concern,

This document is to confirm that Hugo Ramos Abellan has been granted a license to use the BioRender content, including icons, templates and other original artwork, appearing in the attached completed graphic pursuant to BioRender's [Academic License Terms](#). This license permits BioRender content to be sublicensed for use in journal publications.

All rights and ownership of BioRender content are reserved by BioRender. All completed graphics must be accompanied by the following citation: "Created with BioRender.com".

BioRender content included in the completed graphic is not licensed for any commercial uses beyond publication in a journal. For any commercial use of this figure, users may, if allowed, recreate it in BioRender under an Industry BioRender Plan.



For any questions regarding this document, or other questions about publishing with BioRender refer to our [BioRender Publication Guide](#), or contact BioRender Support at support@biorender.com.

Confirmation of Publication and Licensing Rights

December 15th, 2022
Science Suite Inc.

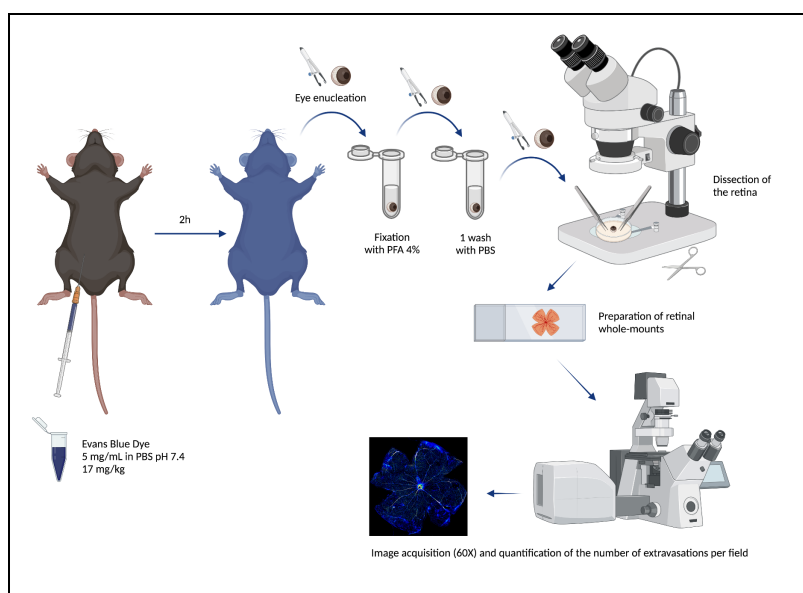
Subscription: *Student Plan*
Agreement number: *GR24RQG79W*
Journal name: *Tesis Doctorales en Red*

To whom this may concern,

This document is to confirm that Hugo Ramos Abellan has been granted a license to use the BioRender content, including icons, templates and other original artwork, appearing in the attached completed graphic pursuant to BioRender's [Academic License Terms](#). This license permits BioRender content to be sublicensed for use in journal publications.

All rights and ownership of BioRender content are reserved by BioRender. All completed graphics must be accompanied by the following citation: "Created with BioRender.com".

BioRender content included in the completed graphic is not licensed for any commercial uses beyond publication in a journal. For any commercial use of this figure, users may, if allowed, recreate it in BioRender under an Industry BioRender Plan.



For any questions regarding this document, or other questions about publishing with BioRender refer to our [BioRender Publication Guide](#), or contact BioRender Support at support@biorender.com.

Confirmation of Publication and Licensing Rights

September 12th, 2023
Science Suite Inc.

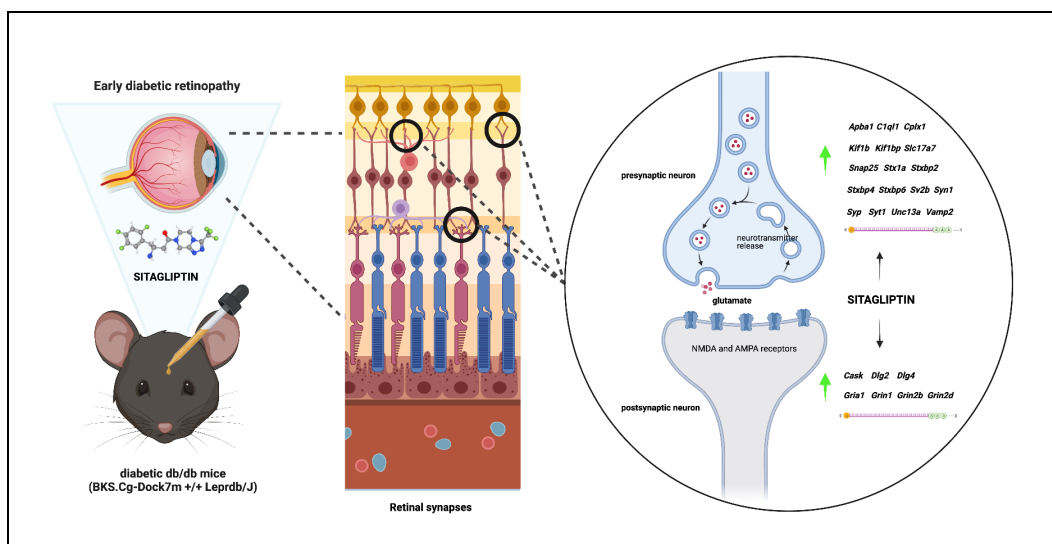
Subscription: Student Plan
Agreement number: AA25UEUXLK
Journal name: Tesis Doctorales en Red

To whom this may concern,

This document is to confirm that Hugo Ramos Abellan has been granted a license to use the BioRender content, including icons, templates and other original artwork, appearing in the attached completed graphic pursuant to BioRender's [Academic License Terms](#). This license permits BioRender content to be sublicensed for use in journal publications.

All rights and ownership of BioRender content are reserved by BioRender. All completed graphics must be accompanied by the following citation: "Created with BioRender.com".

BioRender content included in the completed graphic is not licensed for any commercial uses beyond publication in a journal. For any commercial use of this figure, users may, if allowed, recreate it in BioRender under an Industry BioRender Plan.



For any questions regarding this document, or other questions about publishing with BioRender refer to our [BioRender Publication Guide](#), or contact BioRender Support at support@biorender.com.

Confirmation of Publication and Licensing Rights

September 14th, 2023
Science Suite Inc.

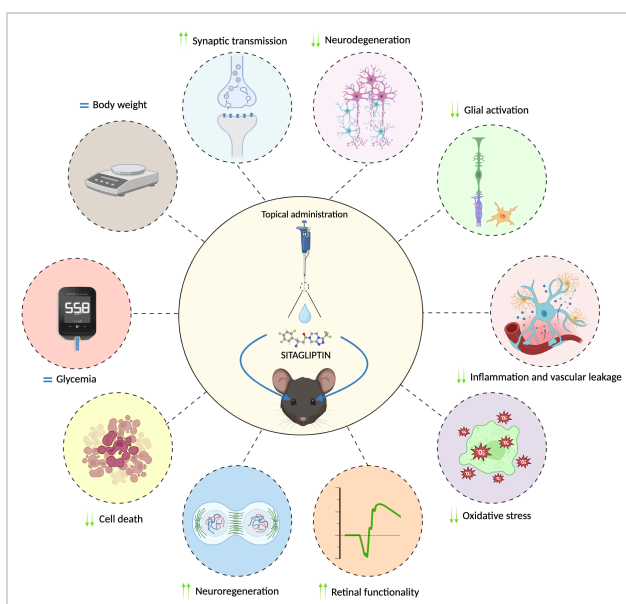
Subscription: *Student Plan*
Agreement number: *UC25UQM0BM*
Journal name: *Tesis Doctorales en Red*

To whom this may concern,

This document is to confirm that Hugo Ramos Abellan has been granted a license to use the BioRender content, including icons, templates and other original artwork, appearing in the attached completed graphic pursuant to BioRender's [Academic License Terms](#). This license permits BioRender content to be sublicensed for use in journal publications.

All rights and ownership of BioRender content are reserved by BioRender. All completed graphics must be accompanied by the following citation: "Created with BioRender.com".

BioRender content included in the completed graphic is not licensed for any commercial uses beyond publication in a journal. For any commercial use of this figure, users may, if allowed, recreate it in BioRender under an Industry BioRender Plan.



For any questions regarding this document, or other questions about publishing with BioRender refer to our [BioRender Publication Guide](#), or contact BioRender Support at support@biorender.com.

8.4. Scientific publications

List of publications derived from this doctoral thesis:

- 1) Ramos, H. *et al.* Neuromodulation Induced by Sitagliptin: A New Strategy for Treating Diabetic Retinopathy. *Biomedicines* **9**, 1772 (2021).
- 2) Bogdanov, P. *et al.* Minimum Effective Dose of DPP-4 Inhibitors for Treating Early Stages of Diabetic Retinopathy in an Experimental Model. *Biomedicines* **10**, 465 (2022).
- 3) Ramos, H. *et al.* Antioxidant Effects of DPP-4 Inhibitors in Early Stages of Experimental Diabetic Retinopathy. *Antioxidants* **11**, 1418 (2022).
- 4) Ramos, H., Bogdanov, P., Simó, R., Deàs-Just, A. & Hernández, C. Transcriptomic Analysis Reveals That Retinal Neuromodulation Is a Relevant Mechanism in the Neuroprotective Effect of Sitagliptin in an Experimental Model of Diabetic Retinopathy. *International Journal of Molecular Sciences* **24**, 571 (2022).



Article

Neuromodulation Induced by Sitagliptin: A New Strategy for Treating Diabetic Retinopathy

Hugo Ramos ^{1,2,†}, Patricia Bogdanov ^{1,2,†}, David Sabater ¹, Jordi Huerta ¹, Marta Valeri ³, Cristina Hernández ^{1,2,*} and Rafael Simó ^{1,2,*}

¹ Diabetes and Metabolism Research Unit, Vall d'Hebron Research Institute, Universitat Autònoma de Barcelona, 08035 Barcelona, Spain; hugo.ramos@vhir.org (H.R.); patricia.bogdanov@vhir.org (P.B.); david.sabater@vhir.org (D.S.); jordi.huerta@vhir.org (J.H.)

² Centro de Investigación Biomédica en Red de Diabetes y Enfermedades Metabólicas Asociadas (CIBERDEM), Instituto de Salud Carlos III (ICSIII), 28029 Madrid, Spain

³ Unit of High Technology, Vall d'Hebron Research Institute, 08035 Barcelona, Spain; marta.valeri@vhir.org

* Correspondence: cristina.hernandez@vhir.org (C.H.); rafael.simo@vhir.org (R.S.)

† Hugo Ramos and Patricia Bogdanov contributed equally to this study.



Citation: Ramos, H.; Bogdanov, P.; Sabater, D.; Huerta, J.; Valeri, M.; Hernández, C.; Simó, R.

Neuromodulation Induced by Sitagliptin: A New Strategy for Treating Diabetic Retinopathy.

Biomedicines **2021**, *9*, 1772. <https://doi.org/10.3390/biomedicines9121772>

Academic Editor: Josef Troger

Received: 8 November 2021

Accepted: 24 November 2021

Published: 26 November 2021

Publisher's Note: MDPI stays neutral with regard to jurisdictional claims in published maps and institutional affiliations.



Copyright: © 2021 by the authors. Licensee MDPI, Basel, Switzerland. This article is an open access article distributed under the terms and conditions of the Creative Commons Attribution (CC BY) license (<https://creativecommons.org/licenses/by/4.0/>).

Abstract: Diabetic retinopathy (DR) involves progressive neurovascular degeneration of the retina. Reduction in synaptic protein expression has been observed in retinas from several diabetic animal models and human retinas. We previously reported that the topical administration (eye drops) of sitagliptin, a dipeptidyl peptidase-4 (DPP-4) inhibitor, prevented retinal neurodegeneration induced by diabetes in db/db mice. The aim of the present study is to examine whether the modulation of presynaptic proteins is a mechanism involved in the neuroprotective effect of sitagliptin. For this purpose, 12 db/db mice, aged 12 weeks, received a topical administration of sitagliptin (5 µL; concentration: 10 mg/mL) twice per day for 2 weeks, while other 12 db/db mice were treated with vehicle (5 µL). Twelve non-diabetic mice (db/+) were used as a control group. Protein levels were assessed by western blot and immunohistochemistry (IHC), and mRNA levels were evaluated by reverse transcription polymerase chain reaction (RT-PCR). Our results revealed a downregulation (protein and mRNA levels) of several presynaptic proteins such as synapsin I (*Syn1*), synaptophysin (*Syp*), synaptotagmin (*Syt1*), syntaxin 1A (*Stx1a*), vesicle-associated membrane protein 2 (*Vamp2*), and synaptosomal-associated protein of 25 kDa (*Snapt25*) in diabetic mice treated with vehicle in comparison with non-diabetic mice. These proteins are involved in vesicle biogenesis, mobilization and docking, membrane fusion and recycling, and synaptic neurotransmission. Sitagliptin was able to significantly prevent the downregulation of all these proteins. We conclude that sitagliptin exerts beneficial effects in the retinas of db/db mice by preventing the downregulation of crucial presynaptic proteins. These neuroprotective effects open a new avenue for treating DR as well other retinal diseases in which neurodegeneration/synaptic abnormalities play a relevant role.

Keywords: diabetic retinopathy; retinal neurodegeneration; dipeptidyl peptidase 4 inhibitors; sitagliptin; presynaptic proteins; db/db mouse model

1. Introduction

The concept of diabetic retina (DR) as a microvascular disease has evolved into that of a more complex diabetic complication in which neurodegeneration plays a significant role [1,2]. Thus, DR is now defined as a highly tissue-specific neurovascular complication [3]. Neurodegeneration and glial activation are primary events in the pathogenesis of DR and have been observed to occur before overt microangiopathy in experimental models of DR and in the retina of diabetic donors [4–6].

Neuronal damage associated with DR is not limited to cell apoptosis and glial activation but also includes other changes such as a reduction in synaptic protein expression [7,8].

In this regard, there is evidence that diabetes reduces the retinal content of several presynaptic proteins critical to the exocytosis of neurotransmitters and synaptic maintenance in murine models [8–10]. In postmortem human retinas, it has been reported that the protein content of presynaptic was depleted compared to non-diabetic donors [11]. Therefore, to prevent or ameliorate the downregulation of presynaptic proteins induced by diabetes would be a desirable effect of any neuroprotective drug.

We have previously demonstrated that topical administration of sitagliptin, a DPP-4 inhibitor, is effective in preventing retinal neurodegeneration (glial activation and neuronal apoptosis), as well as vascular leakage in db/db mouse model [12]. On this basis, the aim of the present study is to examine in an experimental model of diabetes (db/db mice) whether the modulation of presynaptic proteins is a mechanism involved in the neuroprotective effect of sitagliptin.

2. Materials and Methods

2.1. Animals

A total of 24 diabetic male db/db (BKS.Cg-Dock7m +/+ Leprdb/J) mice and 12 non-diabetic mice (db/+; (BKS.Cg-Dock7m + Leprdb/+)) aged 7 weeks were obtained from Charles River Laboratories Inc (Calco Italy for the study). We have characterized the neurodegenerative process that occurs in the retinas of db/db mice, and we found that db/db mouse reproduces the features of the neurodegenerative process that occurs in the human diabetic retina [13]. Animals were bred and maintained at VHIR's animal facility. Animals had free access to ad libitum food (ENVIGO Global Diet Complete Feed for Rodents, Mucedola, Milan, Italy) and filtered water. In order to minimize variability, animals were randomly housed (block randomization) in groups of 2 mice per cage, in Tecniplast GM-500 cages under standard laboratory conditions at 22 ± 2 °C, with 12 h light/dark cycle and relative humidity of 50–60%. Each cage held absorbent bedding and nesting material (BioFresh Performance Bedding 1/800 Pelleted Cellulose, Absorption Corp., Ferndale, WA, USA). Blood glucose levels were weekly measured through tail vein sampling (glucose assay kit; Abbott, Chicago, IL, USA).

All performed experiments with animals were conducted in compliance with European Community (86/609/CEE) and ARVO (Association for Research in Vision and Ophthalmology) tenets for the use of laboratory animals. This study was approved by the Animal Care and Use Committee of Vall d'Hebron Research Institute (VHIR) (Passeig de la Vall d'Hebron 119–129, Barcelona, Spain. Approval code 75/15, approval date 2 December 2015).

2.2. Topical Ocular Treatment

Sitagliptin [sitagliptin phosphate monohydrate (Y0001812, Merck KGaA, Darmstadt, Germany) eyedrops (10 mg/mL; 5 μ L; n = 12) or vehicle [phosphate buffered saline (PBS)] eyedrops (5 μ L; n = 12) were randomly administered directly onto the superior corneal surface of each eye using a micropipette in 10-week-old mice. The treatment (sitagliptin or vehicle) was administered twice daily for 15 days. Non-diabetic mice (n = 12) matched by age were used as control group. On day 15, the drop of sitagliptin or vehicle was administered animals 1h before euthanasia.

2.3. Electoretinogram (ERG)

Full field electoretinography (ERG) recordings were estimated using the Ganzfeld ERG platform (Phoenix Research Laboratories, Pleasanton, CA, USA) following ISCEV (International Society for Clinical Electrophysiology of Vision) recommendations [14]. Animals were dark adapted for at least 8 h prior to ERG recording and then anesthetized with isoflurane. Tropicamide (1%) was utilized to each eye prior to the test. A cutaneous ground electrode was placed near the base of the tail, a needle electrode was placed on the head between the two eyes, and a corneal electrode was placed near each eye. Carboxymethylcellulose (1%) drops were applied to the interior surface of the contact lens

electrodes prior to their placement on the eyes. Three ERG components were assessed in terms of amplitude and timing.

2.4. Retinal Tissue Processing

On day 15, each animal was transcardially perfused with paraformaldehyde 4% (sc-281692, Santa Cruz Biotechnology, Dallas, TX, USA). Previously they received a 200 µL intraperitoneal injection of anesthesia, prepared with a mix containing 1 mL ketamine (GmbH, Hameln, Germany) and 0.3 mL xylazine (Laboratorios Calier S.A., Barcelona, Spain). Eyes were rapidly enucleated and for mRNA and protein evaluations the retinas were separated instantly after enucleation, frozen in liquid nitrogen, and stored at -80°C . For RNA extraction, the retinas were introduced in individual tubes with 140 µL of TRIzol reagent (15596018, InvitrogenTM, Carlsbad, CA, USA). For Western Blot assays, retinas were directly dispensed in an empty tube until protein extraction. Finally, for immunohistochemistry assessment, eyes were not dissected after enucleation and were fixed in 4% paraformaldehyde during 5 h before paraffin embedding. Sections were mounted on slides and stored at 4°C .

2.4.1. RNA Extraction and Quantitative Reverse Transcription Polymerase Chain Reaction (RT-PCR) Assay

Neuroretinas (previously stored at -80°C in TRIzol) were treated with DNase (18068015, ThermoFisher Scientific, Waltham, MA, USA) to eliminate genomic contamination and were purified on RNeasy MinElute column (74106, Qiagen, Hilden, Germany). After supernatant removal, RNA sediment was obtained and resuspended in 30 µL of RNase free water (AM9937, ThermoFisher Scientific, Waltham, MA, USA). An Agilent 2100 Bioanalyzer and a Nanodrop spectrophotometer were used for samples integrity and quantity respectively. cDNA reverse transcription was performed in a T100 Thermal Cycler (Bio-rad, Hercules, CA, USA) using High-Capacity cDNA Reverse Transcription Kit (4368814, ThermoFisher Scientific, Waltham, MA, USA) and Oligo(dT)18 Primer (SO131, ThermoFisher Scientific, Waltham, MA, USA). RT-PCR was carried out using SYBR Green PCR Master Mix (4309155, Applied Biosystems, Warrington, UK) and a 7.900 HT Sequence Detection System in 384-well optical plates with specific primers (displayed in Table 1). Relative quantities were calculated using the ABI SDS 2.4 RQ software and presented as a ratio between them and the endogenous controls (*B2m* and *Actin B* (*Actb*)).

Table 1. Primers used for RT-PCR.

Primers		Nucleotide Sequence
<i>B2m</i>	Forward (5'-3')	5'-GTATGCTATCCAGAAAACCC-3'
	Reverse (5'-3')	5'-CTGAAGGACATATCTGACATC-3'
<i>Actb</i>	Forward (5'-3')	5'-CTAAGGCCAACCGTGAAAG-3'
	Reverse (5'-3')	5'-CAGTATGTTCCGGCTTCCCATTC-3'
<i>Syn1</i>	Forward (5'-3')	5'-AATCACAAGAGATGCTCAG-3'
	Reverse (5'-3')	5'-GGACACGCACATCATATTAG-3'
<i>Syp</i>	Forward (5'-3')	5'-TGCCAACAAGACGGAGAGTG-3'
	Reverse (5'-3')	5'-TAGTGCCCCCTTTAACGCAG-3'
<i>Syt1</i>	Forward (5'-3')	5'-ACCCTGGGCTCTGTATCCC-3'
	Reverse (5'-3')	5'-CCCTGACCACTGAGTGCAAA-3'
<i>Stx1a</i>	Forward (5'-3')	5'-CGCTGTCCCGAAAGTTTGTG-3'
	Reverse (5'-3')	5'-GTGTCTGGTCTCGATCTCACT-3'
<i>Vamp2</i>	Forward (5'-3')	5'-ATCATCGTTTACTTCAGCAC-3'
	Reverse (5'-3')	5'-TGAAAGATATGCTGAGAGG-3'
<i>Snap25</i>	Forward (5'-3')	5'-CAACTGGAACGATTGAGGAA-3'
	Reverse (5'-3')	5'-GGCCACTACTCCATCCTGATTAT-3'

2.4.2. Western Blotting

Protein extraction consisted in a sonication of neuroretinas for 10–15 s in 80 µL of lysis buffer [phenylmethanesulfonylfluoride (PMSF), 1mM; NaF, 100mM; Na₃VO₄ 2mM; RIPA buffer (R0278, Sigma-Aldrich, St Louis, MO, USA); 1x protease inhibitor cocktail (P8340, Sigma-Aldrich, St. Louis, MO, USA)]. 25 µg of extracted protein were loaded in a 4–20% (vol./vol.) precast gels for SDS-PAGE (4561096, Bio-rad, Hercules, CA, USA), and electrophoresis was carried out at 100 V for 90 min. Proteins were then transferred to a polyvinylidene difluoride (PVDF) membrane (1620177, Bio-Rad Laboratories, Hercules, CA, USA) at 400 mA for 90 min and blocked in 5% powder milk (Central Lechera Asturiana, Spain) in 0.1% TBS-Tween. Primary antibodies (Table 2) were overnight incubated at 4 °C. On the next day, secondary antibodies (goat anti-rabbit and goat anti-mouse (Dako Agilent, Santa Clara, CA, USA)) were applied (1:10,000). Immunoreactive bands were detected using a WesternBright ECL HRP substrate kit (K-12045-D50, Advansta, CA, USA). Anti-vinculin (1:7,000, sc-73614; Santa Cruz, Dallas, TX, USA) was used as housekeeping to normalize protein levels. The densitometric analysis was assessed with Image J software (Version 1.8, National Institutes of Health, Bethesda, MD, USA).

Table 2. Primary antibodies used for Western blotting.

Primary Antibodies	Description
Synapsin I	Rabbit polyclonal; 1:2000; ab64581; Abcam, Cambridge, UK
Synaptophysin	Rabbit monoclonal; 1:200,000; ab32127; Abcam, Cambridge, UK
Synaptotagmin	Mouse monoclonal; 1:1,000; ab13259; Abcam, Cambridge, UK
Syntaxin 1A	Rabbit polyclonal; 1:100,000; ab41453; Abcam, Cambridge, UK
SNAP-25	Rabbit polyclonal; 1:1000; 14903-1-AP; Proteintech, Rosemont, IL, USA
Vamp2	Rabbit polyclonal; 1:1000; 10135-1-AP; Proteintech, Rosemont, IL, USA
Cyclophilin A	1:10,000; BML-SA296; Enzo, NY, USA
Vinculin	Mouse monoclonal; 1:7000; sc-73614; Santa Cruz, Dallas, TX, USA

2.4.3. Immunofluorescence Analysis

Paraffin-embedded ocular globes were sectioned (3 µm) and mounted on 25.5 × 75.5 × 1.0 mm Poly-L-Lysine positive charged slides (S21.2113.A, Leica Biosystems, Wetzlar, Germany). Samples were deparaffinized in xylene, rehydrated in grade ethanol series, fixed in ice-cold acid methanol (−20 °C), and washed with PBS 0.01M at pH 7.4. Consecutively, eye sections were heated in a pressure cooker at 150 °C for 4 min in 250 mL of 1:10 diluted antigen retrieval with sodium citrate 10 mM, pH 6 (ab973, Abcam, Cambridge, UK). Then, sections were blocked with blocking solution (X0909, Dako Agilent, Santa Clara, CA, USA) for 1h at room temperature and then incubated overnight at 4 °C with specific primary antibodies (Table 3). The next day, after three washes in PBS, sections were incubated for 1 h in darkness with secondary antibodies (Alexa 488 and Alexa 594; 1/600, Molecular Probes). Samples were washed with PBS, counterstained with Hoechst 33342 (bisbenzimidazole) (14533, ThermoFisher Scientific, Waltham, MA, USA), and mounted with Prolong Mounting Medium Fluorescence (P36930, Prolong, InvitrogenTM, Thermo Fisher Scientific, Eugene, OR, USA) and a coverslip (15747592, ThermoFisher Scientific, Waltham, MA, USA). The images were obtained at a resolution of 1024 × 1024 pixels using laser confocal microscopy (Fluoview FV1000 Laser Scanning Confocal Microscope Olympus, Hamburg, Germany) and immunofluorescences were quantified with ImageJ software (U. S. National Institutes of Health, Bethesda, MD, USA).

Table 3. Primary and secondary antibodies used for immunofluorescence experiments.

Primary Antibodies	Description
Synapsin I	Rabbit polyclonal; 1:100; ab64581; Abcam, Cambridge, UK
Synaptophysin	Rabbit monoclonal; 1:100; ab32127; Abcam, Cambridge, UK
Synaptotagmin	Mouse monoclonal; 1:200; ab13259; Abcam, Cambridge, UK
Syntaxin 1A	Rabbit polyclonal; 1:200; ab41453; Abcam, Cambridge, UK
Vamp2	Rabbit polyclonal; 1:100; 10135-1-AP; Proteintech, Rosemont, IL, USA
SNAP-25	Rabbit polyclonal; 1:100; 14903-1-AP; Proteintech, Rosemont, IL, USA
Secondary Antibodies	Description
Alexa Fluor 488 Goat anti-mouse	Goat polyclonal; 1:600; ab150113; Abcam, Cambridge, UK
Alexa Fluor 488 Goat anti-rabbit	Goat polyclonal; 1:600; ab150081; Abcam, Cambridge, UK
Alexa Fluor 594 Goat anti-mouse	Goat polyclonal; 1:600; A-11032; ThermoFisher Scientific, Waltham, MA, USA
Alexa Fluor 594 Goat anti-rabbit	Goat polyclonal; 1:600; A-11012; ThermoFisher Scientific, Waltham, MA, USA

2.4.4. Statistical Analysis

Data are presented as mean \pm SEM. Statistical comparisons were performed with Student unpaired test. When multiple comparisons were performed, one-way ANOVA followed by the Bonferroni test was used. Statistical significance was set at $p < 0.05$.

3. Results

We found a downregulation (protein and mRNA levels) of several presynaptic proteins such as synapsin I (Figure 1), synaptophysin (Figure 2), synaptotagmin (Figure 3), syntaxin 1A (Figure 4), vesicle-associated membrane protein 2 (VAMP2) (Figure 5), and synaptosomal-associated protein of 25 kDa (SNAP25) (Figure 6) in db/db mice treated with vehicle in comparison with non-diabetic mice. All these presynaptic proteins are involved in vesicle biogenesis, mobilization and docking, membrane fusion and recycling, and synaptic neurotransmission [15].

In addition, we found that topical administration of sitagliptin was able to prevent the downregulation of all these synaptic proteins (Figures 1–6) in diabetic mice. These effects were associated with an improvement of functional abnormalities induced by diabetes assessed by full-field ERG (Figure 7). The amplitude of a wave (predominantly produced by photoreceptors cells) was significantly lower in diabetic mice treated with the vehicle than in non-diabetic mice (Figure 7A). An example of an electroretinogram in response to low and high stimulus intensities in a representative non-diabetic mouse, a db/db mouse treated with vehicle, and a db/db mouse treated with saxagliptin or sitagliptin is shown in Figure 7B.

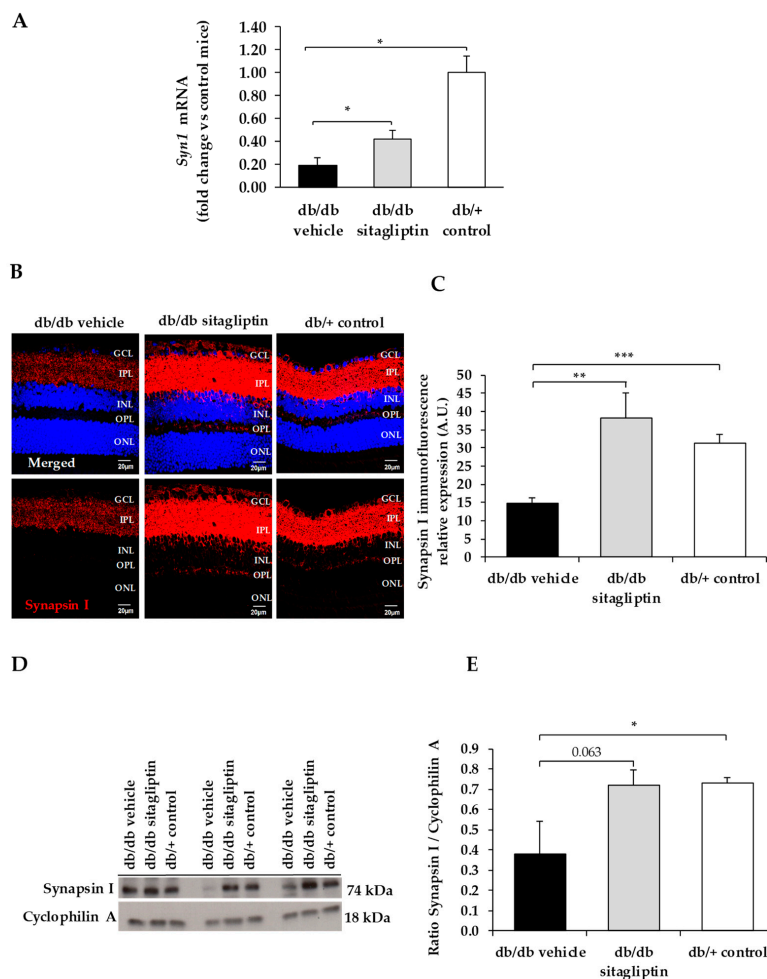


Figure 1. (A) Real-time quantitative RT-PCR analysis of synapsin I gene (*Syn1*) in db/db mice treated with vehicle (black bars), sitagliptin eye drops (grey bars), and in non-diabetic mice (white bars). (B) Immunofluorescence of synapsin I (red) among representative samples of diabetic retinas of experimental groups. Hoechst staining (blue) was used for nuclei labeling. ONL: outer nuclear layer; OPL: outer plexiform layer; INL: inner nuclear layer; IPL: inner plexiform layer; GCL: ganglion cell layer. Scale bars, 20 μ m. (C) Quantification of synapsin I immunofluorescence in diabetic mice treated with vehicle eye drops (black bars), sitagliptin eye drops (grey bars), and in non-diabetic retinas (white bars). (D) Western blot bands of synapsin I and (E) Densitometric analysis in db/db mice treated with vehicle eye drops (black bars), sitagliptin eye drops (grey bars), and in non-diabetic mice retinas (white bars). Protein levels were normalized with cyclophilin A. * $p < 0.05$, ** $p < 0.01$, *** $p < 0.001$.

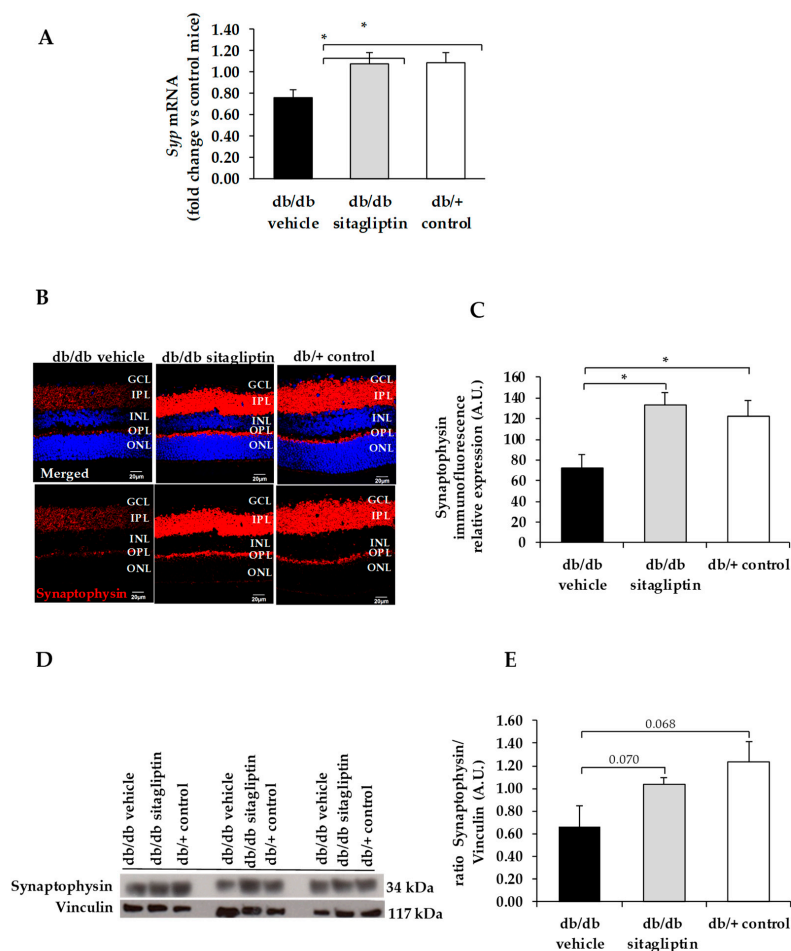


Figure 2. (A) Real-time quantitative RT-PCR analysis of synaptophysin gene (*Syp*) in db/db mice treated with vehicle (black bars), sitagliptin eye drops (grey bars), and in non-diabetic mice (white bars). (B) Immunofluorescence of synaptophysin (red) among representative samples of diabetic retinas of experimental groups. Hoechst staining (blue) was used for nuclei labeling. ONL: outer nuclear layer; OPL: outer plexiform layer; INL: inner nuclear layer; IPL: inner plexiform layer; GCL: ganglion cell layer. Scale bars, 20 μm. (C) Quantification of synaptophysin immunofluorescence in diabetic mice treated with vehicle eye drops (black bars), sitagliptin eye drops (grey bars), and in non-diabetic retinas (white bars). (D) Western blot bands of synaptophysin and (E) Densitometric analysis in db/db mice treated with vehicle eye drops (black bars), sitagliptin eye drops (grey bars), and in non-diabetic mice retinas (white bars). Protein levels were normalized with vinculin. * $p < 0.05$.

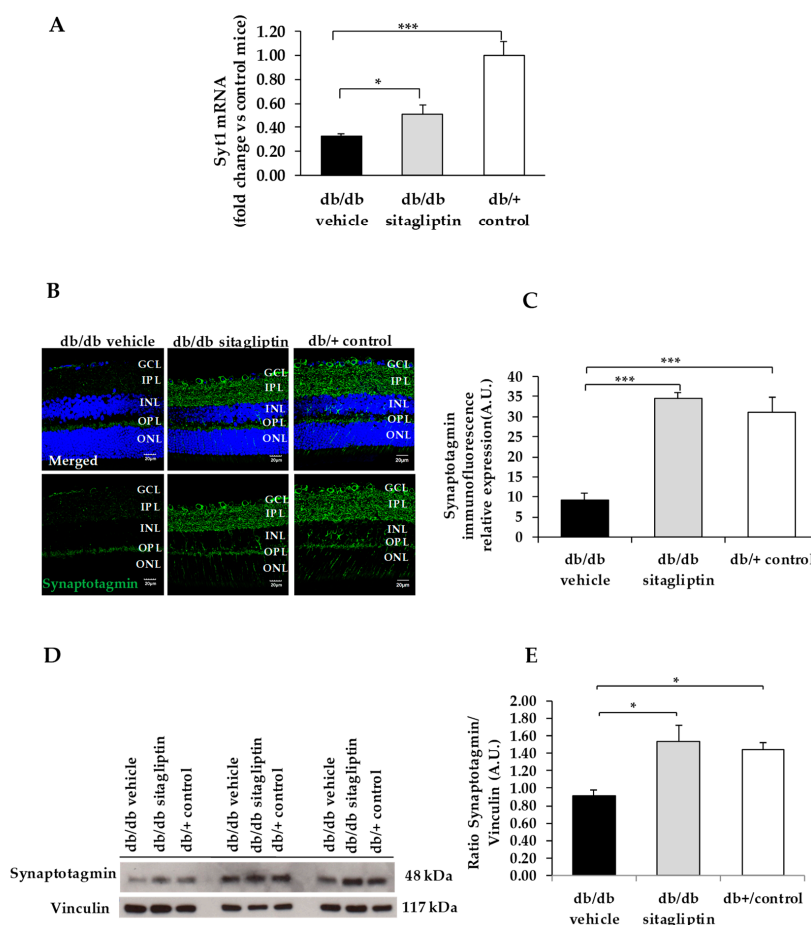


Figure 3. (A) Real-time quantitative RT-PCR analysis of synaptotagmin gene (*Syt1*) in db/db mice treated with vehicle (black bars), sitagliptin eye drops (grey bars), and in non-diabetic mice (white bars). (B) Immunofluorescence of synaptotagmin (green) among representative samples of diabetic retinas of experimental groups. Hoechst staining (blue) was used for nuclei labeling. ONL: outer nuclear layer; OPL: outer plexiform layer; INL: inner nuclear layer; IPL: inner plexiform layer; GCL: ganglion cell layer. Scale bars, 20 μm. (C) Quantification of synaptotagmin immunofluorescence in diabetic mice treated with vehicle eye drops (black bars), sitagliptin eye drops (grey bars), and in non-diabetic retinas (white bars). (D) Western blot bands of synaptotagmin, and (E) Densitometric analysis in db/db mice treated with vehicle eye drops (black bars), sitagliptin eye drops (grey bars), and in non-diabetic mice retinas (white bars). Protein levels were normalized with vinculin. * $p < 0.05$, *** $p < 0.001$.

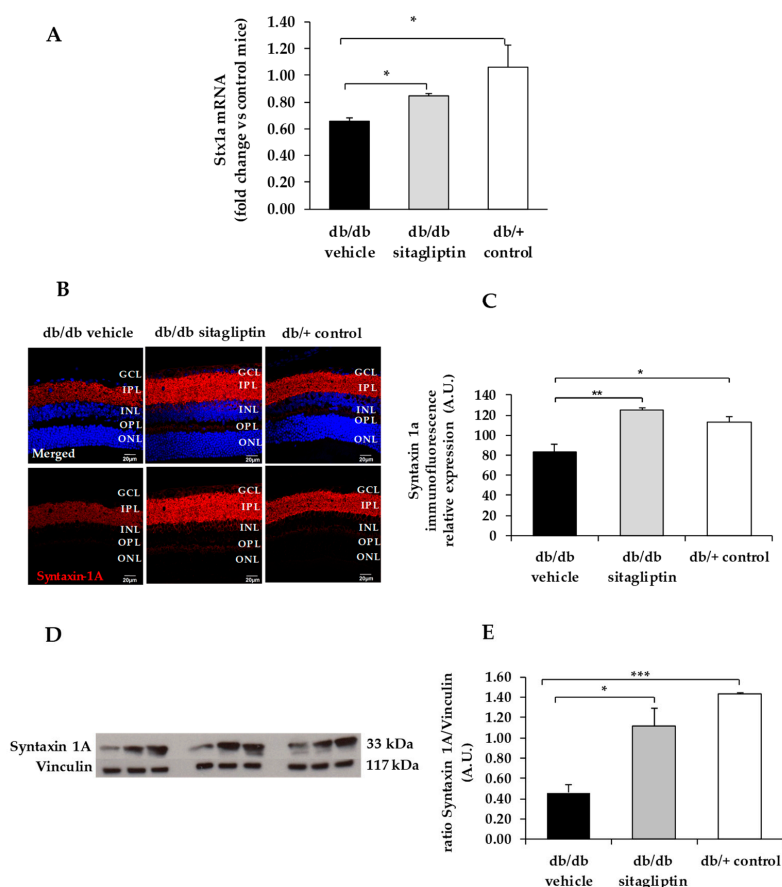


Figure 4. (A) Real-time quantitative RT-PCR analysis of syntxin 1A gene (*Stx1a*) in db/db mice treated with vehicle (black bars), sitagliptin eye drops (grey bars), and in non-diabetic mice (white bars). (B) Immunofluorescence of syntxin 1A (red) among representative samples of diabetic retinas of experimental groups. Hoechst staining (blue) was used for nuclei labeling. ONL: outer nuclear layer; OPL: outer plexiform layer; INL: inner nuclear layer; IPL: inner plexiform layer; GCL: ganglion cell layer. Scale bars, 20 μ m. (C) Quantification of syntxin 1A immunofluorescence in diabetic mice treated with vehicle eye drops (black bars), sitagliptin eye drops (grey bars), and in non-diabetic retinas (white bars). (D) Western blot bands of syntxin 1A and (E) Densitometric analysis in db/db mice treated with vehicle eye drops (black bars), sitagliptin eye drops (grey bars), and in non-diabetic mice retinas (white bars). Protein levels were normalized with vinculin. * $p < 0.05$, ** $p < 0.01$, *** $p < 0.001$.

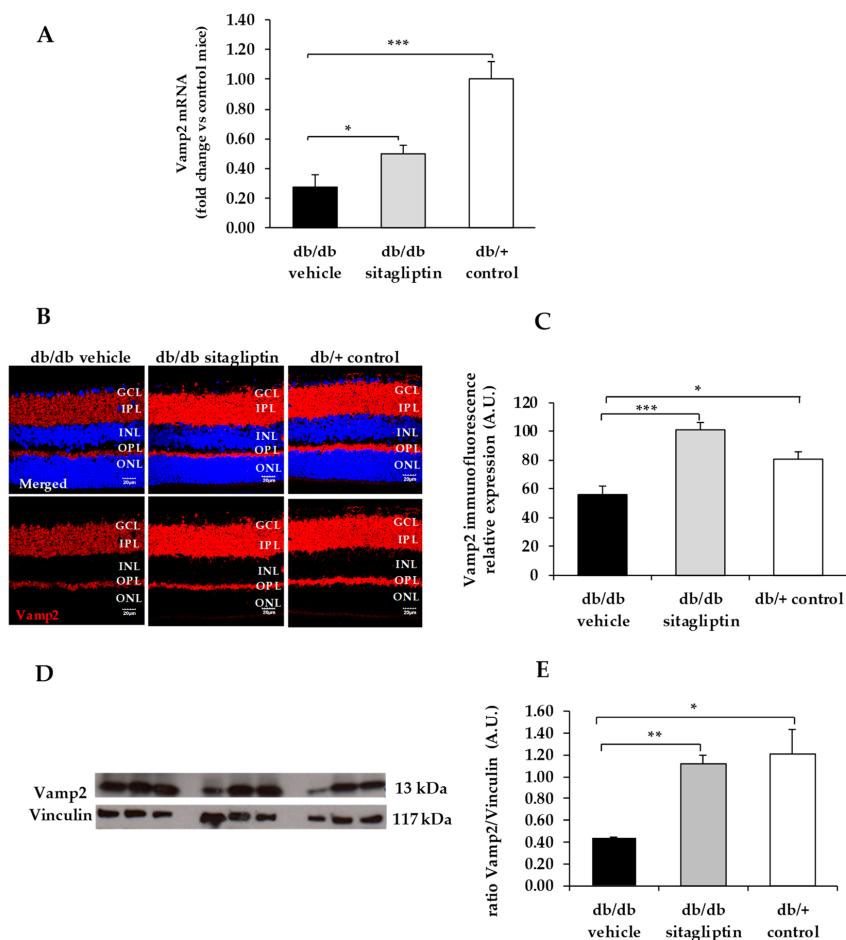


Figure 5. (A) Real-time quantitative RT-PCR analysis of VAMP2 gene (*Vamp2*) in db/db mice treated with vehicle (black bars), sitagliptin eye drops (grey bars), and in non-diabetic mice (white bars). (B) Immunofluorescence of VAMP2 (red) among representative samples of diabetic retinas of experimental groups. Hoechst staining (blue) was used for nuclei labeling. ONL: outer nuclear layer; OPL: outer plexiform layer; INL: inner nuclear layer; IPL: inner plexiform layer; GCL: ganglion cell layer. Scale bars, 20 μ m. (C) Quantification of VAMP2 immunofluorescence in diabetic mice treated with vehicle eye drops (black bars), sitagliptin eye drops (grey bars), and in non-diabetic retinas (white bars). (D) Western blot bands of VAMP2 and (E) Densitometric analysis in db/db mice treated with vehicle eye drops (black bars), sitagliptin eye drops (grey bars), and in non-diabetic mice retinas (white bars). Protein levels were normalized with vinculin. * $p < 0.05$, ** $p < 0.01$, *** $p < 0.001$.

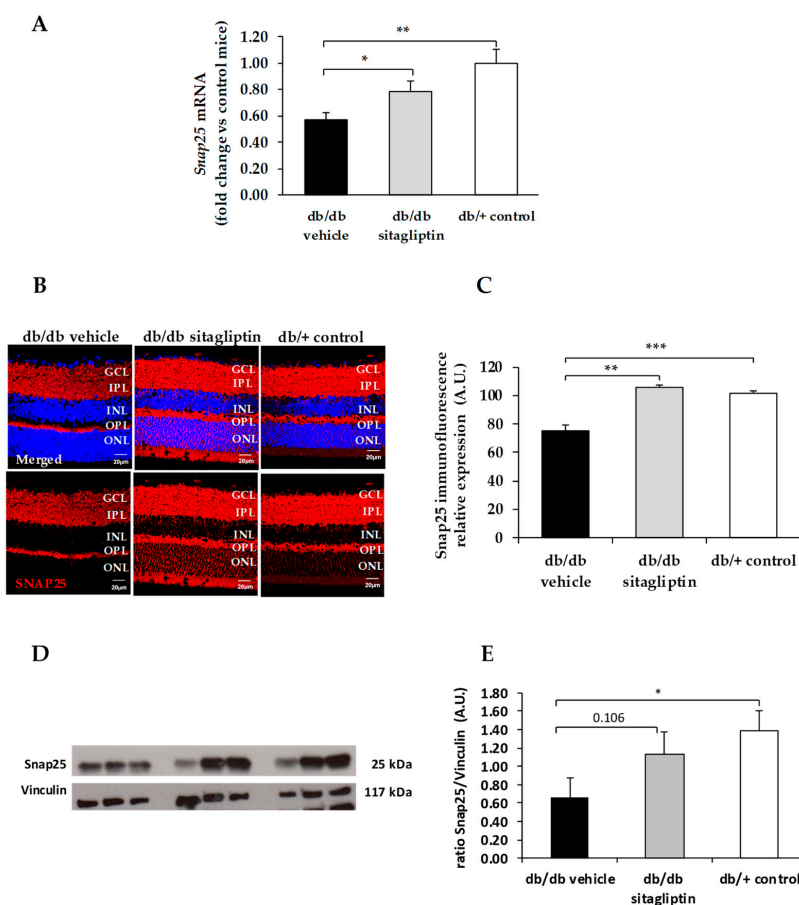


Figure 6. (A) Real-time quantitative RT-PCR analysis of SNAP25 gene (*Snap25*) in db/db mice treated with vehicle (black bars), sitagliptin eye drops (grey bars), and in non-diabetic mice (white bars). (B) Immunofluorescence of SNAP25 (red) among representative samples of diabetic retinas of experimental groups. Hoechst staining (blue) was used for nuclei labeling. ONL: outer nuclear layer; OPL: outer plexiform layer; INL: inner nuclear layer; IPL: inner plexiform layer; GCL: ganglion cell layer. Scale bars, 20 μ m. (C) Quantification of SNAP25 immunofluorescence in diabetic mice treated with vehicle eye drops (black bars), sitagliptin eye drops (grey bars), and in non-diabetic retinas (white bars). (D) Western blot bands of SNAP25 and (E) Densitometric analysis in db/db mice treated with vehicle eye drops (black bars), sitagliptin eye drops (grey bars), and in non-diabetic mice retinas (white bars). Protein levels were normalized with vinculin. * $p < 0.05$, ** $p < 0.01$, *** $p < 0.001$.

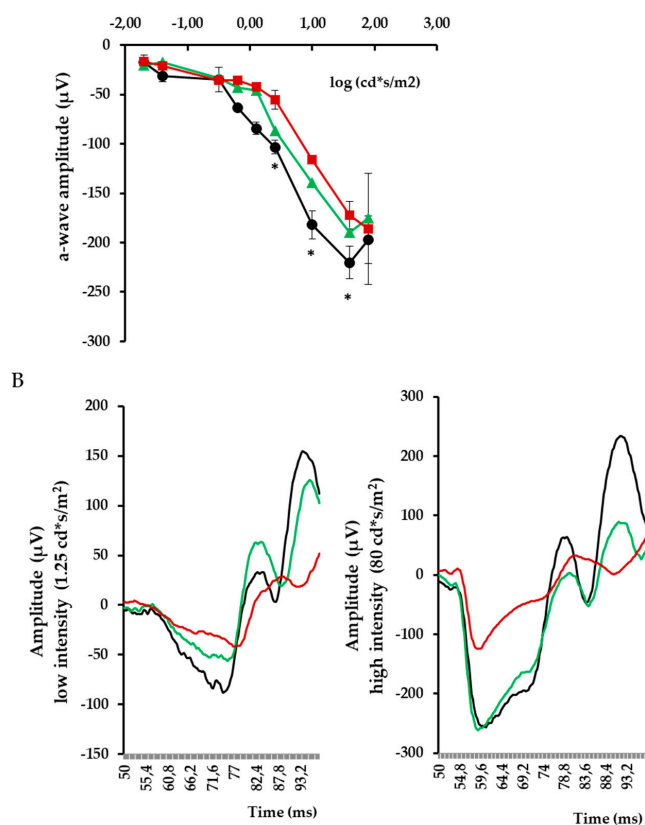


Figure 7. (A) Quantitative analyses of a-wave amplitude in db/db mice treated with vehicle (red), db/db mice treated with sitagliptin (green), and non-diabetic mice (black). * $p < 0.05$ vs. db/db mice treated with vehicle. (B) Electrophoretogram traces in response to low and high stimulus intensities in a representative non-diabetic mouse (black), a db/db mouse treated with vehicle (red), and a db/db mouse treated with sitagliptin (green).

It is worth mentioning that blood glucose concentrations and body weight during treatment were similar in db/db mice treated with sitagliptin and in db/db mice treated with vehicle (Figure 8). These findings indicate that the observed effects of sitagliptine are due to direct effect on the retina rather than a result of an improvement of systemic metabolic control.

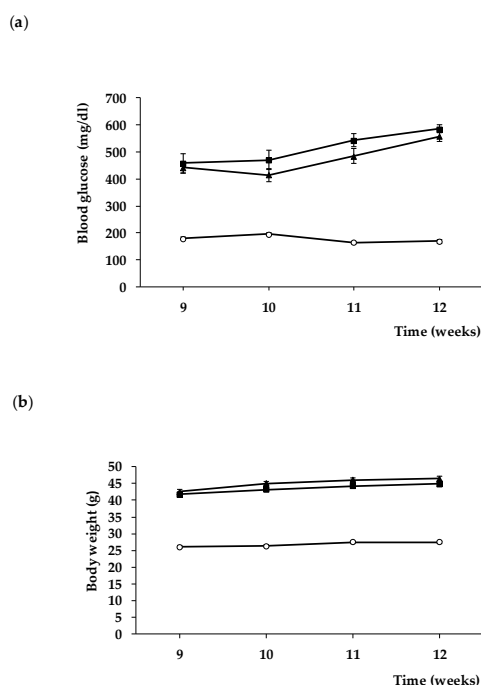


Figure 8. Evolution of blood glucose (a) and body weight (b) in db/+ mice (white circles), db/db mice treated with vehicle (black squares), and db/db mice treated with sitagliptin eye drops (black triangles).

4. Discussion

In the present study we provide evidence that topical ocular administration of sitagliptin (eye drops) was able to prevent the downregulation of presynaptic proteins in retinal neurons in db/db mice. This neuroprotective effect was associated with the improvement of retinal function assessed by ERG.

Synapsin and synaptophysin are the most abundant synaptic vesicle proteins and they are the most commonly used markers for presynaptic terminals [16]. Synapsin is the major peripheral membrane protein accounting for 6% of the total synaptic vesicle protein [17]; it regulates the reserve pool of synaptic vesicles available for exocytosis [18] and maintains the organization and abundance of vesicles at presynaptic terminals [19]. Synaptophysin is the major integral membrane protein accounting for 6–10% of total synaptic vesicle protein [20–22], which regulates the kinetics of synaptic vesicle endocytosis [23] as well as the synaptic vesicle retrieval through its interaction with VAMP2 [24]. SNAP25, VAMP2, syntaxin, and synaptotagmin are SNARE proteins (soluble N-ethylmaleimide-sensitive fusion protein attachment protein receptors) which regulate the synaptic vesicles exocytosis and neurotransmitter release [25].

Synaptophysin was the first synaptic vesicle protein to be cloned and since its discovery in 1985 [20,21] has been the most used marker to study the distribution of synapses. Masser et al. reported that diabetes causes a reduction in the retinal content of synaptophysin in STZ-induced diabetic rats, and this abnormality was corrected by insulin treatment when it was initiated soon after the onset of diabetes [26]. By contrast, when

insulin was given later (i.e., after 1.5 months of uncontrolled diabetes), the synaptic protein content was not returned to control levels [26]. The authors concluded that retinal synapses were lost within 1 month of uncontrolled diabetes and suggest that synapses are not regained with glycemic control and restoration of insulin signaling. We found that the reduction of synaptophysin, as well as other relevant synaptic proteins also occurs in db/db mouse, a type 2 diabetic model with hyperinsulinemia and insulin resistance. In addition, and most importantly, we provide evidence that sitagliptin was able to restore synaptophysin and the other synaptic proteins after several weeks of significant hyperglycemia without any change in systemic blood glucose levels. Therefore, the effects of sitagliptin were due to its direct effects in the retina and unrelated to the improvement of the systemic diabetic milieu.

Regarding the mechanisms involved in the neuroprotective action of sitagliptin, we previously demonstrated that sitagliptin increases retinal content of GLP-1, a neuroprotective peptide for the retina [27], by inhibiting its degradation [12]. In this regard, it has been reported that sitagliptin regulates GABAergic transmission via the GLP-1/GLP-1R pathway [28]. Moreover, we found that sitagliptin prevents the increase of glutamate induced by diabetes by inhibiting GLAST downregulation and had also a strong anti-inflammatory action [12]. Although the main actions of sitagliptin seem mediated by an increase of retinal GLP-1 levels, the simultaneous activation of other mechanisms unrelated to GLP-1/GLP-1R cannot be ruled out [29].

It should be noted that DPP4 has been found embedded in synaptophysin stained elements, thus suggesting a close relationship between synaptic and DPP4 activity in the brain [30]. In addition, inflammation causes a five-fold increase in DPP4 protein level, suggesting a very potent posttranscriptional control of DPP4 expression during developing inflammation [30]. Given that the retina is ontogenically a brain-derived tissue, it could be expected that similar findings will be expected in retinas. Our data support this hypothesis given that we found that the inhibition of DPP4 by sitagliptin has a particular role in the presynaptic protein expression.

The global prevalence of DR in the population with diabetes is around one-third and approximately one-tenth of these patients have the vision-threatening states [31]. In addition, the number of people with visual impairment owing to DR worldwide is rising and this represents an increasing proportion of all causes of blindness and moderate or severe vision impairment [32]. In early stages of DR, aggressive treatments such as laser photocoagulation or intravitreal injections of corticosteroids or anti-VEGF agents are inconceivable. For this purpose, it is desirable to achieve a topical administration (i.e., eye drops) of therapeutic agents, such as sitagliptin. Apart from allowing self-administration, the topical administration of sitagliptin can also limit its action to the eye and minimize the associated systemic effects. Furthermore, it should be noted that it is not proved that sitagliptin systemically administered can cross the blood–retinal barrier. Therefore, for achieving the direct beneficial effects of sitagliptin, the ocular topical route seems mandatory.

In summary, we conclude that sitagliptin exerts beneficial effects in the retinas of diabetic mice by preventing the downregulation of crucial presynaptic proteins. This effect can be added to the mechanisms involved in neuroprotective action of sitagliptin, an open and new avenue for treating DR as well as other retinal diseases in which neurodegeneration plays a relevant role.

Author Contributions: Conceptualization, P.B., C.H. and R.S.; methodology, H.R., P.B., D.S., J.H., M.V., R.S. and C.H.; formal analysis, H.R., P.B., D.S., J.H., M.V., C.H. and R.S.; investigation, P.B., H.R., C.H. and R.S.; resources, R.S. and C.H.; writing—original draft preparation, H.R. and P.B.; writing—review and editing, R.S. and C.H.; supervision, R.S. and C.H.; project administration, C.H.; funding acquisition, R.S. and C.H. All authors have read and agreed to the published version of the manuscript. R.S. is the guarantor of this work and, as such, had full access to all the data in the study and takes responsibility for the integrity of the data and the accuracy of the data analysis.

Funding: This research was funded by grants from the Ministerio de Economía y Competitividad (PID2019-104225RB-I00) and the Instituto de Salud Carlos III (DTS18/0163, PI19/01215, and ICI20/00129). The study funder was not involved in the design of the study.

Institutional Review Board Statement: This study was approved by the Animal Care and Use Committee of Vall d'Hebron Research Institute (VHIR). Approval Code: 75/15. Approval Date: 2 December 2015.

Informed Consent Statement: Not applicable.

Data Availability Statement: The data presented in this study are available on request from the corresponding author.

Acknowledgments: H.R. is the recipient of a grant from the Ministerio de Economía y Competitividad (BES-2017-081690). The histological processing was performed by ICTS "NANBIOSIS", more specifically by Unit 20 of CIBER in Bioengineering, Biomaterials and Nanomedicine (CIBER-BBN) at the Vall d'Hebron Research Institute.

Conflicts of Interest: Vall d'Hebron Research Institute holds intellectual property related to the use of ocular DPP-4 inhibitors to treat diabetic retinopathy. No other potential conflict of interest relevant to this article were reported.






References

- Simó, R.; Hernández, C. European Consortium for the Early Treatment of Diabetic Retinopathy (EUROCONDOR). Neurodegeneration in the diabetic eye: New insights and therapeutic perspectives. *Trends Endocrinol. Metab.* **2014**, *25*, 23–33. [\[CrossRef\]](#) [\[PubMed\]](#)
- Simó, R.; Stitt, A.W.; Gardner, T.W. Neurodegeneration in diabetic retinopathy: Does it really matter? *Diabetologia* **2018**, *61*, 1902–1912. [\[CrossRef\]](#) [\[PubMed\]](#)
- Solomon, S.D.; Chew, E.; Duh, E.J.; Sobrin, L.; Sun, J.K.; VanderBeek, B.L.; Wykoff, C.C.; Gardner, T.W. Diabetic retinopathy: A position statement by the American Diabetes Association. *Diabetes Care* **2017**, *40*, 412–418. [\[CrossRef\]](#) [\[PubMed\]](#)
- Barber, A.J.; Lieth, E.; Khin, S.A.; Antonetti, D.A.; Buchanan, A.G.; Gardner, T.W. Neural apoptosis in the retina during experimental and human diabetes. Early onset and effect of insulin. *J. Clin. Investig.* **1998**, *102*, 783–791. [\[CrossRef\]](#) [\[PubMed\]](#)
- Carrasco, E.; Hernández, C.; Miralles, A.; Huguet, P.; Farrés, J.; Simó, R. Lower somatostatin expression is an early event in diabetic retinopathy and is associated with retinal neurodegeneration. *Diabetes Care* **2007**, *30*, 2902–2908. [\[CrossRef\]](#)
- García-Ramírez, M.; Hernández, C.; Villarreal, M.; Canals, F.; Alonso, M.A.; Fortuny, R.; Masmiquel, L.; Navarro, A.; García-Arumí, J.; Simó, R. Interphotoreceptor retinoid-binding protein (IRBP) is downregulated at early stages of diabetic retinopathy. *Diabetologia* **2009**, *52*, 2633–2641. [\[CrossRef\]](#) [\[PubMed\]](#)
- Barber, A.J.; Gardner, T.W.; Abcouwer, S.F. The significance of vascular and neural apoptosis to the pathology of diabetic retinopathy. *Investig. Ophthalmol. Vis. Sci.* **2011**, *52*, 1156–1163. [\[CrossRef\]](#)
- VanGuilder, H.D.; Brucklacher, R.M.; Patel, K.; Ellis, R.W.; Freeman, W.M.; Barber, A.J. Diabetes downregulates presynaptic proteins and reduces basal synapsin I phosphorylation in rat retina. *Eur. J. Neurosci.* **2008**, *28*, 1–11. [\[CrossRef\]](#)
- Gaspar, J.M.; Baptista, F.I.; Galvão, J.; Castilho, A.F.; Cunha, R.A.; Ambrósio, A.F. Diabetes differentially affects the content of exocytotic proteins in hippocampal and retinal nerve terminals. *Neuroscience* **2010**, *169*, 1589–1600. [\[CrossRef\]](#)
- Ly, A.; Scheerer, M.F.; Zukunft, S.; Muschet, C.; Merl, J.; Adamski, J.; de Angelis, M.H.; Neschen, S.; Hauck, S.M.; Ueffing, M. Retinal proteome alterations in a mouse model of type 2 diabetes. *Diabetologia* **2014**, *57*, 192–203. [\[CrossRef\]](#)
- Robinson, W.F.; VanGuilder, H.D.; D'Cruz, T.S.; El-Remessy, A.B.; Barber, A.J. Synapsin 1 Protein Expression and Phosphorylation Are Compromised by Diabetes in Rodent and Human Retinas. *Investig. Ophthalmol. Vis. Sci.* **2008**, *49*, 4920.
- Hernández, C.; Bogdanov, P.; Solà-Adell, C.; Sampedro, J.; Valeri, M.; Genís, X.; Simó-Servat, O.; García-Ramírez, M.; Simó, R. Topical administration of DPP-IV inhibitors prevents retinal neurodegeneration in experimental diabetes. *Diabetologia* **2017**, *60*, 2285–2298. [\[CrossRef\]](#) [\[PubMed\]](#)
- Bogdanov, P.; Corraliza, L.; Villena, J.A.; Carvalho, A.R.; García-Arumí, J.; Ramos, D.; Ruberte, J.; Simó, R.; Hernández, C. The db/db mouse: A useful model for the study of diabetic retinal neurodegeneration. *PLoS ONE* **2014**, *9*, e97302. [\[CrossRef\]](#) [\[PubMed\]](#)
- Marmor, M.F.; Holder, G.E.; Seeliger, M.W.; Yamamoto, S.; International Society for Clinical Electrophysiology of Vision. Standard for clinical electroretinography (2004 update). *Doc. Ophthalmol.* **2004**, *108*, 107–114. [\[CrossRef\]](#)
- Simó, R.; Simó-Servat, O.; Bogdanov, P.; Hernández, C. Neurovascular Unit: A New Target for Treating Early Stages of Diabetic Retinopathy. *Pharmaceutics* **2021**, *13*, 1320. [\[CrossRef\]](#) [\[PubMed\]](#)
- Micheva, K.D.; Busse, B.; Weiler, N.C.; O'Rourke, N.; Smith, S.J. Single-synapse analysis of a diverse synapse population: Proteomic imaging methods and markers. *Neuron* **2010**, *68*, 639–653. [\[CrossRef\]](#)

17. Huttner, W.B.; Schiebler, W.; Greengard, P.; De Camilli, P. Synapsin I (protein I), a nerve terminal-specific phosphoprotein. III. Its association with synaptic vesicles studied in a highly purified synaptic vesicle preparation. *J. Cell Biol.* **1983**, *96*, 1374–1388. [\[CrossRef\]](#)
18. Böhler, M.; Benfenati, F.; Valtorta, F.; Greengard, P. The synapsins and the regulation of synaptic function. *BioEssays News Rev. Mol. Cell. Dev. Biol.* **1990**, *12*, 259–263. [\[CrossRef\]](#)
19. Bykhovskaia, M. Synapsin regulation of vesicle organization and functional pools. *Semin. Cell Dev. Biol.* **2011**, *22*, 387–392. [\[CrossRef\]](#)
20. Wiedenmann, B.; Franke, W.W. Identification and localization of synaptophysin, an integral membrane glycoprotein of Mr 38,000 characteristic of presynaptic vesicles. *Cell* **1985**, *41*, 1017–1028. [\[CrossRef\]](#)
21. Jahn, R.; Schiebler, W.; Ouimet, C.; Greengard, P.A. 38,000-dalton membrane protein (p38) present in synaptic vesicles. *Proc. Natl. Acad. Sci. USA* **1985**, *82*, 4137–4141. [\[CrossRef\]](#) [\[PubMed\]](#)
22. Takamori, S.; Holt, M.; Stenius, K.; Lemke, E.A.; Grønborg, M.; Riedel, D.; Urlaub, H.; Schenck, S.; Brügger, B.; Ringler, P.; et al. Molecular anatomy of a trafficking organelle. *Cell* **2006**, *127*, 831–846. [\[CrossRef\]](#)
23. Kwon, S.E.; Chapman, E.R. Synaptophysin regulates the kinetics of synaptic vesicle endocytosis in central neurons. *Neuron* **2011**, *70*, 847–854. [\[CrossRef\]](#)
24. Gordon, S.L.; Leube, R.E.; Cousin, M.A. Synaptophysin is required for synaptobrevin retrieval during synaptic vesicle endocytosis. *J. Neurosci.* **2011**, *31*, 14032–14036. [\[CrossRef\]](#) [\[PubMed\]](#)
25. Ramakrishnan, N.A.; Drescher, M.J.; Drescher, D.G. The SNARE complex in neuronal and sensory cells. *Mol. Cell Neurosci.* **2012**, *50*, 58–69. [\[CrossRef\]](#)
26. Masser, D.R.; VanGuilder, H.D.; Bixler, G.V.; Dunton, W.; Bronson, S.K.; Freeman, W.M. Insulin treatment normalizes retinal neuroinflammation but not markers of synapse loss in diabetic rats. *Exp. Eye Res.* **2014**, *125*, 95–106. [\[CrossRef\]](#) [\[PubMed\]](#)
27. Hernández, C.; Bogdanov, P.; Corraliza, L.; García-Ramírez, M.; Solà-Adell, C.; Arranz, J.A.; Arroba, A.I.; Valverde, A.M.; Simó, R. Topical administration of GLP-1 receptor agonists prevents retinal neurodegeneration in experimental diabetes. *Diabetes* **2016**, *65*, 172–187. [\[CrossRef\]](#)
28. Zhang, Y.; Liu, Y.; Xu, J.; Sun, Q.; Yu, F.; Cheng, J.; Peng, B.; Liu, W.; Xiao, Z.; Yin, J.; et al. Inhibition of DPP4 enhances inhibitory synaptic transmission through activating the GLP-1/GLP-1R signaling pathway in a rat model of febrile seizures. *Biochem. Pharmacol.* **2018**, *156*, 78–85. [\[CrossRef\]](#)
29. Dietrich, N.; Kolibabka, M.; Busch, S.; Bugert, P.; Kaiser, U.; Lin, J.; Fleming, T.; Morcos, M.; Klein, T.; Schlotterer, A.; et al. The DPP4 inhibitor linagliptin protects from experimental diabetic retinopathy. *PLoS ONE* **2016**, *11*, e0167853. [\[CrossRef\]](#)
30. Király, K.; Kozsúrek, M.; Lukács, E.; Barta, B.; Alpár, A.; Balázs, T.; Fekete, C.; Szabon, J.; Helyes, Z.; Bölskei, K.; et al. Glial cell type-specific changes in spinal dipeptidyl peptidase 4 expression and effects of its inhibitors in inflammatory and neuropathic pain. *Sci. Rep.* **2018**, *8*, 3490. [\[CrossRef\]](#)
31. Yau, J.W.; Rogers, S.L.; Kawasaki, R.; Lamoureux, E.L.; Kowalski, J.W.; Bek, T.; Chen, S.J.; Dekker, J.M.; Fletcher, A.; Grauslund, J.; et al. Global prevalence and major risk factors of diabetic retinopathy. *Diabetes Care* **2012**, *35*, 556–564. [\[CrossRef\]](#) [\[PubMed\]](#)
32. Leasher, J.L.; Bourne, R.R.; Flaxman, S.R.; Jonas, J.B.; Keeffe, J.; Naidoo, K.; Pesudovs, K.; Price, H.; White, R.A.; Wong, T.Y.; et al. Global Estimates on the Number of People Blind or Visually Impaired by Diabetic Retinopathy: A Meta-analysis from 1990 to 2010. *Diabetes Care* **2016**, *39*, 1643–1649. [\[CrossRef\]](#) [\[PubMed\]](#)

Article

Minimum Effective Dose of DPP-4 Inhibitors for Treating Early Stages of Diabetic Retinopathy in an Experimental Model

Patricia Bogdanov ^{1,2,†} , Hugo Ramos ^{1,2,†} , Marta Valeri ³, Anna Deàs-Just ¹ , Jordi Huerta ¹ , Rafael Simó ^{1,2,4,*}  and Cristina Hernández ^{1,2,4,*} 

¹ Diabetes and Metabolism Research Unit, Vall d'Hebron Research Institute, 08035 Barcelona, Spain; patricia.bogdanov@vhir.org (P.B.); hugo.ramos@vhir.org (H.R.); anna.deas@vhir.org (A.D.-J.); jordi.huerta@vhir.org (J.H.)

² Centro de Investigación Biomédica en Red de Diabetes y Enfermedades Metabólicas Asociadas (CIBERDEM), Instituto de Salud Carlos III (ICSIII), 28029 Madrid, Spain

³ Unit of High Technology, Vall d'Hebron Research Institute, 08035 Barcelona, Spain; marta.valeri@vhir.org

⁴ Department of Medicine, Universitat Autònoma de Barcelona, 08193 Barcelona, Spain

* Correspondence: rafael.simo@vhir.org (R.S.); cristina.hernandez@vhir.org (C.H.); Tel.: +34-934-894-172 (C.H.)

† These authors contributed equally to this work.

Abstract: The neurovascular unit (NVU) plays an essential role in the development of diabetic retinopathy (DR). We previously reported that the topical administration (eye drops) of sitagliptin and saxagliptin, two dipeptidyl peptidase-4 inhibitors (DPP-4i), prevents retinal neurodegeneration and vascular leakage in db/db mice. The aim of the present study is to evaluate the minimum effective dose of the topical administration of these DPP-4i. For this purpose, sitagliptin and saxagliptin were tested at different concentrations (sitagliptin: 1 mg/mL, 5 and 10 mg/mL, twice per day; saxagliptin: 1 and 10 mg/mL, once or twice per day) in db/db mice. As end points of efficacy, the hallmarks of NVU impairment were evaluated: reactive gliosis, neural apoptosis, and vascular leakage. These parameters were assessed by immunohistochemistry, cell counting, and the Evans blue method, respectively. Our results demonstrated that the minimum effective dose is 5 mg/mL twice per day for sitagliptin, and 10 mg/mL twice per day for saxagliptin. In conclusion, this study provides useful results for the design of future preclinical regulatory studies and for planning clinical trials.

Keywords: diabetic retinopathy; dipeptidyl peptidase-4 inhibitors; sitagliptin; saxagliptin; neurovascular unit; retinal neurodegeneration; experimental diabetes; db/db mice



Citation: Bogdanov, P.; Ramos, H.; Valeri, M.; Deàs-Just, A.; Huerta, J.; Simó, R.; Hernández, C. Minimum Effective Dose of DPP-4 Inhibitors for Treating Early Stages of Diabetic Retinopathy in an Experimental Model. *Biomedicines* **2022**, *10*, 465. <https://doi.org/10.3390/biomedicines10020465>

Academic Editors: Randolph D. Glickman and Igor O. Nasonkin

Received: 14 January 2022

Accepted: 13 February 2022

Published: 16 February 2022

Publisher's Note: MDPI stays neutral with regard to jurisdictional claims in published maps and institutional affiliations.



Copyright: © 2022 by the authors. Licensee MDPI, Basel, Switzerland. This article is an open access article distributed under the terms and conditions of the Creative Commons Attribution (CC BY) license (<https://creativecommons.org/licenses/by/4.0/>).

1. Introduction

Diabetic retinopathy (DR) is the leading cause of visual impairment and preventable blindness and represents a significant socioeconomic cost for healthcare systems worldwide [1,2]. The current treatments for DR, such as laser photocoagulation, intra-vitreous injections of corticosteroids, intra-vitreous injections of anti-vascular endothelial growth factor (VEGF) agents, and vitreoretinal surgery, are expensive, have a significant number of secondary effects, and all of them are only used in the advanced stages of DR [3]. At present, treatment of the classic risk factors of DR (i.e., hyperglycemia and hypertension) is the only therapeutic strategy against the early stages, giving rise to an unmet medical need that has to be filled [4].

Since neurodegeneration is a well-established event in the pathogenesis of DR [5], several neuroprotective strategies have emerged as successful treatments in the early stages of experimental models of DR. One such strategy is based on the replacement of neuroprotective factors, such as pigment epithelium-derived factor (PEDF), somatostatin, and glucagon-like peptide 1 (GLP-1), which are downregulated in the diabetic retina [6]. GLP-1 and GLP-1R agonists (GLP-1RAs) have been the most studied, and the main mechanisms

underlying their neuroprotective properties are: (1) anti-inflammatory action; (2) the inhibition of excitotoxicity and neuron death by reducing glutamate accumulation in the extracellular space; (3) antiapoptotic action by increasing antiapoptotic mediators (i.e., FasL, caspase 8, P53/p-P53, Bax) and downregulating survival pathways (Bcl-xL, Bcl-2); (4) antioxidant properties; and (5) a neurogenic effect by restoring retinal neuron cells and reactive gliosis. In addition to neuroprotective action, GLP-1RAs also have microvascular protection by several mechanisms, including the prevention of the downregulation of tight junction proteins, and the inhibition of the overexpression of VEGF and PlGF, and pro-inflammatory cytokines induced by diabetes [6].

The replacement treatment with these factors seems a reasonable approach for preventing retinal neurodegeneration and has been successfully used in experimental models [7–12]. However, the systemic administration of these neuropeptides can hardly reach the retina at pharmacological concentrations and, by contrast, could have systemic adverse effects [4]. On the other hand, when the early stages of DR are the therapeutic target, it would be inconceivable to recommend an aggressive treatment such as intravitreal injections [4]. For all these reasons, the ocular topical route has emerged as an effective therapeutic approach to deliver these neuroprotective factors into the diabetic retina.

We have previously demonstrated that the topical administration of sitagliptin and saxagliptin (two DPP-4 inhibitors) has a powerful action in preventing both neurodegeneration and vascular leakage, two hallmarks of neurovascular unit impairment that occurs in the early stages of DR [13]. As occurs in the systemic circulation, the main mechanism of action of topical (eye drops) DPP-4 inhibitors relies on its capacity of inhibiting GLP-1 degradation. This effect favors the enhancement of GLP-1 content in the neuroretina, thus accounting for the dual action (neuroprotective and vasculotropic). In addition, sitagliptin and saxagliptin were able to significantly increase the levels of exchange protein activated by cAMP (EPAC-1), which plays an important role in the maintenance of the endothelial barrier and neuronal functions. However, the simultaneous activation of other mechanisms unrelated to GLP-1R activation cannot be ruled out.

Given the reported powerful effect of eye drops of sitagliptin and saxagliptin (at doses of 50 mg/mL and 31.5 mg/mL, respectively) in preventing neurodegeneration and vascular leakage [13], we wanted to determine whether a lower dose could also be effective. Therefore, the aim of the present study was to determine the minimum effective dose of sitagliptin and saxagliptin in eye drops for preclinical regulatory purposes and planning future clinical trials.

2. Materials and Methods

2.1. Experimental Design

A total of 63 diabetic male db/db (BKS.Cg-Dock7m $+/+$ Leprdb/J) mice and 14 non-diabetic mice db/+; (BKS.Cg-Dock7m $+/+$ Leprdb/+), aged 8 weeks, were purchased (Charles River Laboratories, Calco, Italy) for the study. Db/db mice carry a mutated leptin receptor that leads to obesity-induced type 2 diabetes. The animals had free access to ad libitum food (ENVIGO Global Diet Complete Feed for Rodents, Mucedola, Milan, Italy) and filtered water. They were maintained at all times at 20 °C temperature and 60% humidity. In order to minimize variability, the animals were randomly housed (block randomization) in groups of 4 mice per cage. Each cage held absorbent bedding and nesting material (BioFresh Performance Bedding 1/800 Pelleted Cellulose, Absorption Corp, Ferndale, WA, USA).

2.2. Interventional Study

At the age of 10 weeks, sitagliptin 1 mg/mL (twice daily, $n = 7$), sitagliptin 5 mg/mL (twice daily, $n = 7$), sitagliptin 10 mg/mL (twice daily, $n = 7$), saxagliptin 1 mg/mL ($n = 14$) (once and twice daily, $n = 7$ in each case), saxagliptin 10 mg/mL ($n = 14$) (once and twice daily, $n = 7$ in each case) and vehicle eye drops ($n = 14$) were randomly administered directly onto the superior corneal surface of each db/db eye using a micropipette (one

drop: 5 μ L). Sitagliptin (1, 5 or 10 mg/mL), saxagliptin (1 or 10 mg/mL) or vehicle (5 μ L phosphate-buffered saline (PBS), pH 7.4) was administrated for 15 days in each eye. On the last day (12 weeks of age), one drop of sitagliptin, saxagliptin or vehicle was administered to each eye 1 h before euthanasia. Fourteen non-diabetic mice (db/+) matched by age served as the control group.

This study was approved by the Animal Care and Use Committee of VHIR (Vall d'Hebron Research Institute, Barcelona, Spain). All the experiments were performed in accordance with the tenets of the European Community (86/609/CEE) and the Association for Research in Vision and Ophthalmology (ARVO).

2.3. Retinal Tissue Processing

On day 15, 4 mice of each experimental group were transcardiacally perfused with p-formaldehyde 4% (sc-281692, Santa Cruz Biotechnology, Dallas, TX, USA), and the eyes were immediately enucleated, fixed in paraformaldehyde 4% for 5 hours, and embedded in paraffin blocks. Previously, each animal was intraperitoneally injected with 200 μ L of anaesthesia prepared with a mix containing 1 mL ketamine (GmbH, Hameln, Germany) and 0.3 mL xylazine (Laboratorios Calier S.A., Barcelona, Spain).

2.4. Retinal Vascular Permeability by Evans Blue Ex Vivo Assay

We determined the permeability of retinal vasculature using the ex vivo Evans blue albumin method. A solution of Evans blue (E2129, Millipore Sigma, Burlington, MA, USA) (5 mg/mL dissolved in PBS pH 7.4) was introduced through an intraperitoneal injection in 3 animals per experimental group (17 mg/Kg). After injection, the animals turned blue, confirming dye uptake and distribution. After 2 h, the mice were euthanized by cervical dislocation and the eyes were enucleated. We obtained the retinas of each animal, which were flat mounted in $25.5 \times 75.5 \times 1.0$ mm³ poly-L-Lysine positively charged microscopic slides (S21.2113.A, Leica Biosystems, Wetzlar, Germany) with Prolong Mounting Medium Fluorescence (P36930, Invitrogen TM, Thermo Fisher Scientific, Eugene, OR, USA) and coverslips (15747592, ThermoFisher Scientific, Waltham, MA, USA). Images were acquired from different fields at 60x using a 561 nm laser line in a confocal laser scanning microscope (Fluoview FV1000 Laser Scanning Confocal Microscope Olympus, Hamburg, Germany). All images were recorded with identical beam intensity at a size of 1024 pixels \times 1024 pixels. The number of extravasations per field of 60 \times was counted for the quantitative analysis using Image J software (U. S. National Institutes of Health, Bethesda, MD, USA).

2.5. Glial Fibrillary Acidic Protein (GFAP) and DPP-4 Immunofluorescence Analysis

Paraffined ocular globes were sectioned (3 μ m) and mounted on $25.5 \times 75.5 \times 1.0$ mm³ poly-L-Lysine positively charged microscopic slides (S21.2113.A, Leica Biosystems, Wetzlar, Germany). Samples were deparaffinized in xylene (28975360, VWR International Euro-lab, Barcelona, Spain), rehydrated in grade ethanol series (1009832500, Millipore Sigma, Burlington, MA, USA), fixed in ice-cold acid methanol (−20 °C), and washed with PBS 0.01 M at pH 7.4. Successively, slides were heated in a pressure cooker at 150 °C for 4 min in 250 mL of antigen retrieval buffer (100X citrate buffer) pH 6 diluted 1:100 (ab93678, Abcam, Cambridge, UK). Then, sections were blocked with blocking solution (10% normal goat serum (31873, ThermoFisher Scientific, Waltham, MA, USA) + 1% BSA (A3059-100G, Millipore Sigma, Burlington, MA, USA) in PBS) for 1 h at room temperature, and afterwards, they were incubated overnight at 4 °C with the anti-GFAP (rabbit monoclonal; 1:500; ab7260; Abcam, Cambridge, UK) or the anti-DPP-4 (rabbit polyclonal; 1:200; ab28340; Abcam, Cambridge, UK) primary antibodies. The next day, after three washes in PBS, sections were incubated for 1 hour in darkness with Alexa Fluor[®] 488 (goat polyclonal; 1:600; ab150081; Abcam, Cambridge, UK) or Alexa Fluor[®] 594 (goat polyclonal; 1:600; A-110012; Life Technologies, Waltham, MA, USA) secondary antibody. Sections were washed with PBS again, counterstained with Hoechst 33342 (bisbenzimidazole) (14533, ThermoFisher Scientific, Waltham, MA, USA), and mounted with Prolong Mounting Medium Fluores-

cence (P36930, Invitrogen™, Thermo Fisher Scientific, Eugene, OR, USA) and a coverslip (15747592, ThermoFisher Scientific, Waltham, MA, USA). The images were obtained at a resolution of 1024×1024 pixels using laser scanning confocal microscopy (Fluoview FV1000 Laser Scanning Confocal Microscope Olympus, Hamburg, Germany) and the immunofluorescences were quantified with ImageJ software (U. S. National Institutes of Health, Bethesda, MD, USA).

2.6. Measurements of Glial Activation

Glial activation was evaluated by laser scanning confocal microscopy at a magnification of $60\times$ using specific staining antibodies against GFAP. To evaluate the degree of glial activation, we used a scoring system based on the extent of GFAP staining, following the methodology described [14]. This scoring system (previously used by our group) was as follows: Müller cell endfeet region/ganglion cell layer (GCL) only (score 1); Müller cell endfeet region/GCL plus a few proximal processes (score 2); Müller cell endfeet plus many processes, but not extending to inner nuclear layer (INL) (score 3); Müller cell endfeet plus processes throughout with some in the ONL (score 4); and Müller cell endfeet plus many dark processes from GCL to the outer margin of ONL (score 5).

2.7. Histological Assessment with Hematoxylin-Eosin (H&E) Staining

2.7.1. Cell Counting in GCL and INL

Eyes were collected and fixed in 4% paraformaldehyde (sc-281692, Santa Cruz Biotechnology, Dallas, TX, USA). After paraffin embedding, retinas were cross-sectioned ($3\ \mu\text{m}$) and a hematoxylin and eosin (H&E) staining was performed for a systematic morphometric analysis of retinal layers. Images of H&E-stained sections were captured with a microscope (FSX100 Inverted Microscope Olympus, Hamburg, Germany) at a magnification of $35\times$ and quantified using the software ImageJ (U. S. National Institutes of Health, Bethesda, MD, USA). Measurements were taken in three different regions of the central retina. Similar and comparative locations for all studied retinas were determined using the same demarcation, which consists in selecting regions close to the optic nerve but with a minimum extension of $300\ \mu\text{m}$ from both sides of the optic nerve head rim (posterior pole of the eye). Cell counts of GCL and INL were averaged and compared among all the experimental groups.

2.7.2. Analysis of Retinal Thickness

Total and INL thicknesses were measured using the ImageJ software (U. S. National Institutes of Health, Bethesda, MD, USA). Five distinct images of each retina were analyzed, quantified, and averaged for obtaining both thicknesses. Imaged regions were selected according to the demarcation described in the cell-counting section, and for each region, a representative value was obtained through the arithmetical mean of ten different measures.

2.8. Statistical Analysis

Data are expressed as the mean \pm standard error of the mean (SEM). For multiple comparisons, a one-way ANOVA followed by the Bonferroni test was used. For statistical purposes, the GFAP extent score was categorized as “normal” (scores 1 and 2) and “pathological” (scores 3, 4 and 5), and for comparisons between groups, Fisher’s exact test was used. Statistical significance was set at $p < 0.05$.

3. Results

3.1. Dose–Response Effect of Topical Administration of Sitagliptin and Saxagliptin on DPP-4 Content

Both DPP-4 inhibitors reduced the DPP-4 protein content in the diabetic retina (Figure 1). No differences were observed among sitagliptin concentrations. However, saxagliptin administered twice a day achieve a higher reduction in DPP-4 levels than when it was administered once daily.

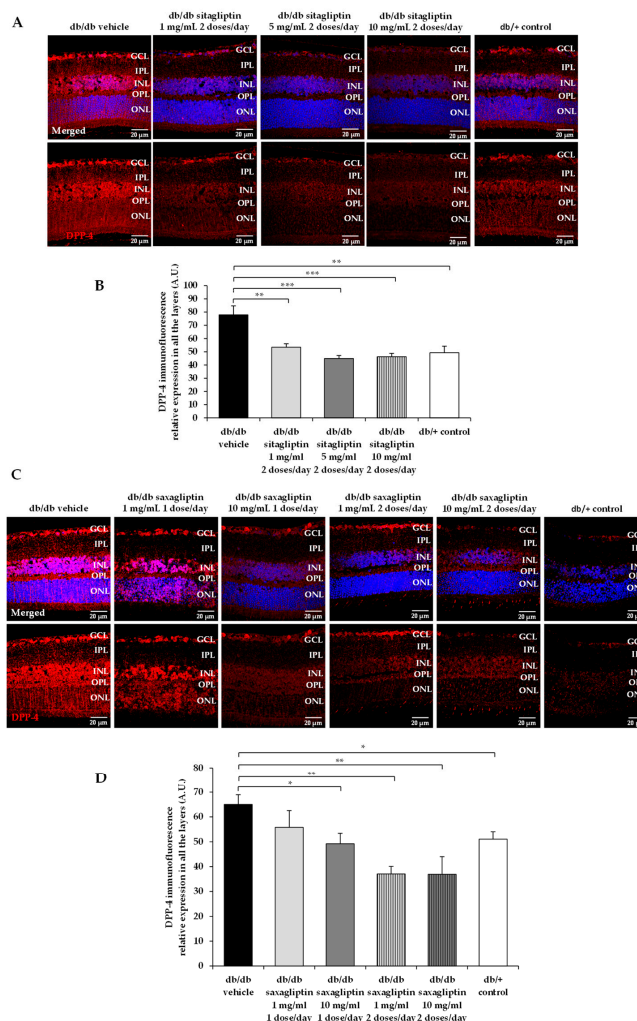


Figure 1. DPP-4 protein abundance. (A,C) Comparison of retinal DPP-4 immunofluorescence reactivity (red) among representative samples of each experimental group. DPP-4 relative fluorescence intensity is presented alone and merged with Hoechst nuclei staining (blue). ONL: outer nuclear layer; OPL: outer plexiform layer; INL: inner nuclear layer; IPL: inner plexiform layer; GCL: ganglion cell layer. Scale bars, 20 μ m. (B,D) Quantification of the DPP-4 immunofluorescence intensity. $n = 4$ mice per group and 5 retinal sections for each retina. * $p < 0.05$; ** $p < 0.01$; *** $p < 0.001$.

3.2. Dose–Response Effect of Topical Administration of Sitagliptin and Saxagliptin on Glial Activation

Non-diabetic mice exhibited GFAP scores < 3 (Figure 2A–D), whereas vehicle-treated diabetic mice displayed a minimum score of four as a result of the aberrant expression of

GFAP (Figure 2A–D). Sitagliptin (with the exception of the lowest concentration, 1 mg/mL) prevented reactive gliosis, 5 mg/mL being the more effective concentration (Figure 2A,B). Regarding saxagliptin, the higher concentration (10 mg/mL) produced the higher reduction in glial activation (Figure 2C,D), regardless if it was administered once or twice per day.

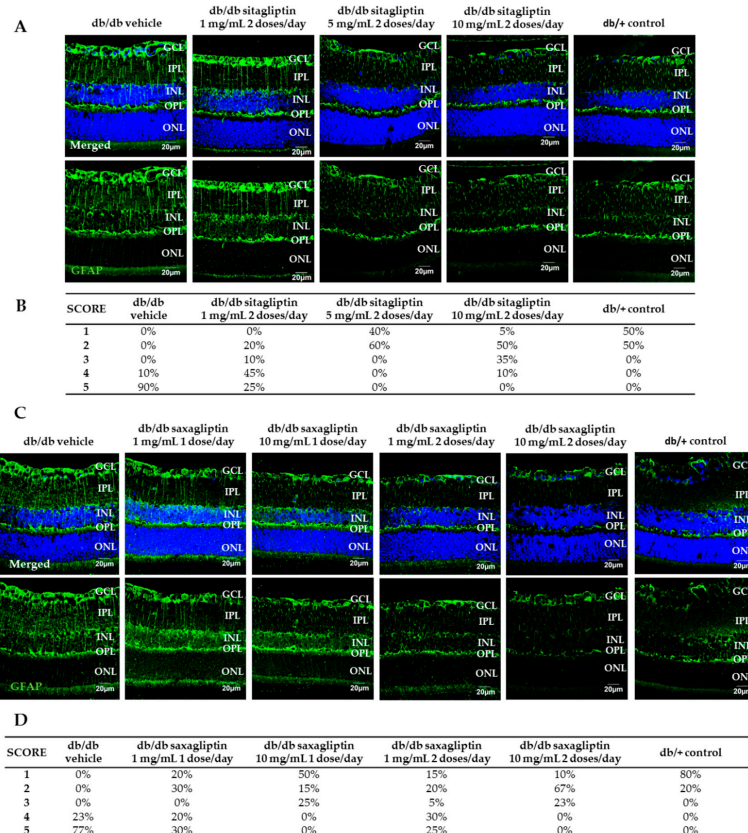


Figure 2. Reactive gliosis. (A,C) Comparison of GFAP immunofluorescence reactivity (green) among experimental groups to assess the dose-efficacy effect of sitagliptin (A), and saxagliptin (C). GFAP relative fluorescence intensity is displayed isolated and merged with Hoechst nuclei staining (blue). ONL: outer nuclear layer; OPL: outer plexiform layer; INL: inner nuclear layer; IPL: inner plexiform layer; GCL: ganglion cell layer. Scale bars, 20 μ m. (B,D) Quantification of reactive gliosis based on the extent of GFAP staining. $n = 4$ mice per group and 5 retinal sections for each retina.

3.3. Dose–Response Effect of Sitagliptin and Saxagliptin Eye Drops on Cell Death and Retinal Thinning

Diabetic mice treated with vehicle showed a clear reduction in the GCL and INL cell counts and in the retinal thickness measurements in comparison to control mice (Figure 3A–F).

Topical administered sitagliptin at concentrations of 5 mg/mL and 10 mg/mL were able to promote cell survival and to preserve retinal thinning, while the results obtained with 1 mg/mL were similar to those obtained in diabetic animals treated with vehicle (Figure 3A–C). Regarding saxagliptin, both concentrations reduced neuronal cell death in the GCL and INL, but only when it was administered twice daily did it result in a significant impact on the INL and total retinal thicknesses.

3.4. Dose–Response Effect of Topical Administration of Sitagliptin and Saxagliptin on Vascular Leakage

As a consequence of multiple extravasations points, higher Evans blue fluorescence was observed in blood vessels in diabetic mice treated with vehicle in comparison to control mice (Figure 4A,C). The higher concentrations of sitagliptin (5 and 10 mg/mL) clearly ameliorated this vascular abnormality, while 1 mg/mL did not prevent vascular leakage (Figure 4A,B). Saxagliptin was also able to prevent vascular leakage, being more effective when administered twice per day, independently of the concentration (Figure 4C,D).

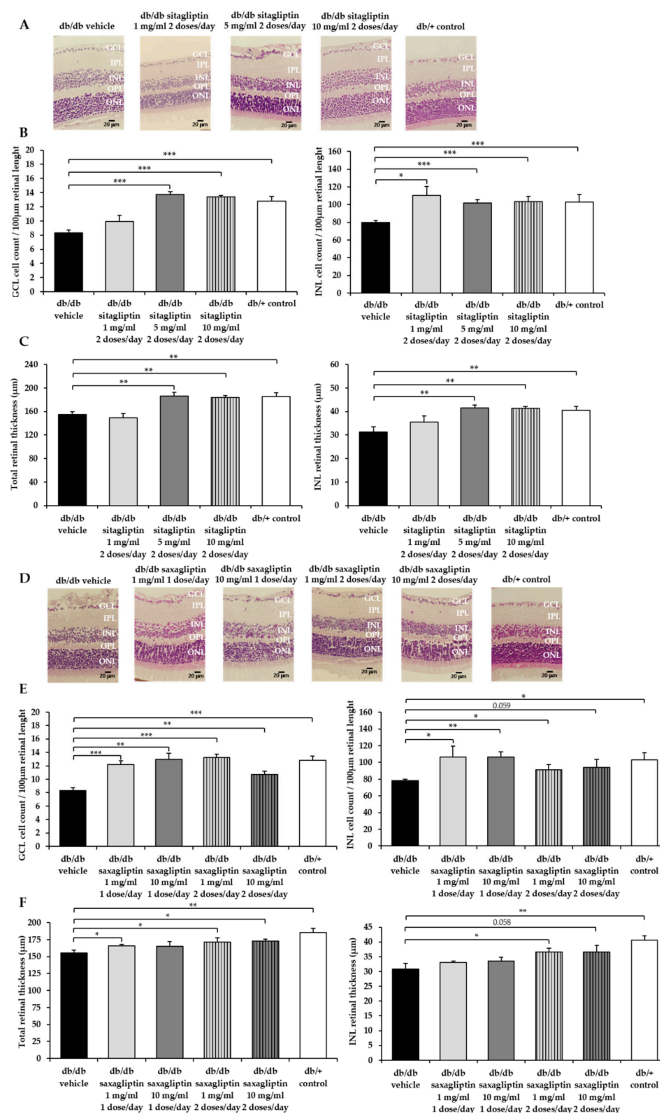


Figure 3. Cell count and retinal thinning. (A,D) Comparison of hematoxylin/eosin (HE)-stained retinas among representative samples of each experimental group. ONL: outer nuclear layer; OPL: outer plexiform layer; INL: inner nuclear layer; IPL: inner plexiform layer; GCL: ganglion cell layer. Scale bars, 20 µm. (B,E) Quantification of the number of cells in the GCL and INL layers. (C,F) Retinal thickness of the INL layer and the whole retina. $n = 4$ mice per group and five retinal sections for each mouse. * $p < 0.05$; ** $p < 0.01$; *** $p < 0.001$.

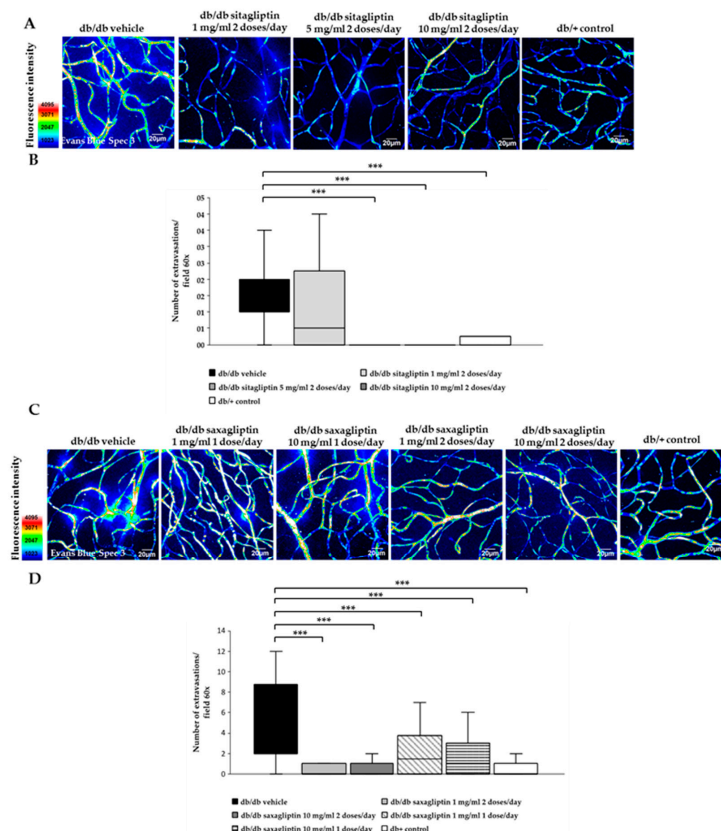


Figure 4. Microvascular abnormalities. (A,C) Confocal images of vascular permeability assessed by Evans blue dye leakage in retinal whole mounts. Treatments with sitagliptin are compared in panel (A) and saxagliptin treatments in panel (C). Spec3, fluorescent spectral signature 3. Scale bars, 20 μ m. (B,D) Quantification of extravasations per 60 \times field of the retina. Treatments with sitagliptin are compared in panel (B) with saxagliptin treatments in panel (D). In graph (B) vehicle is presented with black bars, sitagliptin 5 mg/mL 2 doses/day with grey bars, sitagliptin 10 mg/mL 2 doses/day with dark grey bars and control mice with white bars. In graph (D) vehicle is presented with black bars, saxagliptin 1 mg/mL 1 dose/day with white bars with diagonal lines, saxagliptin 10 mg/mL 1 dose/day with white bars with horizontal lines, saxagliptin 1 mg/mL 2 doses/day with grey bars, saxagliptin 10 mg/mL 2 doses/day with dark grey bars and control mice with white bars. $n = 3$ mice per group, 25–30 fields per animal were analyzed. *** $p < 0.001$.

4. Discussion

In the present study, we evaluated the lower effective dose of a topical (eye drops) administration of sitagliptin and saxagliptin for preventing the hallmarks of NVU impairment: reactive gliosis, neural apoptosis, and vascular leakage. We found that 5 mg/mL for sitagliptin, and 10 mg/mL for saxagliptin, both administered twice daily, were the

minimum effective doses to prevent all these retinal abnormalities, which are essential in the early stages of experimental DR.

Whereas sitagliptin inhibits DPP-4 enzyme by forming non-covalent bonds with its catalytic site, saxagliptin forms a covalent enzyme–inhibitor complex with slow rates of dissociation and consequently longer durations of action [15]. For this reason, we wanted to examine whether saxagliptin could be administered once per day instead of twice per day. We found that whereas glial activation was abrogated when using saxagliptin once per day, neuroretinal thinning and vascular leakage were not significantly reduced. Therefore, as occurs with sitagliptin, saxagliptin should be administered twice per day to obtain full neurovascular protection.

We observed that sitagliptin and saxagliptin downregulated the DPP-4 content in the diabetic retina. Although we do not have any reliable explanation for this finding, it would be related to the reported GLP-1 enhancement that occurs after topical ocular administration of DPP-4 inhibitors in the same experimental model [13].

Neuroprotection is considered an essential part of the treatment of the early stages of DR. Recently, the term DRD instead of DR has been proposed to emphasize the concept that DR is not only a microvascular disease [16]. In this regard, the American Diabetes Association currently defines DR as a specific neurovascular disease [17]. In this setting, topical ocular administration of neuroprotective agents has emerged as a new strategy for treating the early stages of DR due to several reasons: (1) It is a non-invasive route that permits self-application by the patient. (2) There is evidence that a lot of drugs are able to reach the retina at pharmacological concentrations, and multiple experimental studies have demonstrated the effectiveness of eye drops for treating the early stages of DR in experimental models [18]. (3) The systemic side effects are significantly lower than when using systemic administration. (4) The blood–retinal barrier, a serious limiting factor when trying to reach the retina when systemic administration is used, can be sorted out by a topical ocular route.

A topical (eye drops) administration of DPP-4 inhibitors not only exerts a powerful neuroprotective action but also prevent vascular leakage and, therefore, these inhibitors can be envisaged as excellent candidates for treating the early stages of DR. The rationale for using eye drops containing DPP-4 inhibitors is based on the presence of GLP-1 and DPP-4 in the retinas of mice and humans [7,13]. GLP-1 is expressed mainly in the ganglion cell layer and is downregulated in diabetes [7]. In addition, the retinal pigment epithelium of subjects with diabetes present higher DPP-4 concentrations than non-diabetic controls matched by age [13]. Therefore, the already decreased amount of GLP-1 in the diabetic retina can be even worsened by its exaggerated degradation induced by DPP-4. Consequently, the replacement of GLP-1 in the retina can be considered a target for treating DR. This can be achieved by administering GLP-1, by preventing its degradation or by combining both strategies. The advantage of using DPP-4 inhibitors is that they are cheaper, more stable than GLP-1, and can exert other pleiotropic actions unrelated to GLP-1, which are always welcome in a complex and multi-pathway disease such as DR. In this regard, Dietrich et al. [19] have shown that the DPP-4 linagliptin has a neuroprotective effect in *Caenorhabditis elegans*, a model of hyperglycemia-induced neurodegeneration in which GLP-1R is not produced. It could be argued that given that DPP-4 is a well-established oral treatment for type 2 diabetes, it would be unnecessary to use the topical (eye drops) administration, at least in patients undergoing DPP-4 treatment. However, current evidence does not indicate any beneficial effect of the systemic administration of DPP-4 inhibitors [20,21] on DR. This could be due to their inability to cross the blood–retinal barrier (BRB). Since DPP-4 inhibitors are unable to cross the blood–brain barrier [22,23], it is broadly assumed that they do not cross the BRB.

In conclusion, in the present study the minimum effective doses of sitagliptin and saxagliptin, administered by eye drops, for treating the early stages of DR have been established in the db/db mouse model. These data can be used for the design not only for preclinical regulatory purposes but also for planning future clinical trials.

Author Contributions: Conceptualization, P.B., H.R., R.S. and C.H.; methodology, P.B., H.R., M.V., A.D.-J., J.H., R.S. and C.H.; formal analysis, P.B., H.R., M.V., A.D.-J., J.H., R.S. and C.H.; investigation, P.B., H.R., C.H. and R.S.; resources, R.S. and C.H.; writing—original draft preparation, P.B. and H.R.; writing—review and editing, R.S. and C.H.; supervision, R.S. and C.H.; project administration, C.H.; funding acquisition, R.S. and C.H. R.S. is the guarantor of this work and, as such, had full access to all the data in the study and takes responsibility for the integrity of the data and the accuracy of the data analysis. All authors have read and agreed to the published version of the manuscript.

Funding: This research was funded by grants from the Ministerio de Economía y Competitividad (PID2019-104225RB-I00) and the Instituto de Salud Carlos III (DTS18/0163, PI19/01215 and ICI20/00129). The study funder was not involved in the design of the study.

Institutional Review Board Statement: This study was approved by the Animal Care and Use Committee of Vall d’Hebron Research Institute (VHIR). Approval Code: 75/15. Approval Date: 2 December 2015.

Informed Consent Statement: Not applicable.

Data Availability Statement: The data presented in this study are available on request from the corresponding author.

Acknowledgments: H.R. is the recipient of a grant from the Ministerio de Economía y Competitividad (BES-2017-081690). The histological processing was performed by ICTS “NANBIOSIS”, more specifically by Unit 20 of CIBER in Bioengineering, Biomaterials & Nanomedicine (CIBER-BBN) at the Vall d’Hebron Research Institute.

Conflicts of Interest: The authors declare no conflict of interest. Vall d’Hebron Research Institute holds intellectual property related to the use of ocular DPP-4 inhibitors to treat diabetic retinopathy. No other potential conflict of interest relevant to this article were reported.

References

- Leasher, J.L.; Bourne, R.R.; Flaxman, S.R.; Jonas, J.B.; Keeffe, J.; Naidoo, K.; Pesudovs, K.; Price, H.; White, R.A.; Wong, T.Y.; et al. Vision Loss Expert Group of the Global Burden of Disease Study. Global estimates on the number of people blind or visually impaired by diabetic retinopathy: A meta-analysis from 1990 to 2010. *Diabetes Care* **2016**, *39*, 1643–1649. [\[CrossRef\]](#)
- Teo, Z.L.; Tham, Y.C.; Yu, M.; Chee, M.L.; Rim, T.H.; Cheung, N.; Bikbov, M.M.; Wang, Y.X.; Tang, Y.; Lu, Y.; et al. Global Prevalence of Diabetic Retinopathy and Projection of Burden through 2045: Systematic Review and Meta-analysis. *Ophthalmology* **2021**, *128*, 1580–1591. [\[CrossRef\]](#)
- Wong, T.Y.; Cheung, C.M.; Larsen, M.; Sharma, S.; Simó, R. Diabetic retinopathy. *Nat. Rev. Dis. Primers* **2016**, *17*, 16012. [\[CrossRef\]](#)
- Simó, R.; Hernández, C. Novel approaches for treating diabetic retinopathy based on recent pathogenic evidence. *Prog. Retin. Eye Res.* **2015**, *48*, 160–180. [\[CrossRef\]](#)
- Simó, R.; Stitt, A.W.; Gardner, T.W. Neurodegeneration in diabetic retinopathy: Does it really matter? *Diabetologia* **2018**, *61*, 1902–1912. [\[CrossRef\]](#)
- Simó, R.; Simó-Servat, O.; Bogdanov, P.; Hernández, C. Neurovascular Unit: A New Target for Treating Early Stages of Diabetic Retinopathy. *Pharmaceutics* **2021**, *13*, 1320. [\[CrossRef\]](#)
- Hernández, C.; Bogdanov, P.; Corraliza, L.; García-Ramírez, M.; Solà-Adell, C.; Arranz, J.A.; Arroba, A.I.; Valverde, A.M.; Simó, R. Topical administration of GLP-1 receptor agonists prevents retinal neurodegeneration in experimental diabetes. *Diabetes* **2016**, *65*, 172–187. [\[CrossRef\]](#)
- Sampedro, J.; Bogdanov, P.; Ramos, H.; Solà-Adell, C.; Turch, M.; Valeri, M.; Simó-Servat, O.; Lagunas, C.; Simó, R.; Hernández, C. New Insights into the Mechanisms of Action of Topical Administration of GLP-1 in an Experimental Model of Diabetic Retinopathy. *J. Clin. Med.* **2019**, *8*, 339. [\[CrossRef\]](#)
- Simó, R.; Bogdanov, P.; Ramos, H.; Huerta, J.; Simó-Servat, O.; Hernández, C. Effects of the Topical Administration of Semaglutide on Retinal Neuroinflammation and Vascular Leakage in Experimental Diabetes. *Biomedicines* **2021**, *9*, 926. [\[CrossRef\]](#)
- Hernández, C.; García-Ramírez, M.; Corraliza, L.; Fernández-Cameado, J.; Farrera-Sinfreu, J.; Ponsati, B.; González-Rodríguez, A.D.; Valverde, A.M.; Simó, R. Topical Administration of Somatostatin Prevents Retinal Neurodegeneration in Experimental Diabetes. *Diabetes* **2013**, *62*, 2569–2578. [\[CrossRef\]](#)
- Hernández, C.; Arroba, A.I.; Bogdanov, P.; Ramos, H.; Simó-Servat, O.; Simó, R.; Valverde, A.M. Effect of Topical Administration of Somatostatin on Retinal Inflammation and Neurodegeneration in an Experimental Model of Diabetes. *J. Clin. Med.* **2020**, *9*, 2579. [\[CrossRef\]](#)
- Liu, Y.; Leo, L.F.; McGregor, C.; Grivtishvili, A.; Barnstable, C.J.; Tombran-Tink, J. Pigment epithelium-derived factor (PEDF) peptide eye drops reduce inflammation, cell death and vascular leakage in diabetic retinopathy in Ins2(Akita) mice. *Mol. Med.* **2012**, *18*, 1387–1401. [\[CrossRef\]](#)

13. Hernández, C.; Bogdanov, P.; Solà-Adell, C.; Sampedro, J.; Valeri, M.; Genís, X.; Simó-Servat, O.; García-Ramírez, M.; Simó, R. Topical administration of DPP-IV inhibitors prevents retinal neurodegeneration in experimental diabetes. *Diabetologia* **2017**, *60*, 2285–2298. [\[CrossRef\]](#)
14. Anderson, P.J.; Watts, H.; Hille, C.; Philpott, K.; Clark, P.; Gentleman, M.C.S.; Jen, L.-S. Glial and endothelial blood-retinal barrier responses to amyloid-beta in the neural retina of the rat. *Clin. Ophthalmol.* **2008**, *2*, 801–816. [\[CrossRef\]](#)
15. Golightly, L.K.; Drayna, C.C.; McDermott, M.T. Comparative Clinical Pharmacokinetics of Dipeptidyl Peptidase-4 Inhibitors. *Clin. Pharmacokinet* **2012**, *51*, 501–514. [\[CrossRef\]](#)
16. Sun, J.K.; Aiello, L.P.; Abràmoff, M.D.; Antonetti, D.A.; Dutta, S.; Pragnell, M.; Levine, S.R.; Gardner, T.W. Updating the Staging System for Diabetic Retinal Disease. *Ophthalmology* **2021**, *128*, 490–493. [\[CrossRef\]](#)
17. Solomon, S.D.; Chew, E.; Duh, E.J.; Sobrin, L.; Sun, J.K.; VanderBeek, B.L.; Wykoff, C.C.; Gardner, T.W. Diabetic Retinopathy: A Position Statement by the American Diabetes Association. *Diabetes Care* **2017**, *40*, 412–418. [\[CrossRef\]](#)
18. Thagaard, M.S.; Vergmann, A.S.; Grauslund, J. Topical treatment of diabetic retinopathy: A systematic review. *Acta Ophthalmol.* **2021**, *100*, 136–147. [\[CrossRef\]](#)
19. Dietrich, N.; Kolibabka, M.; Busch, S.; Bugert, P.; Kaiser, U.; Lin, J.; Fleming, T.; Morcos, M.; Klein, T.; Schlotterer, A.; et al. The DPP4 Inhibitor Linagliptin Protects from Experimental Diabetic Retinopathy. *PLoS ONE* **2016**, *11*, e0167853. [\[CrossRef\]](#)
20. Tang, H.; Li, G.; Zhao, Y.; Wang, F.; Gower, E.W.; Shi, L.; Wang, T. Comparisons of diabetic retinopathy events associated with glucose-lowering drugs in patients with type 2 diabetes mellitus: A network meta-analysis. *Diabetes Obes. Metab.* **2018**, *20*, 1262–1279. [\[CrossRef\]](#)
21. Chung, Y.R.; Ha, K.H.; Kim, H.C.; Park, S.J.; Lee, K.; Kim, D.J. Dipeptidyl Peptidase-4 Inhibitors versus Other Antidiabetic Drugs Added to Metformin Monotherapy in Diabetic Retinopathy Progression: A Real World-Based Cohort Study. *Diabetes Metab. J.* **2019**, *43*, 640–648. [\[CrossRef\]](#)
22. Fura, A.; Khanna, A.; Vyas, V.; Koplowitz, B.; Chang, S.Y.; Caporuscio, C.; Boulton, D.W.; Christopher, L.J.; Chadwick, K.D.; Hamann, L.G.; et al. Pharmacokinetics of the dipeptidyl peptidase 4 inhibitor saxagliptin in rats, dogs, and monkeys and clinical projections. *Drug Metab. Dispos.* **2009**, *37*, 1164–1171. [\[CrossRef\]](#)
23. Fuchs, H.; Binder, R.; Greischel, A. Tissue distribution of the novel DPP-4 inhibitor BI 1356 is dominated by saturable binding to its target in rats. *Biopharm. Drug. Dispos.* **2009**, *30*, 229–240. [\[CrossRef\]](#)



Article

Antioxidant Effects of DPP-4 Inhibitors in Early Stages of Experimental Diabetic Retinopathy

Hugo Ramos ^{1,2,†} , Patricia Bogdanov ^{1,2,†} , Jordi Huerta ¹ , Anna Deàs-Just ^{1,2} , Cristina Hernández ^{1,2,3,*} and Rafael Simó ^{1,2,3,*}

- ¹ Diabetes and Metabolism Research Unit, Vall d'Hebron Research Institute (VHIR), 08035 Barcelona, Spain; hugo.ramos@vhir.org (H.R.); patricia.bogdanov@vhir.org (P.B.); jordi.huerta@vhir.org (J.H.); anna.deas@vhir.org (A.D.-J.)
- ² Center for Networked Biomedical Research of Diabetes and Associated Metabolic Diseases (CIBERDEM), Carlos III Health Institute (ICSIII), 28029 Madrid, Spain
- ³ Department of Medicine, Autonomous University of Barcelona, 08193 Barcelona, Spain
- * Correspondence: cristina.hernandez@vhir.org (C.H.); rafael.simo@vhir.org (R.S.); Tel.: +34-934-894-172 (C.H.)
- † These authors contributed equally to this work.

Abstract: Hyperglycemia-induced oxidative stress plays a key role in the impairment of the retinal neurovascular unit, an early event in the pathogenesis of DR. The aim of this study was to assess the antioxidant properties of topical administration (eye drops) of sitagliptin in the diabetic retina. For this purpose, db/db mice received sitagliptin or vehicle eye drops twice per day for two weeks. Age-matched db/+ mice were used as the control group. We evaluated retinal mRNA (RT-PCR) and protein levels (Western blotting and immunohistochemistry) of different components from both the antioxidant system (NRF2, CAT, GPX, GR, CuZnSOD, and MnSOD) and the prooxidant machinery (PKC and TXNIP). We also studied superoxide levels (dihydroethidium staining) and oxidative damage to DNA/RNA (8-hydroxyguanosine immunostaining) and proteins (nitrotyrosine immunostaining). Finally, NF-κB translocation and IL-1β production were assessed through Western blotting and/or immunohistochemistry. We found that sitagliptin protected against diabetes-induced oxidative stress by reducing superoxide, TXNIP, PKC, and DNA/RNA/protein oxidative damage, and it prevented the downregulation of NRF2 and antioxidant enzymes, with the exception of catalase. Sitagliptin also exerted anti-inflammatory effects, avoiding both NF-κB translocation and IL-1β production. Sitagliptin prevents the diabetes-induced imbalance between ROS production and antioxidant defenses that occurs in diabetic retinas.

Keywords: diabetes; diabetic retinopathy; sitagliptin; dipeptidyl peptidase-4; DPP-4 inhibitors; oxidative stress; antioxidant; NRF2



Citation: Ramos, H.; Bogdanov, P.; Huerta, J.; Deàs-Just, A.; Hernández, C.; Simó, R. Antioxidant Effects of DPP-4 Inhibitors in Early Stages of Experimental Diabetic Retinopathy. *Antioxidants* **2022**, *11*, 1418. <https://doi.org/10.3390/antiox11071418>

Academic Editor: Marcella Nebbioso

Received: 30 June 2022

Accepted: 19 July 2022

Published: 21 July 2022

Publisher's Note: MDPI stays neutral with regard to jurisdictional claims in published maps and institutional affiliations.



Copyright: © 2022 by the authors. Licensee MDPI, Basel, Switzerland. This article is an open access article distributed under the terms and conditions of the Creative Commons Attribution (CC BY) license (<https://creativecommons.org/licenses/by/4.0/>).

1. Introduction

Oxidative stress is defined as the imbalance between the formation and accumulation of reactive oxygen species (ROS) and the capacity of a biological system to neutralize them [1]. ROS as superoxide anion ($O_2^{\bullet-}$), peroxyl radical (ROO^{\bullet}), and reactive hydroxyl radical ($^{\bullet}OH$) are molecular species with one or more unpaired electrons that are consequently unstable, highly reactive, and can lead to protein, lipid, and DNA damage at high concentrations [2]. These products are produced physiologically and are necessary for the proper functioning of multiple cellular processes. The maintenance of physiological and non-damaging levels of ROS is regulated by antioxidant defenses [3]. Overproduction of ROS or defects in the antioxidant machinery can result in oxidative stress, which is strongly implicated in the development of several diseases, such as diabetes and its complications [4].

Diabetic retinopathy (DR) is one of the most frequent complications of diabetes and the leading cause of preventable blindness among the work-aged population in high-income

countries [5]. DR is currently considered a neurovascular complication, as hyperglycemia and its associated metabolic pathways cause not only microvascular damage but also neurodegeneration and impairment of the retinal neurovascular unit (NVU) [6]. This unit is an interdependent and functional coupling between neurons, glial cells, and blood vessels that coordinates vascular flow with metabolic activity. Any disruption in this functional unit may result in deleterious consequences, resulting in a structural and functional impairment of microvasculature and neurons [7]. NVU impairment is an early event in the pathogenesis of DR, and one of the major triggers is oxidative stress. It should be noted that the retina has a high metabolic and high oxygen-consuming rate, and therefore has special susceptibility to oxidative events [8]. The NVU is equipped with powerful antioxidant mechanisms, including nonenzymatic and enzymatic antioxidants to neutralize ROS and a repair system for those molecules that have been already oxidized [9]. Nevertheless, chronic hyperglycemia leads to excessive accumulation of ROS and reduces the activity and efficiency of these antioxidant defenses, enhancing ROS production [4]. Little is known about how exactly hyperglycemia induces these abnormalities, but four classical pathways have been highly related: the augmented influx of glucose by polyol and hexosamine pathways, the activation of protein kinase C (PKC) and the formation of advanced glycation end products (AGEs) [4,10]. The consequences of hyperglycemia-induced oxidative stress in the retina are mitochondrial dysfunction, inflammation, cellular apoptosis, and structural and functional modifications that consequently may result in neurodegeneration and early microvascular impairment [10].

Current treatments for DR are indicated only in advanced stages of the disease, and are expensive, invasive, and associated with severe side effects. Therefore, the search for new treatments targeting the earliest and asymptomatic stages of DR at the onset of NVU impairment is an unmet medical need that has to be urgently addressed [11]. In this context, a new therapeutic strategy is the topical administration (eye drops) of dipeptidyl peptidase-4 (DPP-4) inhibitors (DPP-4i), which have demonstrated promising results in experimental models of DR [12,13]. Through the nondegradation of glucagon-like peptide-1 (GLP-1), the main target of the DPP-4 enzyme, and through other independent and not clearly elucidated mechanisms, DPP-4i significantly prevents the appearance of the main hallmarks of DR, glial activation, and neuronal cell death, as well as preserving the functionality of the retina [12–14]. In the present study, we explored the potential antioxidant effects of topical administration of DPP-4i in an experimental model of DR.

2. Materials and Methods

2.1. Animals

Twenty diabetic male db/db (BKS.Cg-Dock7m +/+ Leprdb/J) mice and 10 nondiabetic mice (db/+; (BKS.Cg-Dock7m + Leprdb/+)) were acquired from Charles River Laboratories (Calco, Italy) at 7 weeks of age for the experiments. The mutated leptin receptor carried by db/db mice gave rise to an obesity-induced type 2 diabetes phenotype. Mice were bred and maintained in the animal facilities of the Vall d'Hebrón Research Institute (VHIR). With the aim of minimizing variability, mice were randomly distributed (block randomization) into groups of two mice per cage in Tecniplast GM-500 cages (36 cm × 19 cm × 13.5 cm) under standard laboratory conditions at 22 ± 2 °C, with relative humidity of 50–60% and a 12 h light/dark cycle. The cages were equipped with nesting material, absorbent bedding (BioFresh Performance Bedding 1/800 Pelleted Cellulose, Absorption Corp, Ferndale, WA, USA), ad libitum food (ENVIGO Global Diet Complete Feed for Rodents, Mucedola, Milan, Italy), and filtered water. Glycemia was measured weekly through tail-vein blood sampling and a blood glucose meter (71371-80, FreeStyle Optium Neo; Abbott, IL, USA).

All animal experiments were directed in agreement with the European Community (86/609/CEE) and the guidelines of the Association for Research in Vision and Ophthalmology (ARVO) for the utilization of laboratory animals. The Animal Care and Use Committee of VHIR (CEE 14/21) authorized the present study.

2.2. Topical Ocular Treatment

Db/db mice aged 10 weeks received a topical ocular administration of 10 mg/mL sitagliptin phosphate monohydrate (Y0001812, Merck KGaA, Darmstadt, Germany) or vehicle eye drops [phosphate buffered saline (PBS)] for 2 weeks twice per day. Eye drops were randomly administered with the aid of a micropipette (5 µL), onto the superior corneal surfaces of both eyes of diabetic mice. On day 15, 1 h before euthanasia, animals received an additional dose of each treatment. Db/+ mice matched by age were used as the control group.

2.3. Retinal Tissue Processing

On day 15, mice were intraperitoneally injected with 200 µL of anesthesia, composed of a mix of ketamine (1 mL) (GmbH, Hameln, Germany) and xylazine (0.3 mL) (Laboratorios Calier S.A., Barcelona, Spain). Once anesthetized, animals that were intended to be used for immunofluorescence experiments were transcardially perfused with 4% paraformaldehyde (sc-281692, Santa Cruz Biotechnology, Dallas, TX, USA), while others were euthanized through cervical dislocation. Ocular globes were rapidly enucleated and differently processed depending on their purpose. All eyes, with the exception of those used for the immunofluorescence experiment, were dissected and the retinas obtained. Six retinas from each experimental group were submerged in 140 µL of TRIzol reagent (15596018, Invitrogen, Carlsbad, CA, USA) and assigned in different tubes until RNA extraction. Another six retinas from each group were immediately distributed in empty and distinct tubes until protein extraction. All of them were stored at -80°C . Finally, the retinas from four animals of each group were not obtained after enucleation, and the entire ocular globes were fixed again in 4% paraformaldehyde for 5 h before paraffin embedding.

2.4. RNA Isolation and Quantitative Reverse Transcription Polymerase Chain Reaction (RT-PCR) Assay

Retinas (stored at -80°C in 140 µL of TRIzol) were treated with DNase (18068015, ThermoFisher Scientific, Waltham, MA, USA) to avoid genomic contamination and were purified on an RNeasy MinElute column (74106, Qiagen, Hilden, Germany). After supernatant removal, RNA sediment was obtained and resuspended in 30 µL of RNase free water (AM9937, ThermoFisher Scientific, Waltham, MA, USA). A Nanodrop spectrophotometer and an Agilent 2100 Bioanalyzer were used for both RNA quantification and integrity, respectively. Reverse transcription of cDNA was assessed using Oligo(dT)18 Primers (SO131, ThermoFisher Scientific, Waltham, MA, USA) and a High-Capacity cDNA Reverse Transcription Kit (4368814, ThermoFisher Scientific, Waltham, MA, USA) and with the help of a T100 Thermal Cycler (Bio-Rad, Hercules, CA, USA). RT-PCR was performed using SYBR Green PCR Master Mix (04707516001 Roche Diagnostics, Mannheim, Germany), specific primers (Table 1), a LightCycler480 System (05015243001, Roche Diagnostics, Mannheim, Germany), and 384-well optical plates (04729749001, Roche Diagnostics, Mannheim, Germany). Relative quantifications were obtained using the LightCycler480 SW 1.5.1 software and displayed as fold change versus control mice. *B2m* and *Actin* were used as housekeeping genes.

Table 1. Primers used for RT-PCR experiments.

Primers	Gene ID	Nucleotide Sequence	
<i>Actb</i>	11461	Forward (5'-3')	5'-CTAAGGCCAACCGTGAAAG-3'
		Reverse (5'-3')	5'-CAGTATGTTCCGGCTTCCCATTC-3'
<i>B2m</i>	12010	Forward (5'-3')	5'-GTATGCTATCCAGAAAACCC-3'
		Reverse (5'-3')	5'-CTGAAGGACATATCTGACATC-3'
<i>Cat</i>	12359	Forward (5'-3')	5'-AGCGACCAGATGAAGCAGTG-3'
		Reverse (5'-3')	5'-TCCGCTCTCTGTCAAAGTGTG-3'
<i>Gpx1</i>	14775	Forward (5'-3')	5'-CTCACC CGCTCTTACCTTCT-3'
		Reverse (5'-3')	5'-ACACCGGAGACCAATGATGTACT-3'
<i>Gsr</i>	14782	Forward (5'-3')	5'-GACACCTCTTCCTTCGACTACC-3'
		Reverse (5'-3')	5'-CCCAGCTTGTGACTCTCCAC-3'
<i>Il1b</i>	16176	Forward (5'-3')	5'-GCAACTGTCTCTGAACCTCAACT-3'
		Reverse (5'-3')	5'-ATCTTTTGGGGTCCGTCAACT-3'
<i>Nrf2</i>	18024	Forward (5'-3')	5'-TCTTGGAGTAAGTCGAGAAGTGT-3'
		Reverse (5'-3')	5'-GTTGAAACTGAGCGAAAAGGC-3'
<i>Sod1</i>	20655	Forward (5'-3')	5'-AACCAGTTGTGTTGTCAAGAC-3'
		Reverse (5'-3')	5'-CCACCATGTTTCTTAGAGTGAGG-3'
<i>Sod2</i>	20656	Forward (5'-3')	5'-CAGACCTGCCTTACGACTATG-3'
		Reverse (5'-3')	5'-CTCGGTGGCGTTGAGATTGT-3'

2.5. Western Blotting

Ten to fifteen seconds of sonication in 80 μ L of lysis buffer [phenylmethanesulfonylfluoride (PMSF), 1 mM; Na₃VO₄ 2 mM; NaF, 100 mM; 1 \times protease inhibitor cocktail (P8340, Sigma-Aldrich, St. Louis, MO, USA); and RIPA buffer (R0278, Sigma-Aldrich, St. Louis, MO, USA)] were used for retinal protein extraction. Extracted protein (25 μ g) was loaded in 4–20% (v/v) mini-PROTEAN TGX precast protein gels (4561096, Bio-rad, Hercules, CA, USA). Electrophoresis was carried out for 90 min at 100 V. Proteins were then transferred from gradient gels to a polyvinylidene difluoride (PVDF) membrane (1620177, Bio-Rad Laboratories, Hercules, CA, USA) for 90 min at 400 mA. Membranes were then blocked in 5% bovine serum albumin (A3059-100G, Sigma-Aldrich, St. Louis, MO, USA) or 5% powdered milk (Central Lechera Asturiana, Spain). Both blocking solutions were prepared in 0.1% TBS-Tween. Primary antibodies (Table 2) were applied overnight at 4 $^{\circ}$ C. Secondary antibodies [goat anti-rabbit and goat anti-mouse (Dako Agilent, Santa Clara, CA, USA)] were incubated (1:10,000). Immunoreactive bands were acquired using a WesternBright ECL HRP substrate kit (K-12045-D50, Advansta, CA, USA) and quantified with Image J software (version 1.53. U. S. National Institutes of Health, Bethesda, MD, USA). Vinculin protein was assigned as loading control to normalize protein expression.

Table 2. Primary antibodies used for Western blot experiments.

Primary Antibodies	Description
Catalase	Rabbit polyclonal; 1:1000; GTX110704; GeneTex, Alton Pkwy Irvine, CA, USA
Copper-zinc superoxide dismutase	Rabbit polyclonal; 1:1000; GTX100554; GeneTex, Alton Pkwy Irvine, CA, USA
Glutathione peroxidase 1	Rabbit polyclonal; 1:1000; 55053-1-AP; Proteintech, Rosemont, IL, USA
Glutathione reductase	Mouse monoclonal; 1:1000; sc-133245; Santa Cruz, Dallas, TX, USA
Manganese superoxide dismutase	Rabbit polyclonal; 1:1000; ab13533; Abcam, Cambridge, UK
NRF2	Rabbit polyclonal; 1:1000; 16396-1-AP; Proteintech, Rosemont, IL, USA
Vinculin	Mouse monoclonal; 1:7000; sc-73614; Santa Cruz, Dallas, TX, USA

2.6. Immunofluorescence Analysis

Eyes were embedded in paraffin, then sectioned (3 μ m) and mounted on 25.5 mm \times 75.5 mm \times 1.0 mm poly-L-lysine positively charged slides (S21.2113.A, Leica Biosystems, Wetzlar, Germany). For sample deparaffinization and rehydration, slides were consecutively submerged in 100% xylene (3 \times 5 min), 100% ethanol (1 \times 5 min), 96% ethanol (1 \times 5 min), 70% ethanol (1 \times 5 min), 50% ethanol (1 \times 5 min), and distilled water (1 \times 5 min). Samples were fixed again in ice-cold acid methanol (−20 °C) for 1 min and washed 3 times with PBS 0.01 M pH 7.4. For antigen retrieval, slides were warmed with a pressure cooker at 150 °C for 4 min in 250 mL of 1:10 diluted antigen retrieval solution with sodium citrate 10 mM, pH 6 (ab973, Abcam, Cambridge, UK). After 3 washes with PBS, sectioned eyes were incubated in blocking solution (X0909, Dako Agilent, Santa Clara, CA, USA) for 1 h at room temperature to avoid aspecific binding. Consecutively, specific primary antibodies (Table 3) were applied nightly at 4 °C. Next morning, after 3 washes in PBS, slides were incubated for 1 h in the dark with secondary antibodies (Table 3). Eye sections were washed one more time with PBS, counterstained with Hoechst 33342 (bisbenzimidide) (14533, ThermoFisher Scientific, Waltham, MA, USA), and finally mounted with a coverslip (15747592, ThermoFisher Scientific, Waltham, MA, USA) and prolonged mounting medium fluorescence (P36930, Prolong, Invitrogen™, Thermo Fisher Scientific, Eugene, OR, USA). A laser confocal microscope (Fluoview FV1000 Laser Scanning Confocal Microscope Olympus, Hamburg, Germany) was used for image acquisition (1024 \times 1024 pixels). For detecting superoxide levels, dihydroethidium was applied as a primary antibody, and after three washes in PBS was counterstained with Hoescht and mounted.

Table 3. Primary and secondary antibodies used for immunofluorescence experiments.

Primary Antibodies	Description
8-Hydroxyguanosine	Mouse monoclonal; 1:100; ab62623; Abcam, Cambridge, UK
Collagen IV	Rabbit monoclonal; 1:200; ab236640; Abcam, Cambridge, UK
Copper-zinc superoxide dismutase	Rabbit polyclonal; 1:100; GTX100554; GeneTex, Alton Pkwy Irvine, CA, USA
Dihydroethidium	D23107; ThermoFisher Scientific, Waltham, MA, USA
IL-1 β	Rabbit polyclonal; 1:200; ab9722; Abcam, Cambridge, UK
Ki67	Rabbit polyclonal; 1:500; ab15580; Abcam, Cambridge, UK
Manganese superoxide dismutase	Rabbit polyclonal; 1:100; ab13533; Abcam, Cambridge, UK
NeuN	Mouse monoclonal; 1:200; ab104224; Abcam, Cambridge, UK
NF- κ B	Mouse monoclonal; 1:100; sc-8008; Santa Cruz, Dallas, TX, USA
Nitrotyrosine	Mouse monoclonal; 1:100; ab7048; Abcam, Cambridge, UK
NRF2	Rabbit polyclonal; 1:1000; 16396-1-AP; Proteintech, Rosemont, IL, USA
Protein kinase C- β	Rabbit polyclonal; 1:100; ab189782; Abcam, Cambridge, UK
Protein kinase C- δ	Rabbit monoclonal; 1:100; ab182126; Abcam, Cambridge, UK
TXNIP	Rabbit monoclonal; 1:200; ab188865; Abcam, Cambridge, UK
Secondary antibodies	Description
Alexa Fluor 488 Goat anti-mouse	Goat polyclonal; 1:600; ab150113; Abcam, Cambridge, UK
Alexa Fluor 488 Goat anti-rabbit	Goat polyclonal; 1:600; ab150081; Abcam, Cambridge, UK
Alexa Fluor 594 Goat anti-mouse	Goat polyclonal; 1:600; A-11032; ThermoFisher Scientific, Waltham, MA, USA
Alexa Fluor 594 Goat anti-rabbit	Goat polyclonal; 1:600; A-11012; ThermoFisher Scientific, Waltham, MA, USA

2.7. Statistical Analysis

Graph bars are displayed as the mean value followed by the standard error of the mean (SEM). Means of the different experimental groups were compared using both Students *t*-test and one-way ANOVA, which was accompanied by Bonferroni multiple-comparison post hoc test. Differences were considered statistically significant when $p < 0.05$.

3. Results

3.1. Body Weight and Systemic Blood Glucose Levels of db/db Mice Not Modified after Topical Ocular Administration of Sitagliptin

Db/db mice presented significantly higher blood glucose levels than nondiabetic mice (Figure 1A), confirming the diabetic status of the animals. No differences in body weight or blood glucose levels were found between diabetic mice treated with sitagliptin or vehicle eye drops (Figure 1A,B). This finding indicates that all the observed effects can only be attributed to the direct effect of the drug on the retina and not to a systemic metabolic improvement.

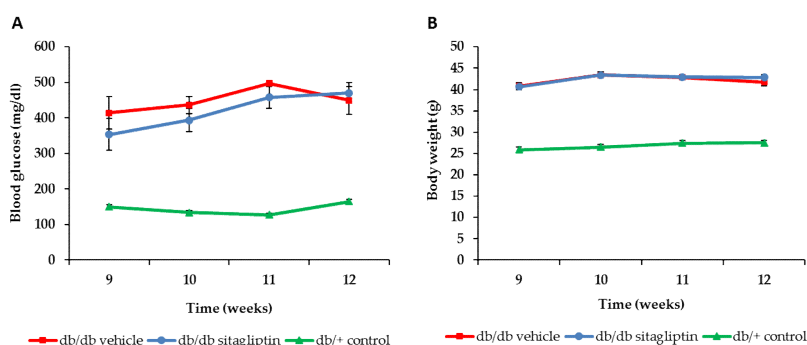


Figure 1. Evaluation of body weight and systemic blood glucose levels. (A) Blood glucose measurements during the experimental course of db/db mice treated with sitagliptin (blue circles) or vehicle (red squares) and db/+ mice (green triangles); $n = 10$. (B) Body weight course of db/db mice treated with sitagliptin (blue circles) or vehicle (red squares) and db/+ mice (green triangles); $n = 10$.

3.2. Sitagliptin Eye Drops Prevented the Antioxidant Deficiencies of the Diabetic Retina

Nuclear factor (erythroid-derived 2)-like 2 (NRF2) is a redox-sensitive transcription factor that plays a major defensive role in the NVU by modulating the expression of antioxidant enzymes, regulating microglial dynamics, and protecting neurons and astrocytes from toxins [15]. It binds to the antioxidant response elements (ARE), which are located in the promoter region of genes that encode many antioxidant enzymes, such as copper–zinc superoxide dismutase (CuZnSOD), manganese superoxide dismutase (MnSOD), catalase (CAT), glutathione peroxidase (GPX), or glutathione reductase (GR) [16]. In db/db mice, mRNA and protein levels of NRF2 were downregulated and topical sitagliptin treatment prevented decreased protein levels in all retinal layers (Figure 2A–C). Regarding all the aforementioned antioxidant enzymes, their retinal mRNA and protein levels were also downregulated in db/db mice, while sitagliptin prevented these abnormalities with the exception of catalase, on which it exerted a neutral effect (Figure 3A–E). Topical administration of sitagliptin prevented this downregulation in all the retinal layers (i.e., MnSOD) or just in GCL (i.e., CuZnSOD) (Figure 3D,E).

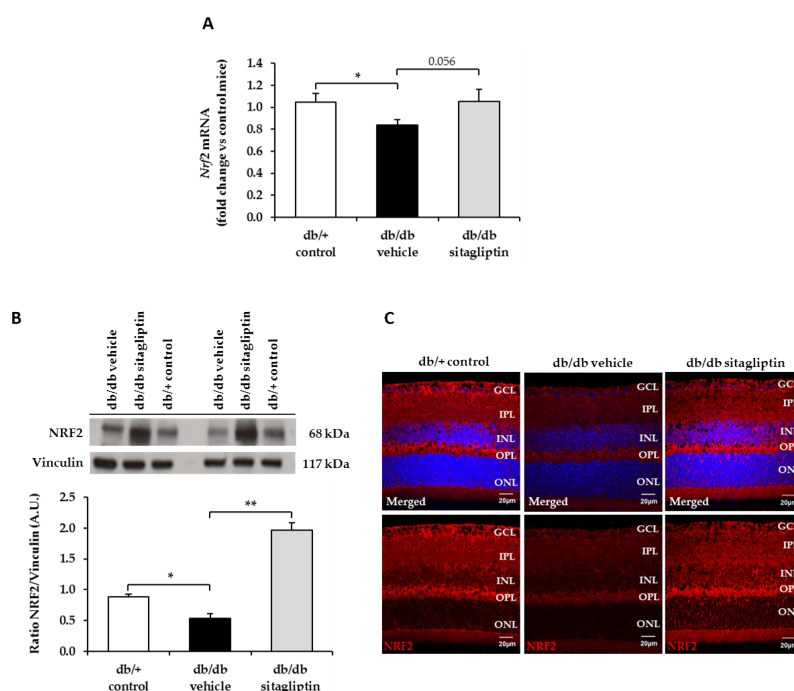


Figure 2. Study of the mRNA and protein levels of NRF2. (A) RT-PCR analysis of the gene that codifies for NRF2 (Nrf2) in db/db mice topically treated with vehicle (black bars), sitagliptin (gray bars), and in db/+ mice (white bars). Results are presented as fold change vs. control mice; $n = 4$. (B) Western blot bands and densitometric analysis of NRF2 protein levels in retinas of vehicle-treated db/db mice (black bars), sitagliptin-treated db/db mice (gray bars) and nondiabetic mice (white bars); $n = 3$. (C) Representative images of NRF2 (red) retinal immunofluorescence in diabetic mice treated with vehicle or sitagliptin eye drops and in nondiabetic mice. Hoechst staining (blue) was used for nuclei labeling. Scale bars, 20 μm ; $n = 4$. GCL (ganglion cell layer), IPL (inner plexiform layer), INL (inner nuclear layer), OPL (outer plexiform layer), ONL (outer nuclear layer). * $p < 0.05$; ** $p < 0.01$.

NRF2 regulates the transcription of other genes whose physiological expression is altered by hyperglycemia and oxidative stress, such as the gene encoding thioredoxin interacting protein (TXNIP) [17,18]. TXNIP is a prooxidant and proapoptotic protein up-regulated in DR, which acts by inhibiting the ROS scavenging and thiol-reducing capability of the antioxidant enzyme thioredoxin (TRX). TXNIP expression has been strongly linked to hyperglycemia in retinal cell cultures, and its sustained expression over time leads to oxidative stress, inflammation, and premature cell death [18]. In db/db mice treated with vehicle, the number of TXNIP-positive cells was significantly higher than in control mice, while the values obtained in sitagliptin-treated db/db mice were similar to controls (Figure 4A,B).

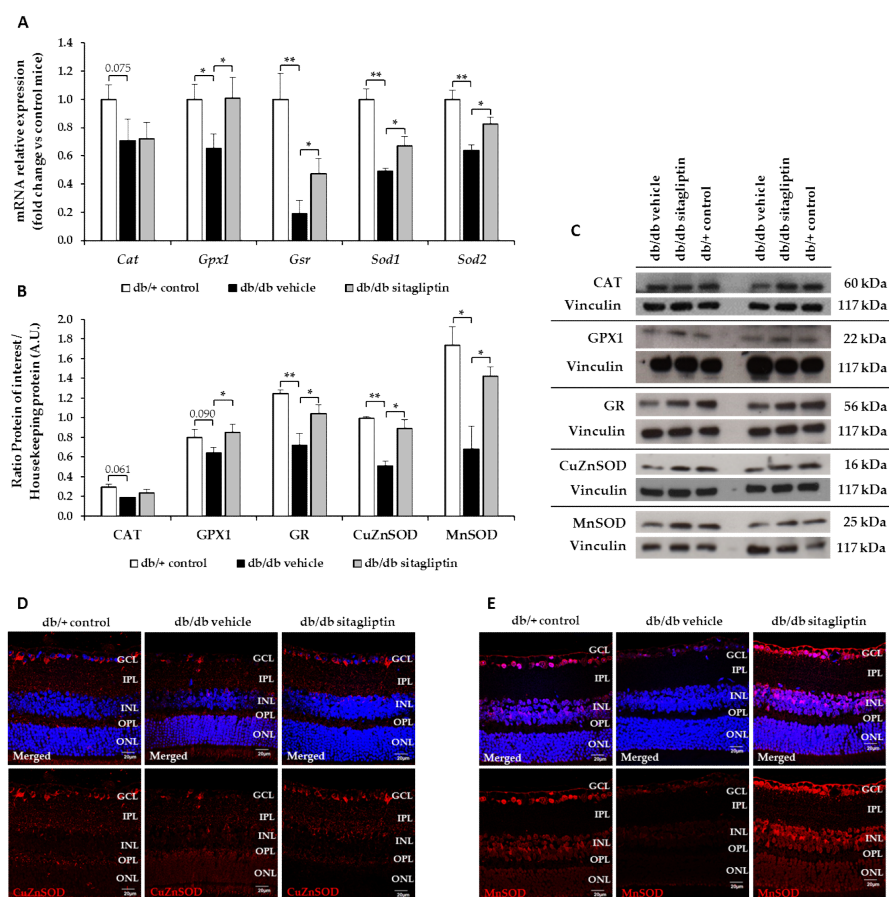


Figure 3. Study of the mRNA and protein levels of the most relevant antioxidant enzymes. (A) RT-PCR analysis of the genes that codify for CAT (Cat), GPX isoform 1 (Gpx1), GR (Gsr), CuZnSOD (Sod1), and MnSOD (Sod2) in db/db mice topically treated with vehicle (black bars) or sitagliptin (gray bars) and in db/+ mice (white bars). Results are presented as fold change vs. control mice; $n = 4$. (B,C) Densitometric analysis and Western blot bands of CAT, GPX isoform 1 (GPX1), GR, CuZnSOD and MnSOD protein levels in retinas of vehicle-treated db/db mice (black bars), sitagliptin-treated db/db mice (gray bars), and nondiabetic mice (white bars); $n = 3$. (D,E) Representative images of the retinal immunofluorescence of CuZnSOD (red) (D) and MnSOD (red) (E) in diabetic mice treated with vehicle or sitagliptin eye drops and in nondiabetic mice. Hoechst staining (blue) was used for nuclei labeling. Scale bars, 20 μ m; $n = 4$. GCL (ganglion cell layer), IPL (inner plexiform layer), INL (inner nuclear layer), OPL (outer plexiform layer), ONL (outer nuclear layer). * $p < 0.05$; ** $p < 0.01$.

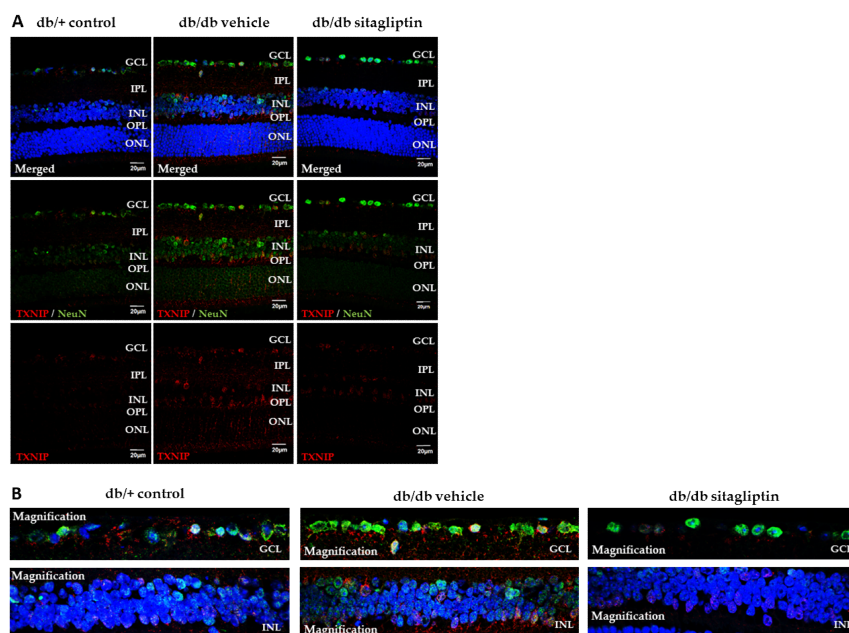


Figure 4. TXNIP immunofluorescence assay. (A,B) Representative images (A), with a magnification of the GCL and INL layers (B) of TXNIP (red) retinal immunofluorescence in db/db mice treated with vehicle or sitagliptin eye drops and in db/+ mice. NeuN (green) and Hoechst staining (blue) were used as neuronal and nuclei markers, respectively. Scale bars, 20 μ m; $n = 4$. GCL (ganglion cell layer), IPL (inner plexiform layer), INL (inner nuclear layer), OPL (outer plexiform layer), ONL (outer nuclear layer).

3.3. Topical Administration of Sitagliptin Reduced the Aberrant Levels of Superoxide and Their Consequent Oxidative Damage to Biological Macromolecules in Diabetic Retinas

Excessive production of superoxide radicals is one of the main contributors to hyperglycemia-related oxidative stress in the diabetic retina [19]. Dihydroethidium (5-ethyl-5,6-dihydro-6-phenyl-3,8-diaminophenanthridine, hydroethidine, DHE) is a hydrophobic and uncharged molecule that has the capacity of crossing extra and intracellular membranes, where it can be oxidized by superoxide, giving rise to two different fluorescent products: ethidium, which is formed by specific redox reactions, and 2-hydroxyethidium, which is a specific adduct of superoxide. Therefore, DHE staining can be used to assess superoxide detection [20]. We found that relative DHE immunofluorescence expression was higher in the nuclear layers of diabetic mice than in the same layers of nondiabetic mice, and that sitagliptin reduced the hyperglycemia-related overproduction of $O_2^{\bullet-}$ (Figure 5A).

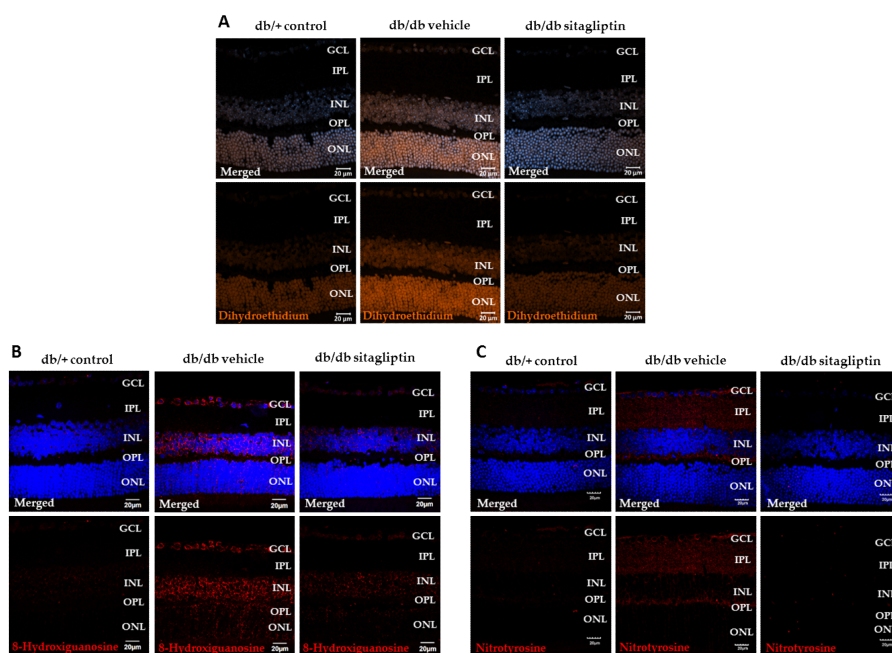


Figure 5. Evaluation of superoxide levels and consequent damage to biological macromolecules. (A–C) Representative images of retinal immunofluorescence of dihydroethidium (orange) (A), 8-hydroxyguanosine (red) (B), and nitrotyrosine (red); (C) immunostaining in db/db mice topically treated with vehicle or sitagliptin and in control mice. Hoechst staining (blue) was used for nuclei labeling. Scale bars, 20 μm; $n = 4$. GCL (ganglion cell layer), IPL (inner plexiform layer), INL (inner nuclear layer), OPL (outer plexiform layer), ONL (outer nuclear layer).

High levels of ROS and reactive nitrogen species (RNS) facilitate their binding to biological such macromolecules as DNA, proteins, and lipids. These interactions promote damage to cell components, thus resulting in biological dysfunctions [21]. One of the most used markers is 8-hydroxyguanosine (8-OHG), the predominant product of DNA/RNA oxidative damage [22]. Nitrotyrosine is another excellent biomarker of oxidative stress, and is formed as a result of protein nitration of free tyrosine residues by reactive peroxynitrite molecules [23]. In our study, both indicators of oxidative damage were significantly higher in the nuclear layers of diabetic retinas treated with vehicle than in the same layers of nondiabetic retinas. We observed that sitagliptin significantly prevented these DR-related abnormalities (Figure 5B,C).

3.4. High PKC Presence in Diabetic Retinas was Reduced by Topical Treatment with Sitagliptin

Hyperactivation of protein kinase C (PKC) isoforms is produced by oxidative stress, and, in turn, contributes to oxidative stress. The PKC family is composed of 12 isoforms, in which PKC- α , - β , - δ , and - ϵ activation play a key role in the development of DR [10]. In the present study, the relative immunofluorescence expression of PKC- β and the number of PKC- δ positive cells were significantly higher in db/db mice treated with vehicle than in control mice. Treatment with sitagliptin eye drops avoided this abnormal increase of both PKC isoforms (Figure 6A,B).

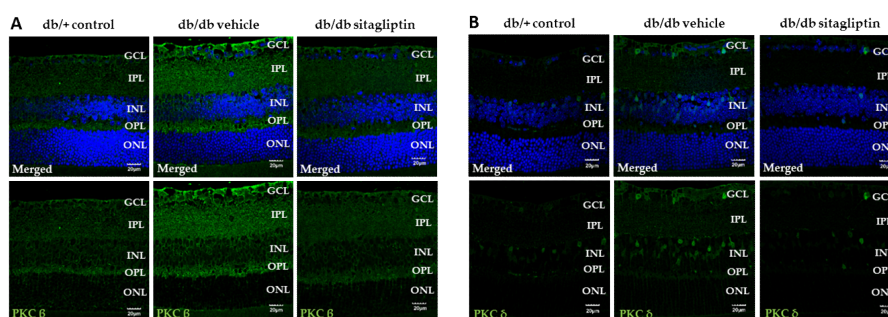


Figure 6. Study of PKC activation. (A,B) Representative images of the retinal immunofluorescence of PKC- β (green) (A) and PKC- δ (green) (B) in db/db mice topically treated with vehicle or sitagliptin and in db/+ mice. Hoechst staining (blue) was used for nuclei labeling. Scale bars, 20 μ m; $n = 4$. GCL (ganglion cell layer), IPL (inner plexiform layer), INL (inner nuclear layer), OPL (outer plexiform layer), ONL (outer nuclear layer).

3.5. Sitagliptin Exhibited Anti-Inflammatory Properties When Administered Topically in Diabetic Retinas

PKC pathway activation not only increases ROS production but also promotes nuclear factor kappa-light-chain-enhancer of activated B cells (NF- κ B). Inactive NF- κ B is located in the cytosol of almost all cell types, forming a complex with the inhibitory protein nuclear factor of kappa light polypeptide gene enhancer in B-cells inhibitor alpha (I κ B α). Several mechanisms, including hyperglycemia or oxidized proteins, can activate the enzyme I κ B kinase (IKK) which phosphorylates I κ B α . As result of phosphorylation, I κ B α is ubiquitinated, dissociated from the NF- κ B complex, and finally degraded by the proteasome. This signaling pathway provokes the activation of NF- κ B and its consequent translocation to the cell nucleus, where it regulates inflammatory responses (i.e., cytokine production) [24]. Regarding our study, topical ocular administration of sitagliptin in db/db mice reduced NF- κ B translocation in comparison to vehicle-treated db/db mice, showing similar results to the nondiabetic condition (Figure 7). Furthermore, we observed an increase in mRNA and protein levels of interleukin 1 beta (IL-1 β) in vehicle-treated diabetic mice, which was attenuated by sitagliptin (Figure 8A,B).

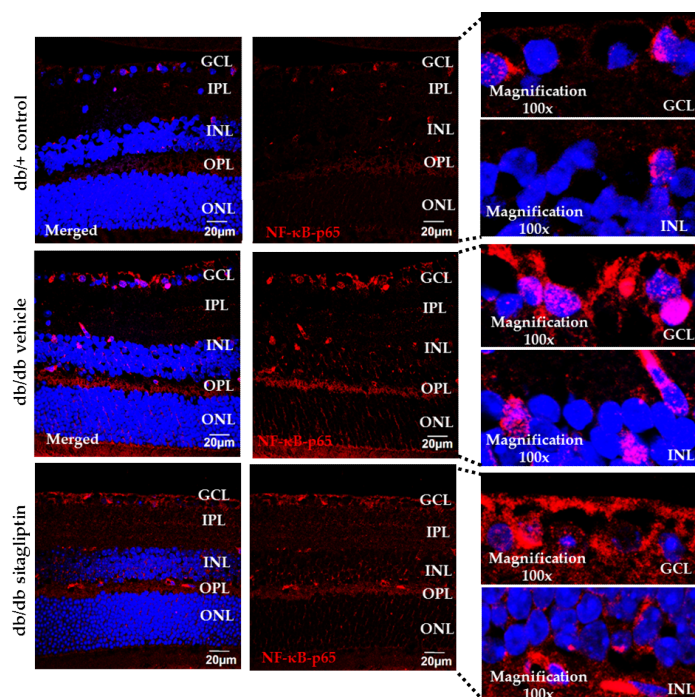


Figure 7. Comparison of NF- κ B translocated cells (red) through immunofluorescence. NF- κ B relative fluorescence intensity is displayed alone and merged with Hoechst nuclei staining (blue). A 100 \times magnification of merged images for each group is attached. Scale bars, 20 μ m; $n = 4$. GCL (ganglion cell layer), IPL (inner plexiform layer), INL (inner nuclear layer), OPL (outer plexiform layer), ONL (outer nuclear layer).

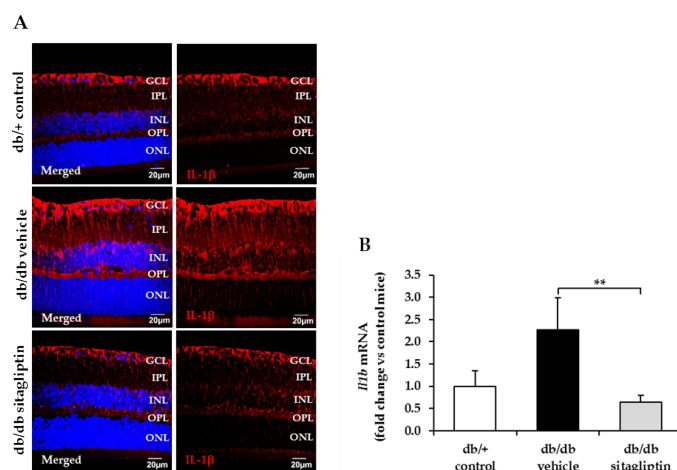


Figure 8. IL-1 β expression. **(A)** Representative images of IL-1 β protein levels (red) through immunofluorescence in db/db mice treated with vehicle or sitagliptin and in db/+ mice. Relative fluorescence intensity is displayed alone and merged with Hoechst nuclei staining (blue). Scale bars, 20 μ m; $n = 4$. **(B)** Comparison of IL-1 β mRNA levels. Results are presented as fold change vs. control mice. Black bar for vehicle treatment, gray bar for sitagliptin treatment, and white bar for nondiabetic mice; $n = 4$. GCL (ganglion cell layer), IPL (inner plexiform layer), INL (inner nuclear layer), OPL (outer plexiform layer), ONL (outer nuclear layer). ** $p < 0.01$.

4. Discussion

In the present study, we demonstrated the antioxidant and the anti-inflammatory properties of sitagliptin, a DPP-4i, in an experimental model of DR. These findings support and reinforce previous evidence showing the beneficial effects of topical administration of sitagliptin in early stages of DR [12,13].

Hyperglycemia-induced oxidative stress is one of the greatest threats to the retinal NVU. The oxygen consumption rate of the retina is extremely high, and it has an abundance of polyunsaturated acids, which are very susceptible to lipid peroxidation [9]. A clear relationship between the diabetic milieu and both ROS overproduction and deficiencies in the antioxidant machinery has been reported in multiple studies [25]. The physiological sources of ROS, mainly the mitochondrial electron transport chain (ETC) and the nicotinamide adenine dinucleotide (NAD⁺/NADH) phosphate (NADPH) oxidase family of enzymes (NOX), are disrupted in DR, leading to an excessive generation of ROS [26]. By contrast, the activity of antioxidant enzymes, which are directly or indirectly responsible for ROS and RNS scavenging, and the transcriptional functionality of the antioxidant factor NRF2 are both diminished in DR [27]. NRF2 is a major regulator of redox homeostasis, with an important role as a negative regulator of inflammation, attenuating oxidative stress by scavenging reactive oxygen species (ROS) and preventing genomic instability due to DNA damage. In the present study, we provide evidence that in db/db mice there exists a significant increase in superoxide levels and oxidative damage to DNA/RNA and proteins and a notable downregulation of NRF2 and the antioxidant enzymes CAT, GPX, GR, CuZnSOD, and MnSOD in comparison with db/+ nondiabetic control mice.

The capacity of sitagliptin to activate the NRF2/ARE pathway and ameliorate the pathological outcome of diseases where oxidative stress plays a key role has already been evidenced. For example, in a β -amyloid-induced rat model of Alzheimer's disease, sitagliptin improved cognitive status by its antioxidant effects mediated by the activation of

NRF2 [28]. Sitagliptin was also able to increase the activities of some antioxidant enzymes, such as SOD, independently of their glucose-lowering abilities [29]. In the present study, we found that topical (eye drops) administration of sitagliptin modulated positively mRNA and protein production by the murine retina of both antioxidant elements: the NRF2/ARE pathway and the enzymatic defenses GPX, GR, CuZnSOD, and MnSOD. In addition, we found that sitagliptin prevented the upregulation of TXNIP (a prooxidant and proapoptotic protein) induced by diabetes, which plays a relevant role in the pathogenesis of DR [18]. Remarkably, we further detected that the topical administration of sitagliptin also reduced the RNA/DNA oxidative damage induced by RNS and ROS in the retinas of db/db mice.

It should be emphasized that the absence of differences in blood glucose levels between diabetic mice treated with vehicle or with sitagliptin eye drops support the idea that sitagliptin has antioxidant properties that cannot be attributed to its glucose-lowering capacity. Although there is some information regarding the antioxidant effect of sitagliptin when administered systemically [30,31], it is impossible to know whether this effect is due to the lowering effect of blood glucose levels or a direct effect of sitagliptin. In addition, the second possibility is unlikely, because it has been reported that sitagliptin is unable to cross the blood–retina barrier. Taken together, to the best of our knowledge, this is the first evidence of direct antioxidant effects of sitagliptin in the diabetic retina after its topical ocular administration.

Little is known about how DPP-4i exert their antioxidant and intrinsic functions. Since the increase in GLP-1 availability is one of the main consequences of DPP-4i administration, it could be postulated that GLP-1, rather than DPP-4i, exerts the antioxidant effect. In fact, in previous studies we demonstrated that topically administered GLP-1 also has the capability of reducing oxidative damage in the same experimental model of DR [32]. However, the antioxidant effects of DPP-4i have also been observed in *in vitro* models without GLP-1 [33]. In addition, we have found that sitagliptin, but not GLP-1 eye drops, improved the deficiencies in GPX and GR protein expressions and prevented the downregulation of CuZnSOD levels in the GCL layer. These findings suggest that sitagliptin may have GLP-1-independent mechanisms of action. These GLP-1-independent beneficial properties together with GLP-1-mediated effects, the lower price, and higher stability in comparison with GLP-1, make sitagliptin eye drops an ideal candidate to be tested in clinical trials for treating early stages of DR.

One of the biggest obstacles in the study of retinal NVU impairment in the context of early stages of DR is to establish a chronological order between the different disrupters (i.e., inflammation, glial activation, oxidative stress, neurodegeneration, and vascular leakage). PKC hyperactivation is one of the mechanisms that has been postulated as a possible link between hyperglycemia and oxidative stress in DR [34]. It is not still clear whether PKC activation contributes more to oxidative stress than oxidative stress contributes to its enhancement [10]. Geraldes et al. [35] reported that hyperglycemia promotes through PKC- δ two different fundamental pathways: cumulative ROS production and NF- κ B activation. Notably, we have found that sitagliptin eye drops prevented the diabetes-induced upregulation of PKC- β and PKC- δ .

Hyperglycemia-induced oxidative stress leads to other pathological events, such as inflammation [36]. In the present study, we observed that topical administration of sitagliptin reduced NF- κ B translocation and the production of IL-1 β , proving the anti-inflammatory properties of DPP-4i. Likewise, Li et al. [37] demonstrated that linagliptin, another DPP-4i, reduced TNF- α accumulation and NF- κ B activation in retinal endothelial cells. Gonçalves et al. [30] also proved sitagliptin's capability to reduce nitrosative stress and IL-1 β in the retinas of Zucker Diabetic Fatty (ZDF) rats. However, in this case, since sitagliptin was administered by the oral route, the beneficial effects could be attributed to the improvement in blood glucose control.

As a limiting factor, it could be argued that the duration of treatment (2 weeks) was too short. However, all the papers testing the effectiveness of DPP-IV inhibitors and other molecules addressed to treat early stages of DR using topical administration

have been performed using similar treatment duration [12,38–43]. It should be noted that we are treating early stages of DR in which microvascular retinal lesions are still absent on fundoscopic examination. However, neurodegeneration and impairment of the neurovascular unit could already be present. These abnormalities can occur very shortly after the onset of diabetes, and the time needed for any treatment to prevent or arrest them in the clinical arena remains to be elucidated. Nevertheless, although we are assuming that the effect of sitagliptin would persist if the treatment were longer, specific studies addressed to confirm this assumption are needed.

5. Conclusions

Although a close relationship between the diabetic milieu and both ROS overproduction and deficiencies in the antioxidant machinery have been reported in multiple studies, the underlying mechanisms involved in diabetes-induced oxidative stress remain to be elucidated. Our results suggest that the db/db mouse model recapitulates well the imbalance between ROS production and antioxidant defenses that exists in the diabetic retina. In addition, we provide the first evidence of the effectiveness of topical (eye drops) administration of sitagliptin in preventing diabetes-induced oxidative stress in the retina. This finding, together with our previous reports showing neurovascular protection of sitagliptin, suggest this therapeutic strategy is promising, and therefore specific clinical trials seem warranted.

Author Contributions: Conceptualization, H.R., P.B., C.H. and R.S.; methodology, H.R., P.B., J.H., R.S. and C.H.; formal analysis, H.R., P.B., J.H., A.D.-J., C.H. and R.S.; investigation, P.B., H.R., A.D.-J., C.H. and R.S.; resources, R.S. and C.H.; writing—original draft preparation, H.R. and P.B.; writing—review and editing, R.S. and C.H.; supervision, R.S. and C.H.; project administration, C.H.; funding acquisition, R.S. and C.H. All authors have read and agreed to the published version of the manuscript. R.S. is the guarantor of this work, and as such, had full access to all the data in the study and takes responsibility for the integrity of the data and the accuracy of the data analysis.

Funding: This research was funded by grants from the Ministerio de Economía y Competitividad (PID2019-104225RB-I00) and the Instituto de Salud Carlos III (DTS18/0163, PI19/01215, and ICI20/00129). The study funders were not involved in the design of the study.

Institutional Review Board Statement: This study was approved by the Animal Care and Use Committee of Vall d’Hebron Research Institute (VHIR). Approval code: 14/21. Approval date: 9 July 2021.

Informed Consent Statement: Not applicable.

Data Availability Statement: The data presented in this study are available in the article.

Acknowledgments: H.R. is the recipient of a grant from the Ministerio de Economía y Competitividad (BES-2017-081690). A.D. is the recipient of a grant from the Ministerio de Economía y Competitividad (PRE2020-095747). Histological processing was carried out by ICTS “NANBIOSIS” (Unit 20 of CIBER in Bioengineering, Biomaterials and Nanomedicine (CIBER-BBN) at the Vall d’Hebron Research Institute). We thank the VHIR High Technology Unit (UAT) core facilities and staff for their contribution in this publication.

Conflicts of Interest: Vall d’Hebron Research Institute owns the intellectual property related to ocular administration of DPP-4 inhibitors to treat diabetic retinopathy. No other potential conflicts of interest relevant to this article are reported.

References

1. Hussain, T.; Tan, B.; Yin, Y.; Blachier, F.; Tossou, M.C.; Rahu, N. Oxidative Stress and Inflammation: What Polyphenols Can Do for Us? *Oxid. Med. Cell Longev.* **2016**, *2016*, 7432797. [\[CrossRef\]](#)
2. Ahsan, H.; Ali, A.; Ali, R. Oxygen free radicals and systemic autoimmunity. *Clin. Exp. Immunol.* **2003**, *131*, 398–404. [\[CrossRef\]](#) [\[PubMed\]](#)
3. Pizzino, G.; Irrera, N.; Cucinotta, M.; Pallio, G.; Mannino, F.; Arcoraci, V.; Squadrito, F.; Altavilla, D.; Bitto, A. Oxidative Stress: Harms and Benefits for Human Health. *Oxid. Med. Cell Longev.* **2017**, *2017*, 8416763. [\[CrossRef\]](#)
4. Kowluru, R.A.; Chan, P.S. Oxidative stress and diabetic retinopathy. *Exp. Diabetes Res.* **2007**, *2007*, 43603. [\[CrossRef\]](#) [\[PubMed\]](#)

5. Cheung, N.; Mitchell, P.; Wong, T.Y. Diabetic retinopathy. *Lancet* **2010**, *376*, 124–136. [\[CrossRef\]](#)
6. Wong, T.Y.; Cheung, C.M.; Larsen, M.; Sharma, S.; Simó, R. Diabetic retinopathy. *Nat. Rev. Dis. Primers* **2016**, *2*, 16012. [\[CrossRef\]](#)
7. Nian, S.; Lo, A.C.Y.; Mi, Y.; Ren, K.; Yang, D. Neurovascular unit in diabetic retinopathy: Pathophysiological roles and potential therapeutic targets. *Eye Vis.* **2021**, *8*, 15. [\[CrossRef\]](#)
8. Dammak, A.; Huete-Toral, F.; Carpena-Torres, C.; Martín-Gil, A.; Pastrana, C.; Carracedo, G. From Oxidative Stress to Inflammation in the Posterior Ocular Diseases: Diagnosis and Treatment. *Pharmaceutics* **2021**, *13*, 1376. [\[CrossRef\]](#)
9. Álvarez-Barrios, A.; Álvarez, L.; García, M.; Artime, E.; Pereiro, R.; González-Iglesias, H. Antioxidant Defenses in the Human Eye: A Focus on Metallothioneins. *Antioxidants* **2021**, *10*, 89. [\[CrossRef\]](#)
10. Kang, Q.; Yang, C. Oxidative stress and diabetic retinopathy: Molecular mechanisms, pathogenetic role and therapeutic implications. *Redox. Biol.* **2020**, *37*, 101799. [\[CrossRef\]](#)
11. Simó, R.; Hernández, C. Novel approaches for treating diabetic retinopathy based on recent pathogenic evidence. *Prog. Retin. Eye Res.* **2015**, *48*, 160–180. [\[CrossRef\]](#) [\[PubMed\]](#)
12. Hernández, C.; Bogdanov, P.; Solà-Adell, C.; Sampedro, J.; Valeri, M.; Genís, X.; Simó-Servat, O.; García-Ramírez, M.; Simó, R. Topical administration of DPP-IV inhibitors prevents retinal neurodegeneration in experimental diabetes. *Diabetologia* **2017**, *60*, 2285–2298. [\[CrossRef\]](#) [\[PubMed\]](#)
13. Ramos, H.; Bogdanov, P.; Sabater, D.; Huerta, J.; Valeri, M.; Hernández, C.; Simó, R. Neuromodulation Induced by Sitagliptin: A New Strategy for Treating Diabetic Retinopathy. *Biomedicines* **2021**, *9*, 1772. [\[CrossRef\]](#) [\[PubMed\]](#)
14. Sampedro, J.; Bogdanov, P.; Ramos, H.; Solà-Adell, C.; Turch, M.; Valeri, M.; Simó-Servat, O.; Lagunas, C.; Simó, R.; Hernández, C. New Insights into the Mechanisms of Action of Topical Administration of GLP-1 in an Experimental Model of Diabetic Retinopathy. *J. Clin. Med.* **2019**, *8*, 339. [\[CrossRef\]](#) [\[PubMed\]](#)
15. Carvalho, C.; Moreira, P.I. Oxidative Stress: A Major Player in Cerebrovascular Alterations Associated to Neurodegenerative Events. *Front. Physiol.* **2018**, *9*, 806. [\[CrossRef\]](#)
16. Bajpai, V.K.; Alam, M.B.; Quan, K.T.; Kwon, K.R.; Ju, M.K.; Choi, H.J.; Lee, J.S.; Yoon, J.I.; Majumder, R.; Rather, I.A.; et al. Antioxidant efficacy and the upregulation of Nrf2-mediated HO-1 expression by (+)-laricresinol, a lignan isolated from *Rubia philippinensis*, through the activation of p38. *Sci. Rep.* **2017**, *7*, 46035. [\[CrossRef\]](#)
17. He, X.; Ma, Q. Redox regulation by nuclear factor erythroid 2-related factor 2: Gatekeeping for the basal and diabetes-induced expression of thioredoxin-interacting protein. *Mol. Pharmacol.* **2012**, *82*, 887–897. [\[CrossRef\]](#)
18. Singh, L.P. Thioredoxin Interacting Protein (TXNIP) and Pathogenesis of Diabetic Retinopathy. *J. Clin. Exp. Ophthalmol.* **2013**, *4*, 10. [\[CrossRef\]](#)
19. Zheng, L.; Kern, T.S. Role of nitric oxide, superoxide, peroxynitrite and PARP in diabetic retinopathy. *Front. Biosci. Landmark* **2009**, *14*, 3974–3987. [\[CrossRef\]](#)
20. Wang, Q.; Zou, M.H. Measurement of Reactive Oxygen Species (ROS) and Mitochondrial ROS in AMPK Knockout Mice Blood Vessels. *Methods Mol. Biol.* **2018**, *1732*, 507–517.
21. Juan, C.A.; Pérez de la Lastra, J.M.; Plou, F.J.; Pérez-Lebeña, E. The Chemistry of Reactive Oxygen Species (ROS) Revisited: Outlining Their Role in Biological Macromolecules (DNA, Lipids and Proteins) and Induced Pathologies. *Int. J. Mol. Sci.* **2021**, *22*, 4642. [\[CrossRef\]](#) [\[PubMed\]](#)
22. Guo, C.; Chen, Q.; Chen, J.; Yu, J.; Hu, Y.; Zhang, S.; Zheng, S. 8-Hydroxyguanosine as a possible RNA oxidative modification marker in urine from colorectal cancer patients: Evaluation by ultra performance liquid chromatography-tandem mass spectrometry. *J. Chromatogr. B Anal. Technol. Biomed. Life Sci.* **2020**, *1136*, 121931. [\[CrossRef\]](#) [\[PubMed\]](#)
23. Bandookwala, M.; Sengupta, P. 3-Nitrotyrosine: A versatile oxidative stress biomarker for major neurodegenerative diseases. *Int. J. Neurosci.* **2020**, *130*, 1047–1062. [\[CrossRef\]](#)
24. Liu, T.; Zhang, L.; Joo, D.; Sun, S.C. NF- κ B signaling in inflammation. *Signal. Transduct. Target. Ther.* **2017**, *2*, 17023. [\[CrossRef\]](#) [\[PubMed\]](#)
25. Santos, J.M.; Mohammad, G.; Zhong, Q.; Kowluru, R.A. Diabetic retinopathy, superoxide damage and antioxidants. *Curr. Pharm. Biotechnol.* **2011**, *12*, 352–361. [\[CrossRef\]](#)
26. Kowluru, R.A.; Mishra, M. Oxidative stress, mitochondrial damage and diabetic retinopathy. *Biochim. Biophys. Acta.* **2015**, *1852*, 2474–2483. [\[CrossRef\]](#)
27. Kowluru, R.A.; Kowluru, A.; Mishra, M.; Kumar, B. Oxidative stress and epigenetic modifications in the pathogenesis of diabetic retinopathy. *Prog. Retin. Eye Res.* **2015**, *48*, 40–61. [\[CrossRef\]](#)
28. Li, Y.; Tian, Q.; Li, Z.; Dang, M.; Lin, Y.; Hou, X. Activation of Nrf2 signaling by sitagliptin and quercetin combination against β -amyloid induced Alzheimer's disease in rats. *Drug. Dev. Res.* **2019**, *80*, 837–845. [\[CrossRef\]](#)
29. Kawanami, D.; Takashi, Y.; Takahashi, H.; Motonaga, R.; Tanabe, M. Renoprotective Effects of DPP-4 Inhibitors. *Antioxidants* **2021**, *10*, 246. [\[CrossRef\]](#)
30. Gonçalves, A.; Leal, E.; Paiva, A.; Teixeira Lemos, E.; Teixeira, F.; Ribeiro, C.F.; Reis, F.; Ambrósio, A.F.; Fernandes, R. Protective effects of the dipeptidyl peptidase IV inhibitor sitagliptin in the blood–retinal barrier in a type 2 diabetes animal model. *Diabetes Obes. Metab.* **2012**, *14*, 453–463. [\[CrossRef\]](#)
31. Civantos, E.; Bosch, E.; Ramirez, E.; Zhenyukh, O.; Egido, J.; Lorenzo, O.; Mas, S. Sitagliptin ameliorates oxidative stress in experimental diabetic nephropathy by diminishing the miR-200a/Keap-1/Nrf2 antioxidant pathway. *Diabetes Metab. Syndr. Obes.* **2017**, *10*, 207–222. [\[CrossRef\]](#) [\[PubMed\]](#)

32. Ramos, H.; Bogdanov, P.; Sampedro, J.; Huerta, J.; Simó, R.; Hernández, C. Beneficial Effects of Glucagon-Like Peptide-1 (GLP-1) in Diabetes-Induced Retinal Abnormalities: Involvement of Oxidative Stress. *Antioxidants* **2020**, *9*, 846. [\[CrossRef\]](#) [\[PubMed\]](#)
33. Wang, C.; Xiao, F.; Qu, X.; Zhai, Z.; Hu, G.; Chen, X.; Zhang, X. Sitagliptin, An Anti-diabetic Drug, Suppresses Estrogen Deficiency-Induced Osteoporosis In Vivo and Inhibits RANKL-Induced Osteoclast Formation and Bone Resorption In Vitro. *Front. Pharmacol.* **2017**, *8*, 407. [\[CrossRef\]](#) [\[PubMed\]](#)
34. Giacco, F.; Brownlee, M. Oxidative stress and diabetic complications. *Circ. Res.* **2010**, *107*, 1058–1070. [\[CrossRef\]](#)
35. Geraldès, P.; King, G.L. Activation of protein kinase C isoforms and its impact on diabetic complications. *Circ. Res.* **2010**, *106*, 1319–1331. [\[CrossRef\]](#)
36. Rübsam, A.; Parikh, S.; Fort, P.E. Role of Inflammation in Diabetic Retinopathy. *Int. J. Mol. Sci.* **2018**, *19*, 942. [\[CrossRef\]](#)
37. Li, H.; Zhang, J.; Lin, L.; Xu, L. Vascular protection of DPP-4 inhibitors in retinal endothelial cells in vitro culture. *Int. Immunopharmacol.* **2019**, *66*, 162–168. [\[CrossRef\]](#)
38. Hernández, C.; García-Ramírez, M.; Corraliza, L.; Fernández-Carreado, J.; Farrera-Sinfreu, J.; Ponsati, B.; González-Rodríguez, A.; Valverde, A.M.; Simó, R. Topical administration of somatostatin prevents retinal neurodegeneration in experimental diabetes. *Diabetes* **2013**, *62*, 2569–2578. [\[CrossRef\]](#)
39. Hernández, C.; Bogdanov, P.; Corraliza, L.; García-Ramírez, M.; Solà-Adell, C.; Arranz, J.A.; Arroba, A.I.; Valverde, A.M.; Simó, R. Topical Administration of GLP-1 Receptor Agonists Prevents Retinal Neurodegeneration in Experimental Diabetes. *Diabetes* **2016**, *65*, 172–187. [\[CrossRef\]](#)
40. Bogdanov, P.; Simó-Servat, O.; Sampedro, J.; Solà-Adell, C.; García-Ramírez, M.; Ramos, H.; Guerrero, M.; Suñé-Negre, J.M.; Ticó, J.R.; Montoro, B.; et al. Topical Administration of Bosentan Prevents Retinal Neurodegeneration in Experimental Diabetes. *Int. J. Mol. Sci.* **2018**, *19*, 3578. [\[CrossRef\]](#)
41. Hernández, C.; Bogdanov, P.; Gómez-Guerrero, C.; Sampedro, J.; Solà-Adell, C.; Espejo, C.; García-Ramírez, M.; Prieto, I.; Egidio, J.; Simó, R. SOCS1-Derived Peptide Administered by Eye Drops Prevents Retinal Neuroinflammation and Vascular Leakage in Experimental Diabetes. *Int. J. Mol. Sci.* **2019**, *20*, 3615. [\[CrossRef\]](#) [\[PubMed\]](#)
42. Ibán-Arias, R.; Lisa, S.; Poulaki, S.; Mastrodimou, N.; Charalampopoulos, I.; Gravanis, A.; Thermos, K. Effect of topical administration of the microneurotrophin BDNF in the diabetic rat retina. *Graefes Arch. Clin. Exp. Ophthalmol.* **2019**, *257*, 2429–2436. [\[CrossRef\]](#) [\[PubMed\]](#)
43. Huang, L.; Liang, W.; Zhou, K.; Wassel, R.A.; Ridge, Z.D.; Ma, J.X.; Wang, B. Therapeutic Effects of Fenofibrate Nano-Emulsion Eye Drops on Retinal Vascular Leakage and Neovascularization. *Biology* **2021**, *10*, 1328. [\[CrossRef\]](#) [\[PubMed\]](#)



Article

Transcriptomic Analysis Reveals That Retinal Neuromodulation Is a Relevant Mechanism in the Neuroprotective Effect of Sitagliptin in an Experimental Model of Diabetic Retinopathy

Hugo Ramos ^{1,2,*}, Patricia Bogdanov ^{1,2,*}, Rafael Simó ^{1,2}, Anna Deàs-Just ^{1,2} and Cristina Hernández ^{1,2,*}

- ¹ Diabetes and Metabolism Research Unit, Vall d'Hebron Research Institute, Universitat Autònoma de Barcelona, 08035 Barcelona, Spain
 - ² Centro de Investigación Biomédica en Red de Diabetes y Enfermedades Metabólicas Asociadas (CIBERDEM), Instituto de Salud Carlos III (ICSIII), 28029 Madrid, Spain
- * Correspondence: patricia.bogdanov@vhir.org (P.B.); cristina.hernandez@vhir.org (C.H.)
 † These authors contributed equally to this work.



Citation: Ramos, H.; Bogdanov, P.; Simó, R.; Deàs-Just, A.; Hernández, C. Transcriptomic Analysis Reveals That Retinal Neuromodulation Is a Relevant Mechanism in the Neuroprotective Effect of Sitagliptin in an Experimental Model of Diabetic Retinopathy. *Int. J. Mol. Sci.* **2023**, *24*, 571. <https://doi.org/10.3390/ijms24010571>

Academic Editors:
Solmaz Abdolrahimzadeh and Mariachiara Di Pippo

Received: 27 October 2022
 Revised: 23 December 2022
 Accepted: 24 December 2022
 Published: 29 December 2022



Copyright: © 2022 by the authors. Licensee MDPI, Basel, Switzerland. This article is an open access article distributed under the terms and conditions of the Creative Commons Attribution (CC BY) license (<https://creativecommons.org/licenses/by/4.0/>).

Abstract: Synaptic dysfunction and neuronal damage have been extensively associated with diabetic retinopathy (DR). Our group evidenced that chronic hyperglycemia reduces the retinal expression of presynaptic proteins, which are crucial for proper synaptic function. The aim of the study was to explore the effect of topically administered sitagliptin, an inhibitor of the enzyme dipeptidyl peptidase-4, on the retinal expression patterns of an experimental model of DR. Transcriptome analysis was performed, comparing the retinas of 10 diabetic (db/db) mice randomly treated with sitagliptin eye drops (10 mg/mL) twice daily and the retinas of 10 additional db/db mice that received vehicle eye drops. Ten non-diabetic mice (db/+) were used as a control group. The Gene Ontology (GO) and Reactome databases were used to perform the gene set enrichment analysis (GSEA) in order to explore the most enriched biological pathways among the groups. The most differentiated genes of these pathways were validated through quantitative RT-PCR. Transcriptome analysis revealed that sitagliptin eye drops have a significant effect on retinal expression patterns and that neurotransmission is the most enriched biological process. Our study evidenced enriched pathways that contain genes involved in membrane trafficking, transmission across chemical synapses, vesicle-mediated transport, neurotransmitter receptors and postsynaptic signal transmission with negative regulation of signaling as a consequence of neuroprotector treatment with sitagliptin. This improves the modulation of the macromolecule biosynthetic process with positive regulation of cell communication, which provides beneficial effects for the neuronal metabolism. This study suggests that topical administration of sitagliptin ameliorates the abnormalities on presynaptic and postsynaptic signal transmission during experimental DR and that this improvement is one of the main mechanisms behind the previously demonstrated beneficial effects.

Keywords: dipeptidyl peptidase-4 inhibitors; sitagliptin; differentially expressed RNAs; synaptic signal transmission; diabetic retinopathy

1. Introduction

The ceaseless progression of diabetes mellitus is turning diabetic retinopathy (DR) into the major source of preventable blindness among working-aged adults worldwide [1]. Due to the lack of symptoms during the early stages of DR, current diagnostic and therapeutic strategies address the advanced stages of the disease [2]. Furthermore, current treatments are expensive, invasive and are associated with side effects. Targeting classic risk factors of diabetes (mainly hyperglycemia and hypertension) is the only strategy against the early stages, giving rise to an unmet medical necessity [3].

The impairment of the neurovascular unit (NVU) of the retina, a functional coupling that integrates vascular flow with metabolic activity and that maintains the integrity of the inner blood–retinal barrier (iBRB), is an early event in the pathogenesis of DR [4,5]. Neurodegeneration, glial activation and early microvascular abnormalities are its main hallmarks [5].

New experimental approaches targeting the early neurodegenerative processes that occur in diabetic retinas are currently being explored [6]. The incretin glucagon-like peptide-1 (GLP-1) is a hormone that has been related to neuroprotection in the central nervous system (CNS) and, consequently, has been postulated as a potential candidate for the treatment of DR due to the direct embryological relationship between the CNS and the retina [7]. Recently, GLP-1, its receptor, the GLP-1 receptor (GLP-1R), mainly responsible for its degradation, and the enzyme dipeptidyl peptidase-4 (DPP-4) were detected in murine and human retinas [8,9]. The low retinal levels of GLP-1 reported in diabetic patients suggest that its replacement treatment could have a neuroprotective role against early DR [5].

Topical administration (eye drops) of GLP-1R agonists (GLP-1RAs) and topical administration of DPP-4 inhibitors (DPP-4i) are two different strategies that seek a common neuroprotective effect: GLP-1R activation. Their effectiveness has been already demonstrated in an experimental model of DR, preventing glial activation, cell death, glutamate excitotoxicity, vascular leakage and electroretinogram (ERG) abnormalities [8,9]. Nevertheless, the lower price, the higher stability and the emergence of new evidence that proves the neuroprotective role of other DPP-4 substrates place DPP-4i as a more attractive therapeutic strategy against the early stages of DR. The complexity of DPP-4i, derived from the multifunctional activity of the inhibited enzyme, and the need for enough preclinical evidence invite elucidation of the mechanisms behind their neuroprotective effects [10]. For this purpose, a transcriptome analysis was performed to study the effect of one DPP-4i, sitagliptin, in an experimental model of DR.

2. Results

2.1. Multiple Comparisons between Transcriptomes Revealed a Clear Effect of Both the Diabetic Condition and Sitagliptin Treatment

The largest number of differentially expressed genes (DEGs) was found in the comparison between sitagliptin-treated db/db mice and control db/+ mice (108 up-regulated and 33 down-regulated genes with an adjusted *p*-value (Adj.P. Val) of less than 0.05). The effect of the diabetic condition was represented by the comparative analysis between the vehicle-treated db/db and the control db/+ mice, which resulted in 19 DEGs (10 up-regulated and 9 down-regulated genes). At the same level of significance, transcriptomic analysis revealed a clear effect of sitagliptin eye drops in diabetic mice, which can be seen in the comparison between the sitagliptin-treated db/db mice and the vehicle-treated db/db mice, where 20 DEGs (17 up-regulated and 3 down-regulated genes) were obtained (Table 1).

2.2. Db/db Mice Topically Treated with Sitagliptin Showed Different Expression Patterns in the Retina Compared to Those Treated with Vehicle

Focusing on the effect of the topical treatment with sitagliptin, we only continued exploring the “db/db sitagliptin vs. db/db vehicle” comparison. HeatMap clustering between both groups using transcripts with an $\text{absLogFC} \geq 0.3$ and an $\text{Adj.P.Val} < 0.05$ revealed two main clusters of different expression patterns (Figure 1). With the exception of sample “Db/db vehicle_15_1”, all samples of each compared condition were grouped together in the same cluster. Genes more differentially expressed are displayed in a summary table (top 10) and in a volcano plot (top 20) (Figure 2A,B).

Table 1. Multiple comparisons of DEGs between groups. Summary table of the number of DEGs acquired for each comparison at distinct significance thresholds (green: db/db sitagliptin vs. db/+ control; red: db/db vehicle vs. db/+ control; blue: db/db sitagliptin vs. db/db vehicle) ($n = 10$).

	db/db Sitagliptin vs. db/+ Control	db/db Vehicle vs. db/+ Control	db/db Sitagliptin vs. db/db Vehicle
UpReg_B	65	15	33
DownReg_B	20	13	9
UpRegAdj0.01	18	5	0
DownRegAdj0.01	6	3	0
UpRegAdj0.05	108	10	17
DownRegAdj0.05	33	9	3
UpRegAdj0.15	369	16	185
DownRegAdj0.15	122	14	65
UpRegAdj0.25	728	24	494
DownRegAdj0.25	291	19	195
UpRegP0.01	363	71	275
DownRegP0.01	116	56	96
UpRegP0.05	852	218	82
DownRegP0.01	376	223	329

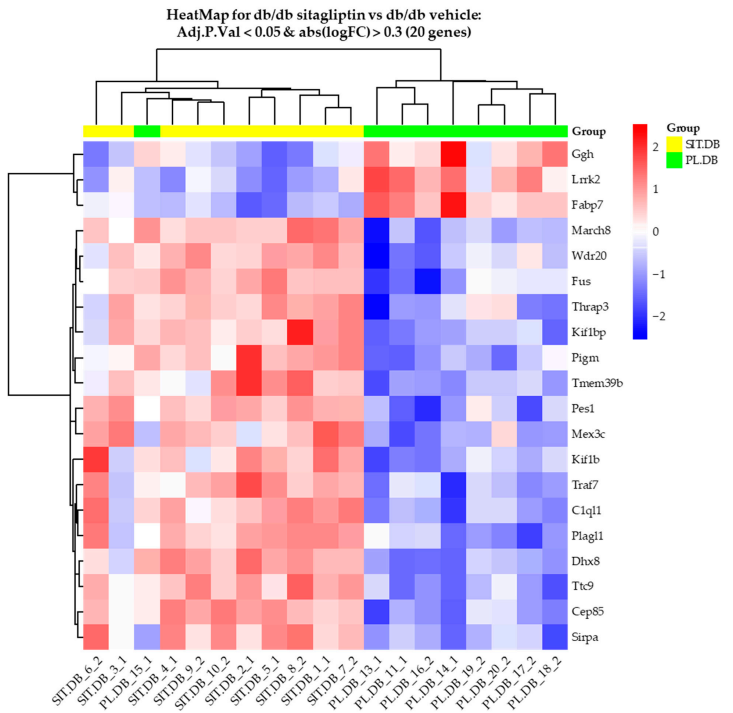


Figure 1. Comparison of retinal expression patterns between sitagliptin-treated and vehicle-treated db/db mice. (A) HeatMap for comparison of sitagliptin-treated db/db mice and vehicle-treated db/db mice with genes with an adjusted p -value of less than 0.05 and an absLogFC greater than 0.3 (20 genes). High and low row z -scores are represented in red and blue, respectively ($n = 10$).

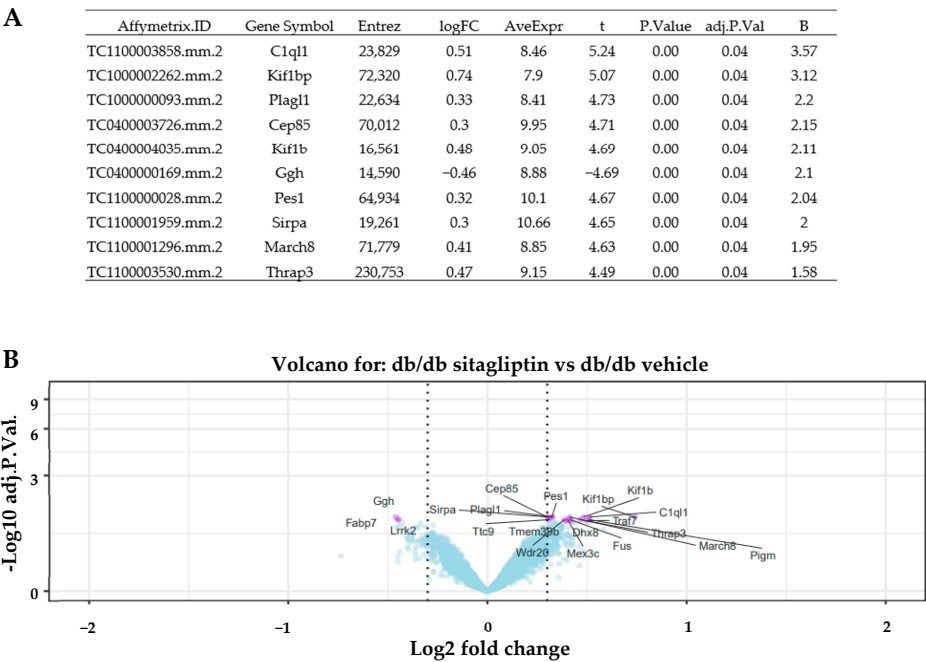


Figure 2. Most differentiated genes. (A) Table of top 10 genes more differentially expressed in the comparison between vehicle-treated and sitagliptin-treated mice. AveExpr is the average expression of the gene across all the arrays in log2 scale. t is a “moderated-t” statistic similar to the usual Student’s t statistic (n = 10). (B) Volcano plot of db/db sitagliptin and db/db vehicle comparison. Genes are shown in purple when adjusted p-value was under 0.05, and absolute logarithmic fold change was above 0.3. Gene symbols are shown for the top 20 most significant genes (n = 10).

2.3. Gene Set Enrichment Analyses (GSEA) Revealed That the Most Differentiated Biological Process Is Neurotransmission

GSEA is a powerful analysis method for interpreting gene expression data [11]. The analysis of biological significance was approached by GSEA using two different annotation databases: the Go Ontology Database (GO) (Biological Process (BP) subcategory) and the Reactome Pathway Database. Most enriched GO (BP) and Reactome terms revealed neurotransmission to be the most differentiated biological process between the transcriptomes of db/db mice treated with sitagliptin and those of the vehicle-treated mice. In GO analysis, more general and non-cell-type-specific terminology was found: transmembrane transport, cytoskeleton organization, secretion, negative regulation of cell communication, etc. (Figure 3A–C).

Nevertheless, Reactome analysis showed us the influence of sitagliptin in the neuronal components of the retina through terms such as: neuronal system, transmission across chemical synapses, neurotransmitters receptors and postsynaptic signal transmission, membrane trafficking, vesicle-mediated transport, etc. (Figure 4A–C). A positive enrichment score or NES indicates that the enriched term is mainly composed of up-regulated genes, whereas a negative score indicates the opposite. In relation to the most enriched biological pathways, the specific heatmaps show clear differential expression patterns between both groups and also expose which genes belong to these pathways (Figure 5A–C).

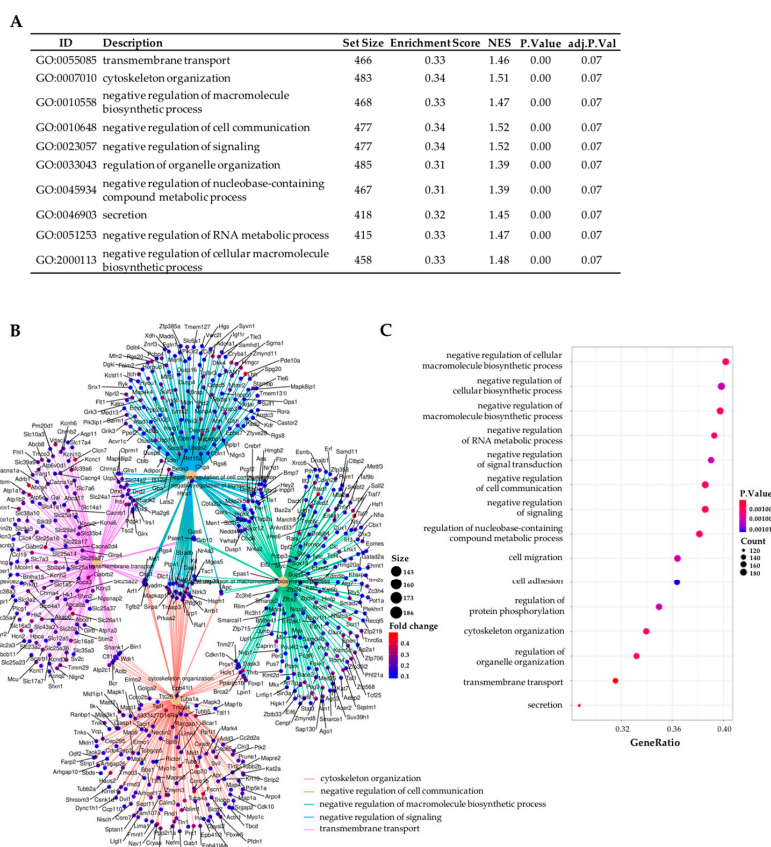


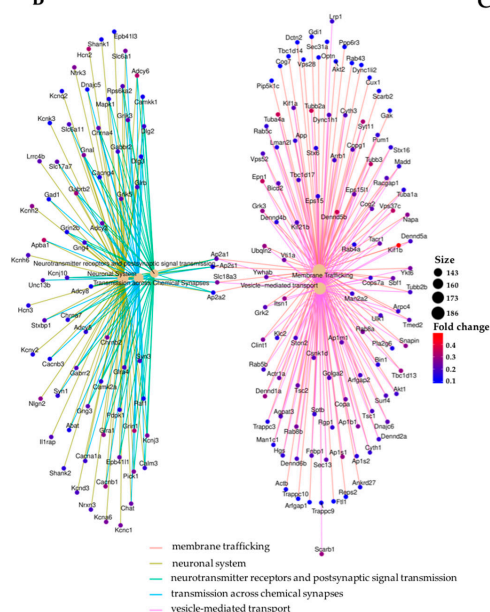
Figure 3. Enrichment analysis of the transcriptome study between vehicle-treated db/db mice and db/db mice treated with sitagliptin using the GO Database (BP subcategory). (A) Table of top 10 enriched GO terms (BP) for the comparison “db/db sitagliptin vs. db/db vehicle”. (B) Network plot of the top five enriched GO term (BP) for “db/db sitagliptin vs. db/db vehicle”. (C) Dot plot of the top 15 enriched GO terms (BP) for the “db/db sitagliptin vs. db/db vehicle” comparison. Results were adjusted with a p -value less than 0.25. The results shown correspond to the top enriched terms with an adjusted p -value < 0.07 .

Reanalysis of the GO study, not only using the BP category but also incorporating the Molecular Function (MF) and Cellular Component (CC) categories and limiting the search to neuronal terms, confirmed the Reactome results (Figure 6A–C). An enrichment map of the most differentiated gene sets associated with synaptic transmission (BP category) can also be observed for the sitagliptin vs. vehicle comparison in Figure 6D.

A

ID	Description	Set Size	Enrichment Score	NES	P.Value	adj.P.Val
R-MMU-112316	neuronal system	130	0.52	2.13	0.00	0.03
R-MMU-112315	transmission across chemical synapses	90	0.58	2.27	0.00	0.03
R-MMU-112314	neurotransmitter receptors and postsynaptic signal transmission	65	0.58	2.16	0.00	0.03
R-MMU-199991	membrane trafficking	258	0.37	1.61	0.00	0.03
R-MMU-5653656	vesicle-mediated transport	269	0.36	1.59	0.00	0.03
R-MMU-5389840	mitochondrial translation elongation	48	-0.51	-2.17	0.00	0.03
R-MMU-5368287	mitochondrial translation	50	-0.48	-2.05	0.00	0.03
R-MMU-15419276	mitochondrial translation termination	50	-0.48	-2.05	0.00	0.03
R-MMU-1483257	phospholipid metabolism	74	0.48	1.81	0.00	0.03
R-MMU-2046104	alpha-linolenic (omega3) and linoleic (omega6) acid metabolism	10	0.78	1.89	0.00	0.03

B



C

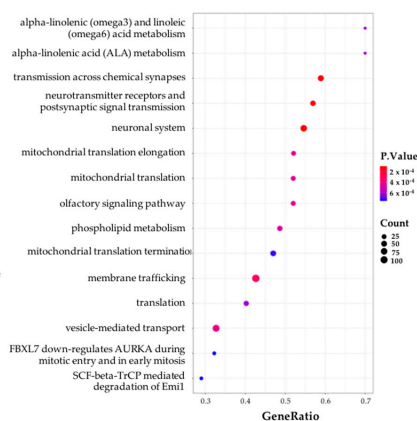


Figure 4. Enrichment analysis of the transcriptome comparison between vehicle-treated db/db mice and db/db mice treated with sitagliptin using the Reactome Pathway Database. (A) Table of the top 10 enriched pathways (Reactome Pathway Database) for the comparative study “db/db sitagliptin vs. db/db vehicle”. (B) Network plot of the top five enriched pathways for the comparison between db/db sitagliptin and db/db vehicle conditions (Reactome Pathway Database). (C) Dot plot of the top 15 enriched pathways (Reactome Pathway Database). The results shown correspond to the top enriched terms with an adjusted p -value < 0.05 .

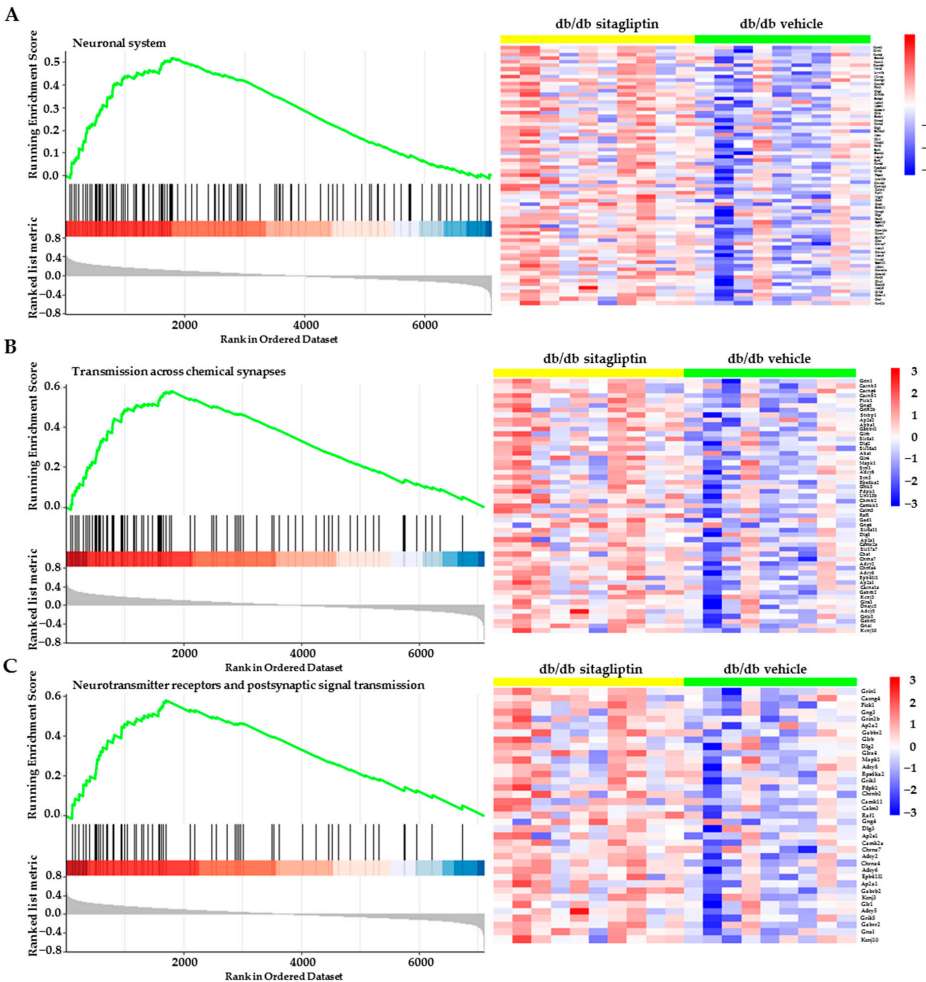


Figure 5. Gene set enrichment analysis (GSEA). (A–C) Heatmaps of the most enriched neurotransmission-related pathways between vehicle-treated db/db mice and sitagliptin-treated db/db mice.

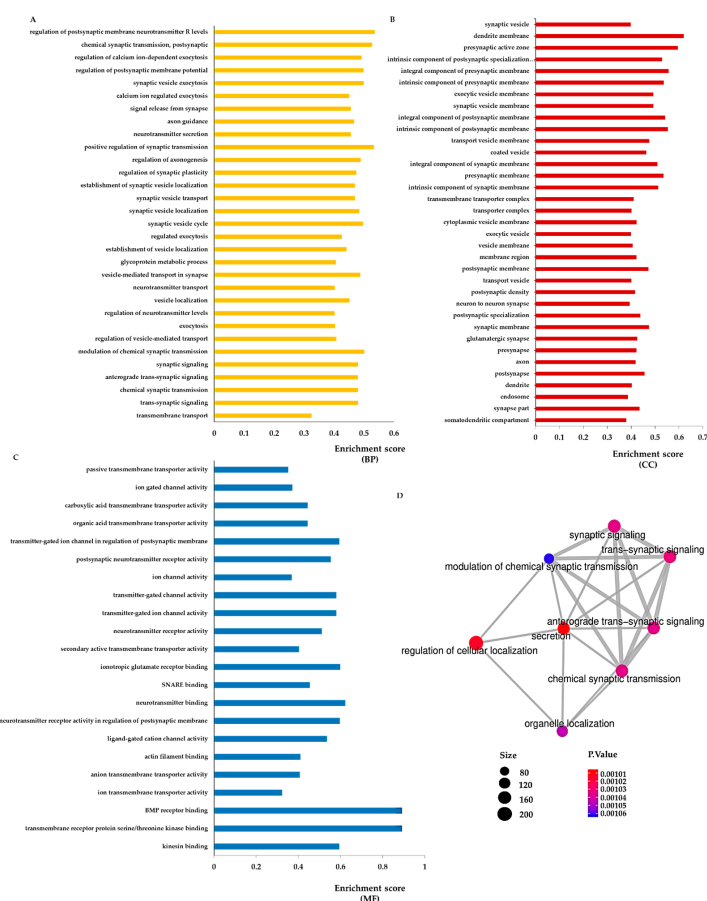


Figure 6. Sitagliptin-enhanced pathways related to synaptic transmission. (A–C) Most enriched terms involved in neurotransmission between sitagliptin-treated db/db mice and db/db mice treated with vehicle using the GO database (Biological Process (BP), Cellular Component (CC) and Molecular Function (MF) subcategories, respectively) (p -value < 0.005). X-axis shows the enrichment score in each category. (D) Cluster related to synaptic transmission from the GO enrichment map of the top 60 enriched terms (BP) between db/db sitagliptin and db/db vehicle.

2.4. Topical Administration of Sitagliptin Prevented DR-Induced Down-Regulation of Genes Related to Synapse Formation, Maintenance and Synaptic Transmission

Most differentiated genes from the top enriched terms are not the main regulators of these biological processes. In view of this, gene expression of other and more crucial proteins was also addressed. Diabetic mice, in comparison to db/+ control mice, presented a significant down-regulation of several genes related to synapse formation and maintenance (complement C1q-like 1 (*C1ql1*); kinesin family member 1B (*Kif1b*); KIF-1 binding protein (*Kif1bp*)), synaptic transmission at presynaptic level (amyloid beta precursor protein-binding family A member 1 (*Apha1*); complexin 1 (*Cplx1*); solute carrier family

17 member 7 (*Slc17a7*); synaptosome-associated protein 25 (*Snapt25*); syntaxin-1A (*Stx1a*); syntaxin-binding protein 2, 4 and 6 (*Stxbp2*, *Stxbp4* and *Stxbp6*); synaptic vesicle glycoprotein 2B (*Sv2b*); synapsin I (*Syn1*); synaptophysin (*Syp*); synaptotagmin (*Syt1*); Unc-13 homolog A (*Unc13A*); vesicle-associated membrane protein 2 (*Vamp2*) and postsynaptic level (calcium/calmodulin-dependent serine protein kinase (*Cask*); discs large MAGUK scaffold protein 2 and 4 (*Dlg2* and *Dlg4*); glutamate ionotropic receptor AMPA-type subunit 1 (*Gria1*); glutamate ionotropic receptor NMDA-type subunit 1, 2B and 2D (*Grin1*, *Grin2b* and *Grin2d*)) (Figure 7A,B). Nevertheless, topical administration of sitagliptin in db/db mice significantly prevented these abnormal expression patterns (Figure 7A,B). In addition, STRING interactions between all the analyzed genes demonstrated the close relationship linking all of them (Figure 7C).

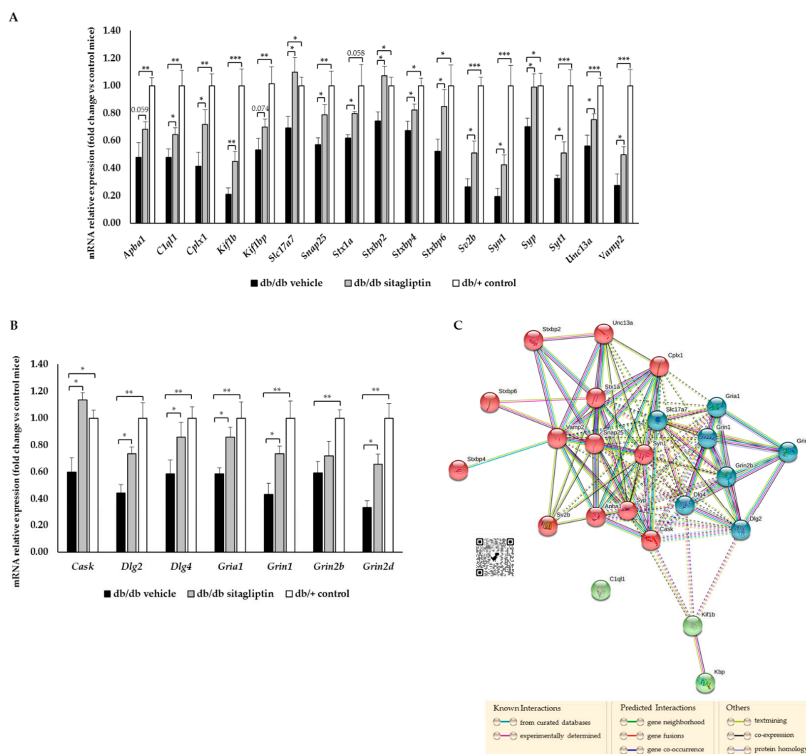


Figure 7. Study of gene expression. (A) RT-PCR analysis of genes related to synapse formation and neurotransmission at presynaptic level in db/db mice treated with vehicle (black bars) or sitagliptin eye drops (gray bars) and in non-diabetic mice (white bars) ($n = 4$). * $p < 0.05$, ** $p < 0.01$, *** $p < 0.001$. (B) RT-PCR analysis of genes associated with neurotransmission at postsynaptic level in db/db mice treated with vehicle (black bars) or sitagliptin eye drops (gray bars) and in non-diabetic mice (white bars) ($n = 4$). * $p < 0.05$, ** $p < 0.01$. (C) Gene interactions of studied genes (STRING ver. 11.5). The red cluster displays genes related to presynaptic proteins, the blue cluster displays those related to postsynaptic proteins and green cluster displays those related to proteins involved in synapse formation. Dashed lines represent interactions between genes from different clusters, while solid lines are the interactions of genes of the same cluster.

3. Discussion

In the context of shedding light on the mechanisms behind the beneficial effects that DPP-4i exerted on an experimental model of DR, we provide a preliminary and comparative study of the retinal transcriptomes of db/db mice topically treated with sitagliptin or vehicle. Our results evidence that neurotransmission, wherein sitagliptin has a protective role, is the main biological process affected by DR. A detailed characterization of the genes involved in this improvement is also provided.

Proper functioning of retinal synapses is essential for the neural processing of visual perception. Any morphological change of synaptic terminals or protein content could impair neuronal behaviour and, consequently, the efficiency of the retina to sense and process light stimuli. DR has been widely associated with synaptic loss and with deficits in neurotransmitter release and uptake systems, leading to altered synaptic activity and electrophysiological abnormalities in the retina [12].

Using two different annotations databases (GO and Reactome) and under restrictive statistical conditions, the retinal GSEA revealed positive enrichment after sitagliptin treatment of multiple terms linked to synaptic transmission, such as: neuronal system, transmission across chemical synapses, neurotransmitters receptors and postsynaptic signal transmission, neurotransmitter transport, regulation of postsynaptic membrane potential, membrane trafficking, vesicle-mediated transport in synapse, axon guidance, etc. The neuroprotective role of DPP-4i in relation to eye complications, where synaptic transmission is altered, has been already reported. In a mouse model of retinitis pigmentosa, sitagliptin preserved presynaptic and postsynaptic elements and synaptic contacts between photoreceptors and bipolar/horizontal cells [13]. Furthermore, in type I diabetes STZ rats with continued hyperglycaemia, sitagliptin prevented neuronal cell death in the retina [8,14]. In both studies, sitagliptin was administered orally, and the effects can be attributed to the systemic improvement due to the lowering of blood glucose levels. Nevertheless, our group demonstrated that sitagliptin eye drops are able, in a non-glycaemia-dependent fashion, to significantly prevent the diabetes-induced synaptic failure that occurred in the retina of db/db mice, evidencing the intrinsic neuroprotective properties of DPP-4i [15]. Considering these previous studies, the GSEA results obtained reveal that, among the different beneficial effects of DPP-4i in DR models, retinal neuroprotection is the most relevant one. In addition, it seems that the retinal GLP-1/GLP-1R pathway is the main mediator of these neuroprotective effects [16]. Nonetheless, independent and synergic mechanisms of DPP-4i should not be ruled out [17].

Current evidence does not indicate any beneficial effect of the systemic administration of DPP-4i on DR in addition to their hypoglycemic action. In fact, systematic reviews and meta-analyses reported a neutral effect of DPP-4i on DR [18–20]. This can be explained because DPP-4i, and, in particular, sitagliptin, is unable to cross the blood–retinal barrier [21,22]. For this reason, we examined the effect of topical administration of sitagliptin. By using this route, sitagliptin was able to reach the retina and exert its effects independently from its capacity to lower blood glucose levels. In fact, this is an advantage because it permitted us to demonstrate the direct effect of the drug in the retina independently of metabolic control. It should be noted that the capacity of antidiabetic agents to lower blood glucose levels is a confounding factor in studies aimed at evaluating their potential effect in the development or progression of DR.

It is not entirely possible to elucidate the neuroprotective impact that dependent or independent GLP-1/GLP-1R pathways have; however, we provide a characterization of some potential targets of both mechanisms (direct or indirect targets). On the one hand, *C1ql1*, the most differentiated gene, codifies for a secreted protein that interacts with hippocampal receptors that promote spinogenesis, synaptogenesis and synaptic territory constitution, essential processes for a functional neuronal connectivity [23]. On the other hand, *Kif1bp* and *Kif1b* genes (top two and five) give rise to a KIF1B-KBP complex, necessary for proper axon elongation [24]. The presence of three genes intimately linked to crucial

functions of the neuronal system among the five most differentiated genes is a clear proof of the neuroprotective role of sitagliptin that cannot go unnoticed.

In addition, multiple genes involved in neurotransmitter uptake and release are up-regulated by sitagliptin (*Apha1*, *Cplx1*, *Slc17a7*, *Stxbp2*, *Stxbp4*, *Stxbp6*, *Sv2b* and *Unc13a*). The proteins that these genes codify are responsible for vesicle biogenesis, mobilization, docking, fusion and recycling [25]. Nevertheless, they are not the most characterized proteins of this biological process, and, therefore, in our RT-PCR validation, we also assessed the mRNA levels of *Snap25*, *Stx1a*, *Syn1*, *Syp*, *Syt1* and *Vamp2*. The core of the neurotransmitter release machinery is composed of the N-ethylmaleimide-sensitive factor attachment protein (SNAP) receptors (SNAREs) syntaxin-1 (*Stx1a*), SNAP-25 (*Snap25*) and synaptobrevin (*Vamp2*), which form the SNARE complex, a four-helix bundle that brings close both vesicle and plasma membrane for proper vesicle docking and fusion. Munc-18 (*Stxbp2*, *Stxbp4*, *Stxbp6*) and Munc-13 (*Unc13a*) modulate SNARE complex formation. Munc-18 binds to a “closed” conformation of syntaxin-1 and to synaptobrevin to stabilize the assembly of the SNARE complex. Munc-13 is responsible for syntaxin-1 “opening” and permits vesicle binding to the plasma membrane [26]. Mint-1 (*Apha1*) mediates the function of Munc-18 [27]. Synaptotagmin 1 (*Syt1*) is a transmembrane protein present in synaptic vesicles which senses and couples Ca^{2+} influx to synchronize neurotransmitter releases. The role of complexin I (*Cplx1*) is not well understood, but it has been related to vesicle fusion [28]. Synaptophysin (*Syp*) is the most abundant synaptic protein, and it modulates the endocytosis of synaptic vesicles [29]. Synapsin I (*Syn1*) orchestrates the reserve pool of synaptic vesicles available for exocytosis and organises the abundance of vesicles at presynaptic terminals [30,31]. Synaptic vesicle glycoprotein 2B (SV2B) (*Sv2b*) stabilizes the vesicle content, maintains and orients the releasable pool of vesicles and modulates vesicular calcium sensitivity to coordinate efficient neurotransmitter release [32]. Finally, vesicular glutamate transporter 1 (VGLUT1) (*Slc17a7*) refills presynaptic recycling vesicles with glutamate, the major excitatory transmitter in the retina, the excitotoxicity of which is a hallmark of DR [33].

Not only genes related to neurotransmitter uptake and release but also genes linked to the next biological step, the postsynaptic processing, have been found. In our transcriptomic analysis, we detected that sitagliptin up-regulates genes that codify for three different subunits of the glutamate ionotropic receptor (N-methyl-D-aspartate) NMDA (*Grin1*, *Grin2b*, *Grin2d*), one subunit of the glutamate α -amino-3-hydroxy-5-methyl-4-isoxazolepropionic acid (AMPA) receptor (*Gria1*), two different postsynaptic density proteins (PSD) (*Dlg2*, *Dlg4*) and the calcium/calmodulin-dependent serine protein kinase (CASK) (*Cask*). Glutamate interacts with both ionotropic and metabotropic receptors to activate and mediate postsynaptic responses. AMPA and NMDA receptors are crucial modulators of synaptic plasticity, the dysregulation of which leads to neurodegenerative processes, including DR [34,35]. PSD-93, PSD-95 and CASK, codified by *Dlg2*, *Dlg4* and *Cask*, respectively, are postsynaptic scaffolding proteins that regulate the synaptic localization of many receptors, channels and signalling proteins [36,37].

In the RT-PCR assay, we found that db/db mice treated with the vehicle, in comparison to non-diabetic animals, presented a down-regulation of all the studied proteins involved in synapse formation, maintenance, neurotransmitter release and postsynaptic response. Sitagliptin eye drops preserved the levels of all these proteins, which reflects its beneficial and significant impact on the retinal neuronal system. As a proper content of synaptic proteins is necessary for the functionality of the retina, we can assume that the results obtained in the present study represent the underlying mechanisms behind the functional recovery (ERG) that we previously reported [8].

It is important to notice the several enriched pathways from our transcriptomic analysis that demonstrate the multiple beneficial effects of DPP-4i not only related to neuroprotection, but also associated with anti-inflammatory or anti-angiogenic properties. Further analysis specifically addressed to confirm this issue is needed.

In summary, topical administration of sitagliptin had neuroprotective effects in an experimental model of DR by preventing the dysregulation of pre- and postsynaptic proteins and other molecules involved in synapse formation and maintenance. This evidence could represent an important approach for the great unmet medical need that diabetic retinopathy represents and even for other retinal diseases in which neurodegeneration/synaptic abnormalities play a key role.

4. Materials and Methods

4.1. Mice

A total of 24 diabetic male db/db (BKS.Cg-Dock7m $+/+$ Leprdb/J) mice and 12 non-diabetic mice (db/+; (BKS.Cg-Dock7m $+$ Leprdb/+)) aged 7 weeks were obtained from Charles River Laboratories Inc. (Calco, Italy) for the study. Db/db mice carry a mutated leptin receptor that leads to obesity-induced type 2 diabetes. Animals were bred and maintained in VHIR's animal facility. Animals had free access to ad libitum food (ENVIGO Global Diet Complete Feed for Rodents, Mucedola, Milan, Italy) and filtered water. In order to minimize variability, animals were randomly housed (block randomization) in groups of 2 mice per cage in Tecniplast GM-500 cages ($36 \times 19 \times 13.5$ cm) under standard laboratory conditions at 22 ± 2 °C, with a 12 h light/dark cycle and relative humidity of 50–60%. Each cage held absorbent bedding and nesting material (BioFresh Performance Bedding 1/800 Pelleted Cellulose, Absorption Corp, Ferndale, WA, USA). Blood glucose levels were measured weekly through tail vein sampling (glucose assay kit; Abbott, IL, USA).

All accomplished experiments with animals were adjusted in compliance with European Community (86/609/CEE) and ARVO (Association for Research in Vision and Ophthalmology) tenets for the use of laboratory animals. This study was approved by the Animal Care and Use Committee of Vall d'Hebron Research Institute (VHIR) (CEEA 75/15).

4.2. Interventional Study

At the age of 10 weeks, sitagliptin (sitagliptin phosphate monohydrate (Y0001812, Merck KGaA, Darmstadt, Germany)) eyedrops (10 mg/mL; $n = 12$) and vehicle (phosphate-buffered saline (PBS)) eyedrops ($n = 12$) were randomly administered twice per day directly onto the superior corneal surface of each eye of diabetic mice with the aid of a micropipette (5 μ L). On day 15, animals (12 weeks of age) received one drop of sitagliptin or vehicle 1 h before euthanasia. Twelve non-diabetic mice, matched by age, were used as a control group.

4.3. Retinal Tissue Processing

On day 15, each animal received a 200 μ L intraperitoneal injection of anesthesia prepared with a mix containing 1 mL ketamine (GmbH, Hameln, Germany) and 0.3 mL xylazine (Laboratorios Calier S.A., Barcelona, Spain). Eyes were rapidly enucleated, and the neuroretinas were dissected. The neuroretina of each animal was directly stored in an empty tube at -80 °C for transcriptomic experiments. The neuroretinas were introduced in individual tubes with 140 μ L of TRIzol reagent (15596018, Invitrogen™, Carlsbad, CA, USA) until RNA extraction. For the RNA extraction, neuroretinas were treated with DNase (18068015, ThermoFisher Scientific, Waltham, MA, USA) to remove genomic contamination and were purified on RNeasy MinElute column (74106, Qiagen, Hilden, Germany). After supernatant elimination, RNA sediment was obtained and resuspended in 30 μ L of RNase free water (AM9937, ThermoFisher Scientific, Waltham, MA, USA). An Agilent 2100 Bioanalyzer and a NanoDrop Spectrophotometer were used for sample integrity and quantity, respectively.

4.4. Transcriptome Analysis

The data for the analysis were obtained from Genomic's UAT core facility at VHIR, where the microarrays were performed. The study was based on 30 samples (the 10 highest quality RNA samples of each group) hybridized in Clariom S Mouse Arrays (ThermoFisher Scientific, Waltham, MA, USA). Bioinformatics analysis was carried out in the Statistics

and Bioinformatics Unit (UEB) at VHIR. Quality approaches (principal component analysis (PCA), hierarchical clustering and heatmaps depicting distances between arrays) were performed before normalization. Any sample was excluded. All samples were normalized following the robust microchip average (RMA) algorithm [38,39]. PCA and hierarchical clustering quality controls were assessed again, and one outlier from the vehicle group was excluded. Using principal variance component analysis (PVCA), we estimated that the main cause of variance was the batch effect. The analysis to select differentially expressed genes (DEG) was based on adjusting a linear model with empirical Bayes moderation of the variance, including a batch factor to adjust batch effects. This is a technique similar to ANOVA specifically developed for microarray data analysis by Gordon K Smyth [40]. *p*-values were adjusted to obtain strong control over the false discovery rate using the Benjamini and Hochberg method. Statistical significance was set at 0.05 for adjusted *p*-values. The analysis of biological significance was based on gene set enrichment analysis (GSEA) using clusterProfiler package in R/Bioconductor [41], which implements the GSEA algorithm proposed by Subramanian [11]. In GSEA, the genes can be ordered in a ranked list according to their differential expression between the classes using different annotation databases (Gene Ontology (GO) and Reactome Pathway Knowledge base). The statistical analysis was performed using the statistical language “R” (R, version 3.5.1 (2 July 2018), copyright (C) 2018, The R Foundation for Statistical Computing) and the libraries developed for the microarray analysis in the Bioconductor Project (www.bioconductor.org) (accessed on 18 October 2021). Functional association networks were constructed and annotated using STRING version 11.5 (<https://string-db.org/>) (accessed on 18 October 2021). The *Mus musculus* genome was used as background genome. The data discussed in this publication were deposited in NCBI’s Gene Expression Omnibus (Edgar et al., 2002) and are accessible through GEO Series accession number GSE219084 (<https://www.ncbi.nlm.nih.gov/geo/query/acc.cgi?acc=GSE219084>).

4.5. cDNA Reverse Transcription and Quantitative Reverse Transcription Polymerase Chain Reaction (RT-PCR) Assay

According to the manufacturer’s instructions, cDNA reverse transcription was performed in a T100 Thermal Cycler (Bio-Rad, Hercules, CA, USA) using a High-Capacity cDNA Reverse Transcription Kit (4368814, ThermoFisher Scientific, Waltham, MA, USA) and Oligo(dT)18 Primer (SO131, ThermoFisher Scientific, Waltham, MA, USA). RT-PCR was carried out using SYBR Green PCR Master Mix (4309155, Applied Biosystems, Warrington, UK) and a 7.900 HT Sequence Detection System in 384-well optical plates with specific primers (displayed in Table 2). Relative quantities were calculated using the ABI SDS 2.4 RQ software and presented as a ratio between them and the endogenous controls (*B2m* and *Actin*).

Table 2. Primers used for RT-PCR.

Primers		Nucleotide Sequence
<i>Actb</i>	Forward (5′-3′)	5′-CTAAGGCCAACCCTGAAAG-3′
	Reverse (5′-3′)	5′-CAGTATGTTCCGGCTTCCCATTC-3′
<i>Atpa1</i>	Forward (5′-3′)	5′-GGTGCTGAGTCATCAAGCATAC-3′
	Reverse (5′-3′)	5′-GAACTTCAACGTAGGTTGGGAA-3′
<i>B2m</i>	Forward (5′-3′)	5′-GTATGCTATCCAGAAAACCC-3′
	Reverse (5′-3′)	5′-CTGAAGGACATATCTGACATC-3′
<i>C1ql1</i>	Forward (5′-3′)	5′-GGCACCTACTTTTTCACCTACC-3′
	Reverse (5′-3′)	5′-AGTCGTAGTCTTGGTCTGCAT-3′
<i>Cask1</i>	Forward (5′-3′)	5′-TGAAGAAGTAGTCAAACCTGCCAG-3′
	Reverse (5′-3′)	5′-TTTGTCCCGTACATTGCATCC-3′
<i>Cplx1</i>	Forward (5′-3′)	5′-AGTTCGTGATGAAACAAGCCC-3′
	Reverse (5′-3′)	5′-TCTTCCTCCTCTTAGCAGCA-3′

Table 2. Cont.

Primers		Nucleotide Sequence
<i>Dlg2</i>	Forward (5'-3')	5'-CTGTCACGAGGCAGGAAATAAA-3'
	Reverse (5'-3')	5'-CGACTTCGTAAGTCACGCTTTG-3'
<i>Dlg4</i>	Forward (5'-3')	5'-TGAGATCAGTCATAGCAGCTACT-3'
	Reverse (5'-3')	5'-CTTCCTCCCCTAGCAGGTCC-3'
<i>Gria1</i>	Forward (5'-3')	5'-AAAGGAGTGTACGCCATCTTTG-3'
	Reverse (5'-3')	5'-TGTCACACGGGAAAACCTGGAG-3'
<i>Grin1</i>	Forward (5'-3')	5'-ATGCACCTGCTGACATTG-3'
	Reverse (5'-3')	5'-TAITGGCCTGGTTTACTGCCT-3'
<i>Grin2b</i>	Forward (5'-3')	5'-GCCATGAACGAGACTGACCC-3'
	Reverse (5'-3')	5'-GCTTCCTGGTCCGTGTCATC-3'
<i>Grin2d</i>	Forward (5'-3')	5'-GCTGCGAGACTATGGCTTCC-3'
	Reverse (5'-3')	5'-CCAGTGACGGGTTTACCAGAAA-3'
<i>Kif1b</i>	Forward (5'-3')	5'-GTCAATCGAATGAACGACCTGG-3'
	Reverse (5'-3')	5'-GCCGATGCAAAAAGTTGAACTG-3'
<i>Kif1bp</i>	Forward (5'-3')	5'-TCTTGACCCGACTGAGCATTT-3'
	Reverse (5'-3')	5'-ATAATGAGCGGCCTTCTCGAA-3'
<i>Slc17a7</i>	Forward (5'-3')	5'-GGTGGAGGGGGTCACATAC-3'
	Reverse (5'-3')	5'-AGATCCCGAAGCTGCCATAGA-3'
<i>Snap25</i>	Forward (5'-3')	5'-CAACTGGAACGCATTGAGGAA-3'
	Reverse (5'-3')	5'-GGCCACTACTCCATCCTGATTAT-3'
<i>Stx1a</i>	Forward (5'-3')	5'-CGCTGTCCCGAAAGTTGTG-3'
	Reverse (5'-3')	5'-GTGTCTGGTCTCGATCTACT-3'
<i>Stxbp2</i>	Forward (5'-3')	5'-AAGGCGGTGTTAGGGGAAA-3'
	Reverse (5'-3')	5'-CAACAGGATGACAAGATTGCGA-3'
<i>Stxbp4</i>	Forward (5'-3')	5'-ACAGGTCTAGGTCTGAAGATCC-3'
	Reverse (5'-3')	5'-CATCCTTGTAACAGTACCTCC-3'
<i>Stxbp6</i>	Forward (5'-3')	5'-CTCTTGATGAAAGAATGCTGGGA-3'
	Reverse (5'-3')	5'-TGACCTTCGTGATAGATGCCT-3'
<i>Sv2b</i>	Forward (5'-3')	5'-AGGTATCGGGACAACATGAGG-3'
	Reverse (5'-3')	5'-GCCTTCTGTAAACATCGCTCTGT-3'
<i>Syn1</i>	Forward (5'-3')	5'-AATCACAAGAGATGCTCAG-3'
	Reverse (5'-3')	5'-GGACACGCACATCATATTTAG-3'
<i>Syp</i>	Forward (5'-3')	5'-TGCCAACAAGACGGAGAGTG-3'
	Reverse (5'-3')	5'-TAGTGCCCCCTTTAACGCAG-3'
<i>Syt1</i>	Forward (5'-3')	5'-ACCCTGGGCTCTGTATCCC-3'
	Reverse (5'-3')	5'-CCCTGACCACTGAGTGCAAA-3'
<i>Unc13A</i>	Forward (5'-3')	5'-GCTGTGCGTGGGAGTCAAA-3'
	Reverse (5'-3')	5'-CAGCTATGGTAGTGCTCTCA-3'
<i>Vamp2</i>	Forward (5'-3')	5'-ATCATCGTTTACTTCAGCAC-3'
	Reverse (5'-3')	5'-TGAAAGATATGGCTGAGAGG-3'

4.6. Statistical Analysis of RT-PCR

Data are presented as mean \pm SEM. Statistical evaluations were performed with Student's unpaired *t*-test for RT-PCR. When multiple comparisons were performed, one-way ANOVA followed by the Bonferroni test was used. Statistical significance was set at $p < 0.05$.

5. Conclusions

This work indicates that the prevention of synaptic abnormalities plays a key role in the reported beneficial effects of topical (eye drops) administration of sitagliptin. These results, in addition to its already demonstrated ability to reduce inflammation, glial activation and vascular leakage, suggest that topical administration of sitagliptin may become a new therapeutic strategy against early stages of DR.

Author Contributions: Conceptualization, P.B., C.H. and R.S.; methodology, H.R., P.B., A.D.-J., R.S. and C.H.; formal analysis, H.R., P.B., A.D.-J., C.H. and R.S.; investigation, P.B., H.R., C.H. and R.S.; resources, R.S. and C.H.; writing—original draft preparation, H.R. and P.B.; writing—review and editing, R.S. and C.H.; supervision, R.S. and C.H.; project administration, C.H.; funding acquisition, R.S. and C.H. R.S. is the guarantor of this work and, as such, had full access to all the data in the study and takes responsibility for the integrity of the data and the accuracy of the data analysis. All authors have read and agreed to the published version of the manuscript.

Funding: This research was funded by grants from the Ministerio de Economía y Competitividad (PID2019-104225RB-I00) and the Instituto de Salud Carlos III (DTS18/0163, PI19/01215 and ICI20/00129). The study funder was not involved in the design of the study.

Institutional Review Board Statement: The animal study protocol was approved by the Animal Care and Use Committee of Vall d'Hebron Research Institute (VHIR). Approval Code: 14/21. Approval Date: 9 July 2021.

Informed Consent Statement: Not applicable.

Data Availability Statement: The raw data of this manuscript are in the GEO repository. Accession “GSE219084” is currently private and is scheduled to be released on 30 November 2025. When the manuscript is published, it will be changed to open access.

Acknowledgments: H.R. is the recipient of a grant from the Ministerio de Economía y Competitividad (BES-2017-081690). We thank the Statistics and Bioinformatics Unit (UEB) and VHIR High Technology Unit (UAT) core facilities and staff for their contribution in this publication.

Conflicts of Interest: Vall d'Hebron Research Institute holds intellectual property related to the use of ocular DPP-4 inhibitors to treat diabetic retinopathy. No other potential conflicts of interest relevant to this article were reported.

References

- Leasher, J.L.; Bourne, R.R.; Flaxman, S.R.; Jonas, J.B.; Keeffe, J.; Naidoo, K.; Pesudovs, K.; Price, H.; White, R.A.; Wong, T.Y.; et al. Vision Loss Expert Group of the Global Burden of Disease Study. Global estimates of people blind or visually impaired by diabetic retinopathy: A meta-analysis from 1990 to 2010. *Diabetes Care* **2016**, *39*, 1643–1649. [\[CrossRef\]](#) [\[PubMed\]](#)
- Wong, T.Y.; Cheung, C.M.; Larsen, M.; Sharma, S.; Simó, R. Diabetic retinopathy. *Nat. Rev. Dis. Primers* **2016**, *17*, 16012. [\[CrossRef\]](#) [\[PubMed\]](#)
- Simó, R.; Hernández, C. Novel approaches for treating diabetic retinopathy based on recent pathogenic evidence. *Prog. Retin. Eye Res.* **2015**, *48*, 160–180. [\[CrossRef\]](#) [\[PubMed\]](#)
- Solomon, S.D.; Chew, E.; Duh, E.J.; Sobrin, L.; Sun, J.K.; VanderBeek, B.L.; Wykoff, C.C.; Gardner, T.W. Diabetic Retinopathy: A Position Statement by the American Diabetes Association. *Diabetes Care* **2017**, *40*, 412–418. [\[CrossRef\]](#) [\[PubMed\]](#)
- Simó, R.; Stitt, A.W.; Gardner, T.W. Neurodegeneration in diabetic retinopathy: Does it really matter? *Diabetologia* **2018**, *61*, 1902–1912. [\[CrossRef\]](#)
- Simó, R.; Simó-Servat, O.; Bogdanov, P.; Hernández, C. Neurovascular Unit: A New Target for Treating Early Stages of Diabetic Retinopathy. *Pharmaceutics* **2021**, *13*, 1320. [\[CrossRef\]](#)
- Salcedo, I.; Tweedie, D.; Li, Y.; Greig, N.H. Neuroprotective and neurotrophic actions of glucagon-like peptide-1: An emerging opportunity to treat neurodegenerative and cerebrovascular disorders. *Br. J. Pharmacol.* **2012**, *166*, 1586–1599. [\[CrossRef\]](#)
- Hernández, C.; Bogdanov, P.; Solà-Adell, C.; Sampedro, J.; Valeri, M.; Genís, X.; Simó-Servat, O.; García-Ramírez, M.; Simó, R. Topical administration of DPP-IV inhibitors prevents retinal neurodegeneration in experimental diabetes. *Diabetologia* **2017**, *60*, 2285–2298. [\[CrossRef\]](#)
- Hernández, C.; Bogdanov, P.; Corraliza, L.; García-Ramírez, M.; Solà-Adell, C.; Arranz, J.A.; Arroba, A.I.; Valverde, A.M.; Simó, R. Topical administration of GLP-1 receptor agonists prevents retinal neurodegeneration in experimental diabetes. *Diabetes* **2016**, *65*, 172–187. [\[CrossRef\]](#)
- Röhrborn, D.; Wronkowitz, N.; Eckel, J. DPP4 in Diabetes. *Front. Immunol.* **2015**, *6*, 386. [\[CrossRef\]](#)
- Subramanian, A.; Tamayo, P.; Mootha, V.K.; Mukherjee, S.; Ebert, B.L.; Gillette, M.A.; Paulovich, A.; Pomeroy, S.L.; Golub, T.R.; Lander, E.S.; et al. Gene set enrichment analysis: A knowledge-based approach for interpreting genome-wide expression profiles. *Proc. Natl. Acad. Sci. USA* **2005**, *102*, 15545–15550. [\[CrossRef\]](#)
- Barber, A.J.; Baccouche, B. Neurodegeneration in diabetic retinopathy: Potential for novel therapies. *Vision. Res.* **2017**, *139*, 82–92. [\[CrossRef\]](#)
- Kutsyr, O.; Arango-Gonzalez, B.; Fernandez-Sanchez, L.; Maneu, V.; Lax, P.; Ambrosio, A.F.; Ueffing, M.; Cuenca, N. Dipeptidyl peptidase-IV inhibition by sitagliptin slows down retinal neurodegeneration in rd10 mice retinas. *Investig. Ophthalmol. Vis. Sci.* **2019**, *60*, 4879.

14. Gonçalves, A.; Marques, C.; Leal, E.; Ribeiro, C.F.; Reis, F.; Ambrósio, A.F.; Fernandes, R. Dipeptidyl peptidase-IV inhibition prevents blood-retinal barrier breakdown, inflammation and neuronal cell death in the retina of type 1 diabetic rats. *Biochim. Biophys. Acta* **2014**, *1842*, 1454–1463. [\[CrossRef\]](#)
15. Ramos, H.; Bogdanov, P.; Sabater, D.; Huerta, J.; Valeri, M.; Hernández, C.; Simó, R. Neuromodulation Induced by Sitagliptin: A New Strategy for Treating Diabetic Retinopathy. *Biomedicines* **2021**, *9*, 1772. [\[CrossRef\]](#)
16. Zhang, Y.; Liu, Y.; Xu, J.; Sun, Q.; Yu, F.; Cheng, J.; Peng, B.; Liu, W.; Xiao, Z.; Yin, J.; et al. Inhibition of DPP4 enhances inhibitory synaptic transmission through activating the GLP-1/GLP-1R signaling pathway in a rat model of febrile seizures. *Biochem. Pharmacol.* **2018**, *156*, 78–85. [\[CrossRef\]](#)
17. Dietrich, N.; Kolibabka, M.; Busch, S.; Bugert, P.; Kaiser, U.; Lin, J.; Fleming, T.; Morcos, M.; Klein, T.; Schlotterer, A.; et al. The DPP4 inhibitor linagliptin protects from experimental diabetic retinopathy. *PLoS ONE* **2016**, *11*, e0167853. [\[CrossRef\]](#)
18. Chung, Y.R.; Ha, K.H.; Kim, H.C.; Park, S.J.; Lee, K.; Kim, D.J. Dipeptidyl Peptidase-4 Inhibitors versus Other Antidiabetic Drugs Added to Metformin Monotherapy in Diabetic Retinopathy Progression: A Real World-Based Cohort Study. *Diabetes Metab. J.* **2019**, *43*, 640–648. [\[CrossRef\]](#)
19. Tang, H.; Li, G.; Zhao, Y.; Wang, F.; Gower, E.W.; Shi, L.; Wang, T. Comparisons of diabetic retinopathy events associated with glucose-lowering drugs in patients with type 2 diabetes mellitus: A network meta-analysis. *Diabetes Obes. Metab.* **2018**, *20*, 1262–1279. [\[CrossRef\]](#)
20. Taylor, O.M.; Lam, C. The Effect of Dipeptidyl Peptidase-4 Inhibitors on Macrovascular and Microvascular Complications of Diabetes Mellitus: A Systematic Review. *Curr. Ther. Res. Clin. Exp.* **2020**, *25*, 100596. [\[CrossRef\]](#)
21. Fura, A.; Khanna, A.; Vyas, V.; Kopolowitz, B.; Chang, S.Y.; Caporuscio, C.; Boulton, D.W.; Christopher, L.J.; Chadwick, K.D.; Hamann, L.G.; et al. Pharmacokinetics of the dipeptidyl peptidase 4 inhibitor saxagliptin in rats, dogs, and monkeys and clinical projections. *Drug Metab. Dispos.* **2009**, *37*, 1164–1171. [\[CrossRef\]](#) [\[PubMed\]](#)
22. Fuchs, H.; Binder, R.; Greischel, A. Tissue distribution of the novel DPP-4 inhibitor BI 1356 is dominated by saturable binding to its target in rats. *Biopharm. Drug Dispos.* **2009**, *30*, 229–240. [\[CrossRef\]](#) [\[PubMed\]](#)
23. Sigoiilot, S.M.; Iyer, K.; Binda, F.; González-Calvo, I.; Talleur, M.; Vodjdani, G.; Isopé, P.; Selimi, F. The Secreted Protein C1QL1 and Its Receptor BAI3 Control the Synaptic Connectivity of Excitatory Inputs Converging on Cerebellar Purkinje Cells. *Cell Rep.* **2015**, *10*, 820–832. [\[CrossRef\]](#) [\[PubMed\]](#)
24. Drerup, C.M.; Lusk, S.; Nechiporuk, A. Kif1B Interacts with KBP to Promote Axon Elongation by Localizing a Microtubule Regulator to Growth Cones. *J. Neurosci.* **2016**, *36*, 7014–7026. [\[CrossRef\]](#) [\[PubMed\]](#)
25. Becherer, U.; Rettig, J. Vesicle pools, docking, priming, and release. *Cell Tissue Res.* **2006**, *326*, 393–407. [\[CrossRef\]](#)
26. Stepien, K.P.; Prinslow, E.A.; Rizo, J. Munc18-1 is crucial to overcome the inhibition of synaptic vesicle fusion by αSNAP. *Nat. Commun.* **2019**, *10*, 4326. [\[CrossRef\]](#)
27. Okamoto, M.; Südhof, T.C. Mints, Munc18-interacting proteins in synaptic vesicle exocytosis. *J. Biol. Chem.* **1997**, *272*, 31459–31464. [\[CrossRef\]](#)
28. Courtney, N.A.; Bao, H.; Briguglio, J.S.; Chapman, E.R. Synaptotagmin 1 clamps synaptic vesicle fusion in mammalian neurons independent of complexin. *Nat. Commun.* **2019**, *10*, 4076. [\[CrossRef\]](#)
29. Kwon, S.E.; Chapman, E.R. Synaptophysin regulates the kinetics of synaptic vesicle endocytosis in central neurons. *Neuron* **2011**, *70*, 847–854. [\[CrossRef\]](#)
30. Böhler, M.; Benfenati, F.; Valtorta, F.; Greengard, P. The synapsins and the regulation of synaptic function. *Bioessays* **1990**, *12*, 259–263. [\[CrossRef\]](#)
31. Bykhovskaia, M. Synapsin regulation of vesicle organization and functional pools. *Semin. Cell Dev. Biol.* **2011**, *22*, 387–392. [\[CrossRef\]](#)
32. Stout, K.A.; Dunn, A.R.; Hoffman, C.; Miller, G.W. The Synaptic Vesicle Glycoprotein 2: Structure, Function, and Disease Relevance. *ACS Chem. Neurosci.* **2019**, *10*, 3927–3938. [\[CrossRef\]](#)
33. Martineau, M.; Guzman, R.E.; Fahlke, C.; Klingauf, J. VGLUT1 functions as a glutamate/proton exchanger with chloride channel activity in hippocampal glutamatergic synapses. *Nat. Commun.* **2017**, *8*, 2279. [\[CrossRef\]](#)
34. Huang, S.; Chen, L.; Bladen, C.; Stys, P.K.; Zamponi, G.W. Differential modulation of NMDA and AMPA receptors by cellular prion protein and copper ions. *Mol. Brain* **2018**, *11*, 62. [\[CrossRef\]](#)
35. Smith, S.B. Diabetic Retinopathy and the NMDA Receptor. *Drug News Perspect* **2002**, *15*, 226–232. [\[CrossRef\]](#)
36. Jeong, J.; Pandey, S.; Li, Y.; Badger, J.D., 2nd; Lu, W.; Roche, K.W. PSD-95 binding dynamically regulates NLGN1 trafficking and function. *Proc. Natl. Acad. Sci. USA* **2019**, *116*, 12035–12044. [\[CrossRef\]](#)
37. Hsueh, Y.P. The role of the MAGUK protein CASK in neural development and synaptic function. *Curr. Med. Chem.* **2006**, *13*, 1915–1927. [\[CrossRef\]](#)
38. Gentleman, R.; Carey, V.; Huber, W.; Irizarry, R.A.; Dudoit, S. *Bioinformatics and Computational Biology Solutions Using R and Bioconductor*; Springer: Berlin/Heidelberg, Germany, 2005.
39. Irizarry, R.A.; Hobbs, B.; Collin, F.; Beazer-Barclay, Y.D.; Antonellis, K.J.; Scherf, U.; Speed, T.P. Exploration, normalization, and summaries of high density oligonucleotide array probe level data. *Biostatistics* **2003**, *4*, 249–264. [\[CrossRef\]](#)

40. Smyth, G.K. Linear models and empirical bayes methods for assessing differential expression in microarray experiments. *Stat. Appl. Genet Mol. Biol.* **2004**, *3*. [[CrossRef](#)]
41. Wu, T.; Hu, E.; Xu, S.; Chen, M.; Guo, P.; Dai, Z.; Feng, T.; Zhou, L.; Tang, W.; Zhan, L.; et al. clusterProfiler 4.0: A universal enrichment tool for interpreting omics data. *Innovation* **2021**, *2*, 100141. [[CrossRef](#)]

Disclaimer/Publisher's Note: The statements, opinions and data contained in all publications are solely those of the individual author(s) and contributor(s) and not of MDPI and/or the editor(s). MDPI and/or the editor(s) disclaim responsibility for any injury to people or property resulting from any ideas, methods, instructions or products referred to in the content.

Diabetic retinopathy (DR) is one of the most frequent complications of diabetes and it is considered the leading cause of blindness among the working age population in the most developed countries. Despite this, treatments are only available for the later stages of the disease when vision is already impaired. Moreover, current treatments are invasive, expensive and associated with undesirable side effects. Therefore treatment of DR and in particular in its early stages is considered an unmet medical need.

In the earliest stages of DR, before vision is impaired, there exist alterations in the retinal neurovascular unit (NVU), a functional coupling formed by neurons, glial cells and blood vessels, which modulates blood flow according to metabolic demands. Our research group found that glucagon-like peptide-1 (GLP-1) is locally synthesized by the retina and that a decreased production exist in diabetic patients. This is important because GLP-1 is a neuroprotective agent with viscerotropic actions. In this regard, we also found that topical administration of GLP-1 or GLP-1 receptor agonists were effective in the treatment of early stages of DR in experimental models. Another therapeutic approach related to GLP-1 receptor activation consists in administering topically inhibitors of the enzyme dipeptidyl peptidase-4 (DPP-4i), which degrades endogenous GLP-1. This enzyme degrades other substrates that have been linked to beneficial effects, which may be synergistic with the increase in GLP-1. For this reason, the greater stability and lower price, when compared to GLP-1 and GLP-1 receptor agonists, we hypothesized that topical administration of DPP-4i has great potential for treating early DR. First studies evidenced that these drugs can prevent the main pathophysiological processes of early DR (neuronal death, glial activation and vascular leakage), however more preclinical evidence is needed to reach clinical phases.

In the present thesis, and in order to shed light on the mechanisms of action behind these beneficial effects, a transcriptomic study was conducted between diabetic mice topically treated with vehicle or sitagliptin (a DPP-4i) and non-diabetic animals. The study revealed that the main mechanism of action of sitagliptin is neuromodulatory in nature, preserving key proteins in synaptic transmission at the pre- and postsynaptic level. These proteins are down-regulated in DR. Furthermore, sitagliptin also exhibits antioxidant and anti-inflammatory effects. Topical administration of sitagliptin preserved the physiological balance between reactive oxygen species and antioxidant defenses, thus preventing oxidative damage to DNA and proteins. In addition, sitagliptin reduced the activation of inflammatory pathways in the retina and decreased the production of pro-inflammatory cytokines. These effects were accompanied by a functional improvement of the retina and a recovery of physiological neuronal proliferation rates. Furthermore, the minimum effective doses for sitagliptin and saxagliptin, another DPP-4i, were established. These findings could pave the way for clinical trials to test this new approach in the treatment of early stages of DR or even other retinal diseases.